



DURBAN UNIVERSITY OF TECHNOLOGY
INYUVESI YASETHEKWINI YEZOBUCHWEPHESHE

CREATIVE. DISTINCTIVE. IMPACTFUL.

**REMEDICATION OF EFAVIRENZ USING A MAGNETIC MOLECULARLY
IMPRINTED TITANIA NANOCOMPOSITE**

by

ASENATHI SIBALI

A dissertation submitted to the School of Science and Technology, Durban University of

Technology Sciences University in fulfilment of the requirements for the degree of

Master of Applied Science in Chemistry

DECLARATION

I declare that this dissertation is my own, unaided work. It is being submitted for the degree of Master of Science at Durban University of Technology, South Africa. It has not been submitted before for any degree or examination at any university.

05 May 2025

LIST OF MANUSCRIPTS AND CONFERENCE OUTPUTS

The results of the current study have been drafted into three (3) manuscripts in which the candidate was the principal author. The first manuscript has been published in the Journal of Hazardous Materials Advances (Impact factor – 5.5); the second has been submitted to the Journal of Water Process Engineering (Impact factor – 6.3) for peer review; the third has been drafted and is intended for submission in Environmental Pollution journal (Impact Factor – 7.6). A portion of the work that focussed on the multivariate approach to optimization was recently presented in a conference

1. Asenathi Sibali, Thabang Mokhothu, Samson Mohomane, Vusumzi Emmanuel Pakade, Ramakwal Christinah Chokwe, Somandla Ncube, **Applications of molecularly imprinted titania-based photocatalysis for degradation of pharmaceutical pollutants in the aqueous environment.** *Published in the Journal of Hazardous Materials Advances.*
2. Asenathi Sibali, Devrani Naicker, Nompumelelo Pretty Cele, Vusumzi Emmanuel Pakade, Ramakwala Christinah Chokwe, Thabang Mokhothu, Somandla Ncube, **Removal of efavirenz in wastewater effluents using a magnetic molecularly imprinted polymer: Synthesis, multivariate optimization and application.** *Published in the Journal of Water Process Engineering*
3. Asenathi Sibali, Devrani Naicker, Nompumelelo Cele, Vusumzi Pakade, Thabang Mokhothu, Somandla Ncube, **Photodegradation of efavirenz in wastewater effluents using a hybrid TiO₂ – magnetic molecularly imprinted polymer.** *Submitted to Chemistry Africa journal.*

Conference Output

1. Asenathi Sibali, Thabang Mokhothu, Devran Naicker, Nompumelelo Cele, Samson Mohamane, Vusumzi Pakade and Somandla Ncube “**Understanding adsorption kinetics of efavirenz using a molecularly imprinted nanosorbent based on central composite design**”. Poster Presentation at the South African Chemical Institute, KwaZulu Natal region (SACI-KZN) Postgraduate Research Colloquium (29 November 2024) at the University of Zululand, KwaDlangezwa.

ACKNOWLEDGEMENTS

- To my supervisor Dr S Ncube and my co-supervisor Dr T H Mokhothu I am extremely thankful for guidance, support, encouragement, mostly patience throughout the entire process of researching and writing this dissertation.
- To Devran Naicker (HPLC laboratory technician), I thank for her unwavering support and assistance in handling the instrument and availability.
- To the Durban University of Technology internal Master's Scholarship, I thank them for financially support throughout this study. This research would not have been possible without your assistance.
- I would also like to thank my family (dad, mom, siblings and my son) for believing in me and for emotional support.
- Finally, I would like to thank God for letting me through all the difficulties

ABSTRACT

In the current study, remediation of efavirenz as a model antiretroviral drug in wastewater effluents was investigated using a hybrid photodegrader based on titania embed on a magnetic molecularly imprinted polymer (MMIP). Initially, a MMIP was synthesized to specifically recognize and remove efavirenz from wastewater effluents. The magnetic smart polymer was synthesized via a bulk polymerization technique with efavirenz as the template, and p-vinyl benzoic acid the functional monomer in the presence of magnetite nanoparticles. The MMIP was characterized using Fourier transform infrared spectroscopy and thermogravimetric analysis. The performance of MMIP was optimized using a central composite design. The optimum conditions for effective adsorption of efavirenz were pH 6.5, MMIP mass of 15 mg, 1 mg L⁻¹ efavirenz concentration and contact time of 40 min. The optimal binding capacity achieved after 40 min of contact time and neutral conditions was 44.9 µg g⁻¹.

Batch studies revealed that pseudo-second order and the Langmuir isotherm were the models that explained the kinetics and mechanism of adsorption of efavirenz onto the MMIP. This suggested that the interaction between the MMIP and the efavirenz was through chemisorption and that once efavirenz binding reaches a maximum limit, no more binding occurs. The MMIP was finally applied in the removal of efavirenz from real wastewater effluents polluted with 3.99 ng mL⁻¹ of efavirenz. The polymeric sorbent could achieve 44.8% removal efficiencies. Reusability studies showed less than 4% average loss in the binding capacity with every reuse cycle, while there was no loss in binding capabilities when the polymer was utilized at about half its binding capacity.

Finally, photocatalytic degradation of efavirenz was investigated as a potential remedial tool for efavirenz in wastewater effluents. Titania was imbedded onto the MMIP to form a hybrid MMIP/TiO₂ nanocomposite with the ability to trap efavirenz from wastewater followed by its

photodegradation. Its performance was also investigated using factorial design involving initial concentration of efavirenz (20 - 60 $\mu\text{g L}^{-1}$), mass of the MMIP/TiO₂ (5 -15 mg) and the time of irradiation (20 - 40 min). The results were also observed in a form of contour plots. Up to 99% photodegradation of efavirenz was achieved within 15 min. However, it was observed that the photodegrader performed better under higher concentrations of efavirenz concentrations. In general, the synthesis and optimization of a hybrid molecularly imprinted titania nanocomposite for photodegradation of efavirenz in wastewater effluents was successful. Its performance has proven that it can be a viable tool for remediation of efavirenz in wastewater effluents. Efavirenz cannot be removed by conventional wastewater treatment processes and advanced technologies such as the MMIP/TiO₂ nanocomposite synthesized in the current study could help minimize the release of efavirenz into surface water systems. This work has yielded three manuscripts; a review article and two research papers. The review has been published, one manuscript is under review and the final one has been drafted.

TABLE OF CONTENTS

DECLARATION	ii
LIST OF MANUSCRIPTS AND CONFERENCE OUTPUTS	iii
ACKNOWLEDGEMENTS	v
ABSTRACT.....	vi
LIST OF FIGURES	ix
LIST OF TABLES	xv
LIST OF ABBREVIATIONS.....	xvi
1 INTRODUCTION	17
1.1 Background.....	17
1.2 Problem statement	20
1.3 Aim.....	20
1.4 Objectives	21
2 LITERATURE REVIEW	22
2.1 Antiretroviral drugs	22
2.1.1 Properties of antiretroviral drugs.....	23
2.1.2 Sources of ARVD contamination.....	24
2.1.3 Ecotoxicological impact of antiretroviral drugs	26
2.2 Various methods for the removal of pharmaceuticals in wastewater	26

REFERENCES	27
3 MANUSCRIPTS AND PUBLISHED PAPERS	32
3.1 PAPER 1.....	33
Abstract.....	34
Keywords	35
Abbreviations.....	35
1 Introduction.....	36
2 Overview of pharmaceutical pollution in the aqueous environment	37
3 Principles of photocatalytic degradation.....	39
4 Integration of molecularly imprinted polymers with TiO ₂ photodegradation catalysts ...	41
3.2 Principle of titania photodegradation	41
3.3 Applications of titania-based photocatalyst in degradation of pharmaceutical residues	41
3.4 Challenges of photocatalytic degradation of pharmaceuticals in aqueous environments.....	43
3.5 Principle of molecular imprinting technology.....	43
3.6 Applications of molecularly imprinted TiO ₂ photodegradation catalysts	45
5 Photodegradation activities of other molecularly imprinted photocatalysts.....	49
5.1 Molecularly imprinted metal oxides	49
5.2 Molecularly imprinted graphene-based semiconductors.....	50

5.3	Molecularly imprinted organic semiconductors	51
5.4	Molecularly imprinted metal organic frameworks	52
5.5	Molecularly imprinted schemes based on novel semiconductors	53
6	Challenges and considerations	54
7	Perspectives.....	57
8	Conclusions.....	60
	Funding	61
	References.....	61
	PAPER 2	78
	Abstract	79
1	Introduction.....	80
2	Methods and Materials.....	82
2.1	Chemicals and reagents	82
2.2	Gas chromatography mass spectrometry	82
2.3	Synthesis of a magnetic smart sorbent	83
2.3.1	Synthesis of magnetite.....	83
2.3.2	Synthesis of a magnetic molecularly imprinted polymer	83
2.4	Optimization experiments using central composite design	84
2.5	Investigating the mechanism and kinetics of adsorption.....	85
2.6	Reusability studies.....	86

2.7	Application of the MMIP in wastewater effluent samples	87
2.7.1	Wastewater effluent collection and analysis	87
2.7.2	Removal of efavirenz using the magnetic polymer	87
3	Results and Discussion	88
3.1	Characterization results	88
3.2	Optimization results.....	89
3.2.1	Method validity and interactive effects	89
3.2.2	Adsorption kinetics and mechanism.....	91
3.3	Reusability studies.....	94
3.4	Application in wastewater samples	94
3.4.1	Method validation and levels of efavirenz in wastewater effluents	94
3.4.2	Removal of efavirenz from wastewater effluents.....	95
4	Conclusions.....	96
	Funding	97
	Acknowledgment	97
	References.....	97
	PAPER 3	104
	Abstract.....	105
	Keywords	106
1	Introduction.....	107

2	Methods and materials	108
2.1	Chemicals and Reagents	108
2.2	Instrumentation and method validation	109
2.3	Synthesis of titania.....	109
2.4	Synthesis of a hybrid nanocomposite	109
2.5	Photodegradation optimization.....	110
2.6	Adsorption kinetics.....	111
3	Results and discussion	111
3.1	Characterization results	111
3.2	Adsorption kinetics and mechanism.....	112
3.3	Optimization and degradation kinetics	114
3.4	Degradation results	117
4	Conclusion and recommendations	118
	References.....	119
	GENERAL CONCLUSIONS	125
	APPENDEIX FOR PAPER 1	126
	APPENDEIX FOR PAPER 2	127
	APPENDIX FOR PAPER 3	136
	APPENDIX – Poster Presentation	138

LIST OF FIGURES

Figure 1: Sources of ARVDs into the water bodies.....25

LIST OF TABLES

Table 1: Name, structure, and physicochemical properties of efavirenz	24
---	----

LIST OF ABBREVIATIONS

%RSD	Percentage relative standard deviation
AIBN	1,1'-azobis(isobutyronitrile)
ARVD	Antiretroviral drug
BET	Brunauer -Emmett -Teller
CCD	Central composite design
CCF	Composite centered faces
C_e	Equilibrium concentration
C_o	Initial concentration
DMF	Dimethylformamide
DOE	Design of experiment
EGDMA	Ethylene glycol dimethacrylate
GC-TQMS	Gas chromatography - triple quadrupole mass spectrometer
K_F	Freundlich constant
K_L	Langmuir constant
LC-MS	Liquid chromatography- mass spectrometer
LOD	Limit of detection
LOQ	Limit of quantification
MDL	Method detection limit
MIP	Molecular imprinted polymer

MIT	Molecular imprinting technology
MMIP	Magnetic molecularly imprinted polymer
MMIP-TiO ₂	Magnetic molecularly imprinted polymer-titanium dioxide
MQL	Method quantification limit
NIP	non-imprinted polymer
Q _e	Adsorption capacity at equilibrium
Q _t	Adsorption capacity at time t
R ²	Coefficient of determination
SIM	Single ion monitoring
WWTP	Wastewater treatment plant

1 INTRODUCTION

1.1 Background

The release of pharmaceuticals into the environment causes negative effects on the metabolism of exposed living organisms and possibly humans. A wide range of pharmaceuticals exist but the most common ones can be classified under antibiotics, painkillers, anti-inflammatory drugs, antivirals, hormones, and antidepressants. Among these pharmaceutical residues, antiretroviral drugs may be considered pollutants of emerging concern because studies that report their presence in the environment are recent. Antiretroviral drugs (ARVDs) are among antiviral pharmaceuticals with potentially serious ecotoxicological effects when they make their way into the environment. Exposure to them via contaminated water may be consequential especially for those already taking ARVDs and for new infections because they work against a virus that easily mutates if the drugs are not taken according to prescription. The analysis of ARVDs in the aqueous environment only started in the past 10 years with the first studies in South Africa reported in 2015 (Wood, Duvenage and Rohwer, 2015). Since then, there has been a plethora of other studies that have detected ARVDs in wastewater, rivers and dams in South Africa and the African continent at large (Gwenzi and Chaukura, 2018; Lawrence Mzukisi Madikizela, Ncube and Chimuka, 2020). Major sources of the ARVDs in the environment is mainly through effluents from wastewater treatment plants (WWTPs) (Gwenzi and Chaukura, 2018; Lawrence Mzukisi Madikizela, Ncube and Chimuka, 2020) as well as illicit or indiscriminate disposal of expired drugs. Poor sanitation in most African regions, unavailability of modern ablution facilities that can be flushed with water to direct the human waste into WWTPs and improper disposal of expired or unused medications contributes to the direct contamination of surface water with pharmaceuticals (Zunngu *et al.*, 2017).

A further challenge for Africa is that the infection rates continue to increase resulting in more ARVDs released into the environment as part of excreta. (Adeola and Forbes, 2022) and (Ncube et al., 2018) recently reported findings that Southern Africa is a potential hotspot regarding ARVD contamination due to relatively high therapeutic application and detection thereof in water bodies (Ncube *et al.*, 2018; Adeola, de Lange and Forbes, 2021). The presence of ARVDs in various aqueous systems such as wastewater effluents, surface water, ground water, and even drinking water has been reported extensively in Africa (Wood, Duvenage and Rohwer, 2015; Abafe *et al.*, 2018; Moslah *et al.*, 2018). Efavirenz and nevirapine are the most detected ARVDs in surface environments and some scholars now consider them as priority pollutants in African water bodies (Nannou *et al.*, 2019; Adeola, de Lange and Forbes, 2021). In particular, the levels efavirenz are way higher compared to other ARVDs and was therefore used in the current study as a model ARVD in wastewater effluents.

While most studies on pharmaceutical pollution have focussed on reporting their detection in the aqueous environment, recent research has since shifted focus towards finding sustainable pollution control technologies that can effectively control their levels in the environment. Photocatalytic degradation has offered a viable alternative with the ability to eliminate pharmaceutical residues through degradation and eventual mineralization to less-toxic products (Fiorenza *et al.*, 2019). Other sorbents such as clay and activated carbon have been reported in literature. However, they are also unable to selectively remove organic contaminants at trace levels, even though adsorption is a popular technique for removing both organic and inorganic contaminants from environmental matrices (Fiorenza *et al.*, 2019).

Among metal oxide photocatalyst, titanium dioxide (TiO₂) (also called titania) is one of the most promising for its advantageous properties such as low cost, chemical inertness, and photostability compared to other metal oxide nanoparticles (Scuderi *et al.*, 2016). TiO₂

photocatalyst performs exceptionally well in the photocatalytic degradation of organic compounds and offers the benefits of high catalytic activity, high safety, and non-toxicity.

However, photocatalytic degradation also has its own disadvantages. The photocatalytic oxidation is not a selective process being driven by the formation of radicals that degrade anything organic. Therefore, the organic compounds present in water at high concentration are efficiently degraded, compared to those that exist at low concentration due to competition with interferents such as humic acids.

Therefore, this study was focused on introducing molecular imprinting technology where a smart polymer with cavities specific to the targeted compound is synthesized and the photocatalyst gets imbedded within the polymer matrix. A more detailed discussion of the MIP-TiO₂ and its applications in remediation of pharmaceuticals is presented as review article (**Paper 1**) already published in Journal of Hazardous Materials Advances. The molecularly imprinted polymer (MIP) matrix was also magnetized with magnetite to offer it an advantage of keeping it static using an external magnetic field (Kaya, Cetinkaya and Ozkan, 2023). The hybrid MMIP-TiO₂ was synthesized, characterized and applied in the degradation of efavirenz from wastewater effluents. The idea was that the MIP will selectively trap the efavirenz from wastewater effluents; the magnetite will allow the polymer to be trapped and also be removed from solution using an external magnetic; the TiO₂ would then degrade the trapped efavirenz and the final degradation products will escape from the cavities allowing the cavities to trap more efavirenz from solution.

The performance of the hybrid photodegrader was optimized for various important parameters to determine its optimum operating conditions for the effective remediation of efavirenz. Firstly, parameters that affect the adsorption of efavirenz onto the MMIP cavities were investigated. These included initial concentration, contact time, pH and MMIP dosage. For

photodegradation, three parameters were investigated. These were initial concentration, time of irradiation, and mass of MMIP/TiO₂. All optimization studies were done using a multivariate approach based on central composite designs (CCDs). Modde and Minitab 18 were the two statistical software used to create the CCDs. The advantage of a multivariate approach over one-factor-at-a-time (OFAT) is that it takes potential interactive effects into consideration during optimization while OFAT investigates one factor at a time while keeping other constant. Synthesis of the MMIP, its characterization and application for removal of efavirenz from wastewater effluents is presented as **Paper 2** and has been submitted to Journal of Water Process Engineering for peer review. The synthesis of the hybrid MMIP-TiO₂ nanophotocatalyst, its characterization, optimization and application for degradation of efavirenz in wastewater effluents is presented as **Paper 3** ready for submission in Environmental Pollution journal.

1.2 Problem statement

Conventional wastewater treatment processes are not effective in removal of ARVDs from wastewater and various studies have detected the presence of ARVDs in water systems in South Africa with efavirenz being the most prevalent and its concentrations way above other ARVDs. This raises a serious concern because such exposure can lead to adverse risks to human health and ecotoxicological effects to aquatic organisms. The current study intended to investigate the potential of photocatalytic degradation as a potential remediation tool for removing efavirenz in water sources.

1.3 Aim

To synthesize a hybrid MMIP/TiO₂ nanocomposite for remediation of efavirenz from surface water systems.

1.4 Objectives

- To synthesize a MIP, magnetite and TiO_2 to be used in the production of a hybrid nanocomposite.
- To synthesize the MMIP/ TiO_2 nanocomposite.
- To characterize the MIP, TiO_2 , magnetite and MMIP/ TiO_2 nanocomposite using techniques such as thermogravimetric analysis (TGA), scanning electron microscopy (SEM), transmission electron microscopy (TEM), Fourier transform-infrared (FTIR), Brunauer-Emmett-Teller (BET) and powder X-ray diffraction (XRD).
- To determine the best working conditions for the effective photocatalytic degradation of efavirenz using the MMIP/ TiO_2 nanocomposite.
- To predict the extent of adsorption of efavirenz onto the nanocomposite based on the Langmuir and Freundlich adsorption isotherms.
- To predict the mechanism of adsorption of efavirenz on the nanocomposite based on the pseudo first order (PFO) and pseudo second order (PSO) models.
- To develop and validate an GC/MS method for the analysis of efavirenz in aqueous solution.
- To apply the synthesized hybrid nanocomposite for the photocatalytic removal of efavirenz in water.

2 LITERATURE REVIEW

2.1 Antiretroviral drugs

Antiretroviral drugs (ARVDs) are therapeutic agents for the treatment of retroviral infections such as human immunodeficiency virus (HIV), also popularly called the HIV disease. The HIV virus infects the CD4 T cells responsible for the body's immunity. Antiretroviral treatment against HIV does not eliminate the virus but rather prevents its rapid replication (Ncube *et al.*, 2018). The ARVDs as well as other pharmaceuticals are emerging contaminants that are ultimately discharged into water bodies. Unused drugs and expired drugs are often disposed of indiscriminately and therefore get into drainage systems and ultimately reach waterbodies (Abafe *et al.*, 2018). Antiretroviral drugs are used to treat retroviruses, which are different from other viruses based on the mode of replication within their host, which involves RNA genetic materials and not DNA materials like other viruses. Antiretroviral drugs may cause adverse effects on the central and peripheral nervous systems (Abers, Shandera and Kass, 2014). The rate and extent of neuropsychiatric adverse effects varies with different classes of ARVDs and among each drug in their class. Neurotoxicity induced by nucleoside reverse transcriptase inhibitor (NRTI) occurs due to the inhibition of mitochondrial DNA polymerase. Over half of the antiviral drugs are antiretroviral, and ARVDs are further classified based on their mode of action, such as nucleoside reverse transcriptase inhibitors (NRTIs), non-nucleoside reverse transcriptase inhibitors (NNRTIs), protease inhibitors, fusion inhibitors, post attachment inhibitors, integrase inhibitors, pharmacokinetic enhancers, and so on Chahal 2017. ARVDs are taken by prescribed options therefore they should be taken according to prescription. These ARVDs do not eliminate HIV but rather they prevent its rapid replication, mother to child transmission and, they decrease the amount of virus load in the blood stream. However, these ARVDs may cause adverse effects on the central and peripheral nervous systems if not taken carefully according to prescription (Gwenzi and Chaukura, 2018; L M Madikizela, Ncube and

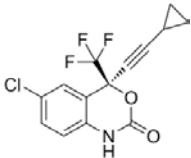
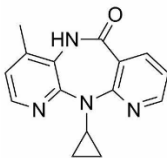
Chimuka, 2020). The rate and extent of these adverse effects varies with different classes of ARVDs and among each drug in their class. For example, efavirenz predominantly affects the central nervous system, leading to insomnia, irritability, and vivid dreams. Furthermore, nevirapine, a first line ARVD, has been associated with chronic liver toxicity in humans after 200 mg was administered once daily for 14 days, followed by 200 mg twice daily (Adeola and Forbes, 2022). Adverse human health effects caused by ARVD exposures include cough, dizziness, fever, diarrhea, nausea, headache, rash, hepatotoxicity, hypersensitivity, psychosis, insomnia, fatigue, vivid dreams, idiosyncratic myalgia, dyslipidemia, pancreatitis, lactic acidosis, hepatic steatosis, and heart disease (Ncube *et al.*, 2018). However, these adverse effects occur only after being exposed to high concentrations, drug abuse, overdose, and/or bioaccumulation of ARVDs over a long period of time and may not be relevant to exposure to low levels in the environment. Currently, wastewater treatment plants are not able to remove ARVDs from wastewater (Ngqwala and Muchesa, 2020). In regard, some studies have detected ARVDs in wastewater effluents, rivers, and dams (Ngqwala and Muchesa, 2020). The detection of ARVDs in surface water sources is an indication of the need for studies to find tools that can be used to reduce or even eliminate their presence in the aquatic systems. In the current study, the intention was to investigate the potential of photocatalytic degradation.

2.1.1 Properties of antiretroviral drugs

The behavior of pharmaceuticals in the environment is mainly dependent on their physical properties such the solubility, acid dissociation constant (pKa) and octanol-water coefficient (Kow). The physicochemical properties of efavirenz are listed in Table 1. The Kow value is used to measure the hydrophobicity or hydrophilicity of a substance (Nannou *et al.*, 2020). Higher Kow value indicates the likeliness that a compound will be found more on a solid matrix than in aqueous solution (Mtolo, Mahlambi and Madikizela, 2019). A pKa value represents the acidity of a compound. Compounds with low pKa value such as efavirenz are strongly

acidic (completely dissociates) and have higher water solubility (Settimo, Bellman and Knechtel, 2014).

Table 1: Name, structure, and physicochemical properties of efavirenz (Wood, Duvenage and Rohwer, 2015)

Name	structure	Mw (g mol ⁻¹)	Kow	pKa	Solubility (mg mL ⁻¹)
Efavirenz		315.675	4.15	-1.5	0.00855
Nevirapine		266.298	3.89	2.5	0.7046

2.1.2 Sources of ARVD contamination

Sources of contamination by ARVDs are summarized in Figure 1. As detailed in the published review article (**Paper 1**), the main source of ARVDs in the environment is through wastewater effluents. Various scholars have observed that developing countries are the most affected because they still use conventional wastewater treatment processes with limited abilities to remove pharmaceutical residues from effluents (Fekadu *et al.*, 2019; Lawrence Mzukisi Madikizela, Ncube and Chimuka, 2020). The situation is made worse because of the lack of disposal directives to guide monitoring programs resulting in an uncontrolled release of improperly treated wastewater with no repercussions or reparations for those responsible. The presence of ARVDs in wastewater can be traced to excreta from people taking ARVD medication (Wood, Duvenage and Rohwer, 2015; Patel *et al.*, 2019). Improper domestic and sewage waste disposal, drug manufacture, and hospital waste disposal are also important sources of ARVD contamination (Wood, Duvenage and Rohwer, 2015; Schoeman, Dlamini

and Okonkwo, 2017). Other sources of ARVD contamination include leachates from landfill, effluents from hospitals, inadequate disposal of expired drugs, and waste dumped by research institutions and pharmaceutical companies. Disposal of out-of-date or unwanted medicines, which may occur via the sink/toilet or municipal landfill sites, means they may also eventually leach into groundwater. Prescription practices leading to some unfinished prescriptions contribute to the illicit disposal of unused drugs, thus compounding environmental pollution concerns regarding pharmaceutical products (Frédéric and Yves, 2014). Aside from ingestion of pharmaceuticals via prescription (or self-medication, which should be discouraged), human exposure to pharmaceuticals also occurs via the food chain, such as drinking contaminated water and eating food sources like crops, vegetables, fish, and dairy products containing metabolized and untransformed ARVD compounds (Ebele, Abou-Elwafa Abdallah and Harrad, 2017).

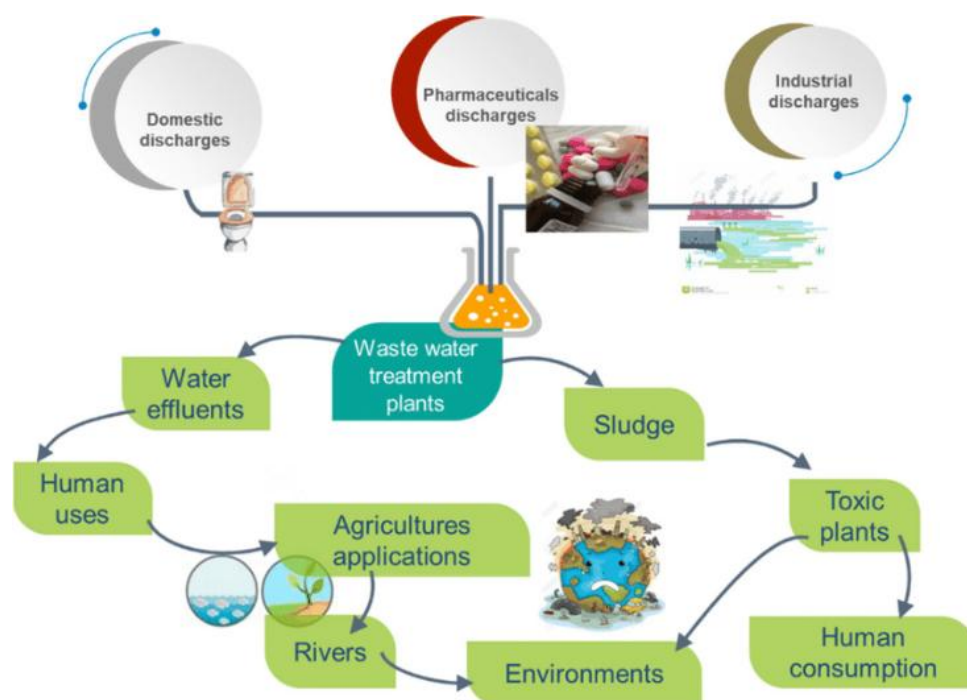


Figure 1: Sources of ARVDs into the water bodies (Mansouri *et al.*, 2021)

2.1.3 Ecotoxicological impact of antiretroviral drugs

The presence of ARVDs in drinking water sources may cause adverse effects on humans and aquatic organisms. The rate and extent of neuropsychiatric adverse effects varies with different classes of ARVDs and among each drug in their class (Abers, Shandera and Kass, 2014). Neurotoxicity induced by NRTI occurs due to the inhibition of mitochondrial DNA polymerase. This mechanism of action is also the reason for the mitochondrial myopathy and lactic acidosis that occurs with the use of zidovudine (Anderson and Rower, 2010). Efavirenz, which is an NNRTI, is predominantly associated with antiretroviral-related central nervous system toxicity, leading to insomnia, irritability, and vivid dreams (Abers, Shandera and Kass, 2014). However, efavirenz has been reported to have a relatively lower risk (8 - 25%) of causing acute and chronic dermatological problems (Tchetnya *et al.*, 2018). Nevirapine, a first-line ARVD that is commonly detected in water sources has been associated with chronic liver toxicity in humans (Gozalo *et al.*, 2011). Adverse human health effects caused by ARVD exposures include cough, dizziness, fever, diarrhea, nausea, headache, rash, hepatotoxicity, hypersensitivity, psychosis, insomnia, fatigue, vivid dreams, idiosyncratic myalgia, dyslipidemia, pancreatitis, lactic acidosis, hepatic steatosis, and heart disease (Ncube *et al.*, 2018).

2.2 Various methods for the removal of pharmaceuticals in wastewater

The removal of pharmaceuticals depends on different water treatment processes that result in different efficiencies. Wastewater treatment plants are not designed to completely remove pharmaceuticals (Patel *et al.*, 2019). Currently, many large-scale water treatment methods are available, such as electrochemical degradation (Li, Wang and Yu, 2021), photodegradation (An *et al.*, 2011; Jallouli *et al.*, 2018; Bhembe *et al.*, 2020), and advanced oxidation process (Huang *et al.*, 2015), precipitation, membrane filtration technology, and biodegradation. These modern

procedures have shown positive results throughout time, but they have significant limitations, such as lower efficacy, a high energy need, and a complicated operating process. In this study, photocatalytic degradation was explored. A review gives a brief overview of photocatalytic degradation and its integration with MIPs for remediation of pharmaceutical residues in aqueous environments is presented as **Paper 1** (Section 3.1) already published in *Journal of Hazardous Materials Advances*.

REFERENCES

Abafe, O.A. *et al.* (2018) ‘LC-MS/MS determination of antiretroviral drugs in influents and effluents from wastewater treatment plants in KwaZulu-Natal, South Africa’, *Chemosphere*, 200, pp. 660–670. Available at: <https://doi.org/10.1016/j.chemosphere.2018.02.105>.

Abers, M.S., Shandera, W.X. and Kass, J.S. (2014) ‘Neurological and psychiatric adverse effects of antiretroviral drugs’, *CNS Drugs*, 28(2), pp. 131–145. Available at: <https://doi.org/10.1007/s40263-013-0132-4>.

Adeola, A.O. and Forbes, P.B.C. (2022) ‘Antiretroviral Drugs in African Surface Waters: Prevalence, Analysis, and Potential Remediation’, *Environmental Toxicology and Chemistry*, 41(2), pp. 247–262. Available at: <https://doi.org/10.1002/etc.5127>.

Adeola, A.O., de Lange, J. and Forbes, P.B.C. (2021) ‘Adsorption of antiretroviral drugs, efavirenz and nevirapine from aqueous solution by graphene wool: Kinetic, equilibrium, thermodynamic and computational studies’, *Applied Surface Science Advances*, p. 100157. Available at: <https://doi.org/10.1016/j.apsadv.2021.100157>.

An, T. *et al.* (2011) ‘Photocatalytic degradation kinetics and mechanism of antiviral drug-lamivudine in TiO₂ dispersion’, *Journal of Hazardous Materials*, 197, pp. 229–236. Available at: <https://doi.org/10.1016/j.jhazmat.2011.09.077>.

Anderson, P.L. and Rower, J.E. (2010) ‘Zidovudine and Lamivudine for HIV Infection’,

Clinical Medicine Reviews in Therapeutics, 2, pp. 115–127. Available at: <https://doi.org/10.4137/cmrt.s4557>.

Bhembe, Y.A. *et al.* (2020) ‘Photocatalytic degradation of nevirapine with a heterostructure of few-layer black phosphorus coupled with niobium (V) oxide nanoflowers (FL-BP@Nb₂O₅)’, *Chemosphere*, 261, p. 128159. Available at: <https://doi.org/10.1016/j.chemosphere.2020.128159>.

Ebele, A.J., Abou-Elwafa Abdallah, M. and Harrad, S. (2017) ‘Pharmaceuticals and personal care products (PPCPs) in the freshwater aquatic environment’, *Emerging Contaminants*, 3(1), pp. 1–16. Available at: <https://doi.org/10.1016/j.emcon.2016.12.004>.

Fekadu, S. *et al.* (2019) ‘Pharmaceuticals in freshwater aquatic environments: A comparison of the African and European challenge’, *Science of the Total Environment*, 654, pp. 324–337. Available at: <https://doi.org/10.1016/j.scitotenv.2018.11.072>.

Fiorenza, R. *et al.* (2019) ‘Selective photodegradation of 2,4-D pesticide from water by molecularly imprinted TiO₂’, *Journal of Photochemistry and Photobiology A: Chemistry*, 380(April), p. 111872. Available at: <https://doi.org/10.1016/j.jphotochem.2019.111872>.

Frédéric, O. and Yves, P. (2014) ‘Pharmaceuticals in hospital wastewater: Their ecotoxicity and contribution to the environmental hazard of the effluent’, *Chemosphere*, 115(1), pp. 31–39. Available at: <https://doi.org/10.1016/j.chemosphere.2014.01.016>.

Gozalo, C. *et al.* (2011) ‘Pharmacogenetics of toxicity, plasma trough concentration and treatment outcome with nevirapine-containing regimen in anti-retroviral-naïve HIV-infected adults: An exploratory study of the TRIANON ANRS 081 trial’, *Basic and Clinical Pharmacology and Toxicology*, 109(6), pp. 513–520. Available at: <https://doi.org/10.1111/j.1742-7843.2011.00780.x>.

Gwenzi, W. and Chaukura, N. (2018) ‘Organic contaminants in African aquatic systems: current knowledge, health risks and future research directions’, *Science of the Total*

Environment, 619–620, pp. 1493–1514. Available at:
<https://doi.org/10.1016/j.scitotenv.2017.11.121>.

Huang, D.L. *et al.* (2015) ‘Application of molecularly imprinted polymers in wastewater treatment: a review’, *Environmental Science and Pollution Research*, 22(2), pp. 963–977. Available at: <https://doi.org/10.1007/s11356-014-3599-8>.

Jallouli, N. *et al.* (2018) ‘Heterogeneous photocatalytic degradation of ibuprofen in ultrapure water, municipal and pharmaceutical industry wastewaters using a TiO₂/UV-LED system’, *Chemical Engineering Journal*, 334(September 2017), pp. 976–984. Available at: <https://doi.org/10.1016/j.cej.2017.10.045>.

Kaya, S.I., Cetinkaya, A. and Ozkan, S.A. (2023) ‘Molecularly imprinted polymers as highly selective sorbents in sample preparation techniques and their applications in environmental water analysis’, *Trends in Environmental Analytical Chemistry*, 37(September 2022), p. e00193. Available at: <https://doi.org/10.1016/j.teac.2022.e00193>.

Li, J., Wang, Y. and Yu, X. (2021) ‘Magnetic molecularly imprinted polymers: synthesis and applications in the selective extraction of antibiotics’, *Frontiers in Chemistry*, 9, pp. 1–17. Available at: <https://doi.org/10.3389/fchem.2021.706311>.

Madikizela, Lawrence Mzukisi, Ncube, S. and Chimuka, L. (2020) ‘Analysis, occurrence and removal of pharmaceuticals in African water resources: A current status’, *Journal of Environmental Management*, 253(August 2019), p. 109741. Available at: <https://doi.org/10.1016/j.jenvman.2019.109741>.

Madikizela, L M, Ncube, S. and Chimuka, L. (2020) ‘Analysis, occurrence and removal of pharmaceuticals in African water resources: A current status’, *Journal of Environmental Management*, 253, p. 109741. Available at: <https://doi.org/10.1016/j.jenvman.2019.109741>.

Mansouri, F. *et al.* (2021) ‘Removal of pharmaceuticals from water by adsorption and advanced oxidation processes: State of the art and trends’, *Applied Sciences (Switzerland)*,

- 11(14). Available at: <https://doi.org/10.3390/app11146659>.
- Moslah, B. *et al.* (2018) ‘Pharmaceuticals and illicit drugs in wastewater samples in north-eastern Tunisia’, *Environmental Science and Pollution Research*, 25, pp. 18226–18241. Available at: <https://doi.org/10.1007/s11356-017-8902-z>.
- Mtolo, S.P., Mahlambi, P.N. and Madikizela, L.M. (2019) ‘Synthesis and application of a molecularly imprinted polymer in selective solid-phase extraction of efavirenz from water’, *Water Science & Technology*, 79, pp. 356–365. Available at: <https://doi.org/10.2166/wst.2019.054>.
- Nannou, C. *et al.* (2019) ‘Analytical strategies for the determination of antiviral drugs in the aquatic environment’, *Trends in Environmental Analytical Chemistry*, 24, p. e00071. Available at: <https://doi.org/10.1016/j.teac.2019.e00071>.
- Nannou, C. *et al.* (2020) ‘Antiviral drugs in aquatic environment and wastewater treatment plants: A review on occurrence, fate, removal and ecotoxicity’, *Science of the Total Environment*, 699, p. 134322. Available at: <https://doi.org/10.1016/j.scitotenv.2019.134322>.
- Ncube, S. *et al.* (2018) ‘Environmental fate and ecotoxicological effects of antiretrovirals: A current global status and future perspectives’, *Water Research*, 145, pp. 231–247. Available at: <https://doi.org/10.1016/j.watres.2018.08.017>.
- Ngqwala, N.P. and Muchesa, P. (2020) ‘Occurrence of pharmaceuticals in aquatic environments: A review and potential impacts in South Africa’, *South African Journal of Science*, 116, pp. 1–7. Available at: <https://doi.org/10.17159/sajs.2020/5730>.
- Patel, M. *et al.* (2019) ‘Pharmaceuticals of emerging concern in aquatic systems: Chemistry, occurrence, effects, and removal methods’, *Chemical Reviews*, 119(6), pp. 3510–3673. Available at: <https://doi.org/10.1021/acs.chemrev.8b00299>.
- Schoeman, C., Dlamini, M. and Okonkwo, O.J. (2017) ‘The impact of a Wastewater Treatment Works in Southern Gauteng, South Africa on efavirenz and nevirapine discharges into the

aquatic environment’, *Emerging Contaminants*, 3(2), pp. 95–106. Available at: <https://doi.org/10.1016/j.emcon.2017.09.001>.

Scuderi, V. *et al.* (2016) ‘Photocatalytic and antibacterial properties of titanium dioxide flat film’, *Materials Science in Semiconductor Processing*, 42, pp. 32–35. Available at: <https://doi.org/10.1016/j.mssp.2015.09.005>.

Settimo, L., Bellman, K. and Knegt, R.M.A. (2014) ‘Comparison of the accuracy of experimental and predicted pKa values of basic and acidic compounds’, *Pharmaceutical Research*, 31(4), pp. 1082–1095. Available at: <https://doi.org/10.1007/s11095-013-1232-z>.

Tchetnya, X. *et al.* (2018) ‘Severe eye complications from toxic epidermal necrolysis following initiation of Nevirapine based HAART regimen in a child with HIV infection: A case from Cameroon’, *BMC Pediatrics*, 18(1), pp. 1–6. Available at: <https://doi.org/10.1186/s12887-018-1088-9>.

Wood, T.P., Duvenage, C.S.J. and Rohwer, E. (2015) ‘The occurrence of anti-retroviral compounds used for HIV treatment in South African surface water’, *Environmental Pollution*, 199, pp. 235–243. Available at: <https://doi.org/10.1016/j.envpol.2015.01.030>.

Zunngu, S.S. *et al.* (2017) ‘Synthesis and application of a molecularly imprinted polymer in the solid-phase extraction of ketoprofen from wastewater’, *Comptes Rendus Chimie*, 20(5), pp. 585–591. Available at: <https://doi.org/10.1016/j.crci.2016.09.006>.

3 MANUSCRIPTS AND PUBLISHED PAPERS

The following sub sections present the two published articles and a manuscript that is under review in the Chemistry Africa journal. Each paper is presented with its own introduction, methodology, results and discussion, conclusions and references. Referencing style is based on the journal in which the paper was submitted. These manuscripts form part of the dissertation and should be examined.

Section 5.1 presents a paper published in Journal of Hazardous Materials Advances.

Section 5.2 presents a paper published in Journal of Water Process Engineering

Section 5.3 presents a revised manuscript submitted in the Chemistry Africa journal.

3.1 PAPER 1

Paper 1 presents the published version of a review article published in the Journal of Hazardous Materials Advances with Impact Factor of 5.5. The title of the review is; “**Applications of molecularly imprinted titania-based photocatalysis for degradation of pharmaceutical pollutants in the aqueous environment**”.

<https://doi.org/10.1016/j.hazadv.2024.100513>

Author contributions

Asenathi Sibali - Writing the original draft, conceptualization.

Thabang Hendrica Mokhothu: Reviewing & editing, Supervision, Conceptualization.

Samson Masulubanye Mohomane: Reviewing & editing, Conceptualization.

Vusumzi Emmanuel Pakade: Reviewing & editing, Conceptualization.

Ramakwala Christinah Chokwe: Reviewing & editing, Conceptualization.

Somandla Ncube: Reviewing & editing, Supervision, Conceptualization.

Applications of molecularly imprinted titania-based photocatalysis for degradation of pharmaceutical pollutants in the aqueous environment

Asenathi Sibali^a, Thabang Mokhothu^a, Samson Mohomane^b, Vusumzi Emmanuel Pakade^c, Ramakwala Christinah Chokwe^c, Somandla Ncube^{a*}

^aDepartment of Chemistry, Durban University of Technology, P O Box 1334, Durban 4000, South Africa

^bDepartment of Chemistry, KwaDlangezwa Campus, University of Zululand, Empangeni 3886, South Africa

^cDepartment of Chemistry, University of South Africa, Private Bag X6, Florida, 1710, South Africa

Corresponding author: SomandlaN@dut.ac.za (S. Ncube), +27738618567

Abstract

Pharmaceutical residues and their ecotoxicological impact on aquatic organisms are well documented which has forced researchers to shift focus towards finding sustainable pollution control technologies that can effectively control their levels in the environment. Photocatalytic degradation has offered a viable alternative with the ability to eliminate pharmaceutical residues through degradation and eventual mineralization to less-toxic products. Despite its documented successes, photocatalysis still has its challenges that relate to the presence of scavengers of photogenerated radicals and decomposed matrices accumulating on the surface of the photocatalyst. This has led to the incorporation of molecularly imprinted polymers on the surface of the photocatalyst to allow only selected targets to reach the photocatalyst. This review provides a concise yet comprehensive look at the integration of photocatalysis with molecular imprinting technology focussing on titania-based photocatalysts combined with

molecularly imprinted polymers for selective degradation of pharmaceutical pollutants in the aqueous environment. The principles, applications, challenges and future directions of molecularly imprinted photocatalytic degradation as a technology for the remediation of pharmaceuticals in aqueous environments are highlighted.

Keywords

MIPs, TiO₂, photocatalytic degradation, pharmaceuticals, pollution

Abbreviations

ARG - antibiotic resistant genes

g-C₃N₄ - graphitic carbon nitride

MIPs - molecularly imprinted polymers

MOFs - Metal-Organic Frameworks

PEDOT - poly-3,4-ethylenedioxythiophene

POPD - poly-o-phenylenediamine

1 Introduction

Photocatalytic degradation represents a promising approach for mitigating environmental pollution by harnessing the power of light and semiconductor catalysts to degrade organic contaminants. As research progresses and technology matures, photocatalysis is expected to play a pivotal role in achieving sustainable development goals related to water and air quality management worldwide. However, there still exists some challenges that have hindered progress towards total acceptance of doped-TiO₂ as an ultimate remedial tool for pollutants in the aqueous environment, and this has opened some avenues for improvement including integration with molecular imprinting technology. Various photocatalysts in combination with molecularly imprinted polymers (MIPs) and their applications in eradicating organic pollutants in general have been presented in literature [1–12]. Some reviews have detailed synthesis techniques for MIPs modified with TiO₂ and their application in pollution remediation [13,14]. Reviews that touch on different nanostructure-based photocatalysts for degradation of pharmaceuticals [15,16], antibiotics [17–19], antivirals [20], antipsychotics [21], nonsteroidal anti-inflammatory drugs and analgesics [22], and some that target specific pharmaceuticals such as sulfamethoxazole [23] have been presented in literature. A recent review also presented studies that have reported remediation of antibiotics using various hybrid MIPs [24]. The application of photocatalytic degradation and molecular imprinting in environmental pollution research has gained much interest and their integration towards the production of hybrid schemes targeting pharmaceutical pollution is an area that deserves a focussed review. The current review seeks to provide a concise yet comprehensive look at the principles, applications, challenges, and future directions of molecularly imprinted TiO₂-based photocatalytic degradation of pharmaceutical residues in the environment. It differs from all other reviews in that it is a focussed review that details the integration of titania-based photocatalysts with molecular imprinting technology for the purposes of pharmaceutical

remediation in aqueous environments. Other molecularly imprinted photocatalysts are also discussed to better understand the potential value that molecular imprinting might bring to pharmaceutical pollution control based on semiconductor photocatalysts. Interest in the applications of molecularly imprinted TiO₂ as a technology for the remediation of pharmaceuticals in aqueous environments is a recent niche area with 83% of the referenced studies done in the last 5 years (2019 - 2024). Only three studies were done more than 10 years ago. The three papers were all published in 2012 for the degradation of oxytetracycline [25], ciprofloxacin [26] and tetracycline [27].

2 Overview of pharmaceutical pollution in the aqueous environment

Pharmaceuticals are critical components of modern healthcare systems, contributing significantly to public health improvements and quality of life. Their production is regulated by health authorities in each country to ensure they meet stringent standards for safety, quality, and efficacy. However, their fate after performing their therapeutic effect in the body has not been prioritized with most of the residues making their way into the aqueous environment, thus creating a challenge to environmental sustainability and water quality. Various scholars have observed that developing countries are the most affected because they still use conventional wastewater treatment processes with limited abilities to remove pharmaceutical residues from effluents [28,29]. The situation is made worse because of the lack of disposal directives to guide monitoring programs resulting in an uncontrolled release of improperly treated wastewater with no repercussions or reparations for those responsible.

The presence of pharmaceutical residues in the aqueous environment poses a significant concern due to their potential ecotoxicological and health impacts on the organisms that depend on water if the water gets polluted. Pharmaceutical residues originate from the excretion of pharmaceuticals by humans and animals, as well as improper disposal of unused medications either by consumers or pharmaceutical manufacturing companies. A plethora of studies have

attributed the presence of pharmaceutical residues in the aqueous environments to high pharmaceutical consumption trends, the inability of conventional wastewater treatment processes to fully degrade the pharmaceuticals, and the lack of pollution directives in some countries [28,29]. Most pharmaceuticals enter aqueous environments primarily through wastewater effluents from hospitals, households, and pharmaceutical industries while relatively low amounts enter via improper disposal of unused or expired pharmaceuticals [30].

A wide range of pharmaceuticals exist but the most common ones can be classified under antibiotics, painkillers, anti-inflammatory drugs, antivirals, antiretrovirals, hormones, and antidepressants. Antibiotics and antiretrovirals are probably the worst pharmaceuticals to enter the aquatic environment. Chronic exposure to low concentrations of antibiotics can contribute to antibiotic resistance in bacteria [31–33] while antiretrovirals have the potential to promote drug resistance in the human body if not taken according to prescription [34]. The other classes also have endocrine-disrupting effects with the potential to cause behavioural changes in aquatic organisms. Detection and monitoring of these residues have been crucial in pollution management. The provision of monitoring data has led to a better understanding of the potential risks of pharmaceuticals to ecosystems and human health and the drafting of policies that address pharmaceutical residues in water bodies. Efforts typically focus on monitoring of pharmaceuticals in aqueous environments, health risk assessment, and setting limits for permissible concentrations in effluents. However, it is important to note that regulatory frameworks vary globally and most developing countries have not yet defined frameworks for pharmaceuticals in wastewater effluents. Another challenge is that the availability of pharmaceutical pollution directives does not guarantee compliance with those directives due to a lack of stringent measures against those that defy or ignore the guideline limits in effluents. With data showing evidence of the presence of elevated levels of pharmaceutical residues in the aqueous environment, researchers have since diverted to remediation. This is because

pharmaceutical consumption continues to rise globally with new medicines being introduced regularly. In addition, attempts at keeping effluents within guideline limits have failed due to a lack of measures that enforce compliance. Remedial action that eliminates pharmaceuticals by mineralization has provided hope for pollution management. Photocatalytic degradation using radicals generated through the illumination of semiconductor materials has gained traction in pollution remediation. Its intergradation with molecular imprinting technology has offered a viable direction towards more effective management of pharmaceutical contaminants in the environment.

3 Principles of photocatalytic degradation

Photocatalytic degradation is an advanced oxidation process that utilizes light and a semiconductor catalyst to degrade organic pollutants into harmless by-products. It differs from photolysis in that UV photolysis of H₂O molecules is a result of light at 309 nm with energy of about 4 eV resulting in dissociation of H₂O molecules into $\cdot\text{OH}$ species and H₂O₂. On the other hand, photocatalysis is a process that harnesses the power of light to accelerate chemical reactions on the surface of semiconductor materials used as catalysts [7,11]. When a semiconductor absorbs light, electrons are excited from the valence band to the conduction band leaving behind positively charged holes in the valence band [18]. These electron-hole pairs can initiate oxidation or reduction reactions with surrounding molecules. Electrons in the conduction band are free to move within the semiconductor material and can participate in reduction reactions by donating their energy to react with molecules on the surface or dissolved in the surrounding solution. The holes in the valence band are positively charged and decompose pollutants through oxidation. In the presence of water and O₂, the electrons in the conduction band reduce O₂ into superoxide radicals ($\cdot\text{O}_2^-$), while the holes can attract electrons from water molecules and hydroxyl ions (OH⁻) forming hydroxyl radicals ($\cdot\text{OH}$) with strong oxidant properties [18]. The $\cdot\text{OH}$ and $\cdot\text{O}_2^-$ radicals are highly reactive and initiate the

decomposition of organic molecules in solution breaking down complex molecules into simpler, less-toxic substances. The $\cdot\text{OH}$ radical achieves this by either removing an electron or H atom, or by adding itself to unsaturated bonds. The process is depicted in Fig. 1.

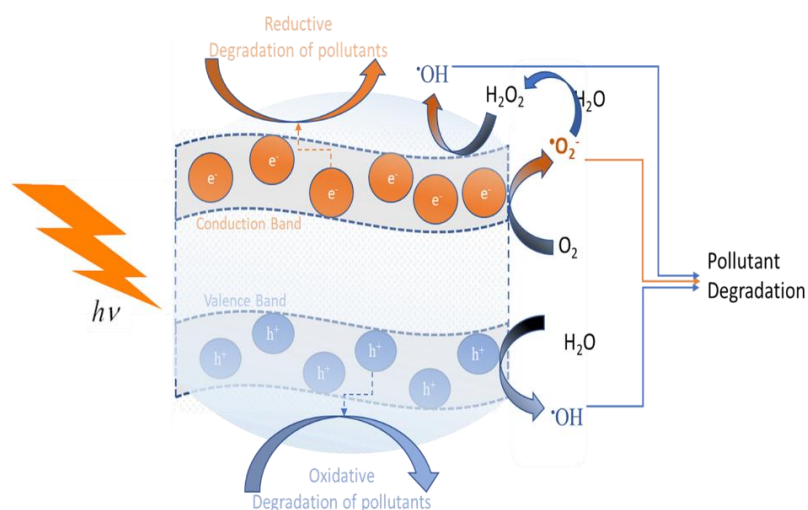


Fig. 1 Photocatalytic degradation schematic diagram

The most common semiconductor photocatalyst that has been utilized extensively in pollution control is TiO_2 . Its preference as a photocatalyst stems from the fact that it is low-cost, readily available and it is more stable in an aqueous solution [35]. Furthermore, TiO_2 is non-corrosive, highly stable and the degradation products are largely non-toxic compared to other semiconductors with better photocatalytic activity such as ZnO [36]. Other important photodegraders include graphitic carbon nitride ($g\text{-C}_3\text{N}_4$), Metal-Organic Frameworks (MOFs) as well as some organic semiconductors such as poly-*o*-phenylenediamine (POPD). These photocatalytic semiconductors have been applied in the photodegradation of pharmaceuticals in aqueous environments and some reviews on them are available in the literature [4,37]. However, the focus of the current review is TiO_2 and its modification with MIPs for application in the remediation of pharmaceutical residues in aqueous environments.

4 Integration of molecularly imprinted polymers with TiO₂ photodegradation catalysts

3.2 Principle of titania photodegradation

The wavelength range in which TiO₂ shows light response has been reported between 200 to 400 nm due to electron transition from the valence band (O_{2p}) to the conduction band (Ti_{3d}). The valence band position for TiO₂ is at 2.77 eV while the conduction band is at -0.33 eV giving a band gap of 3.1 eV [38]. Electron transitions therefore only occurs when TiO₂ is illuminated with photons having $h\nu > 3.1$ eV. The band gap of the different types of TiO₂ is larger than 3 eV (~3.0 eV for rutile to ~3.2 eV for anatase), thus making pure TiO₂ primarily active for UV light. Anatase TiO₂ with 3.2 eV, corresponds to the absorption of light at 387 nm and below which falls at the lowest end of visible light [3]. The mechanism of photodegradation by TiO₂ doped with either metals or non-metals has been detailed in different review articles [7,11,18]. The reviews emphasized that dopants act by minimizing the bandgap of TiO₂ allowing it to use higher wavelengths in the visible light region to transfer its photoelectrons to the conduction band. The doped-TiO₂ therefore becomes active in the visible light region.

3.3 Applications of titania-based photocatalyst in degradation of pharmaceutical residues

Applications of TiO₂ as a single isolated photocatalyst in the degradation of pharmaceutical residues have been less represented in literature with relatively lower degradation efficiencies compared to advanced or doped TiO₂ photocatalysts. For example, Shaykhi and Zinatizadeh [39] reported a photocatalytic-perozonation (O₃/H₂O₂/UV/TiO₂) reactor for degradation of amoxicillin in a simulated wastewater treatment plant achieving 58% removal efficiencies in 250 min. The degradation of carbamazepine has been reported to attain complete mineralization after 6 h of irradiation [40]. It is however, important to mention that most of the

reported efficiencies are comparable with advanced degradation schemes. A study reported TiO₂ irradiated with UV rays at 365 nm resulting in 90% removal of amoxicillin and 98% for metformin over 150 min in a laboratory-scale synthetic hospital wastewater [41]. Recently, some researchers arguably reported commercial Degussa P25 TiO₂ with the ability to remove three pharmaceuticals (propranolol-99.3%, mebeverine-98.5%, and carbamazepine-83.2%) after irradiation with light of 253 nm for 30 min [42]. A large portion of TiO₂-based photocatalysis has been reported for the remediation of antiviral drugs. For example, a TiO₂/H₂O₂ system irradiated at 300 nm yielded 89.23% degradation rates of nevirapine in wastewater within 60 min [43] while 87.1% was reported for lamivudine [44].

Doped TiO₂ has been explored successfully as a replacement for plain TiO₂ and its application in the removal of pharmaceuticals has been a success story with various studies reporting better catalytic performance and degradation efficiency under visible light. The purpose of doping is to narrow the band gap or provide acceptors of the photoelectrons from the conduction band. Decreasing the band gap results in more electrons being excited to the conduction band. The end result is an improved photocatalytic activity. When doped, a hybridized valence band occupying a higher energy level is formed which results in the reduction of the band gap. For example, for a graphene/TiO₂, a new hybridized valence band consisting of C_{2p} (from graphene) and O_{2p} (from TiO₂) is formed [45]. The resultant graphene/TiO₂ can be attributed to graphene's enhanced quantum efficiency due to the plasmon resonance effect on its surface which relates to its strong light absorbing ability. Another example is that of a TiO₂/Ge photocatalyst with a band gap of 2.83 eV compared to 3.21 eV for TiO₂ [46]. TiO₂ doped with other semiconductors has been explored successfully in pharmaceutical pollution remediation and a plethora of studies are presented in literature reporting impressive photocatalytic activity towards target pharmaceuticals [18,47,48].

3.4 Challenges of photocatalytic degradation of pharmaceuticals in aqueous environments

Despite advancements in photocatalytic degradation approaches as shown by the applications of doped semiconductors for removal of pharmaceutical residues in aqueous environments, total pharmaceutical elimination still presents several challenges. Notably is the issue of matrix effects. Water samples contain numerous organic and inorganic compounds [49,50], which can limit the ability of a photodegrader to effectively perform its photocatalytic activity on the intended pharmaceutical residue [38,51,52]. Another important challenge that complicates the task of comprehensive remediation of pharmaceuticals is their existence in aqueous environments at extremely low concentrations compared to matrices. Furthermore, aqueous surface sources contain multiple pollutants that require remediation simultaneously [53]. Most photodegraders are non-specific and their photogenerated radicals will react with anything organic that exist on their surfaces. In this regard, it is observed that researchers have recently introduced MIPs with the aim of selectively bringing the target pollutants to the surface of the photodegrader [1,8]. MIPs are valued for their tailor-made selectivity, which can be advantageous in applications requiring precise recognition and manipulation of specific molecules [54–56]. The interrelationship between the MIP and the nanoparticle is synergistic. The MIP offers specific binding sites that bring the target pollutant to the surface of the photodegrader nanoparticle, while embedding the MIP on the nanoparticle itself enhances its binding capability by offering a high surface area with more binding sites per unit area.

3.5 Principle of molecular imprinting technology

A MIP is created by polymerization of functional monomers with peripheral vinyl groups in the presence of a template molecule. In most cases, the template molecule is the target compound for which the MIP is intended to absorb from the aqueous solution. The functional monomer and the template molecule must have complementary functional groups that interact

through weak non-covalent intermolecular forces such as Van der Waals forces and H-bonding. Once the functional monomers have occupied strategic positions around the monomer, a cross linker with terminal vinyl groups is added to the reaction mixture. Polymerization is then initiated using a radical initiator such as azobisisobutyronitrile. The crosslinker helps create a link between the functional monomers allowing them to maintain their positions around the template molecules as the polymerization process progresses. Ethylene glycol dimethacrylate is commonly used as the crosslinker [57]. The final product is a covalent solid structure with the template molecules still trapped within its matrix. Since the interaction between the monomer functional groups and those of the template are non-covalent, the trapped template molecules can be washed out using an appropriate organic solvent leaving behind cavities or imprints that are complementary in shape, size and functionality to the template molecule [58,59]. These cavities have the ability to selectively isolate the target molecule or molecules with similar structures and functional groups from aqueous solution in the presence of potential interferences. These features have since permitted integration of molecular imprinting technology with photocatalysis as remediation tools for pharmaceuticals in the environment. Notably, the imprinted layer does not take part in photocatalysis but merely provides recognition sites that help bring the targeted pollutant to the photocatalyst. In this regard, the presence of the MIP on the surface of the photocatalyst is not expected to affect the degradation pathways but offers channels that allow specific targets to reach the photocatalyst. Various studies have reported applications of MIPs for isolation of pharmaceuticals from aqueous samples and some review articles are present in literature [60–62]. The current review assesses the integration of MIPs with photocatalysts including TiO_2 for remediation of pharmaceutical residues in the aqueous environment.

3.6 Applications of molecularly imprinted TiO₂ photodegradation catalysts

While the purpose of doping TiO₂ is to reduce the band gap, in MIP-TiO₂ systems the target is to create specific binding sites to bring specific targets closer to TiO₂. The concept of molecularly imprinted photocatalytic degradation has been clearly illustrated in a graphical abstract by Feng et al., (Fig. 2) that represented a MIP-TiO₂ for degradation of norfloxacin [63]. The schematic diagram shows TiO₂ nanoparticles embedded within a MIP particle with holes/cavities that channel towards the nanoparticles. The advantage is that the MIP isolates the target pollutant from a complex aqueous system. The isolated pollutant is brought closer to the TiO₂ and this minimizes potential interference from matrices in solution. With the process of photocatalysis dependent on the photogenerated radicals, molecular imprinting on the surface of photocatalysts has also been shown to greatly reduce the impact of radical scavengers on the photocatalytic activity by keeping them away from the surface of the photocatalyst [64]. While photocatalysis offers a green alternative to chemical oxidation methods, the environmental impact of photocatalytic nanoparticles that can potentially leach into the environment is another drawback for using metal oxides as photocatalysts [65–67]. However, copolymerization during synthesis of the MIP ensures that these nanoparticles remain trapped within the polymer reducing their potential to leach into the environment. Recent studies have further incorporated magnetite nanoparticles for the purpose of trapping the MIP-TiO₂ nano-scheme and keeping it stationary and also remove it from aqueous solution using an external magnetic field [68–70]. This helps prevent the entire polymer from washing away with the water in cases where they need to be deployed in the environment. The concept of application of a magnetic MIP-TiO₂ scheme for degradation of pharmaceuticals in aqueous environment is summarized in Fig. 3. This simplified version represents a pharmaceutical compound being selectively trapped within the MIP-TiO₂ scheme and eventually getting mineralized to less toxic products.

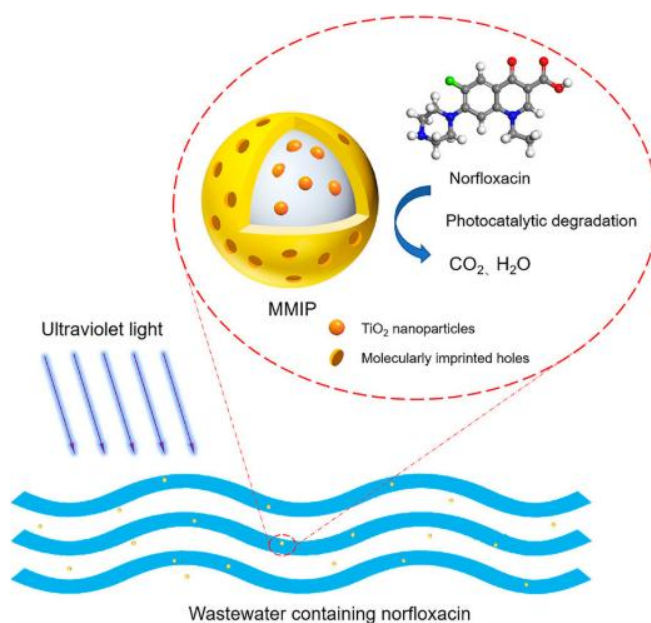


Fig. 2 Graphical representation of magnetic molecularly imprinted photocatalytic degradation of norfloxacin. Adapted with permission from Taylor & Francis [63].

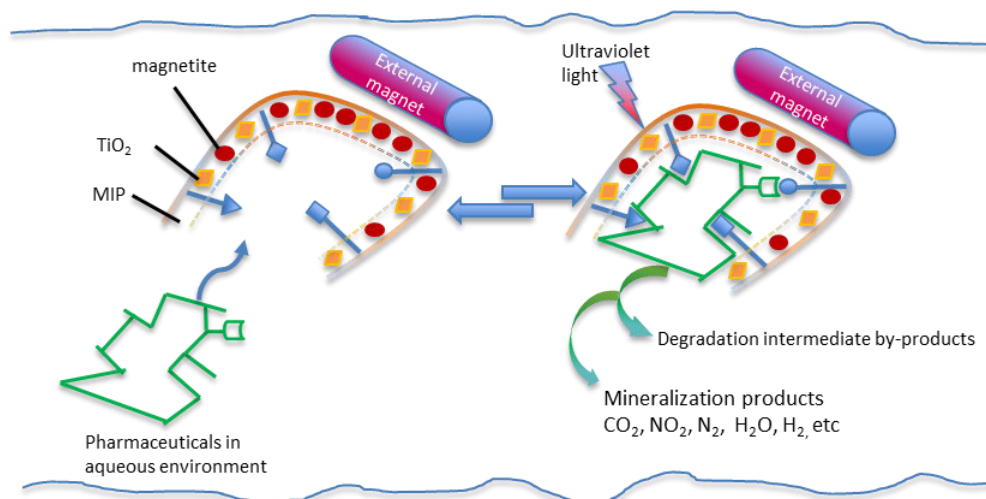


Fig. 3 Degradation schematic diagram for pharmaceutical pollutants based on a magnetized molecularly imprinted polymer embedded with titania

TiO₂ embedded on MIP cavities for photocatalytic degradation of pharmaceutical residues in the environment has been reported in literature as shown in Table 1. Diclofenac is well studied with the first application of MIP-TiO₂ yielding just over 48% degradation efficiencies in 2018 [71]. However, the preceding studies have observed better efficiencies such as 91.4% efficiency in 10 min [51]. Diclofenac has also been included in multiresidue remediation using MIP-TiO₂ as the photocatalyst with fairly high degradation rates observed (Table 1). For example, a study that reported degradation rates for seven pharmaceuticals, the rates for diclofenac ranked second with about 42% [72]. Diclofenac is one of the most commonly used over-the-counter anti-inflammatory medication for mild to moderate pain and is frequently detected in the aqueous environment [73].

Table 1 Molecularly imprinted-TiO₂ photocatalysts applied in pharmaceutical degradation

Target(s)	Photocatalyst	Template	Time (min)	Efficiency (%)	Reference
Chlortetracycline	Fe ₃ O ₄ /g-C ₃ N ₄ /TiO ₂ /MIP	Chlortetracycline	120	91.87	[38]
Ciprofloxacin	MIP/C/TiO ₂	Ciprofloxacin	90	87	[74]
	MIP/POPD/TiO ₂ /fly-ash	Ciprofloxacin	60	70	[26]
Diclofenac	MIP/TiO ₂	Diclofenac	120	48.72	[71]
	MIP/TiO ₂	Diclofenac	10	91.4	[51]
Enrofloxacin	TiO ₂ @SiO ₂ @Fe ₃ O ₄ /MIP	Enrofloxacin	90	-	[75]
Norfloxacin	CoFe ₂ O ₄ @TiO ₂ @MMIP	Norfloxacin	150	84.2	[63]
Oxytetracycline	MIP/POPD/TiO ₂ /fly-ash	Oxytetracycline	60	76	[25]
Sulfadiazine	N-TiO ₂ /C/MIP	Sulfadiazine	140	99.25	[76]
Sulfamethoxazole	MIP-TiO ₂ @Fe ₂ O ₃ @g-C ₃ N ₄	Sulfamethoxazole		96.8	[77]
Sulfasalazine	MMIP@TiO ₂	Sulfasalazine	10	92	[78]
Tetracycline	MIP/TiO ₂	Tetracycline	180	-	[27]
Sulfadiazine	MIP/TiO ₂	Aniline (dummy)	80	99.9	[79]
Sulfamethoxazole			15	99.9	
Diclofenac	MIP/TiO ₂	Diclofenac	60	86.6	[80]

Ibuprofen		Ibuprofen		75	
Norfloxacin	CoFe ₂ O ₄ @TiO ₂ @MMIP	Norfloxacin		99.4	[81]
Ciprofloxacin				85.9	
Tetracycline	TiO ₂ @MIP	Tetracycline	50	95	[82]
Norfloxacin				80	
Sulfamethoxazole				59	
Thiamphenicol				45	
Chloramphenicol				39	
Diclofenac	MIP/TiO ₂	Diclofenac	60	42	[72]
Valsartan				46	
Tioconazole				25	
Ketoconazole				24	
Ibuprofen				19	
Atorvastatin				19	
Gentamicine				11	

Double heterojunction schemes have also been investigated in the photodegradation of pharmaceuticals using molecularly imprinted TiO₂-based photocatalysts. Examples include a novel molecularly imprinted TiO₂ doped with Fe₂O₃ and g-C₃N₄ [77]. The two doping materials were reported to reduce the rate of recombination of e⁻/h⁺ pairs. Fe₂O₃ provided a Z-heterojunction with TiO₂ while g-C₃N₄ provided a second charge transfer mechanism. Due to the MIP in the scheme, their double Z-scheme was able to selectively isolate sulfamethoxazole from synthetic wastewater in the presence of sulfadiazine, ibuprofen and bisphenol A as potential interferents. Sulfamethoxazole degradation efficiency was found to be 96.8% which was more than double the efficiency observed for the potential interferents.

Most of the degradation studies using molecularly imprinted TiO₂ photocatalysts have validated the need for molecular imprinting by comparing the photocatalytic activity of the target with that of potential competing pharmaceuticals. For example, to prove selectivity, Fang

and colleagues investigated the degradation performance of norfloxacin-imprinted $\text{CoFe}_2\text{O}_4@\text{TiO}_2\text{-MMIP}$ towards norfloxacin, ciprofloxacin, ibuprofen, carbamazepine and phenol then observed its specificity towards fluoroquinolones (norfloxacin-91.1% and ciprofloxacin-85.9%) compared to other classes of pharmaceuticals with degradation of ibuprofen at 34 %, carbamazepine at 3.4% and phenol at only 2.9% [81]. This was attributed to the imprinted cavities on the surface of TiO_2 which preferentially brought the fluoroquinolones closer to the surface of the TiO_2 while the other compounds remained in solution. Another study imprinted TiO_2 with tetracycline and tested it against five antibiotics; sulfamethoxazole, thiamphenicol, chloramphenicol, norfloxacin and tetracycline. The tetracycline-imprinted TiO_2 achieved 95% degradation for tetracycline, 80% for norfloxacin while sulfamethoxazole, thiamphenicol and chloramphenicol had 59, 45 and 39% degradation, respectively [82]. The preference towards tetracycline was attributed to the shape and size of imprinted cavities.

5 Photodegradation activities of other molecularly imprinted photocatalysts

5.1 Molecularly imprinted metal oxides

Some metal oxide nanoparticles with semiconductor properties have been utilized in combination with molecular imprinting for photocatalytic degradation of pharmaceuticals. ZnO is considered to have better semiconductor properties than TiO_2 and its molecularly imprinted version has been utilized in pharmaceutical pollution management. Cantarella et al. [83] has reported molecularly imprinted ZnO nanonuts with the ability to selectively degrade all the paracetamol within 3 h in the presence of four other water pollutants. Similarly, Du et al. [53] reported a molecularly imprinted ZnO composite doped with $\text{NH}_2\text{-UiO-66}$ MOF that removed 61.9% in 30 min. Wang et al. [84] reported a $\text{Fe}_3\text{O}_4/\text{ZnO}@\text{MIP}$ composite that achieved 90.72% degradation of amoxicillin over 140 min. Interaction between ZnO with the

dopants had synergistic effects which limited the e^-/h^+ recombination. Other molecularly imprinted metal oxides have also been investigated. A NiO-CuS/MIP nanocomposite for removal of letrozole in wastewater was found to exhibit over 90% degradation rates [85]. A MIP-CuFeO₂@MnO₂ nanocomposite was group-imprinted using aniline and pyrrole copolymers and acrylamide as a dummy template for targeting tetracycline [52]. The nanocomposite selectively degraded tetracycline achieving 92% efficiency. A surface BiOCl/Bi₃NbO₇ photocatalyst imprinted with ceftriaxone has also been reported with a 92% degradation of ceftriaxone after 100 min [86].

5.2 Molecularly imprinted graphene-based semiconductors

Molecularly imprinted graphene-based photocatalytic degradation has been utilized in pharmaceutical pollution control in the environment. The application of graphene-based nanomaterials in photocatalysis is due to the plasmonic resonance effect possessed by carbon nanoparticles. This integrated approach utilizes the advantages that both molecular imprinting and plasmon resonance can bring in photocatalytic degradation. A magnetic molecularly imprinted bismuth phosphate@graphene oxide (BiPO₄@GO-MMIP) was developed for selective degradation of ciprofloxacin [87]. Its photocatalytic activity was attributed to Bi(PO₄) and GO with the authors noting that Bi(PO₄) has more energy gap than GO resulting in the transfer of photoelectrons from LUMO of GO to HOMO of Bi(PO₄) via π to π^* transitions. About 75% of ciprofloxacin was degraded over 80 min. Lui et al. [76] have developed a molecularly imprinted C-doped TiO₂ nanomaterial for sulfadiazine and recorded a 99.25% degradation efficiency in 140 min. This was an indication that the selectivity of the molecularly imprinted surface coupled with the surface plasmon effect brought by the thin sheets of graphene greatly improved the photocatalytic activity of TiO₂. An Fe₃O₄/g-C₃N₄/TiO₂ heteroscheme imprinted with diclofenac achieved 68.34, 84.76 and 86.27% degradation rates

towards diclofenac in wastewater, river water, and tap water [38]. It was obvious that the complexity of the sample affects the performance of the photocatalyst with its performance in wastewater lower compared to river and tap water.

5.3 Molecularly imprinted organic semiconductors

The potential of organic semiconductors as replacements for TiO_2 and other metal oxide semiconductors has been investigated for pharmaceutical remediation with a list of studies reported in literature where MIPs were combined with organic material as the photocatalysts or as dopants for photocatalysts. The main advantage of organic semiconductors is that their energy level positions can be adjusted. In their study, Huang et al. [88] synthesized a magnetic molecularly imprinted photocatalyst based on poly-o-phenylenediamine doped with silver (Ag-POPD) as an organic semiconductor for selective degradation of ciprofloxacin achieving a 70.85% degradation rate in 90 min. Similarly, an imprinted Ag-POPD was used elsewhere for the same pharmaceutical with similar degradation rates (73.25%) in 90 min [89]. Huo et al. [26] has modified molecularly imprinted TiO_2 /fly ash cenospheres with POPD for degradation of ciprofloxacin in wastewater yielding 70% efficiency in 60 min. The same authors presented a similar approach but this time imprinting their cenospheres with oxytetracycline and La^{3+} for degradation of oxytetracycline yielding 76% in 60 min [25]. However, La^{3+} did not impact the catalytic activity of the cenospheres but merely enhanced the imprinting of oxytetracycline by acting as a bridge between the O atoms of oxytetracycline and the N atoms of the acrylamide monomers. A novel Cu^{2+} -imprinted POPD- CoFe_2O_4 heterojunction mesoporous photocatalyst has been reported with the ability to reduce Cu^{2+} and simultaneously degrade tetracycline [90]. CoFe_2O_4 acted as an acceptor of photo-induced holes from POPD. The CoFe_2O_4 holes were responsible for degradation of tetracycline while Cu^{2+} was reduced by photoelectrons from the conduction band of POPD.

Other semiconducting polymers have been reported in molecularly imprinted photocatalytic degradation of pharmaceuticals. For example, polyaniline integrated with a WS₂ semiconducting material where it acted by transferring charge carriers has been investigated in the photocatalytic degradation of nitrofurantoin with an efficiency of 92% in 75 min [91]. Polyaniline is an organic conducting polymer which tends to keep the e⁻/h⁺ pairs separated by transferring charge carriers from WS₂. Lu et al. [92] developed a magnetic imprinted nanoreactor based on poly-3,4-ethylenedioxythiophene (PEDOT) and CdS with double photocatalytic activity towards danofloxacin. CdS acted as the photocatalyst, magnetite enhanced transfer of conduction band photoelectrons while PEDOT extracted the photoinduced holes. Molecular imprinting enhanced selectivity towards the danofloxacin with photocatalyst achieving 84.8% degradation of danofloxacin. Its photocatalytic activity towards three other pharmaceuticals (gatifloxacin, ciprofloxacin and tetracycline) ranged between 37 and 50%.

5.4 Molecularly imprinted metal organic frameworks

MIPs imbedded on MOFs is another area that has been explored in the degradation of pharmaceutical pollutants in the environment. Yi et al. [17] recently reported a MIL100@MIP for sulfamethoxazole with the study observing a 63.6% increase in the degradation performance compared to non-imprinted scheme. Magnetic MIPs grafted on a MIL-100 MOF have been reported for elimination of ciprofloxacin from wastewater effluents [93], sulfamethoxazole in wastewater [94] and tetracycline in lake water [95]. The reported Fe₃O₄@MIL-100(Fe)@MIP nanocomposites were imprinted with ciprofloxacin, sulfamethoxazole and tetracycline, respectively. The imprinted frameworks displayed a strong preference towards the target pharmaceuticals in the presence of other pharmaceutical residues as potential competitors. In both cases, the presence of Fe₃O₄@MIP on the surface of MOF allowed specific targets only to channel into the MOF. The photocatalytic activity was further

enhanced by addition of H₂O₂ which helped to capture the photogenerated electrons to form more $\cdot\text{OH}$ radicals. For MOF-based schemes, photodegradation occurs by photo-Fenton processes. Lui et al. [96] has also reported a molecularly imprinted MOF anchored on porous carbon forms that selectively removed norfloxacin, ibuprofen, naproxen, sulfadimethoxine and caffeine. Another study created molecularly imprinted MOF channels utilizing the 3D structural configuration of β -cyclodextrin for selective degradation of sulfamethoxazole [97]. Over 91% degradation rates in complex matrices including polluted river water were achieved in 60 min.

5.5 Molecularly imprinted schemes based on novel semiconductors

Other hybrid schemes in which molecularly imprinted polymers were embedded on novel semiconductor materials have been reported in photocatalytic degradation of pharmaceutical pollutants. These include a ZnGa₂O₄/Cr³⁺ heterojunction photocatalyst for degradation of tetracycline [98]. This heterojunction scheme had afterglow photocatalysis abilities in which tetracycline could be degraded day-and-night. A molecularly imprinted magnetic γ -Fe₂O₃/H₂O₂/chitosan composite has been reported for the removal of norfloxacin in pharmaceutical wastewater through Fenton-like oxidative degradation [99,100]. Yan et al. [101] has reported an imprinted P25@IL nanoreactor in which a MIP was synthesized using an imidazole ionic liquid as a monomer and levofloxacin as the template. This novel MIP was embedded on the surface of a TiO₂ photocatalyst for the degradation of levofloxacin and tetracycline in aqueous media. The imprinted nanoreactor had a strong preference for levofloxacin compared to the non-imprinted nanoreactor with degradation rates of 50.69 and 25.58%, respectively. The authors attributed this to the specificity of the levofloxacin-imprinted reactor towards levofloxacin.

6 Challenges and considerations

Despite its promise, photocatalytic degradation still faces several challenges as a potential remedial tool for pharmaceutical pollution control. TiO_2 may be readily available as a commercial photocatalyst but it still needs to be modified or doped appropriately for it to effectively degrade the target pollutant. Commercial TiO_2 is marketed as P25, a combination of about 80% anatase and 20% rutile [3]. Modification of TiO_2 with selective imprinted polymer cavities may help bring the target closer to the photocatalyst's surface however, embedding a solid matrix on the surface may create challenges related to incident light accessibility. Effective photocatalytic degradation solely depends on light striking the semiconductor [75]. In this regard, one of the major questions focuses on whether light can fully transmit through the imprinting layer. Currently, there are limited studies that have reported on the light permeability of imprinted polymers and the potential impact it can have if the imprinted TiO_2 was to be upscaled. The most appropriate position of the TiO_2 nanoparticles within the MIP matrix that could result in better accessibility of the incident light has not yet been reported. More research is required in this regard to assess the potential of upscaling molecularly imprinted photocatalysts for application in the environment.

Another notable observation in the applications of molecularly imprinted TiO_2 -based photocatalysts and any other imprinted photocatalyst is the lack of pilot-scale studies and industrial applications to demonstrate their feasibility and economic viability in large-scale environmental remediation projects. MIPs are tailored for single specific targets and currently, most studies have reported molecularly imprinted photodegraders that target a single pharmaceutical (Table 1). This approach is not environmentally plausible because pharmaceuticals exist in the environment as mixtures, all of which are of ecotoxicological concern, indicating a need for multiresidue remedial tools. It should be noted that some studies have already initiated this approach [72,82]. However, the results are not yet convincing with

efficiencies ranging between 11 and 46% for 7 pharmaceuticals [72], and 39 - 95% for 5 pharmaceuticals [82]. Importantly, a single pharmaceutical was used as the imprinting template which might explain the low degradation efficiencies towards the targeted compounds (Table 1). Multitemplate imprinting might be a solution to this problem.

The type of matrix is also a contributing factor that has proven to limit the potential upscaling and commercialization of photocatalysts. Liu et al. [38] recently observed that their molecularly imprinted $\text{Fe}_3\text{O}_4/\text{g-C}_3\text{N}_4/\text{TiO}_2$ heteroscheme attained different degradation rates towards diclofenac in tap water (86.27%), polluted river water (84.76%), pulping wastewater (65.69%), and pharmaceutical wastewater (68.34%), despite the scheme being imprinted with diclofenac. Tang et al. [97] also observed a reduction in the degradation abilities of a MIP/ZnO/MOF towards sulfamethoxazole in polluted river water (91%) compared to tap water (97%). It is obvious that degradation is lower for samples with more complex matrices and there is a need for proper optimization strategies in consideration of matrices. Related to matrices is the issue of interferents, which reduce the photocatalytic activity by adsorbing on the photocatalyst surface and blocking the active sites, scavenging $\cdot\text{OH}$ and $\cdot\text{O}_2^-$ radicals, and competition for incident light. For example, Liu et al. [38] observed that photodegradation of chlorotetracycline using $\text{Fe}_3\text{O}_4/\text{g-C}_3\text{N}_4/\text{TiO}_2/\text{MIP}$ decreased significantly from 91.87% to 61.29% in the presence of humic acids. They mentioned that humic acid adsorbed on the surface and scavenged for photogenerated O_2 radicals. It also decomposed under continuous illumination and further accumulated on the surface of the photocatalyst. This observation creates a challenge because humic substances including fulvic acids and humic acids are always a part of wastewater treatment [49,50]. They possess other advantages such as the removal of toxic trace metals and other lipophilic constituents from wastewater. Various other important scavengers that inhibit the degradation activities of molecularly imprinted photocatalysts have been mentioned in the literature. One study observed that the degradation rates for diclofenac

decreased from 91.4% to 84.8, 61.7, and 29.5% in the presence of butanol, EDTA-2Na and p-benzoquinone, respectively [51]. Another study reported that isopropanol, triethanolamine, and p-benzoquinone led to a reduction in tetracycline rates from 92% to 62.5, 54.38 and 78.9%, respectively [52]. Alcohols such as isopropanol are scavengers of $\cdot\text{OH}$ radicals, p-benzoquinone targets $\cdot\text{O}_2^-$ radicals while triethanolamine scavenges the holes. Save for humic acids, the levels of these radical scavengers in municipal wastewater are not well defined. In this regard, the focus should shift towards those potential scavengers that are known to exist in relevant concentrations in the aqueous environment.

Other inhibitors to commercialization have been raised when discussing the potential of molecularly imprinted photocatalysts. The production of commercial MIPs has always been a challenge for researchers because they need to be synthesized for a specific target [102]. This has failed because priority pollutants cannot be the same for potential customers from different areas. Another challenge is that regeneration studies which focus on the stability of molecularly imprinted photocatalysts if deployed in the environment have not yet been fully explored. Impressive regeneration results have been presented for most of the molecularly imprinted TiO_2 photocatalysts in which the photocatalyst is reused based on lab-scale stagnant water, usually between 5 and 10 cycles. However, the challenge is that if the photocatalyst was to be applied in the environment it would have to be deployed and be continuously in contact with flowing water. Reusability studies should therefore consider photocatalyst deployment times.

There is also a challenge of the parent pharmaceutical achieving 100% degradation without being completely mineralized. An example was presented by Li et al. [103] in which amoxicillin, methyl orange and 3-chlorophenol all achieved 100% degradation but their mineralization was 78.1, 47.9 and 35.7%, respectively. Another study observed that while diclofenac achieved 89% degradation after 10 min, its mineralization was only 17% [51]. These

observations raise the issue of the toxicity of intermediate degradation products that do not achieve complete mineralization. It is however important to point out that molecularly imprinted photocatalysts give less products since the intermediates can remain in the cavities to permit mineralization [97], but the toxicity of the unmineralized products remains a concern. Different studies have observed different ecotoxicities of the intermediates depending on the target pharmaceutical. For example, Peng et al. [52] observed that the intermediate products of tetracycline were less toxic towards aquatic organisms compared to tetracycline. However, An et al. [104] noted that acyclovir's inhibition towards bacteria, algae, and daphnia ranged between 4.8 and 35.1%, but the ecotoxicities increased to 14.3 - 79.0% when the same organisms were exposed to the treated solution of acyclovir indicating the cumulative ecotoxicity due to intermediates. Even after complete degradation of acyclovir, the biotoxicities remained between 7.2 and 14.4%. The implication was that the unmineralized intermediates were toxic towards bacteria, algae, and daphnia. These conflicting observations are an indication of the challenge of intermediates and the need for further studies that can provide more informed ecotoxicity data.

7 Perspectives

Research continues to seek methodologies that can either substitute or enhance the applicability of photocatalysts for the remediation of pollutants in the environment. The potential of co-doping is one area that could potentially elevate the applicability of molecularly imprinted TiO₂ photocatalysts for the remediation of pharmaceuticals [18]. For example, a typical single Z-scheme has the disadvantage that migration of charge carriers to higher valence bands and lower conduction bands is coupled with a loss of catalytic redox potential. Utilizing multiple heterojunction schemes where TiO₂ is coupled with other semiconductors is one approach that could help increase the catalytic conduction band potential and improve the photocatalytic activity. A recent study has investigated a novel molecularly imprinted TiO₂@Fe₂O₃@g-C₃N₄

in which Fe_2O_3 and $\text{g-C}_3\text{N}_4$ were used as co-dopants on the surface of the MIP- TiO_2 [77]. The inclusion of $\text{g-C}_3\text{N}_4$ provided a second charge transfer mechanism in addition to the Fe_2O_3 Z-heterojunction thus reducing the rate of recombination of e^-/h^+ pairs. Another study observed that $\text{TiO}_2@\text{ZnFe}_2\text{O}_4/\text{Pd}$ gave better catalytic performance than $\text{TiO}_2@\text{ZnFe}_2\text{O}_4$ [105], while co-doping TiO_2 with carbon and nitrogen gave better photocatalytic performances [76,106]. These are indications of the potential of co-doping in enhancing the photocatalytic abilities of TiO_2 .

Having mentioned the potential ecotoxicity effects due to the leaching of nanoparticles into the environment, some researchers have substituted inorganic nanoparticles including metal oxides and graphene with organic semiconductors [88]. These include POPD, PEDOT, and some MOFs as discussed in Sections 5.3 - 5.5. More of these materials need to be identified and their potential as substitutes for TiO_2 should be investigated. Furthermore, the use of organic solvents in synthesizing MIPs requires careful assessment and regulation. With green chemistry procedures advocating for the use of environmentally friendly solvents, deep eutectic solvents and ionic liquids have been mentioned in the synthesis of MIPs [107]. This approach could be adopted in the synthesis of MIP-based photocatalysts.

With most studies still focussing on remediation of single pharmaceuticals, a shift towards multiresidue degradation can be an important approach that could result in upscaling molecularly imprinted photocatalysts. Nearly 10 years ago, de Escobar et al. [72] attempted a MIP/ TiO_2 imprinted with cavities for seven pharmaceuticals belonging to different classes (atorvastatin, diclofenac, ibuprofen, tioconazole, valsartan, ketoconazole, and gentamicine). They observed that degradation rates for the multitemplate imprinted TiO_2 photocatalyst were enhanced by over 400%. Multiple pharmaceutical degradation is an area that needs serious attention because pollutants do not exist in isolation in the environment and photocatalysts with multiresidue degradation capabilities are required. Multiple imprinted photocatalysts with two

or more heterojunctions can be further explored to enhance the degradation abilities of imprinted photocatalysts to remediate multifarious pharmaceuticals from the environment. Furthermore, some studies have observed that using dummy templates results in better degradation activities than when target pharmaceuticals are used as the templates. For example, Li et al. [79] synthesized a MIP/TiO₂ with sulphonamide and sulfamethoxazole as templates. They compared their activities with a MIP/TiO₂ prepared using aniline as a dummy template and observed that it performed better than target-imprinted MIP/TiO₂, with the additional advantage of producing fewer intermediates and by-products.

Various other novel methods that could be further explored have been mentioned in the literature. Zhang et al. [98] have initiated the concept of afterglow photocatalysis with the ability to degrade pollutants day and night. Another area that might excite researchers in the near future has been recently mentioned in literature where a MIP-based photocatalyst was utilized for the mitigation of antibiotic resistant genes (ARGs) in aqueous environment [64]. In their study, the researchers synthesized guanine-imprinted g-C₃N₄ nanosheets and used them to degrade plasmid-encoded (bla_{NDM-1}) multi-drug ARG in wastewater effluents. Imprinting g-C₃N₄ with guanine enhanced the adsorption of the ARG on its surface resulting in photodegradation efficiencies that were 37-fold faster than bare g-C₃N₄. ARGs are of global concern because of their persistence in the environment and photocatalytic degradation might provide a potentially effective way of removing them in the environment. Photodegradation helps fragment and mineralize the DNA of the ARG thus preventing it from repair.

Common MIP/doped-TiO₂ photocatalysts still underperform when compared to MIP/TiO₂ schemes with dopants that possess plasmonic resonance properties. The future of molecularly imprinted photocatalysts might fall on utilizing the advantages of molecularly imprinting and dopants with plasmonic resonance properties. Studies that integrated molecular imprinting with graphene-doped photocatalysts have observed better performances compared to individual

techniques combined with TiO₂. For example, a molecularly imprinted C-doped TiO₂ nanomaterial for sulfadiazine recorded a 99.25% degradation efficiency in 140 min [76]. A tetracycline imprinted Ag/Ag₃VO₄/g-C₃N₄ photocatalyst that utilized Ag⁰ for its surface plasmon resonance resulted in a 90% degradation efficiency of tetracycline over 120 min [108]. These observations are an indication that combined utilization of molecular imprinting and plasmon resonance could shape the future of photocatalytic degradation of organic pollutants, necessitating further studies in this area.

8 Conclusions

Photocatalytic degradation represents a promising approach to controlling environmental pollution. Its integration with molecular imprinting technology is expected to play a pivotal role in achieving sustainable goals related to pharmaceutical control in the environment. Currently, the approach has several drawbacks that need to be addressed before it can be considered as a plausible alternative in pharmaceutical pollution control. One notable drawback is the lack of pilot-scale studies and industrial applications to demonstrate their feasibility and economic viability in large-scale environmental remediation projects. Continued research is therefore essential to further explore innovative solutions around molecularly imprinted photocatalysts for sustainable pharmaceutical residue management including substituting metal oxide nanoparticles with organic semiconductors and exploring multiresidue photodegradation. The review identifies that the integration of molecular imprinted polymers with semiconductor materials for photodegradation of pollutants is a relatively new niche area with 83% of the studies so far done within the last 5 years (2019 - 2024) and more studies are expected in the few coming years.

Funding

DUT University Research Capacity Development Grant:

References

- [1] T. Sajini, M.G. Gigimol, B. Mathew, A brief overview of molecularly imprinted polymers supported on titanium dioxide matrices, *Mater. Today Chem.* 11 (2019) 283–295. <https://doi.org/10.1016/j.mtchem.2018.11.010>.
- [2] Y. Ali, E. Hadj, A. Azzouz, M. Ahrouch, A. Lamaoui, N. Raza, A. Ait, Molecular imprinting technology for next-generation water treatment via photocatalysis and selective pollutant adsorption, *J. Environ. Chem. Eng.* 12 (2024) 112768. <https://doi.org/10.1016/j.jece.2024.112768>.
- [3] R. Krakowiak, J. Musial, P. Bakun, M. Spychała, B. Czarczynska-Goslinska, D.T. Mlynarczyk, T. Koczorowski, L. Sobotta, B. Stanisiz, T. Goslinski, Titanium dioxide-based photocatalysts for degradation of emerging contaminants including pharmaceutical pollutants, *Appl. Sci.* 11 (2021). <https://doi.org/10.3390/app11188674>.
- [4] P. Singh, A. Borthakur, A review on biodegradation and photocatalytic degradation of organic pollutants: A bibliometric and comparative analysis, *J. Clean. Prod.* 196 (2018) 1669–1680. <https://doi.org/10.1016/j.jclepro.2018.05.289>.
- [5] A. Bagheri, N. Aramesh, A. Arif, I. Gul, S. Ghotekar, M. Bilal, Molecularly imprinted polymers-based adsorption and photocatalytic approaches for mitigation of environmentally-hazardous pollutants — A review, *J. Environ. Chem. Eng.* 9 (2021) 104879. <https://doi.org/10.1016/j.jece.2020.104879>.
- [6] C. Lai, X. Zhou, D. Huang, G. Zeng, M. Cheng, A review of titanium dioxide and its

- highlighted application in molecular imprinting technology in environment, *J. Taiwan Inst. Chem. Eng.* 91 (2018) 517–531. <https://doi.org/10.1016/j.jtice.2018.05.035>.
- [7] D. Chen, Y. Cheng, N. Zhou, P. Chen, Y. Wang, K. Li, S. Huo, P. Cheng, P. Peng, R. Zhang, L. Wang, H. Liu, Y. Liu, R. Ruan, Photocatalytic degradation of organic pollutants using TiO₂-based photocatalysts: A review, *J. Clean. Prod.* 268 (2020). <https://doi.org/10.1016/j.jclepro.2020.121725>.
- [8] G. Guan, J.H. Pan, Z. Li, Innovative utilization of molecular imprinting technology for selective adsorption and (photo)catalytic eradication of organic pollutants, *Chemosphere* 265 (2021) 129077. <https://doi.org/10.1016/j.chemosphere.2020.129077>.
- [9] Y. Zhang, X. Zhang, S. Wang, Recent advances in the removal of emerging contaminants from water by novel molecularly imprinted materials in advanced oxidation processes -A review, *Sci. Total Environ.* 883 (2023) 163702. <https://doi.org/10.1016/j.scitotenv.2023.163702>.
- [10] L. Wang, J. Yu, X. Wang, J. Li, L. Chen, Molecular imprinting-based nanocomposite adsorbents for typical pollutants removal, *J. Hazard. Mater. Lett.* 4 (2023) 100073. <https://doi.org/10.1016/j.hazl.2022.100073>.
- [11] W.S. Koe, J.W. Lee, W.C. Chong, An overview of photocatalytic degradation : photocatalysts , mechanisms , and development of photocatalytic membrane, *Environ. Sci. Pollut. Res.* 27 (2019) 1–44. <https://doi.org/10.1007/s11356-019-07193-5>.
- [12] X. Li, H. Wei, T. Song, H. Lu, X. Wang, A review of the photocatalytic degradation of organic pollutants in water by modified TiO₂, *Water Sci. Technol.* 88 (2023) 1495–1507. <https://doi.org/10.2166/wst.2023.288>.
- [13] L. Sun, J. Guan, Q. Xu, X. Yang, J. Wang, X. Hu, Synthesis and applications of

- molecularly imprinted polymers modified TiO₂ nanoparticles: A review, *Polymers* (Basel). 10 (2018) 1–26. <https://doi.org/10.3390/polym10111248>.
- [14] Y. Luo, X. Feng, Z. Chen, X. Shen, Molecularly imprinted photocatalysts: fabrication, application and challenges, *Mater. Adv.* 3 (2022) 8830–8847. <https://doi.org/10.1039/d2ma00848c>.
- [15] D.T. Ruziwa, A.E. Oluwalana, M. Mupa, L. Meili, R. Selvasembian, M.M. Nindi, M. Sillanpaa, W. Gwenzi, N. Chaukura, Pharmaceuticals in wastewater and their photocatalytic degradation using nano-enabled photocatalysts, *J. Water Process Eng.* 54 (2023) 103880. <https://doi.org/10.1016/j.jwpe.2023.103880>.
- [16] A. Majumder, D. Saidulu, A.K. Gupta, P.S. Ghosal, Predicting the trend and utility of different photocatalysts for degradation of pharmaceutically active compounds: A special emphasis on photocatalytic materials, modifications, and performance comparison, *J. Environ. Manage.* 293 (2021) 112858. <https://doi.org/10.1016/j.jenvman.2021.112858>.
- [17] J. Yi, J. Wan, G. Ye, Y. Wang, Y. Ma, Z. Yan, C. Zeng, Targeted degradation of refractory organic pollutants in wastewater based on molecularly imprinted catalytic materials: Adsorption process and degradation mechanism, *Sep. Purif. Technol.* 311 (2023) 123244. <https://doi.org/10.1016/j.seppur.2023.123244>.
- [18] P.S. Basavarajappa, S.B. Patil, N. Ganganagappa, K.R. Reddy, A. V. Raghu, C.V. Reddy, Recent progress in metal-doped TiO₂, non-metal doped/codoped TiO₂ and TiO₂ nanostructured hybrids for enhanced photocatalysis, *Int. J. Hydrogen Energy* 45 (2020) 7764–7778. <https://doi.org/10.1016/j.ijhydene.2019.07.241>.
- [19] Y. Chen, J. Yang, L. Zeng, M. Zhu, Recent progress on the removal of antibiotic pollutants using photocatalytic oxidation process, *Crit. Rev. Environ. Sci. Technol.* 52

- (2022) 1401–1448. <https://doi.org/10.1080/10643389.2020.1859289>.
- [20] G. Rana, P. Dhiman, A. Kumar, A. Chauhan, G. Sharma, Recent advances in photocatalytic removal of antiviral drugs by Z-scheme and S-scheme heterojunction, *Environ. Sci. Pollut. Res.* 31 (2024) 40851–40872. <https://doi.org/10.1007/s11356-024-33876-9>.
- [21] F. Mohamadpour, F. Mohamadpour, Photodegradation of six selected antipsychiatric drugs; carbamazepine, sertraline, amisulpride, amitriptyline, diazepam, and alprazolam in environment: efficiency, pathway, and mechanism—a review, *Sustain. Environ. Res.* 34 (2024) 1–26. <https://doi.org/10.1186/s42834-024-00214-0>.
- [22] M. Vahidifar, Z. Es'haghi, N.M. Oghaz, A.A. Mohammadi, M.S. Kazemi, Multi-template molecularly imprinted polymer hybrid nanoparticles for selective analysis of nonsteroidal anti-inflammatory drugs and analgesics in biological and pharmaceutical samples, *Environ. Sci. Pollut. Res.* 29 (2022) 47416–47435. <https://doi.org/10.1007/s11356-021-18308-2>.
- [23] J. Musial, D.T. Mlynarczyk, B.J. Stanis, Photocatalytic degradation of sulfamethoxazole using TiO₂-based materials – Perspectives for the development of a sustainable water treatment technology, *Sci. Total Environ.* 856 (2023) 159122. <https://doi.org/10.1016/j.scitotenv.2022.159122>.
- [24] F. Mumtaz, M. Atif, F. Naz, B. Li, K. Wang, M.R. AlShehhi, Advanced hybrid molecular imprinted polymers for antibiotics remediation from wastewater, *ChemBioEng Rev.* 11 (2024) 495–512. <https://doi.org/10.1002/cben.202300057>.
- [25] P. Huo, Z. Lu, X. Liu, X. Liu, X. Gao, J. Pan, D. Wu, J. Ying, H. Li, Y. Yan, Preparation molecular/ions imprinted photocatalysts of La³⁺@POPD/TiO₂/fly-ash cenospheres: Preferential photodegradation of TCs antibiotics, *Chem. Eng. J.* 198–199 (2012) 73–80.

<https://doi.org/10.1016/j.cej.2012.05.089>.

- [26] P. Huo, Z. Lu, X. Liu, D. Wu, X. Liu, J. Pan, X. Gao, W. Guo, H. Li, Y. Yan, Preparation photocatalyst of selected photodegradation antibiotics by molecular imprinting technology onto TiO₂/fly-ash cenospheres, *Chem. Eng. J.* 189–190 (2012) 75–83. <https://doi.org/10.1016/j.cej.2012.02.030>.
- [27] H.T. Wang, X. Wu, H.M. Zhao, X. Quan, Enhanced photocatalytic degradation of tetracycline hydrochloride by molecular imprinted film modified TiO₂ nanotubes, *Chinese Sci. Bull.* 57 (2012) 601–605. <https://doi.org/10.1007/s11434-011-4897-x>.
- [28] L.M. Madikizela, S. Ncube, L. Chimuka, Analysis, occurrence and removal of pharmaceuticals in African water resources: A current status, *J. Environ. Manage.* 253 (2020) 109741. <https://doi.org/10.1016/j.jenvman.2019.109741>.
- [29] S. Fekadu, E. Alemayehu, R. Dewil, B. Van der Bruggen, Pharmaceuticals in freshwater aquatic environments: A comparison of the African and European challenge, *Sci. Total Environ.* 654 (2019) 324–337. <https://doi.org/10.1016/j.scitotenv.2018.11.072>.
- [30] J.P. Bavumiragira, J. Ge, H. Yin, Fate and transport of pharmaceuticals in water systems: A processes review, *Sci. Total Environ.* 823 (2022) 153635. <https://doi.org/10.1016/j.scitotenv.2022.153635>.
- [31] U. Theuretzbacher, Global antibacterial resistance: The never-ending story, *J. Glob. Antimicrob. Resist.* 1 (2013) 63–69. <https://doi.org/10.1016/j.jgar.2013.03.010>.
- [32] D.G.J. Larsson, C.F. Flach, Antibiotic resistance in the environment, *Nat. Rev. Microbiol.* 20 (2022) 257–269. <https://doi.org/10.1038/s41579-021-00649-x>.
- [33] N. Skandalis, M. Maeusli, D. Papafotis, S. Miller, B. Lee, I. Theologidis, B. Luna, Environmental spread of antibiotic resistance, *Antibiotics* 10 (2021) 1–14.

<https://doi.org/10.3390/antibiotics10060640>.

- [34] S. Ncube, L.M. Madikizela, L. Chimuka, M.M. Nindi, Environmental fate and ecotoxicological effects of antiretrovirals: A current global status and future perspectives, *Water Res.* 145 (2018) 231–247. <https://doi.org/10.1016/j.watres.2018.08.017>.
- [35] S. Teixeira, R. Gurke, H. Eckert, K. Ku, J. Fauler, G. Cuniberti, Photocatalytic degradation of pharmaceuticals present in conventional treated wastewater by nanoparticle suspensions, *J. Environ. Chem. Eng.* 4 (2016) 287–292. <https://doi.org/10.1016/j.jece.2015.10.045>.
- [36] X. Li, B. Yang, K. Xiao, H. Duan, J. Wan, H. Zhao, Targeted degradation of refractory organic compounds in wastewaters based on molecular imprinting catalysts, *Water Res.* 203 (2021) 117541. <https://doi.org/10.1016/j.watres.2021.117541>.
- [37] T. Xia, Y. Lin, W. Li, M. Ju, Photocatalytic degradation of organic pollutants by MOFs based materials: A review, *Chinese Chem. Lett.* 32 (2021) 2975–2984. <https://doi.org/10.1016/j.ccllet.2021.02.058>.
- [38] R. Liu, X. Han, R. Liu, Z. Qi, B. Ren, Y. Sun, Molecularly imprinted Fe₃O₄/g-C₃N₄/TiO₂ catalyst for selective photodegradation of chlorotetracycline, *Colloids Surfaces A Physicochem. Eng. Asp.* 680 (2024) 132691. <https://doi.org/10.1016/j.colsurfa.2023.132691>.
- [39] Z.M. Shaykhi, A.A.L. Zinatizadeh, Statistical modeling of photocatalytic degradation of synthetic amoxicillin wastewater (SAW) in an immobilized TiO₂ photocatalytic reactor using response surface methodology (RSM), *J. Taiwan Inst. Chem. Eng.* 45 (2014) 1717–1726. <https://doi.org/10.1016/j.jtice.2013.12.024>.

- [40] L. Haroune, M. Salaun, A. Ménard, C.Y. Legault, J.P. Bellenger, Photocatalytic degradation of carbamazepine and three derivatives using TiO₂ and ZnO: Effect of pH, ionic strength, and natural organic matter, *Sci. Total Environ.* 475 (2014) 16–22. <https://doi.org/10.1016/j.scitotenv.2013.12.104>.
- [41] P. Chinnaiyan, S.G. Thampi, M. Kumar, M. Balachandran, Photocatalytic degradation of metformin and amoxicillin in synthetic hospital wastewater: effect of classical parameters, *Int. J. Environ. Sci. Technol.* 16 (2019) 5463–5474. <https://doi.org/10.1007/s13762-018-1935-0>.
- [42] A.H. Navidpour, M.B. Ahmed, J.L. Zhou, Photocatalytic degradation of pharmaceutical residues from water and sewage effluent using different TiO₂ nanomaterials, *Nanomaterials* 14 (2024). <https://doi.org/10.3390/nano14020135>.
- [43] P. Ncube, C. Zvinowanda, M. Belaid, F. Ntuli, Heterogeneous photocatalytic degradation of nevirapine in wastewater using the UV/TiO₂/H₂O₂ process, *Environ. Process.* 10 (2023) 1–24. <https://doi.org/10.1007/s40710-022-00615-6>.
- [44] T. An, J. An, H. Yang, G. Li, H. Feng, X. Nie, Photocatalytic degradation kinetics and mechanism of antiviral drug-lamivudine in TiO₂ dispersion, *J. Hazard. Mater.* 197 (2011) 229–236. <https://doi.org/10.1016/j.jhazmat.2011.09.077>.
- [45] K. Li, J. Xiong, T. Chen, L. Yan, Y. Dai, D. Song, Y. Lv, Z. Zeng, Preparation of graphene/TiO₂ composites by nonionic surfactant strategy and their simulated sunlight and visible light photocatalytic activity towards representative aqueous POPs degradation, *J. Hazard. Mater.* 250–251 (2013) 19–28. <https://doi.org/10.1016/j.jhazmat.2013.01.069>.
- [46] S.Y. Chun, W.J. Chung, S.S. Kim, J.T. Kim, S.W. Chang, Optimization of the TiO₂/Ge composition by the response surface method of photocatalytic degradation under

- ultraviolet-A irradiation and the toxicity reduction of amoxicillin, *J. Ind. Eng. Chem.* 27 (2015) 291–296. <https://doi.org/10.1016/j.jiec.2015.01.003>.
- [47] K.S. Varma, R.J. Tayade, K.J. Shah, P.A. Joshi, A.D. Shukla, V.G. Gandhi, Photocatalytic degradation of pharmaceutical and pesticide compounds (PPCs) using doped TiO₂ nanomaterials: A review, *Water-Energy Nexus* 3 (2020) 46–61. <https://doi.org/10.1016/j.wen.2020.03.008>.
- [48] N. Ahmadpour, M. Nowrouzi, V. Madadi Avargani, M.H. Sayadi, S. Zendehboudi, Design and optimization of TiO₂-based photocatalysts for efficient removal of pharmaceutical pollutants in water: Recent developments and challenges, *J. Water Process Eng.* 57 (2024) 104597. <https://doi.org/10.1016/j.jwpe.2023.104597>.
- [49] X. Zhu, J. Liu, L. Li, G. Zhen, X. Lu, J. Zhang, H. Liu, Z. Zhou, Z. Wu, X. Zhang, Prospects for humic acids treatment and recovery in wastewater: A review, *Chemosphere* 312 (2023) 137193. <https://doi.org/10.1016/j.chemosphere.2022.137193>.
- [50] S. Chianese, A. Fenti, P. Iovino, D. Musmarra, S. Salvestrini, Sorption of organic pollutants by humic acids: A review, *Molecules* 25 (2020) 1–17. <https://doi.org/10.3390/molecules25040918>.
- [51] L. Bi, Z. Chen, L. Li, J. Kang, S. Zhao, B. Wang, P. Yan, Y. Li, X. Zhang, J. Shen, Selective adsorption and enhanced photodegradation of diclofenac in water by molecularly imprinted TiO₂, *J. Hazard. Mater.* 407 (2021) 124759. <https://doi.org/10.1016/j.jhazmat.2020.124759>.
- [52] J. Peng, F. Deng, H. Shi, Z. Wang, X. Li, J. Zou, X. Luo, Target recognition and preferential degradation of toxic chemical groups by innovative group-imprinted photocatalyst with footprint cavity, *Appl. Catal. B Environ.* 340 (2024) 123179. <https://doi.org/10.1016/j.apcatb.2023.123179>.

- [53] Q. Du, P. Wu, Y. Sun, J. Zhang, H. He, Selective photodegradation of tetracycline by molecularly imprinted ZnO @ NH₂-UiO-66 composites, *Chem. Eng. J.* 390 (2020) 1–11. <https://doi.org/10.1016/j.cej.2020.124614>.
- [54] J.J. Belbruno, Molecularly imprinted polymers, *Chem. Rev.* 119 (2019) 94–119. <https://doi.org/10.1021/acs.chemrev.8b00171>.
- [55] A. Martín-Esteban, Molecularly-imprinted polymers as a versatile, highly selective tool in sample preparation, *TrAC - Trends Anal. Chem.* 45 (2013) 169–181. <https://doi.org/10.1016/j.trac.2012.09.023>.
- [56] S.I. Kaya, A. Cetinkaya, S.A. Ozkan, Molecularly imprinted polymers as highly selective sorbents in sample preparation techniques and their applications in environmental water analysis, *Trends Environ. Anal. Chem.* 37 (2023) e00193. <https://doi.org/10.1016/j.teac.2022.e00193>.
- [57] L.M. Madikizela, N.T. Tavengwa, L. Chimuka, Applications of molecularly imprinted polymers for solid-phase extraction of non-steroidal anti-inflammatory drugs and analgesics from environmental waters and biological samples, *J. Pharm. Biomed. Anal.* 147 (2018) 624–633. <https://doi.org/10.1016/j.jpba.2017.04.010>.
- [58] D.A. Gkika, A.K. Tolkou, D.A. Lambropoulou, D.N. Bikiaris, P. Kokkinos, I.K. Kalavrouziotis, G.Z. Kyzas, Application of molecularly imprinted polymers (MIPs) as environmental separation tools, *RSC Appl. Polym.* 2 (2024) 127–148. <https://doi.org/10.1039/d3lp00203a>.
- [59] G. Vasapollo, R. Del Sole, L. Mergola, M.R. Lazzoi, A. Scardino, S. Scorrano, G. Mele, Molecularly imprinted polymers: Present and future prospective, *Int. J. Mol. Sci.* 12 (2011) 5908–5945. <https://doi.org/10.3390/ijms12095908>.

- [60] D.S. Villarreal-Lucio, K.X. Vargas-Berrones, L. Díaz de León-Martínez, R. Flores-Ramírez, Molecularly imprinted polymers for environmental adsorption applications, *Environ. Sci. Pollut. Res.* 29 (2022) 89923–89942. <https://doi.org/10.1007/s11356-022-24025-1>.
- [61] A. Speltini, A. Scalabrini, F. Maraschi, M. Sturini, A. Profumo, Newest applications of molecularly imprinted polymers for extraction of contaminants from environmental and food matrices: A review, *Anal. Chim. Acta* 974 (2017) 1–26. <https://doi.org/10.1016/j.aca.2017.04.042>.
- [62] D. Huang, R. Wang, Y. Liu, Application of molecularly imprinted polymers in wastewater treatment : a review, (2015) 963–977. <https://doi.org/10.1007/s11356-014-3599-8>.
- [63] L. Fang, K. Tang, D. Wei, Y. Zhang, Y. Zhou, Photocatalytic degradation of norfloxacin by magnetic molecularly imprinted polymers: influencing factors and mechanisms, *Environ. Technol. (United Kingdom)* 44 (2023) 1438–1449. <https://doi.org/10.1080/09593330.2021.2003442>.
- [64] Q. Yuan, D. Zhang, P. Yu, R. Sun, H. Javed, G. Wu, P.J.J. Alvarez, Selective Adsorption and Photocatalytic Degradation of Extracellular Antibiotic Resistance Genes by Molecularly-Imprinted Graphitic Carbon Nitride, *Environ. Sci. Technol.* 54 (2020) 4621–4630. <https://doi.org/10.1021/acs.est.9b06926>.
- [65] F. Zhang, Z. Wang, W.J.G.M. Peijnenburg, M.G. Vijver, Review and prospects on the ecotoxicity of mixtures of nanoparticles and hybrid nanomaterials, *Environ. Sci. Technol.* 56 (2022) 15238–15250. <https://doi.org/10.1021/acs.est.2c03333>.
- [66] M. Renzi, A. Blašković, Ecotoxicity of nano-metal oxides: A case study on daphnia magna, *Ecotoxicology* 28 (2019) 878–889. <https://doi.org/10.1007/s10646-019-02085->

3.

- [67] M.K. Nguyen, J.Y. Moon, Y.C. Lee, Microalgal ecotoxicity of nanoparticles: An updated review, *Ecotoxicol. Environ. Saf.* 201 (2020). <https://doi.org/10.1016/j.ecoenv.2020.110781>.
- [68] K. Poonia, P. Raizada, A. Singh, N. Verma, T. Ahamad, S.M. Alshehri, A.A.P. Khan, P. Singh, C.M. Hussain, Magnetic molecularly imprinted polymer photocatalysts: synthesis, applications and future perspective, *J. Ind. Eng. Chem.* 113 (2022) 1–14. <https://doi.org/10.1016/j.jiec.2022.05.029>.
- [69] S. Huang, J. Xu, J. Zheng, F. Zhu, L. Xie, G. Ouyang, Synthesis and application of magnetic molecularly imprinted polymers in sample preparation, (2018) 3991–4014.
- [70] Y. Cui, L. Ding, J. Ding, Recent advances of magnetic molecularly imprinted materials: From materials design to complex sample pretreatment, *TrAC - Trends Anal. Chem.* 147 (2022) 116514. <https://doi.org/10.1016/j.trac.2021.116514>.
- [71] C.C. de Escobar, Y.P. Moreno Ruiz, J.H.Z. dos Santos, L. Ye, Molecularly imprinted TiO₂ photocatalysts for degradation of diclofenac in water, *Colloids Surfaces A Physicochem. Eng. Asp.* 538 (2018) 729–738. <https://doi.org/10.1016/j.colsurfa.2017.11.044>.
- [72] C.C. de Escobar, M.A. Lansarin, J.H. Zimnoch dos Santos, Synthesis of molecularly imprinted photocatalysts containing low TiO₂ loading: Evaluation for the degradation of pharmaceuticals, *J. Hazard. Mater.* 306 (2016) 359–366. <https://doi.org/10.1016/j.jhazmat.2015.11.035>.
- [73] P. Sathishkumar, R.A.A. Meena, T. Palanisami, V. Ashokkumar, T. Palvannan, F.L. Gu, Occurrence, interactive effects and ecological risk of diclofenac in environmental

- compartments and biota - a review, *Sci. Total Environ.* 698 (2020) 134057. <https://doi.org/10.1016/j.scitotenv.2019.134057>.
- [74] L. Li, X. Zheng, Y. Chi, Y. Wang, X. Sun, Q. Yue, B. Gao, S. Xu, Molecularly imprinted carbon nanosheets supported TiO₂: Strong selectivity and synergic adsorption-photocatalysis for antibiotics removal, *J. Hazard. Mater.* 383 (2020) 121211. <https://doi.org/10.1016/j.jhazmat.2019.121211>.
- [75] Z. Lu, F. Chen, M. He, M. Song, Z. Ma, W. Shi, Y. Yan, J. Lan, F. Li, P. Xiao, Microwave synthesis of a novel magnetic imprinted TiO₂ photocatalyst with excellent transparency for selective photodegradation of enrofloxacin hydrochloride residues solution, *Chem. Eng. J.* 249 (2014) 15–26. <https://doi.org/10.1016/j.cej.2014.03.077>.
- [76] Q. Li, Y. Huang, Z. Pan, J. Ni, W. Yang, J. Chen, Y. Zhang, J. Li, Hollow C, N-TiO₂@C surface molecularly imprinted microspheres with visible light photocatalytic regeneration availability for targeted degradation of sulfadiazine, *Sep. Purif. Technol.* 299 (2022) 121814. <https://doi.org/10.1016/j.seppur.2022.121814>.
- [77] J.Y. Zhang, J. Ding, L.M. Liu, R. Wu, L. Ding, J.Q. Jiang, J.W. Pang, Y. Li, N.Q. Ren, S.S. Yang, Selective removal of sulfamethoxazole by a novel double Z-scheme photocatalyst: Preferential recognition and degradation mechanism, *Environ. Sci. Ecotechnology* 17 (2024) 100308. <https://doi.org/10.1016/j.ese.2023.100308>.
- [78] S. Mokhtari, H. Faghihian, M. Mirmohammadi, A core/shell TiO₂ magnetized molecularly imprinted photocatalyst (MMIP@TiO₂): synthesis and its photodegradation activity towards sulfasalazine, *Environ. Sci. Pollut. Res.* 30 (2023) 13624–13638. <https://doi.org/10.1007/s11356-022-22792-5>.
- [79] D. Li, R. Yuan, B. Zhou, H. Chen, Selective photocatalytic removal of sulfonamide antibiotics: The performance differences in molecularly imprinted TiO₂ synthesized

- using four template molecules, *J. Clean. Prod.* 383 (2023) 135470.
<https://doi.org/10.1016/j.jclepro.2022.135470>.
- [80] A. Eslami, M. Rafiee, R. Sedghi, A. Aliyari, B. Heidari, Simultaneous and selective removal of diclofenac and ibuprofen from aqueous matrices by a hybrid TiO₂-dual-template molecularly imprinted polymer, *Int. J. Environ. Anal. Chem.* 00 (2023) 1–23.
<https://doi.org/10.1080/03067319.2023.2178917>.
- [81] L. Fang, Y. Miao, D. Wei, Y. Zhang, Y. Zhou, Efficient removal of norfloxacin in water using magnetic molecularly imprinted polymer, *Chemosphere* 262 (2021).
<https://doi.org/10.1016/j.chemosphere.2020.128032>.
- [82] S. Sheng, Z. Zhang, M. Wang, X. He, C. Jiang, Y. Wang, Synthesis of MIL-125(Ti) derived TiO₂ for selective photoelectrochemical sensing and photocatalytic degradation of tetracycline, *Electrochim. Acta* 420 (2022) 140441.
<https://doi.org/10.1016/j.electacta.2022.140441>.
- [83] M. Cantarella, A. Di Mauro, A. Gulino, L. Spitaleri, G. Nicotra, V. Privitera, G. Impellizzeri, Selective photodegradation of paracetamol by molecularly imprinted ZnO nanonuts, *Appl. Catal. B Environ.* 238 (2018) 509–517.
<https://doi.org/10.1016/j.apcatb.2018.07.055>.
- [84] J. Wang, J. Feng, C. Wei, Molecularly imprinted polyaniline immobilized on Fe₃O₄/ZnO composite for selective degradation of amoxicillin under visible light irradiation, *Appl. Surf. Sci.* 609 (2023) 155324.
<https://doi.org/10.1016/j.apsusc.2022.155324>.
- [85] H. Rabizadeh, A. Feizbakhsh, H.A. Panahi, E. Kono, A convenient synthesis of NiO-CuS/molecularly imprinted polymer nanocomposites with highly enhanced adsorption activity and selectivity for removal of Letrozole, *Polym. Technol. Mater.* 59 (2020) 619–

629. <https://doi.org/10.1080/25740881.2019.1669658>.
- [86] H. Zhang, Y. Xiao, Y. Peng, L. Tian, Y. Wang, Y. Tang, Y. Cao, Z. Wei, Z. Wu, Y. Zhu, Q. Guo, Selective degradation of ceftriaxone sodium by surface molecularly imprinted BiOCl/Bi₃NbO₇ heterojunction photocatalyst, *Sep. Purif. Technol.* 315 (2023) 123716. <https://doi.org/10.1016/j.seppur.2023.123716>.
- [87] S. Kumar, P. Karfa, K.C. Majhi, R. Madhuri, Photocatalytic, fluorescent BiPO₄@Graphene oxide based magnetic molecularly imprinted polymer for detection, removal and degradation of ciprofloxacin, *Mater. Sci. Eng. C* 111 (2020). <https://doi.org/10.1016/j.msec.2020.110777>.
- [88] Y. Huang, P. Wang, F. Chen, G. Zhou, M. Song, X. Liu, C. Ma, S. Han, Y. Yan, Z. Lu, Enhanced controllable degradation ability of magnetic imprinted photocatalyst via photoinduced surface imprinted technique for ciprofloxacin selectively degradation, *J. Photochem. Photobiol. A Chem.* 410 (2021) 113159. <https://doi.org/10.1016/j.jphotochem.2021.113159>.
- [89] X. Liu, L. Tang, L. Xu, G. Zhou, Q. Liu, M. Song, C. Ma, Z. Lu, Y. Yan, A temperature-sensitive modified imprinted Ag-Poly (o-phenylenediamine) photocatalyst synthesized by microwave method for efficient degradation of ciprofloxacin, *React. Kinet. Mech. Catal.* 135 (2022) 2137–2151. <https://doi.org/10.1007/s11144-022-02208-8>.
- [90] F. He, Z. Lu, M. Song, X. Liu, H. Tang, P. Huo, W. Fan, H. Dong, X. Wu, S. Han, Selective reduction of Cu²⁺ with simultaneous degradation of tetracycline by the dual channels ion imprinted POPD-CoFe₂O₄ heterojunction photocatalyst, *Chem. Eng. J.* 360 (2019) 750–761. <https://doi.org/10.1016/j.cej.2018.12.034>.
- [91] T. Fatima, S. Husain, M. Khanuja, Optimization of WS₂ modified polyaniline for superior photocatalytic degradation and electrochemical detection of pharmaceutical

- drug, *FlatChem* 44 (2024) 100624. <https://doi.org/10.1016/j.flatc.2024.100624>.
- [92] Z. Lu, G. Zhou, M. Song, X. Liu, H. Tang, H. Dong, P. Huo, F. Yan, P. Du, G. Xing, Development of magnetic imprinted PEDOT/CdS heterojunction photocatalytic nanoreactors: 3-Dimensional specific recognition for selectively photocatalyzing danofloxacin mesylate, *Appl. Catal. B Environ.* 268 (2020) 118433. <https://doi.org/10.1016/j.apcatb.2019.118433>.
- [93] X. Li, X. Chen, Z. Lv, B. Wang, Ultrahigh ciprofloxacin accumulation and visible-light photocatalytic degradation: Contribution of metal organic frameworks carrier in magnetic surface molecularly imprinted polymers, *J. Colloid Interface Sci.* 616 (2022) 872–885. <https://doi.org/10.1016/j.jcis.2022.02.130>.
- [94] Y. Xie, J. Wan, Z. Yan, Y. Wang, T. Xiao, J. Hou, H. Chen, Targeted degradation of sulfamethoxazole in wastewater by molecularly imprinted MOFs in advanced oxidation processes: Degradation pathways and mechanism, *Chem. Eng. J.* 429 (2022) 132237. <https://doi.org/10.1016/j.cej.2021.132237>.
- [95] J.X. Fu, S.Y. Li, Q.Y. Li, E. Bell, D.D. Yang, T. Li, Y.J. Li, J.Y. He, L. Di Zhou, Q.H. Zhang, C.S. Yuan, Preparation of surface molecular-imprinted MOFs for selective degradation of tetracycline antibiotics in wastewater, *Colloids Surfaces A Physicochem. Eng. Asp.* 687 (2024) 133575. <https://doi.org/10.1016/j.colsurfa.2024.133575>.
- [96] Z. Liu, G. Chen, X. Lu, In-situ growth of molecularly imprinted metal–organic frameworks on 3D carbon foam as an efficient adsorbent for selective removal of antibiotics, *J. Mol. Liq.* 340 (2021) 117232. <https://doi.org/10.1016/j.molliq.2021.117232>.
- [97] M. Tang, J. Wan, Y. Wang, Z. Yan, Y. Ma, J. Sun, S. Ding, Developing a molecularly imprinted channels catalyst based on template effect for targeted removal of organic

- micropollutants from wastewaters, *Chem. Eng. J.* 445 (2022) 136755.
<https://doi.org/10.1016/j.cej.2022.136755>.
- [98] Y. Zhang, Z.W. Wang, X.T. Yang, Y.Z. Zhu, H.F. Wang, Afterglow-catalysis and molecular imprinting: A promising union for elevating selectivity in degradation of antibiotics, *Appl. Catal. B Environ.* 305 (2022) 121025.
<https://doi.org/10.1016/j.apcatb.2021.121025>.
- [99] M. Huang, T. Zhou, X. Wu, J. Mao, Adsorption and degradation of norfloxacin by a novel molecular imprinting magnetic Fenton-like catalyst, *Chinese J. Chem. Eng.* 23 (2015) 1698–1704. <https://doi.org/10.1016/j.cjche.2015.08.030>.
- [100] X. Wu, M. Huang, T. Zhou, J. Mao, Recognizing removal of norfloxacin by novel magnetic molecular imprinted chitosan/ γ -Fe₂O₃ composites: Selective adsorption mechanisms, practical application and regeneration, *Sep. Purif. Technol.* 165 (2016) 92–100. <https://doi.org/10.1016/j.seppur.2016.03.041>.
- [101] H. Yan, Y. Ren, G. Zhou, P. Wang, Y. Xu, M. Song, X. Liu, C. Ma, S. Han, Z. Lu, Aqueous-phase synthesis of heterojunction molecular imprinted photocatalytic nanoreactor via stable interaction forces for improved selectivity and photocatalytic property, *Appl. Surf. Sci.* 579 (2022) 152174.
<https://doi.org/10.1016/j.apsusc.2021.152174>.
- [102] J.W. Lowdon, H. Diliën, P. Singla, M. Peeters, T.J. Cleij, B. van Grinsven, K. Eersels, MIPs for commercial application in low-cost sensors and assays – An overview of the current status quo, *Sensors Actuators, B Chem.* 325 (2020).
<https://doi.org/10.1016/j.snb.2020.128973>.
- [103] D. Li, Q. Zhu, C. Han, Y. Yang, W. Jiang, Z. Zhang, Photocatalytic degradation of recalcitrant organic pollutants in water using a novel cylindrical multi-column

- photoreactor packed with TiO₂-coated silica gel beads, *J. Hazard. Mater.* 285 (2015) 398–408. <https://doi.org/10.1016/j.jhazmat.2014.12.024>.
- [104] T. An, J. An, Y. Gao, G. Li, H. Fang, W. Song, Photocatalytic degradation and mineralization mechanism and toxicity assessment of antiviral drug acyclovir: Experimental and theoretical studies, *Appl. Catal. B Environ.* 164 (2015) 279–287. <https://doi.org/10.1016/j.apcatb.2014.09.009>.
- [105] N. Ahmadpour, M.H. Sayadi, S. Sobhani, M. Hajiani, Photocatalytic degradation of model pharmaceutical pollutant by novel magnetic TiO₂@ZnFe₂O₄/Pd nanocomposite with enhanced photocatalytic activity and stability under solar light irradiation, *J. Environ. Manage.* 271 (2020) 110964. <https://doi.org/10.1016/j.jenvman.2020.110964>.
- [106] L.T. Nguyen, H.T. Nguyen, T.D. Pham, T.D. Tran, H.T. Chu, H.T. Dang, V.H. Nguyen, K.M. Nguyen, T.T. Pham, B. Van der Bruggen, UV–Visible light driven photocatalytic degradation of ciprofloxacin by N,S Co-doped TiO₂: The effect of operational parameters, *Top. Catal.* 63 (2020) 985–995. <https://doi.org/10.1007/s11244-020-01319-7>.
- [107] L.M. Madikizela, S. Ncube, P.N. Nomngongo, V.E. Pakade, Molecular imprinting with deep eutectic solvents: Synthesis, applications, their significance, and benefits, *J. Mol. Liq.* 362 (2022) 119696. <https://doi.org/10.1016/j.molliq.2022.119696>.
- [108] L. Sun, J. Li, X. Li, C. Liu, H. Wang, P. Huo, Y. sheng Yan, Molecularly imprinted Ag/Ag₃VO₄/g-C₃N₄ Z-scheme photocatalysts for enhanced preferential removal of tetracycline, *J. Colloid Interface Sci.* 552 (2019) 271–286. <https://doi.org/10.1016/j.jcis.2019.05.060>.

PAPER 2

Paper 2 presents the published version of a manuscript titled “**Removal of efavirenz in wastewater effluents using a magnetic molecularly imprinted polymer: Synthesis, multivariate optimization and application**”.

In this work, a magnetic molecularly imprinted polymer (MMIP) nanosorbent was synthesized, optimized via central composite design and finally applied in the removal of efavirenz in wastewater effluents. The MMIP boasts the magnetic advantage that allows it to be held static and can be removed from the real effluents in the environment using an external magnetic field. The results of the study observed that the MMIP may be a viable tool for removal of efavirenz from wastewater effluents. The manuscript was published in the Journal of Water Process Engineering for peer review. <https://doi.org/10.1016/j.jwpe.2025.107786>

All supplementary material that gives detailed information used in manuscript 2 is given in the appendix.

Author contributions

Asenathi Sibali - Experiments, Data analysis, Writing the original draft, Conceptualization.

Devrani Naicker - Reviewing & editing, Conceptualization

Nompumelelo Pretty Cele - Reviewing & editing, Conceptualization

Vusumzi Emmanuel Pakade - Reviewing & editing, Conceptualization.

Ramakwala Christinah Chokwe - Reviewing & editing, Conceptualization.

Thabang Hendrica Mokhothu - Reviewing & editing, Supervision, Conceptualization.

Somandla Ncube - Reviewing & editing, Supervision, Conceptualization.

Removal of efavirenz in wastewater effluents using a magnetic molecularly imprinted polymer: Synthesis, multivariate optimization and application

Asenathi Sibali^a, Devrani Naicker^a, Nompumelelo Pretty Cele^a, Vusumzi Emmanuel Pakade^b, Ramakwala Christinah Chokwe^b, Thabang Mokhothu^a, Somandla Ncube^{a*}

^aDepartment of Chemistry, Durban University of Technology, P O Box 1334, Durban 4000, South Africa

^bDepartment of Chemistry, University of South Africa, Private Bag X6, Florida, 1710, South Africa

*Corresponding author. Tel: +27-313732309. E-mail: SomandlaN@dut.ac.za

Abstract

Efavirenz is the most detected antiretroviral drug in the aqueous environment and its levels are way higher compared to other antiretroviral drugs. This is a cause for concern and requires a shift towards finding remedial ways to minimize its potential impact to aquatic organisms. In the current study, a magnetic molecularly imprinted polymer was synthesized, optimized via central composite design and finally applied to remove of efavirenz from wastewater effluents. The magnetic smart polymer was synthesized via a bulk polymerization technique owing to its simplicity, low cost yet it yields a polymer of high purity. Efavirenz was used as the template and p-vinyl benzoic acid as the functional monomer. Based on coefficient plots, summary of fit and contour plots, the removal of efavirenz was directly affected by contact time, initial concentration of efavirenz and the mass of the magnetic polymer used under neutral conditions. The optimal binding capacity achieved after 40 min of contact time and neutral conditions was 44.9 $\mu\text{g g}^{-1}$. The polymeric sorbent could achieve 44.8% removal efficiencies from real

wastewater effluents polluted with 3.99 ng mL⁻¹ of efavirenz. Reusability studies showed less than 4% average loss in the binding capacity with every reuse cycle, while there was no loss in binding capabilities when the polymer was utilized at about half its binding capacity.

Keywords: central composite design; efavirenz; molecularly imprinted polymer; pollution; wastewater

1 Introduction

The release of pharmaceuticals into the aqueous environment has negative effects on humans and other aquatic species. Antiretroviral drugs (ARVDs) are among a group of pharmaceuticals with potentially serious ecotoxicological effects when they make their way into the environment. Exposure to them via contaminated water may be consequential especially for those already taking ARVDs and for new infections because ARVDs work against a virus that easily mutates if the drugs are not taken according to prescription. The analysis of ARVDs in the aqueous environment in South Africa started about 10 years ago and the first paper was published in 2015 [1]. Since then, there has been a plethora of other studies that have detected ARVDs in wastewater, rivers and dams in South Africa and the African continent at large [2,3]. Major sources of the ARVDs in the environment are mainly through effluents from wastewater treatment plants (WWTPs) as well as illicit or indiscriminate disposal of expired drugs [2,3]. Poor sanitation in most African regions, unavailability of modern ablution facilities that can be flushed with water to direct the human waste into WWTPs and improper disposal of expired or unused medications have contributed to the direct contamination of surface water with pharmaceuticals.

A further challenge for Africa is that the infection rates continue to surge resulting in more ARVDs released into the environment as part of excreta [4,5]. South Africa in particular has

been identified as a hotspot regarding ARVD contamination due to the relatively high therapeutic application and lack of wastewater treatment processes that can effectively minimize their release via effluents. In this regard, the presence of ARVDs in various aqueous systems such as wastewater effluents, surface water, ground water, and even drinking water has been reported extensively in South Africa [1,6,7]. Efavirenz is the most detected ARVD in surface environments and some scholars now consider it as a priority pollutant in African water bodies [5,8]. The performance of conventional wastewater treatment processes in South Africa has recently been observed to be less effective in the removal of efavirenz [9]. For example, four WWTPs in the Gauteng Province could only remove between 21 and 27% of efavirenz [10]. In the Eastern Cape Province, WWTPs were reported to achieve between 2 and 12% removal efficiencies [11], while in the KwaZulu Natal Province, removal efficiencies for four of the five WWTPs ranged between 19 and 38% [12]. In view of these observations, it is crucial that alternative removal strategies are explored to minimize entry of efavirenz into the environment through WWTP effluents.

In the current study, we have investigated a magnetic molecularly imprinted polymer (MMIP) as a potential remedial tool for efavirenz in WWTP effluents. MIPs are the synthetic materials with structural cavities designed to selectively isolate a specific target from complex matrices. The MIPs have been utilized in separation science to selectively isolate target analytes from complicated samples [13]. Despite the documented advantages that include low-cost production and stability, classic MIPs still have the challenge of isolating them from the sample matrix once they have adsorbed the target molecule. In this regard, recent studies have emphasize the need for incorporating magnetic materials to allow for their removal using an external magnetic field [14–17]. In our study, the MMIP was synthesized, characterized and its performance was optimized before its application as a sorbent to remove efavirenz from real effluent samples from a WWTP in Durban, South Africa. With the view that the smart polymer

needs to be deployed in wastewater effluents, it was magnetized with magnetite (iron oxide) to offer the advantage of trapping it at the deployment site using an external magnetic force [18,19] The trapped MMIP could be recovered from wastewater effluents, cleaned, and re-deployed to continue adsorbing efavirenz from the effluents. Previously, MIPs for ARVDs have been utilized as sorbents for solid phase extraction (SPE) for the purposes of quantifying ARVDs in various aqueous samples, including efavirenz [12,20–22]. Nevirapine was included in the study as a competitor of efavirenz for the active binding sites on the magnetic polymer cavities.

2 Methods and Materials

2.1 Chemicals and reagents

Analytical grade efavirenz and nevirapine as well as all organic solvents of HPLC grade (acetonitrile, methanol, ethyl acetate, dimethylformamide and toluene) were purchased from Merck (Pty) Ltd, Johannesburg, South Africa. Chemicals for synthesis of the MIP including ethylene glycol dimethacrylate (EGDMA) (the cross-linker), p-vinyl benzoic acid (the monomer) and 1,1'-azobis(isobutyronitrile) (AIBN) as the initiator were also purchased from Merck (Pty) Ltd, Johannesburg, South Africa.

2.2 Gas chromatography mass spectrometry

Chromatographic quantitation was carried out on a gas chromatograph coupled with triple quadrupole mass spectrometry (GC-TQMS) by Scion instruments, Goes, Netherlands. A 100-ng mL⁻¹ standard was first run in full scan mode to determine a suitable temperature program and the retention times of the efavirenz and nevirapine. A temperature program from 170 to 280°C gave retention times of 4.15 and 5.12 min, respectively. The transfer line temperature and source temperature were set at 290°C and 250°C, respectively. The spectra of the two

ARVDs were searched in the NIST library and positively identified with 87 and 92% matches for efavirenz and nevirapine, respectively. A single ion monitoring (SIM) method was then created by setting the 4.15 and 5.12 min as retention times while the m/z values were set at 316 and 266 for efavirenz and nevirapine, respectively. The mass error was set at ± 5 ppm. The GC-TQMS was then calibrated using 10 calibration standards of efavirenz in the concentration range of 10 - 100 ng mL⁻¹. The limit of detection (LOD) and limit of quantitation (LOQ) were computed using the linear regression method based on the Linest function in Excel. These were further used to determine the method detection limit (MDL) and method quantitation limit (MQL) based on the amount of MMIP used and the volume of the effluents.

2.3 Synthesis of a magnetic smart sorbent

2.3.1 Synthesis of magnetite

For synthesis of magnetite, 3 g of FeCl₃.6H₂O and 1.5 g of FeSO₄.7H₂O were dissolved in 100 mL of deionized water in a round bottom flask. The solution was heated to 50°C and then 12 mL of concentrated ammonia solution was added and the mixture stirred vigorously for 30 min. The temperature was then increased and maintained at 90°C for 30 min. Magnetic nanoparticles were magnetically retained at the bottom of the flask, washed with water and ethanol and dried in an oven overnight at 60°C.

2.3.2 Synthesis of a magnetic molecularly imprinted polymer

The synthesis of MMIP was done by transferring 0.0736 mmol of efavirenz as a template into a 50 mL round bottom flask containing 3 mL dimethylformamide as a porogen. The resulting homogeneous solution was stirred at 200 rpm and 40°C for 5 min to completely dissolve the monomer templates in dimethylformamide. Then 41 mg of p-vinyl benzoic acid as a functional monomer was added and the mixture stirred for a further 5 min. A 0.2 g mass of magnetite from Section 2.3.1 was added to the solution followed by mild ultrasonic treatment for 15 min.

Then 208 μL of EGDMA was added as a crosslinker followed by 100 mg of the AIBN initiator. The mixture was allowed to pre-polymerize in an inert atmosphere (nitrogen) for 10 min and the temperature of the mixture was then increased to 70°C and maintained for 30 min. The temperature was finally increased to 90°C until a polymer was formed. The polymer was formed within 2 h but it was allowed to remain in the silicon bath at 90°C for a further 2 h to stabilize. The product was dried in an oven overnight at 70°C. The dried MMIP was then crushed into a fine powder and washed with methanol/acetic acid (9:1 v/v) to remove the ARVD template molecules creating cavities within each grain of the polymer powder. The magnetic polymer was then characterized using Fourier transform infrared spectroscopy (FTIR) and thermogravimetric analysis (TGA). The MIP was synthesized using the same procedure as MMIP in the absence of the magnetite.

2.4 Optimization experiments using central composite design

The interactive effects of four factors that could affect the adsorption of efavirenz from aqueous solution were optimized simultaneously using central composite design (CCD) created on MODDE Pro statistical software by Sartorius, Göttingen, Germany. These were sample pH (4 - 9), mass of MMIP (5 - 15 mg), initial concentration of efavirenz (0.1 - 1 ng mL^{-1}) and contact time (10 - 120 min). The design output based on a quadratic model with star points placed on the faces of the sides composed of 27 experiments of which three of the experiments were randomly set for repeated design runs. The CCD output was then experimented and the peak area was chosen as a response factor. All the 27 design runs were done in triplicate and the average peak area was used for data analysis.

2.5 Investigating the mechanism and kinetics of adsorption

To investigate the extent of adsorption of efavirenz, 50 mg of the MMIP was dispersed into 5 mL spiked solutions over a concentration range of 10 - 300 ng mL⁻¹. The extraction process was allowed to take place under ambient conditions for 10 min. The results were then used to plot two important isotherm models; the Langmuir and Freundlich adsorption isotherms. The Langmuir adsorption isotherm predicts linear adsorption and a maximum surface coverage [23]. The model explains that all binding sites are homogeneous with uniform adsorption energy and that each site can accommodate only one molecule, thus only a single layer of adsorption (a monolayer) occurs [24]. The mathematical representation of the linearized form of the Langmuir model is summarized using Eq. 1. On the other hand, the Freundlich adsorption isotherm model predicts a heterogeneous binding site distribution, meaning binding sites with different adsorption energies [23]. The linearized mathematical representation of the Freundlich model is summarized using Eq. 2. These linearized equations are used to plot linear graphs based on the $y = mx + c$ form. The model whose linear plot gives a higher coefficient of determination (R^2) is accepted as the model that explains the extent of adsorption.

$$1/q_e = \left(1/K_L Q_{max}\right) \left(\frac{1}{C_e}\right) + 1/Q_{max} \quad (1)$$

where q_e is the adsorption capacity of the ARVDs at equilibrium (ng g⁻¹), Q_{max} is the monolayer maximum adsorption capacity of the sorbent (ng g⁻¹) and K_L is the Langmuir equilibrium constant (L g⁻¹) and C_e is the concentration of ARVDs (ng g⁻¹).

$$\log q_e = \log K_F + 1/n \log C_i \quad (2)$$

where K_F is the Freundlich constant (L g⁻¹) and n is the heterogeneity factor.

The pseudo-first-order (PFO) and pseudo-second-order (PSO) adsorption kinetic models are the most commonly used in understanding adsorption kinetics. To investigate the kinetics, a 50

mg mass of the MMIP was added in centrifuge tubes containing 5 mL of water spiked at 200 ng mL⁻¹ of efavirenz. Three tubes were randomly collected for analysis at specific time intervals over a period of 10 to 120 min. The analysis data was then used to plot the linear forms of the PFO and PSO models based on Eq. 3 and 4, respectively. The model with a better R² value was accepted as the one that explained the mechanism of adsorption of efavirenz onto the MMIP cavities. PFO predicts that adsorption occurs by physisorption while PSO predicts chemisorption.

$$\ln(q_e - q_t) = \ln q_e - k_1 t \quad (3)$$

$$t/q_e = 1/k_2 q_e^2 + t/q_e \quad (4)$$

where k_1 and k_2 are the rate constants for the pseudo first- and second-order models (min⁻¹), respectively.

2.6 Reusability studies

To investigate the possibility of reusing the polymer to extract efavirenz from effluent samples, the MMIP was used and regenerated repeatedly under its maximum binding capacity and at half its binding capacity. This was done by placing 10 mg of the MMIP in 5 mL of water spiked at 50 and 100 µg mL⁻¹ of efavirenz then allowing adsorption to occur at 25°C for 40 min. This was followed by trapping the MMIP using an external magnet and the spiked sample decanted. Thereafter, the MMIP was washed with 5 mL methanol to determine the amount of efavirenz extracted. The same MIP was used repeatedly for five consecutive cycles of adsorption/desorption.

2.7 Application of the MMIP in wastewater effluent samples

2.7.1 Wastewater effluent collection and analysis

Samples were collected from a WWTP in Durban, South Africa that treats both domestic and industrial wastewater using conventional treatment methods with chlorination as the final step. After chlorination, the effluents are discharged into a nearby river. Wastewater was collected at the exit point where the treated wastewater discharges into a river after chlorination. All samples were collected into 2.5 L brown glass bottles and transported to the laboratory in cooler boxes. In the laboratory, the samples were sonicated and immediately filtered through 0.45 μm filter paper. The filtered samples were then extracted using solid phase extraction (SPE) with Hydrophilic-Lipophilic-Balance (HLB) (6 cc Vac, 200 mg) cartridges by Waters Corporation, Milford, USA as sorbents followed by analysis using a gas chromatography coupled with triple quadrupole mass spectrometry (GC-TQMS). For SPE, 50 mL of wastewater effluent samples was diluted with 50 mL deionized water. The HLB cartridges were first conditioned with 5 mL of methanol followed by equilibrating with 3 mL of deionized water. The diluted wastewater effluent samples (100 mL) were then loaded at about 1 mL min^{-1} . The pumping process was continued for a further 5 min to dry the cartridges. About 1 mL of 2% methanol in water was then used to wash the cartridges. Finally, 5 mL of methanol was used to elute the analytes from the cartridges followed by immediate analysis using GC-TQ/MS. This process was repeated three times.

2.7.2 Removal of efavirenz using the magnetic polymer

Once the amount of efavirenz had been determined in effluents using SPE-GC-TQMS, the MMIP was then applied to the effluent samples to remove the ARVDs. A volume of 100 mL of undiluted wastewater effluent sample was poured into a 250 mL beaker. Then 20 mg of the MMIP was added and the mixture allowed to settle. After 30 min, a magnet was used to trap the MMIP at the bottom of the beaker and the effluent was decanted. The MMIP was then

washed with 5 mL of methanol to determine the amount of efavirenz trapped by the polymer. The amount trapped was then compared with the amount found in the effluents using SPE. This was used to determine the efficiency of the MMIP in removing the ARVDs from wastewater effluents using Eq. 5.

$$\text{Removal efficiency} = n_{MMIP} / n_E \times 100\% \quad (5)$$

where n_{MMIP} is the amount removed by the MMIP, n_E is the amount of efavirenz in effluents.

3 Results and Discussion

3.1 Characterization results

All the significant peaks observed for the MIP in Fig. 1A agreed with the information acquired from previous studies in which p-vinyl benzoic acid and EDGMA were used during polymer formation [25]. The FTIR of the synthesized magnetite exhibited typical -OH and Fe-O absorption bands as evidence of the purity of the synthesized magnetite nanoparticles [26]. The broad signal band at around 3400 cm^{-1} represented -OH stretching while the two bands at around 1650 and 1480 cm^{-1} were due to -OH and O-H vibrational modes of water particles on the surface of the nanoparticle. The Fe-O stretching was observed at around 580 cm^{-1} . The presence of -OH and Fe-O bands was an indication that the synthesized magnetite nanoparticles were of high purity. After co-polymerization, the -OH stretch initially observed for magnetite was suppressed both at 3400 , 650 and 1480 cm^{-1} which was an indication that the magnetite lost the H_2O particles from its surface as it was incorporated into the MIP during co-polymerization.

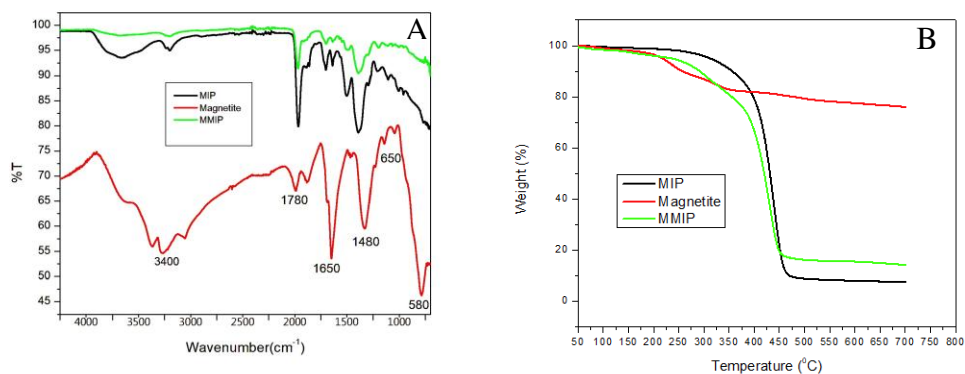


Fig. 1 FTIR spectrum (A) and TGA thermogram (B) of the sorbents.

The TGA results in Fig. 1B show that the MMIP the hybrid polymer maintains its weight up to 250°C and only degrades to about 80% at 350°C. The incorporation of the magnetite nanoparticles tend to destabilize the polymer because the MIP maintained almost 100% stability up to 350°C. Results of similar nature where MIPs maintain more than 80% of its weight at temperatures above 300°C have been reported in literature [27–29]. These observations are an indication that the polymer can be used under extreme environmental conditions without degradation.

3.2 Optimization results

3.2.1 Method validity and interactive effects

The performance of the design model and its fit-for-purpose summary is presented visually in Fig. 2. The coefficient plots in Fig 2A show that initial concentration of the ARVD in solution, the mass of the MMIP used as the sorbent and the time it remains in contact with efavirenz had a positive significant effect on the adsorption kinetics. However, a change in pH of the solution seemed to have a minimal effect which is similar to other studies from the literature [5]. The coefficient plots further show that most factors had minimal dependence on interactive effects except for the pH*pH dual interaction which led to a significant negative effect on the MMIP's

performance, while the MMIP*MMIP interaction had a significantly positive effect. The reliability of these observations is presented as a summary of fit plots (Fig. 2B). Acceptable values for coefficient of determination (R^2), predictive relevance (Q^2), and reproducibility were observed for the model with $R^2 = 0.890$, $Q^2 = 0.833$ and reproducibility of 0.99 indicating minimal error in the response output. The negative value of the model validity in Fig. 2B does not necessarily imply an incorrect model form but rather represents an artificial lack of fit since acceptable values are observed for R^2 , Q^2 and reproducibility. This implies that the model error is still in the same range as the pure error, therefore it can be utilized as a valid model.

Surface response outputs obtained through simultaneous investigation of effects of initial concentration, contact time, sample pH and mass of MMIP were visualized in form of contour plots as shown in Fig. 2C. From the plots, it was observed that initial concentration, mass of the MMIP and contact time had a direct effect on the amount of efavirenz extracted from solution which corroborated with the results of coefficient plots in Fig 2A. As for pH, efavirenz was adsorbed better under neutral conditions with both basic and acidic conditions resulting in less adsorption.

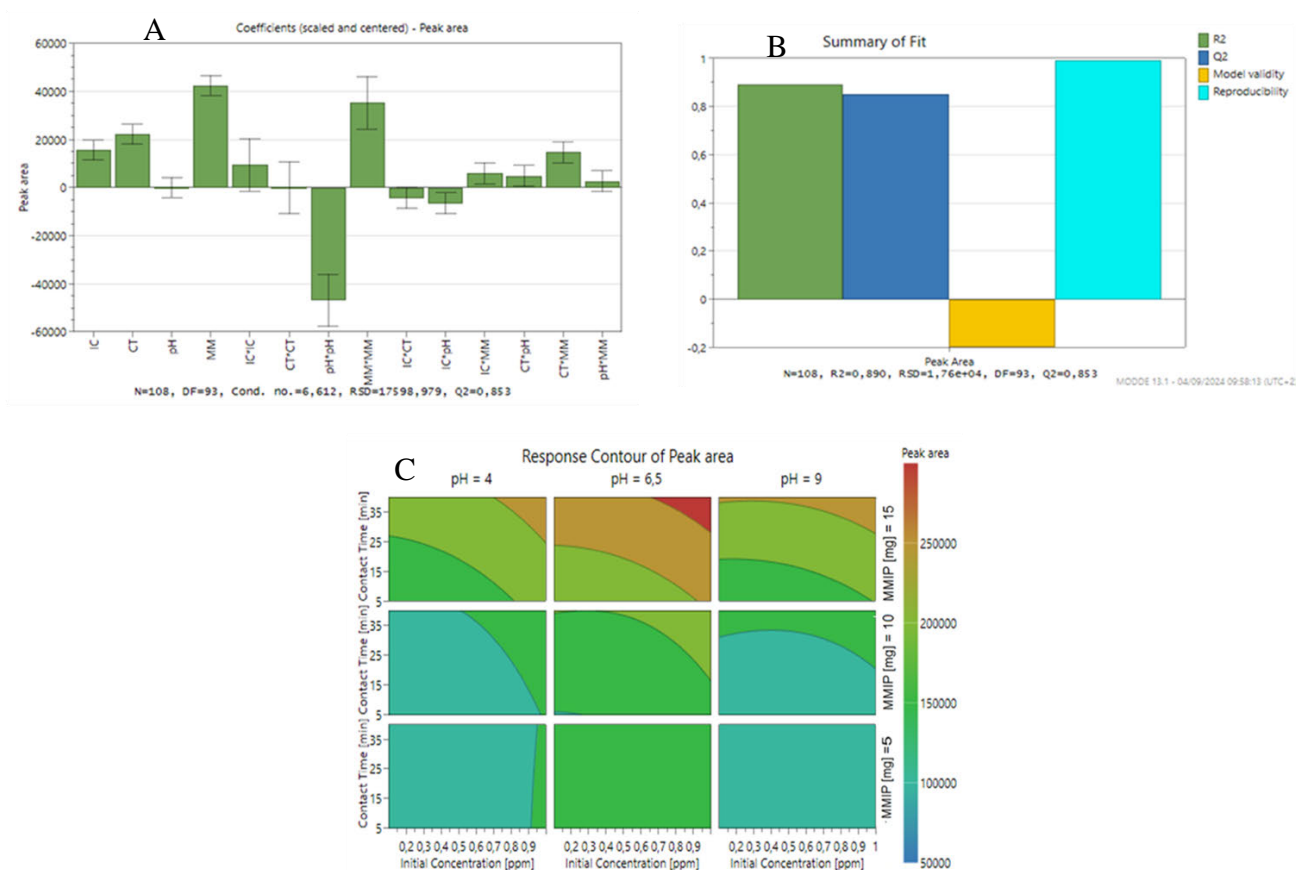


Fig. 2 Coefficient plots (A), summary of fit (B) and contour plots (C) of the optimized factors. IC – initial concentration; CT – contact time; MM – mass of the magnetic molecularly imprinted polymer.

3.2.2 Adsorption kinetics and mechanism

The adsorption of efavirenz followed pseudo second order kinetics (Table 1) suggesting that the interaction between the MMIP and the efavirenz was through chemisorption attaining a maximum adsorption of $44.9 \mu\text{g g}^{-1}$ within 40 min (Fig. 3). Similar adsorption kinetics have been observed where a MMIP was used for extraction of other pharmaceuticals including 17β -estradiol [30]. Other studies on MMIP for pharmaceuticals have obtained faster kinetics including Dai and colleagues who investigated adsorption kinetics of carbamazepine and clofibrac acid and achieved equilibrium after 15 min [31]. When the MMIP was used to bind

nevirapine as an interferent, it was observed that its maximum binding capacity towards nevirapine was just 11.5 ug g^{-1} .

For the adsorption modelling results, it was observed that the Langmuir model was favoured with a higher R^2 value of 0.9975 compared to 0.991 for the Freundlich model (Table 1). The Freundlich model value is still relatively high but Fig. 4B shows that it fails to explain the adsorption mechanism at low concentrations of efavirenz. The Langmuir isotherm model was therefore accepted as the model that explains the extent of adsorption of the efavirenz onto the MMIP cavities. In addition, the R_L value was in the favourable range of $0 < R_L < 1$, while the predicted maximum adsorption capacity of 48.9 ug g^{-1} (Table 1) is comparable with the experimental maximum value of 53.6 ug g^{-1} (Fig. 3). The Langmuir isotherm model assumes that all binding sites are homogeneous with uniform adsorption energy and the adsorption process gives a monolayer coverage. This was an indication that once a MIP cavity is occupied, no further adsorption occurs on that cavity. This agrees with the adsorption kinetic results in which interaction between efavirenz and the MIP cavity functional groups was predicted to occur through chemisorption [12,20,21].

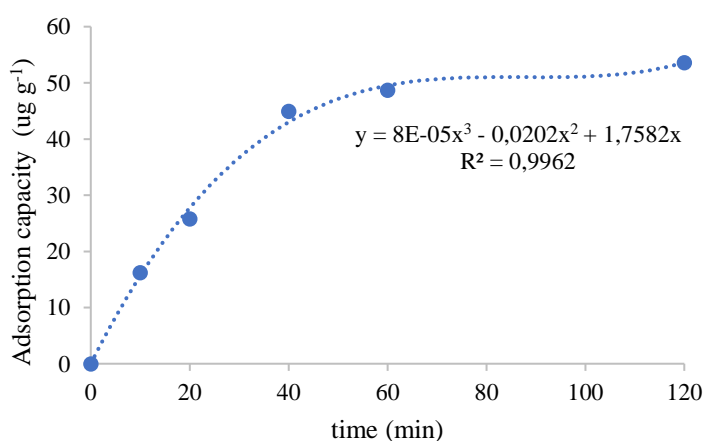


Fig. 3 Effects of contact time on the adsorption capacity. Experimental conditions: initial concentration of efavirenz – 200 ng mL⁻¹, sample pH – 6, adsorbent mass –50 mg and sample volume – 5 mL

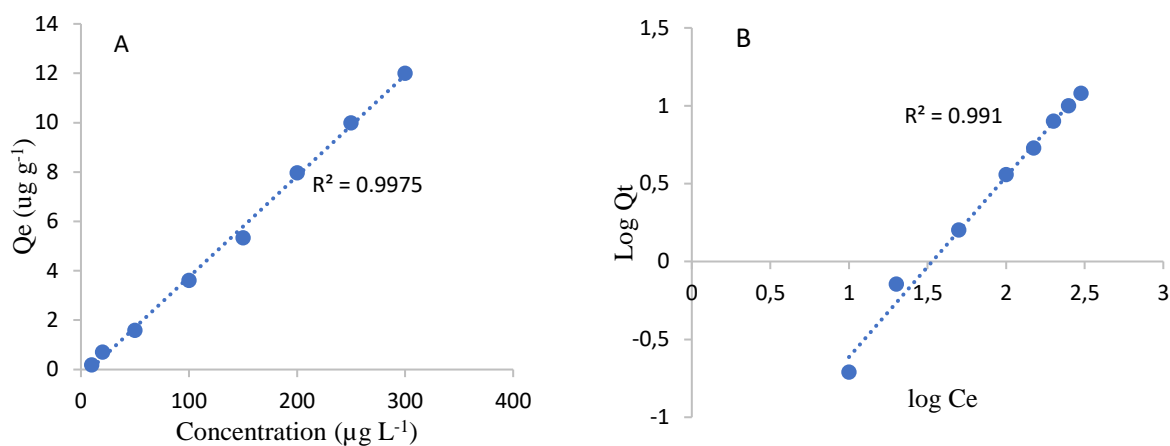


Fig. 4 Effects of initial concentration on the adsorption capacity. A - Langmuir model; B - Freundlich model

Table 1 Modelling results

Pseudo-1 st order		Pseudo-2 nd order		Freundlich model		Langmuir model		
R ²	R ²	K ₂ (g ug ⁻¹ min ⁻¹)		R ²	R ²	K _L (μL g ⁻¹)	R _L	Q _{max} (ug g ⁻¹)
0.9752	0.9833	1.51		0.9910	0.9975	0.1199	0.199	48.9

R² - coefficient of determination; K₂ pseudo-second order constant; q_e - equilibrium adsorption capacity; K_L - the Langmuir equilibrium adsorption constant (L g⁻¹); R_L – the separation factor; Q_{max} - maximum adsorption capacity

3.3 Reusability studies

MMIP regeneration studies in Fig. 5A show a slight gradual decrease in the adsorption capacity if the MMIP is used close to its maximum capacity, however losing only 19% after five consecutive cycles. The reusability of the synthesized MIP corresponds to the behaviour reported in literature for the extraction of abacavir [28]. Minimal loss is observed if the MMIP is used repeatedly at half its binding capacity maintaining an almost 100% reusability (Fig. 5B) which is advantageous considering the concentrations of efavirenz that have been reported in the environment [7,12,21].

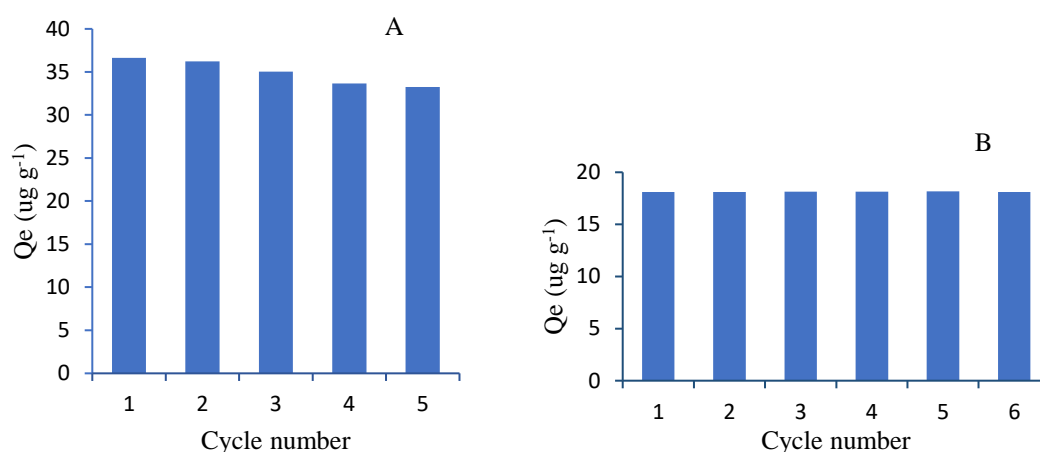


Fig. 5 Reusability of efavirenz in five consecutive cycles at the MMIP maximum binding capacity (A) and at half its capacity (B).

3.4 Application in wastewater samples

3.4.1 Method validation and levels of efavirenz in wastewater effluents

Validation parameters for analysis of efavirenz using GC-TQMS are presented in Table 2. Good sensitivity of the SPE-GC-TQMS was observed with the MDL and MQL for efavirenz at 0.0265 and 0.0804 ng mL^{-1} , respectively. All relative standard deviation values based on triplicate analysis were less than 14%. Most studies have reported LODs such as 0.41 $\mu\text{g L}^{-1}$

[12], and 0.16 ng mL^{-1} , [32]. Studies that report MDLs for efavirenz remain limited in literature [33]. For example, the MDL values were 0.12 and 0.84 ng L^{-1} in river and estuary samples, respectively [11], while 0.70 up to 9 ng L^{-1} have been reported in WWTP effluents using LC-MS [7,10,33].

The amount of efavirenz detected in the effluent using SPE-GC-TQMS was found to be 3.99 ng mL^{-1} (Table 2). The results are comparable with those reported in WWTP effluents across South Africa. In the KwaZulu Natal Province where the current study was conducted, researchers have reported varying concentrations of efavirenz mostly between 0.028 and 34 ng mL^{-1} [7,12,21] while higher concentrations of $46 - 96.11 \text{ ng mL}^{-1}$ have also been recently reported [34]. In other provinces within South Africa, levels of efavirenz in wastewater effluents range between 0.021 and 7.6 ng mL^{-1} [10,35–38]. Nevirapine was not detected in the current study which corroborates with other studies where it was either not detected or just reported in very low levels less than 1.92 ng mL^{-1} [7,10,21,36–39]. Extreme concentrations of up to 92.11 ng mL^{-1} have also been reported [34].

3.4.2 Removal of efavirenz from wastewater effluents

The application of the MMIP as a sorbent that removes efavirenz from undiluted raw wastewater effluents gave an average of 44.8% (Table 2). This performance was considered relatively effective since the effluents were undiluted and unspiked which represented true wastewater effluent with its matrices. These performances are comparable with other advanced treatment processes that have been applied on wastewater effluents for the purposes of removing ARVDs from the effluents. For example, photolysis based on UV/H₂O₂ has been reported to remove between 20 and 50% of nevirapine from effluents [40]. However, other processes that perform better than the current method have been reported in the literature. Adeola and colleagues used graphene wool and reported 80% removal efficiency for efavirenz [5]. An exfoliated graphene sorbent for removal of ARVDs including efavirenz achieved up to

81% efficiency for ARVDs [34]. The same research group further reported up to 86% removal efficiency using activated macadamia nutshells [41]. While the reported sorbents from the literature performed better, the MMIP sorbent used in the current study boasts the magnetic advantage that allows it to be held static and can be removed from the real effluents in the environment using an external magnetic field. It is noteworthy mentioning that most studies that have mentioned recoveries of ARVDs from effluents are almost always done for the purposes of quantitation while studies that report removal efficiencies as a remedial tool remain limited. In this regard, the magnetic sorbent presented in the current study might be a viable remedial approach with potential applicability in the environment.

Table 2 Method validation, concentration of ARVDs in effluents and removal efficiencies

Analyte	SIM ion (m/z)	R ²	Calibration Accuracy (%)	MDL (ng mL ⁻¹)	MQL (ng mL ⁻¹)	*Concentration in effluent (ng mL ⁻¹)	Removal efficiency (% ± RSD%)
Efavirenz	315	0.9908	92.2 - 104.7	0.0265	0.0804	3.99	44.8 ± 11
Nevirapine	266	0.9981	92.3 - 104	0.0331	0.100	n.d	-

n.d - not detected;

*Done using SPE

4 Conclusions

A magnetic smart polymer has been successfully synthesized and applied as a sorbent for efavirenz from wastewater effluents achieving 44.8% removal efficiencies. Its fit for purpose prediction was verified statistically using central composite design outputs such as coefficient plots, summary of fit and contour plots. Although the removal efficiency is still relatively low, the smart sorbent was optimized using environmental wastewater effluent polluted with efavirenz. The sorbent has a further advantage of being magnetized which could permit for its

deployment in the environment and its eventual recovery for reuse using an external magnetic field. The magnetic sorbent has shown great potential and could be a viable alternative to remediation of efavirenz and other ARVDs from surface water sources.

Declaration of interests: The authors declare that they have no known competing financial interests or personal relationships that could have appeared to influence the work reported in this paper.

Funding

This research did not receive any specific grant from funding agencies in the public, commercial, or not-for-profit sectors

Acknowledgment

In loving memory of Nompumelelo Pretty Cele.

References

- [1] T.P. Wood, C.S.J. Duvenage, E. Rohwer, The occurrence of anti-retroviral compounds used for HIV treatment in South African surface water, *Environ. Pollut.* 199 (2015) 235–243. <https://doi.org/10.1016/j.envpol.2015.01.030>.
- [2] L.M. Madikizela, S. Ncube, L. Chimuka, Analysis, occurrence and removal of pharmaceuticals in African water resources: A current status, *J. Environ. Manage.* 253 (2020) 109741. <https://doi.org/10.1016/j.jenvman.2019.109741>.
- [3] W. Gwenzi, N. Chaukura, Organic contaminants in African aquatic systems: current knowledge, health risks and future research directions, *Sci. Total Environ.* 619–620 (2018) 1493–1514. <https://doi.org/10.1016/j.scitotenv.2017.11.121>.

- [4] S. Ncube, L.M. Madikizela, L. Chimuka, M.M. Nindi, Environmental fate and ecotoxicological effects of antiretrovirals: A current global status and future perspectives, *Water Res.* 145 (2018) 231–247. <https://doi.org/10.1016/j.watres.2018.08.017>.
- [5] A.O. Adeola, J. de Lange, P.B.C. Forbes, Adsorption of antiretroviral drugs, efavirenz and nevirapine from aqueous solution by graphene wool: Kinetic, equilibrium, thermodynamic and computational studies, *Appl. Surf. Sci. Adv.* 6 (2021) 100157. <https://doi.org/10.1016/j.apsadv.2021.100157>.
- [6] B. Moslah, E. Hapeshi, A. Jrad, D. Fatta-kassinou, Pharmaceuticals and illicit drugs in wastewater samples in north-eastern Tunisia, *Environ. Sci. Pollut. Res.* 25 (2018) 18226–18241. <https://doi.org/10.1007/s11356-017-8902-z>.
- [7] O.A. Abafe, J. Späth, J. Fick, S. Jansson, C. Buckley, A. Stark, B. Pietruschka, B.S. Martincigh, LC-MS/MS determination of antiretroviral drugs in influents and effluents from wastewater treatment plants in KwaZulu-Natal, South Africa, *Chemosphere* 200 (2018) 660–670. <https://doi.org/10.1016/j.chemosphere.2018.02.105>.
- [8] C. Nannou, A. Ofrydopoulou, E. Evgenidou, D. Heath, E. Heath, D. Lambropoulou, Analytical strategies for the determination of antiviral drugs in the aquatic environment, *Trends Environ. Anal. Chem.* 24 (2019) e00071. <https://doi.org/10.1016/j.teac.2019.e00071>.
- [9] R. Wang, J. Luo, C. Li, J. Chen, N. Zhu, Antiviral drugs in wastewater are on the rise as emerging contaminants: A comprehensive review of spatiotemporal characteristics, removal technologies and environmental risks, *J. Hazard. Mater.* 457 (2023) 131694. <https://doi.org/10.1016/j.jhazmat.2023.131694>.
- [10] C. Schoeman, M. Dlamini, O.J. Okonkwo, The impact of a wastewater treatment works

- in southern Gauteng, South Africa on efavirenz and nevirapine discharges into the aquatic environment, *Emerg. Contam.* 3 (2017) 95–106. <https://doi.org/10.1016/j.emcon.2017.09.001>.
- [11] R. Netshithothole, L.M. Madikizela, Occurrence of selected pharmaceuticals in the East London coastline encompassing major rivers, estuaries, and seawater in the Eastern Cape Province of South Africa, *ACS Meas. Sci. Au* 4 (2024) 283–293. <https://doi.org/10.1021/acsmesuresciau.4c00004>.
- [12] S.P. Mtolo, P.N. Mahlambi, L.M. Madikizela, Synthesis and application of a molecularly imprinted polymer in selective solid-phase extraction of efavirenz from water, *Water Sci. Technol.* 79 (2019) 356–365. <https://doi.org/10.2166/wst.2019.054>.
- [13] J.J. Belbruno, Molecularly imprinted polymers, *Chem. Rev.* 119 (2019) 94–119. <https://doi.org/10.1021/acs.chemrev.8b00171>.
- [14] C. Dong, H. Shi, Y. Han, Y. Yang, R. Wang, J. Men, Molecularly imprinted polymers by the surface imprinting technique, *Eur. Polym. J.* 145 (2021) 110231. <https://doi.org/10.1016/j.eurpolymj.2020.110231>.
- [15] M. Sobiech, K. Synoradzki, T.J. Bednarchuk, K. Sobczak, M. Janczura, J. Giebułtowicz, P. Luliński, Impact of structure and magnetic parameters of nanocrystalline cores on surface properties of molecularly imprinted nanoconjugates for analysis of biomolecules – A case of tyramine, *Microchem. J.* 179 (2022). <https://doi.org/10.1016/j.microc.2022.107571>.
- [16] M.S. Eissa, M.S. Imam, M. Abdelrahman, M.M. Ghoneim, M. Abdullah, R. Bayram, H.M. Ali, N.S. Abdelwahab, M. Gamal, Magnetic molecularly imprinted polymers and carbon dots molecularly imprinted polymers for green micro-extraction and analysis of pharmaceuticals in a variety of matrices, *Microchem. J.* 205 (2024) 111235.

- <https://doi.org/10.1016/j.microc.2024.111235>.
- [17] Y. Liu, L. Wang, H. Li, L. Zhao, Y. Ma, Y. Zhang, J. Liu, Y. Wei, Rigorous recognition mode analysis of molecularly imprinted polymers—Rational design, challenges, and opportunities, *Prog. Polym. Sci.* 150 (2024). <https://doi.org/10.1016/j.progpolymsci.2024.101790>.
- [18] S.I. Kaya, A. Cetinkaya, S.A. Ozkan, Molecularly imprinted polymers as highly selective sorbents in sample preparation techniques and their applications in environmental water analysis, *Trends Environ. Anal. Chem.* 37 (2023) e00193. <https://doi.org/10.1016/j.teac.2022.e00193>.
- [19] R. Nisticò, Magnetic materials and water treatments for a sustainable future, *Res. Chem. Intermed.* 43 (2017) 6911–6949. <https://doi.org/10.1007/s11164-017-3029-x>.
- [20] S. Khulu, S. Ncube, Y. Nuapia, L.M. Madikizela, H. Tutu, H. Richards, K. Ndungu, E. Mavhunga, L. Chimuka, Multivariate optimization of a two-way technique for extraction of pharmaceuticals in surface water using a combination of membrane assisted solvent extraction and a molecularly imprinted polymer, *Chemosphere* 286 (2022) 131973. <https://doi.org/10.1016/j.chemosphere.2021.131973>.
- [21] T. Xolo, P. Mahlambi, Molecularly imprinted polymers as solid-phase and dispersive solid-phase extraction sorbents in the extraction of antiretroviral drugs in water: adsorption, selectivity and reusability studies, *J. Anal. Sci. Technol.* 15 (2024). <https://doi.org/10.1186/s40543-024-00418-4>.
- [22] S. Sigonya, T.C. Mokhena, P.M. Mayer, P.S. Mdluli, T.R. Makhanya, T.H. Mokhothu, Synthesis of a multi-template molecular imprinted bulk polymer for the adsorption of non-steroidal inflammatory and antiretroviral drugs, *Appl. Sci.* 14 (2024). <https://doi.org/10.3390/app14083320>.

- [23] M.A. Al-ghouti, D.A. Da, Guidelines for the use and interpretation of adsorption isotherm models: A review, *J. Hazard. Mater.* 393 (2020) 122383. <https://doi.org/10.1016/j.jhazmat.2020.122383>.
- [24] M. Patel, R. Kumar, K. Kishor, T. Mlsna, C.U. Pittman, D. Mohan, Pharmaceuticals of emerging concern in aquatic systems: Chemistry, occurrence, effects, and removal methods, *Chem. Rev.* 119 (2019) 3510–3673. <https://doi.org/10.1021/acs.chemrev.8b00299>.
- [25] S. Bakhtiar, S.A. Bhawani, S.R. Shafqat, Synthesis and characterization of molecular imprinting polymer for the removal of 2-phenylphenol from spiked blood serum and river water, *Chem. Biol. Technol. Agric.* 6 (2019) 1–10. <https://doi.org/10.1186/s40538-019-0152-5>.
- [26] M. Veneranda, J. Aramendia, L. Bellot-Gurlet, P. Colomban, K. Castro, J.M. Madariaga, FTIR spectroscopic semi-quantification of iron phases: A new method to evaluate the protection ability index (PAI) of archaeological artefacts corrosion systems, *Corros. Sci.* 133 (2018) 68–77. <https://doi.org/10.1016/j.corsci.2018.01.016>.
- [27] S.S. Zunngu, L.M. Madikizela, L. Chimuka, P.S. Mdluli, Synthesis and application of a molecularly imprinted polymer in the solid-phase extraction of ketoprofen from wastewater, *Comptes Rendus Chim.* 20 (2017) 585–591. <https://doi.org/10.1016/j.crci.2016.09.006>.
- [28] S.N. Qwane, P.S. Mdluli, L.M. Madikizela, Synthesis, characterization and application of a molecularly imprinted polymer in selective adsorption of abacavir from polluted water, *South African J. Chem.* 73 (2020) 84–91. <https://doi.org/10.17159/0379-4350/2020/V73A13>.
- [29] S. Khulu, S. Ncube, T. Kgame, Synthesis , characterization and application of a

- molecularly imprinted polymer as an adsorbent for solid - phase extraction of selected pharmaceuticals from water samples, *Polym. Bull.* 79 (2022) 1287–1307. <https://doi.org/10.1007/s00289-021-03553-9>.
- [30] L. Bi, J. Shen, Z. Yao, J. Kang, S. Zhao, P. Yan, B. Wang, Preparation and adsorption properties of magnetic molecularly imprinted polymers for selective recognition of 17 β -Estradiol, *Separations* 9 (2022) 1–15.
- [31] C. Dai, J. Zhang, Y. Zhang, Removal of carbamazepine and clofibric acid from water using double templates – molecularly imprinted polymers, (2013) 5492–5501. <https://doi.org/10.1007/s11356-013-1565-5>.
- [32] H. Mokgope, A.L. Taka, M.J. Klink, V.E. Pakade, T. Walmsley, Quantification of some ARVs' removal efficiency from wastewater using a moving bed biofilm reactor, *Water Sci. Technol.* 86 (2022) 2928–2942. <https://doi.org/10.2166/wst.2022.353>.
- [33] L. Yao, W.Y. Dou, Y.F. Ma, Y.S. Liu, Development and validation of sensitive methods for simultaneous determination of 9 antiviral drugs in different various environmental matrices by UPLC-MS/MS, *Chemosphere* 282 (2021) 131047. <https://doi.org/10.1016/j.chemosphere.2021.131047>.
- [34] P.N. Kunene, P.N. Mahlambi, T. Ndlovu, Adsorption of antiretroviral drugs, abacavir, nevirapine, and efavirenz from river water and wastewater using exfoliated graphite: Isotherm and kinetic studies, *J. Environ. Manage.* 360 (2024) 121200. <https://doi.org/10.1016/j.jenvman.2024.121200>.
- [35] R. Netshithothole, M. Managa, T.L. Botha, L.M. Madikizela, Occurrence of selected pharmaceuticals in wastewater and sludge samples from wastewater treatment plants in Eastern Cape province of South Africa, (2024) 7–14.
- [36] T.T. Mosekiemang, M.A. Stander, A. de Villiers, Simultaneous quantification of

- commonly prescribed antiretroviral drugs and their selected metabolites in aqueous environmental samples by direct injection and solid phase extraction liquid chromatography - tandem mass spectrometry, *Chemosphere* 220 (2019) 983–992. <https://doi.org/10.1016/j.chemosphere.2018.12.205>.
- [37] V. Mhuka, S. Dube, M.M. Nindi, Occurrence of pharmaceutical and personal care products (PPCPs) in wastewater and receiving waters in South Africa using LC-OrbitrapTM MS, *Emerg. Contam.* 6 (2020) 250–258. <https://doi.org/10.1016/j.emcon.2020.07.002>.
- [38] C. Schoeman, M. Mashiane, M. Dlamini, O. Okonkwo, Quantification of selected antiretroviral drugs in a wastewater treatment works in South Africa using GC-TOFMS, *J. Chromatogr. Sep. Tech.* 06 (2015) 1–8. <https://doi.org/10.4172/2157-7064.1000272>.
- [39] M.N. Akawa, K.M. Dimpe, P.N. Nomngongo, Amine - functionalized magnetic activated carbon as an adsorbent for preconcentration and determination of acidic drugs in environmental water samples using HPLC - DAD, *Open Chem.* 18 (2020) 1218–1229.
- [40] E. Ngumba, A. Gachanja, T. Tuhkanen, Removal of selected antibiotics and antiretroviral drugs during post-treatment of municipal wastewater with UV, UV/chlorine and UV/hydrogen peroxide, *Water Environ. J.* 34 (2020) 692–703. <https://doi.org/10.1111/wej.12612>.
- [41] L. Simelane, P. Mahlambi, S. Rochat, B. Baker, Removal of antiretroviral drugs from wastewater using activated macadamia nutshells: Adsorption kinetics, adsorption isotherms, and thermodynamic studies, *Water Environ. Res.* 96 (2024) 1–16. <https://doi.org/10.1002/wer.11020>.

PAPER 3

Paper 3 is revised version of a manuscript submitted to the Chemistry Africa journal. The title of the manuscript is “**Photodegradation of efavirenz in wastewater effluents using a hybrid TiO₂ – magnetic molecularly imprinted polymer**”.

This manuscript reports the synthesis of titania nanoparticles embedded with a magnetic molecularly imprinted polymer (MMIP/TiO₂) as a photocatalyst in the degradation of efavirenz in wastewater effluents under visible light. The manuscript presents a detailed optimization of the degradation process using a multivariate approach. The photocatalytic degradation kinetics were investigated using river water and wastewater effluents with degradation efficiencies up to 95 and 99%, respectively. The results of the study show that photodegradation using the MMIP/TiO₂ could be a solution for remediation of efavirenz in polluted aqueous environments.

Author contributions

Asenathi Sibali - Experiments, Data analysis, Writing the original draft, Conceptualization.

Thabang Hendrica Mokhothu - Reviewing & editing, Supervision, Conceptualization.

Vusumzi Emmanuel Pakade - Reviewing & editing, Conceptualization.

Ramakwala Christinah Chokwe - Reviewing & editing, Conceptualization.

Somandla Ncube - Reviewing & editing, Supervision, Conceptualization.

Photocatalytic degradation of efavirenz in wastewater effluents using a hybrid TiO₂-magnetic molecularly imprinted polymer.

Asenathi Sibali^a, Devrani Naicker^a, Ramakwala Christinah Chokwe^b, Vusumzi Emmanuel Pakade^b, Precious Nokwethemba Mahlambi^c, Thabang Hendrick Mokhothu^a, Somandla Ncube^{a*}

^aDepartment of Chemistry, Durban University of Technology, P O Box 1334, Durban 4000, South Africa

^bDepartment of Chemistry, University of South Africa, Private Bag X6, Florida, 1710, South Africa

^cDepartment of Chemistry, University of KwaZulu-Natal, Private Bag X01, Pietermaritzburg, 3209, South Africa

*somandlan@dut.ac.za

Abstract

Efavirenz has been frequently detected in wastewater effluents which poses health hazards to human beings and the aquatic organisms that may rely on the rivers and dams that receive the polluted effluents. This study reports the synthesis of titania nanoparticles embedded on a magnetic molecularly imprinted polymer (MMIP/TiO₂) as a photocatalyst for the degradation of efavirenz in wastewater effluents and river water samples. The hybrid MMIP/TiO₂ was synthesized via bulk polymerization of p-vinylbenzoic acid in the presence of TiO₂, magnetite and efavirenz as a template. Pareto charts from factorial designs observed that during the photodegradation process, the initial concentration of efavirenz was more important than the mass of MMIP/TiO₂ and time

of irradiation. Optimum degradation was observed for minimal mass of MMIP/TiO₂ (5 mg) within 15 min of irradiation while efficiencies increased with increase in initial concentration of efavirenz in both wastewater effluents and river water. Irradiation was done using light of 365 nm wavelength after 40 min contact time to ensure efavirenz gets adsorbed onto the polymer cavities before irradiation. The maximum adsorption capacity of the MMIP/TiO₂ in wastewater effluent was 176 µg g⁻¹ while in river water it was 158 µg g⁻¹. High degradation efficiencies up to 95% were observed for efavirenz in river water and 99% in wastewater effluents. The photodegraded could be removed from solution after degradation using an external magnetic field. The results of the study show that photodegradation using the MMIP/TiO₂ could be a solution for remediation of efavirenz from wastewater effluents.

Keywords

efavirenz; photocatalytic degradation; molecularly imprinted polymer; titania; wastewater effluents

1 Introduction

The presence of antiretroviral drugs (ARVDs) in water sources can have implications for the development of drug-resistant strains of viruses and their toxicity to aquatic organisms [1]. Among ARVDs, efavirenz is frequently detected in surface water sources and its concentrations are relatively higher compared to other ARVDs [2]. Efavirenz is a non-nucleoside reverse transcriptase inhibitor which has been widely used in South Africa to treat various mutant strains of HIV since 1998 and is the third most used ARVD worldwide which might explain its frequent detection in the aqueous environment [3].

Efavirenz, like other pharmaceuticals, is released into the environment primarily through wastewater effluents as conventional wastewater treatment processes are not designed to remove complex compounds such as pharmaceuticals. Most pharmaceuticals are only partially removed during water purification [4]. Since efavirenz cannot be completely degraded in conventional WWTPs and has been reported in concentrations as high as 96.11 ng mL^{-1} in effluents [5], the search for other effective yet affordable remedial tools becomes important to minimize its release into the environment. Several researchers have investigated various remedial methods mostly based on adsorption [6], [7] while photocatalytic degradation has recently gained much interest in remediation of pharmaceutical pollutants from aqueous environmental sources [8], [9]. However, the photocatalysts used still have challenges related to selectivity prompting researchers to integrate them with molecularly imprinted polymers (MIPs). The selective advantages of MIPs is widely discussed in literature [10], [11].

Molecularly imprinted photocatalysts and their magnetized core/shell counterparts have attracted considerable interest because of their favorable attributes, such as superparamagnetic properties, outstanding selectivity, and remarkable stability [12], [13]. Various advanced photodegraders have been mentioned in combination with MIPs but titania remains a cheap yet effective choice over other photodegraders [8], [14]. Titania is readily available and non-

corrosive in an aqueous solution and the degradation products are largely non-toxic. Furthermore, the titania photocatalysts perform exceptionally well in the photocatalytic degradation of organics in wastewater and offer the benefits of high catalytic activity, high safety, and non-toxicity [15]. As of now there is no photocatalyst that is accepted universally for removal of pollutants from the aqueous environment which prompts for more studies.

In the current study, a hybrid photodegrader was synthesized focusing on the combination of an imprinted polymer and titania to determine its potential as a remedial tool for removing efavirenz from wastewater effluents. The MIP cavities were created using efavirenz as a template. The magnetic MIP impregnated with titania (MMIP/TiO₂) was synthesized by bulk polymerization using p-vinylbenzoic acid as a monomer, efavirenz as a template, magnetite as a magnetic material and TiO₂ as the photodegrading nanomaterial. Optimization studies to determine the best conditions for initial concentration of efavirenz, the MMIP/TiO₂ dosage and the contact time were done based on multivariate analysis.

2 Methods and materials

2.1 Chemicals and Reagents

Analytical grade efavirenz as well as all organic solvents of HPLC grade acetonitrile, methanol, ethanol, ethyl acetate, dimethylformamide (DMF) and toluene) were purchased from Merk Pty Ltd, Johannesburg, South Africa. Chemicals for synthesis of the MMIP/TiO₂ including efavirenz, p-vinyl benzoic acid, ethylene glycol dimethacrylate (EGDMA), 32% hydrochloric acid (HCl), 1,1'-azobis(isobutyronitrile) (AIBN), titanium tetraisopropoxide (TTIP), FeCl₃.6H₂O and FeSO₄.7H₂O were also purchased from Merk Pty Ltd, Johannesburg, South Africa.

2.2 Instrumentation and method validation

The analysis of efavirenz was done using high-performance liquid chromatography coupled with a diode array detector (HPLC-DAD). The column used was a Phenomenex kinetex Gemini® C18 5 μm (150 x 4.6 mm). The mobile phase gradient composed of 25% ultrapure water and 70% acetonitrile in isocratic mode. The injection volume was 20 μL at a flow rate of 1 mL min^{-1} for 7 min. The detector wavelength was set at 247 nm. The HPLC-DAD was calibrated with 10 standard solutions of efavirenz in the concentration range of 0.1 - 1.0 mg L^{-1} with the calibration curve attaining linearity value of 0.9964. The sensitivity of the analytical method computed using the linear regression approach gave a limit of detection of 2.15 $\mu\text{g L}^{-1}$ and limit of quantitation of 7.46 $\mu\text{g L}^{-1}$.

2.3 Synthesis of titania

TiO_2 was synthesized using a sol-gel method. Initially, 14 mL of titanium isopropoxide was added in a beaker followed by addition of 120 mL ethanol and stirring for 30 min (solution A). In a different beaker, 2 mL of 2 M HCl was added to 4 mL of deionized water and gently mixed (solution B). Solution B was then added dropwise to solution A and left to stir at room temperature until a gel was formed. The gel was transferred to an oven at 100°C and left to dry for 24 h. The gel was finally calcined at 550°C for 4 h to remove the volatile substances.

2.4 Synthesis of a hybrid nanocomposite

The MMIP/ TiO_2 was obtained via bulk polymerization on the surface of TiO_2 and magnetite nanoparticles. In the pre-polymerization stage, 23.2 mg of efavirenz was dissolved in 3 mL dimethylformamide at 40°C followed by 41 mg of p-vinyl benzoic acid. TiO_2 (200 mg) and magnetite (0.2 mg) were then added into the mixture followed by mild ultrasonication for 15 min. Finally, 208 μL of EGDMA was added and the temperature raised to 70°C. After 10 min, the temperature was increased to 90°C under vacuum and the polymerization process was

initiated with 100 mg of the AIBN under a nitrogen gas atmosphere. After 4 h, the polymer was transferred into an oven at 70°C and allowed to dry for 12 h. The MMIP/TiO₂ polymer was then crushed into a fine powder of <150 µm, washed with methanol/acetic acid (9:1 v/v) to remove efavirenz leaving cavities whose size and position of functional groups complementary to efavirenz. The washed polymer was returned to the oven for 2 h.

2.5 Photodegradation optimization

The interactive effects of three factors that could affect the adsorption of efavirenz from aqueous solution were optimized simultaneously using a full factorial design created on Minitab 18 statistical software. The three factors were initial concentration of efavirenz, MMIP/TiO₂ dosage and contact time. On the software, initial concentration was set between 20 and 60 µg L⁻¹, MMIP/TiO₂ between 5 and 15 mg, and contact time was from 20 - 40 min. Importantly, the initial concentration range inputted in the design falls within the environmentally relevant concentrations of efavirenz in South Africa aqueous systems where researches have reported up to 96.11 µg L⁻¹ [5], [16]–[21]. The design output composed of 20 randomized experiments based on 8 cube points, 6 centre points in the cube and 1 replicate run. The experiments were then carried out in triplicate and the degradation efficiency was given as the response factor. All experiments were carried out in darkness and the effluent MMIP/TiO₂ mixture was illuminated with light of 365 nm wavelength from a LABOQUIP UV-A lamp. The MMIP/TiO₂ was separated from the solution using a magnet and the concentration of the remaining solution was analysed using HPLC-DAD. The degradation efficiency was calculated using Eq. 1.

$$\text{Degradation efficiency} = \frac{(C_o - C_f)}{C_o} \times 100\% \quad (1)$$

where C_o and C_f are the initial and final concentration of efavirenz, respectively.

2.6 Adsorption kinetics

Before investigating the factors that affect photodegradation, it was important to investigate the kinetics of adsorption of efavirenz on to the sorbent. The idea was to determine the minimum time needed for efavirenz to enter the sorbent cavities before effecting photodegradation. To investigate the kinetics before irradiation, 50 mg mass of the MMIP/TiO₂ was added in 24 vials containing 10 mL of wastewater effluent spiked at 1 mg L⁻¹ of efavirenz. Three vials were randomly collected for analysis at specific times over a period of 5 to 120 min. The experiments were repeated using spiked river water. Wastewater was not filtered while the river water was quite dirty and needed to be filtered before use. The analysis data was also used to determine the mechanism of adsorption of efavirenz on the MMIP/TiO₂ cavities based on Eq. 2 & 3 that represent the linearized forms of the pseudo-first and second order models, respectively.

$$\ln(q_e - q_t) = \ln q_e - k_1 t$$

(2)

$$t/q_e = 1/k_2 q_e^2 + t/q_e$$

(3)

where k_1 and k_2 are the rate constants for the pseudo first- and second-order models (min⁻¹), respectively.

3 Results and discussion

3.1 Characterization results

Characterization results for MMIP/TiO₂ after immersion in efavirenz solution using the Zeiss Ultra Plus Field Emission Gun Scanning Electron Microscopy (Tokyo, Japan) in tandem with

Energy Dispersive X-ray Spectroscopy (SEM-EDS) are shown in Fig 1. The SEM results show a rough surface for the imprinted polymer (Fig 1A) while the EDS identified elementary composition of the polymer. Ti, Fe and Cl which relate to the presence of titania, magnetite and efavirenz, respectively were identified within the polymer. The three important elements (Ti, Fe and Cl) were all identified using EDS with weight percentages of 0.26, 0.17 and 0.17%, respectively as shown in Fig 1. The detection of Cl may suggest the presence of efavirenz molecules within the MMIP/TiO₂ trapped within the MIP cavities before photodegradation. Generally, C and O contributed the highest percentage weights recording 77.38 and 20.33%, respectively. The presence of Cu and Ca could be due to the purity of the analytical grade chemicals used during synthesis of the MMIP/TiO₂.

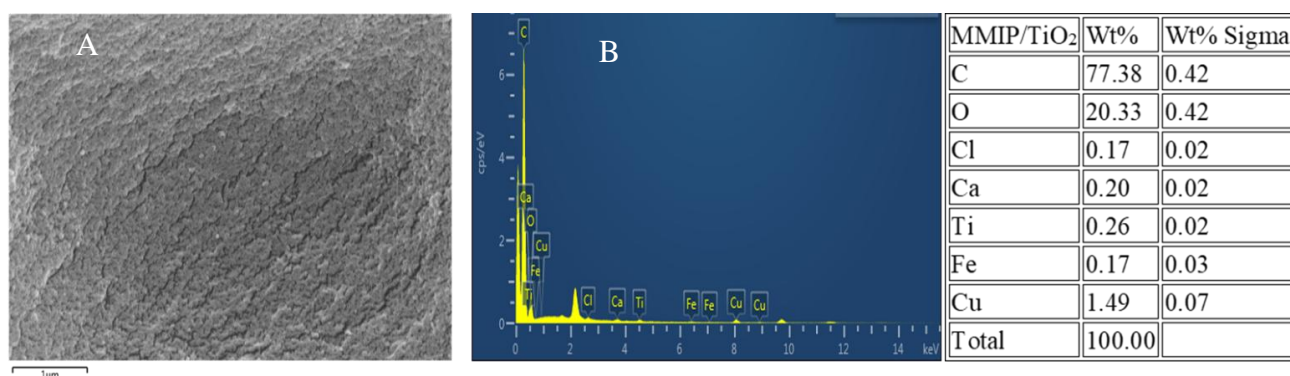


Fig 1. Characterization results using SEM-EDX showing surface (A) and the elementary composition (B) of the hybrid MMIP/TiO₂ polymer.

3.2 Adsorption kinetics and mechanism

The adsorption of efavirenz followed pseudo second order kinetics (Table 2) indicating that the interaction between the MMIP/TiO₂ and the efavirenz was through chemisorption attaining a maximum adsorption capacity of 176 μg g⁻¹ for wastewater effluent and 158 μg g⁻¹ in river water within 40 min (Fig 2). The adsorption capacity of the hybrid (MMIP/TiO₂) was greater than that of the MMIP alone (48.8 μg g⁻¹), probably because of the presence of 200 mg of TiO₂ nanoparticles that offer more surface area to the polymer. The same MMIP was previously

observed to adsorb efavirenz followed a Langmuir isotherm forming a monolayer on the surface cavities [19]. This is in agreement with the kinetics observed during the current study. Better adsorption capacities for pharmaceuticals in deionized water using MIP/TiO₂ nanosorbents and their doped versions have been reported for pollutants including 4.5 mg g⁻¹ for atrazine [22] and 24.54 mg g⁻¹ for chlorotetracycline [23].

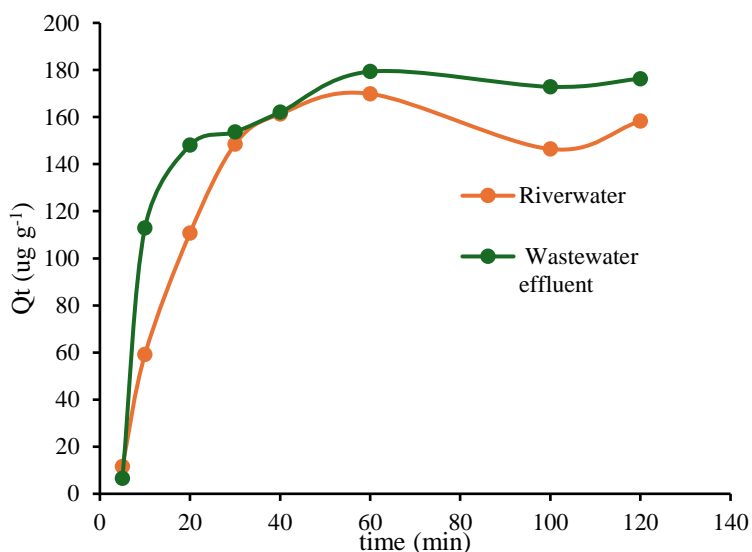


Fig 2. Effects of contact time on the adsorption capacity. Experimental conditions: initial concentration of efavirenz – 1 mg. L⁻¹, MMIP/TiO₂ dosage – 50 mg and sample volume – 10 mL for both wastewater effluent and river water.

Table 2. Modelling results

Sample	R ²	
	Pseudo 1 st order	Pseudo 2 nd order
River water	0.8740	0.9883
Wastewater effluent	0.8693	0.9945

3.3 Optimization and degradation kinetics

The Pareto chart analysis shown in Fig 3 illustrates the percentage level of the influence of each variable independently and their interaction on the response. The initial concentration of efavirenz was the main independent factor affecting photodegradation of efavirenz significantly in both wastewater effluent and river water samples. The pareto charts also show that time of irradiation had a small significant effect on the response in river water while in wastewater effluent it shows that mass of MMIP/TiO₂ had a small effect on the response. The results are similar to the one for tenofovir mineralization even though the significant factors were contact time and initial concentration [24].

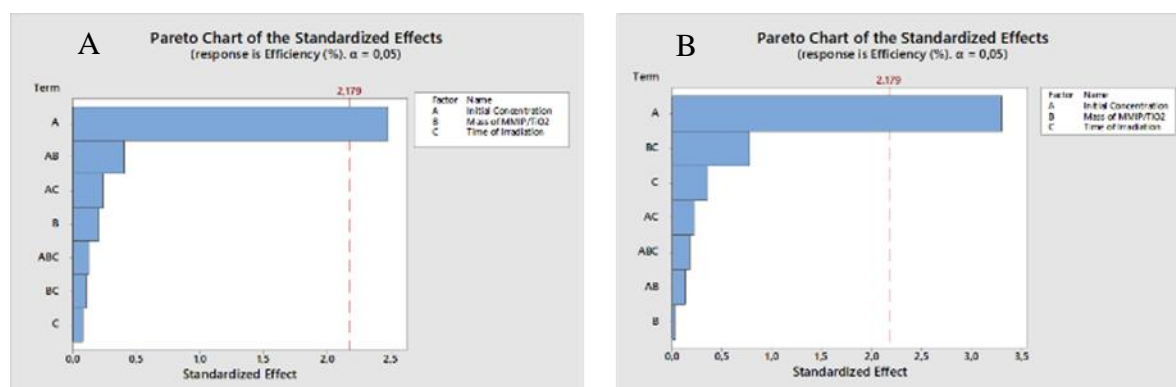


Fig 3. Factor effects for photodegradation of efavirenz in river water (A) and wastewater (B).

The results of the Pareto charts are supported by the contour plots in Fig 4. For example, Fig 4A & D, which represent the interactive effects of initial concentration and MMIP/TiO₂ dose for wastewater and river water, respectively clearly show that an increase in concentration resulted in better degradation efficiencies while the MMIP/TiO₂ dosage remained insignificant. This could be a result of matrix effects that limit the sorption of efavirenz onto the MIP cavities when concentrations are low. However, for wastewater effluents the degradation efficiencies at low efavirenz concentrations were still very high (80%) at lower concentrations of efavirenz (Fig 4A), while they were about 40% for efavirenz in river water. Importantly, the river water

was dirtier and had to be filtered before use during optimization experiments. The same trend was observed for interactive effects of concentration of efavirenz and the time of irradiation (Fig 4B & E).

In both samples, optimum photodegradation was attained within 15 min of irradiation. These observations are in contrast to those reported for nevirapine where the researchers reported a decrease in degradation efficiencies [25]. In their study, the authors had spiked water with very high concentrations of nevirapine (5 - 20 ppm) compared to 0.02 - 0.06 ppm (20 - 60 $\mu\text{g L}^{-1}$) in the current study. It is important to point out that the efavirenz concentration investigated in this study falls within the environmental concentrations reported in literature [2], [5], and real wastewater effluents and river water were used. The 15-min optimum degradation time is similar to what has been reported in literature in which MIP/TiO₂ was used including the degradation of sulfamethoxazole [26], sulfasalazine [27], and diclofenac [28], while most of the studies using MIP/TiO₂ for degradation of pharmaceuticals have reported longer times in the 50 - 180 min range [8].

In Fig 4C & F, which represent the interactive effects of the less important factors (MMIP/TiO₂) dosage and time of irradiation), the contour plots for wastewater effluents represented degradation efficiencies above 92% while for river water they were above 60% in the entire optimization range. Larger amounts of MMIP/TiO₂ dosage gave lower degradation efficiencies probably due to agglomeration effects. For river water samples, a ridge contour response was observed (Fig 4F) in which similar degradation effects were observed when MMIP/TiO₂ dosage was low over a short period but also when the dosage was high after a long contact time. The plot of relative concentration of efavirenz in solution with degradation time given in Fig 5 shows fast degradation kinetics within 20 min.

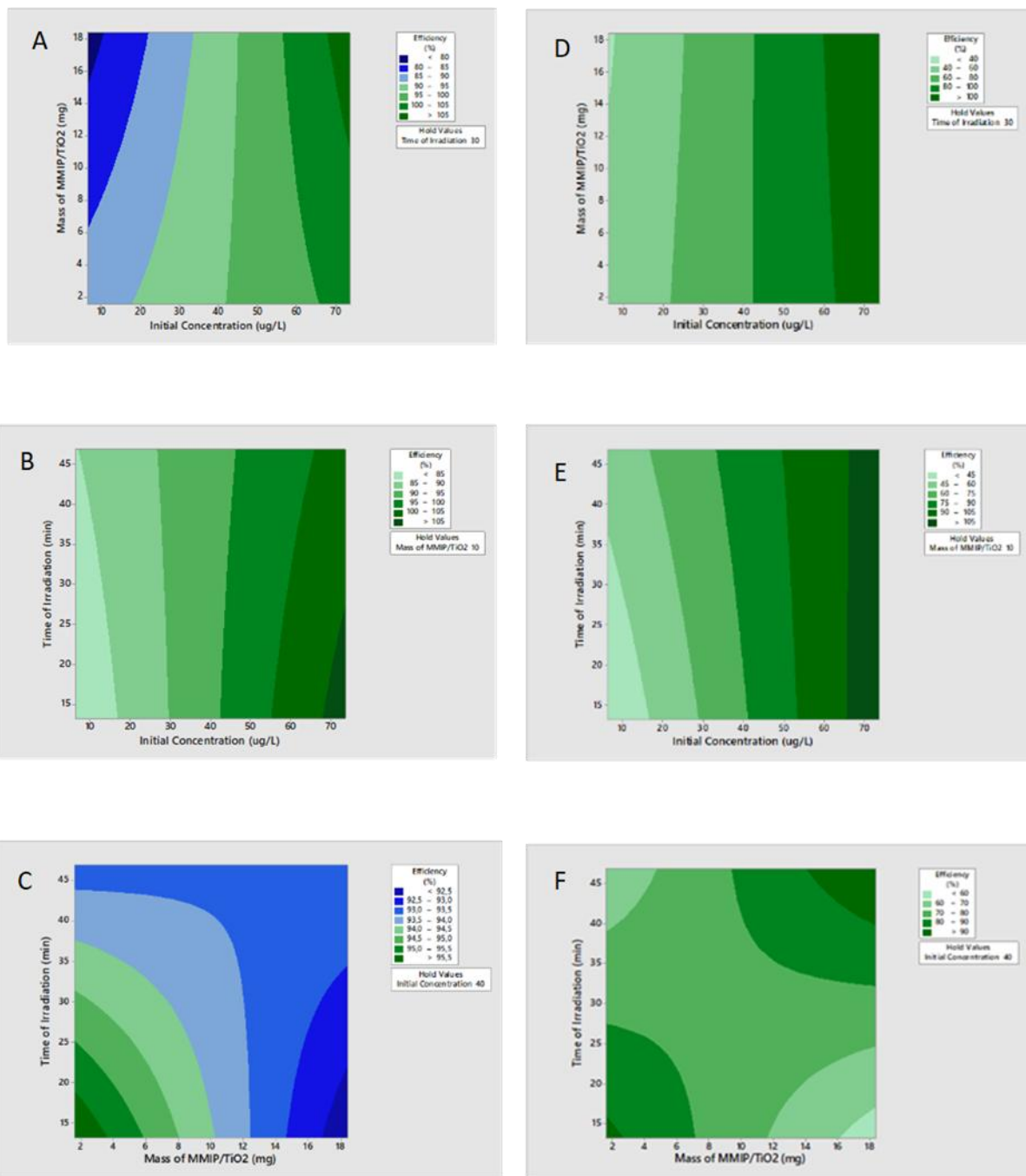


Fig 4. Interactive effects of factors for efavirenz in wastewater (A – C) and in river water (D – F).

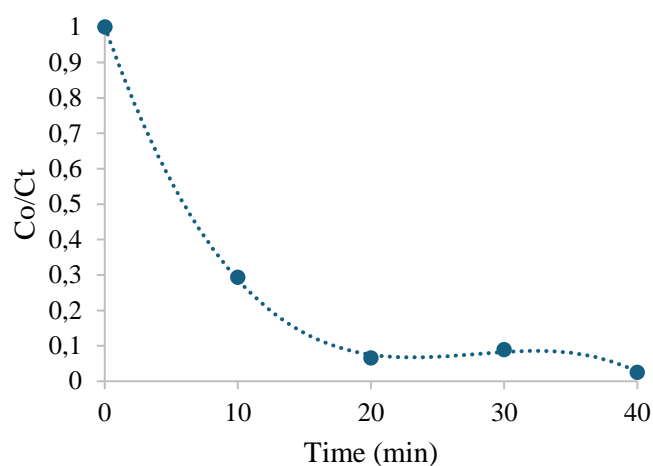


Fig 5. Degradation kinetics for efavirenz in wastewater effluents using UV light of 365 nm wavelength.

3.4 Degradation results

From the optimization studies, it was observed that degradation efficiency of efavirenz in wastewater effluent samples was up to 99% while in river water it was 95%. The river water samples were dirtier than the wastewater effluents which could explain this observation. In addition, the maximum adsorption capacity was higher in wastewater effluents compared to river water samples (Fig 2). While this is the first study that reports photocatalytic degradation of ARVDs using a MIP/TiO₂ photodegrader, similar efficiencies have been reported for other pharmaceuticals [8]. For example, degradation of sulfadiazine and sulfamethoxazole was 99.9% using MIP/TiO₂ [26]. A hybrid MMIP/TiO₂@g-C₃N₄ achieved 96.8% degradation of sulfamethoxazole [29], while another study reported 99.25% degradation of sulfadiazine using N-TiO₂/C/MIP [30]. Lower degradation efficiencies have been reported where TiO₂ was used without molecular imprinting. For example, one study reported 84% degradation efficiency of efavirenz in water using a doped silver nano catalyst [31]. Other studies have used UV/TiO₂/H₂O₂ nanocatalysts for other ARVDs achieving 89.23% degradation for nevirapine

[32] and 87.1% for lamivudine [33]. The results of the current therefore show that molecularly imprinted TiO_2 photocatalysts perform better as remediation tools for ARVDs in wastewater effluents. Conventional wastewater treatment processes are inefficient in preventing exit of efavirenz from wastewater treatment plants, and a magnetic photodegrader imprinted with cavities specific for efavirenz and deployed at the effluent exit point could help reduce entry of efavirenz into effluent-receiving rivers.

4 Conclusion and recommendations

A hybrid MMIP/ TiO_2 nanocomposite was successfully synthesized and optimized using multivariate approaches. It was then applied to degrade efavirenz in wastewater effluents spiked at environmentally relevant concentrations with the degradation efficiencies reaching 99% in wastewater effluents and 95% in polluted river water samples. The response surface model showed that initial concentration of efavirenz was the most significant factor with degradation efficiencies relatively lower in trace concentrations of efavirenz. Generally, the magnetic component of the nanocomposite allows it to be deployed in exit points of wastewater effluents and kept static using an external magnetic field. The MIP component allows for selective isolation of efavirenz from solution and bringing it close to TiO_2 embedded within the polymer matrix. The degradation process is continuous because as the efavirenz gets degraded, the degradation products move out of the cavities allowing the MIP to adsorb more efavirenz. The hybrid MMIP/ TiO_2 has proven to be a viable remediation tool that could prevent efavirenz from entering surface water systems through wastewater effluents. Considering that the current study was done in a laboratory scale, it would be important to perform further studies to upscale the MMIP/ TiO_2 for application in wastewater treatment plants. More studies are required to better understand the economic aspects as well as the stability of the sorbent and the potential environmental implications due to unintended leaching of its components into

the environment. The capabilities of the sorbent towards other ARVDs and different matrices can also be explored.

Declarations: The authors declare that they have no known competing financial interests or personal relationships that could have appeared to influence the work reported in this paper.

Funding: The authors did not receive support from any organization for the submitted work.

Ethical approval: Not applicable

Informed consent: Not applicable

References

- [1] B. Chimukangara *et al.*, “Trends in pretreatment HIV-1 drug resistance in antiretroviral therapy-naive adults in South Africa, 2000–2016: A pooled sequence analysis,” *EClinicalMedicine*, vol. 9, pp. 26–34, 2019, doi: 10.1016/j.eclinm.2019.03.006.
- [2] C. Nannou, A. Ofrydopoulou, E. Evgenidou, D. Heath, E. Heath, and D. Lambropoulou, “Antiviral drugs in aquatic environment and wastewater treatment plants: A review on occurrence, fate, removal and ecotoxicity,” *Sci. Total Environ.*, vol. 699, p. 134322, 2020, doi: 10.1016/j.scitotenv.2019.134322.
- [3] M. M. Bastos, C. C. P. Costa, T. C. Bezerra, F. D. C. Da Silva, and N. Boechat, “Efavirenz a nonnucleoside reverse transcriptase inhibitor of first-generation: Approaches based on its medicinal chemistry,” *Eur. J. Med. Chem.*, vol. 108, pp. 455–465, 2016, doi: 10.1016/j.ejmech.2015.11.025.
- [4] O. Frédéric and P. Yves, “Pharmaceuticals in hospital wastewater: Their ecotoxicity and

- contribution to the environmental hazard of the effluent,” *Chemosphere*, vol. 115, no. 1, pp. 31–39, 2014, doi: 10.1016/j.chemosphere.2014.01.016.
- [5] P. N. Kunene, P. N. Mahlambi, and T. Ndlovu, “Adsorption of antiretroviral drugs, abacavir, nevirapine, and efavirenz from river water and wastewater using exfoliated graphite: Isotherm and kinetic studies,” *J. Environ. Manage.*, vol. 360, no. May, p. 121200, 2024, doi: 10.1016/j.jenvman.2024.121200.
- [6] N. A. Ahammad, M. A. Ahmad, B. H. Hameed, and A. T. Mohd Din, “A mini review of recent progress in the removal of emerging contaminants from pharmaceutical waste using various adsorbents,” *Environ. Sci. Pollut. Res.*, vol. 30, no. 60, pp. 124459–124473, 2023, doi: 10.1007/s11356-022-19829-0.
- [7] V. Vinayagam *et al.*, “Sustainable adsorbents for the removal of pharmaceuticals from wastewater: A review,” *Chemosphere*, vol. 300, no. February, 2022, doi: 10.1016/j.chemosphere.2022.134597.
- [8] A. Sibali, T. H. Mokhothu, S. M. Mohomane, V. E. Pakade, R. C. Chokwe, and S. Ncube, “Applications of molecularly imprinted titania-based photocatalysis for degradation of pharmaceutical pollutants in the aqueous environment,” *J. Hazard. Mater. Adv.*, vol. 16, no. August, p. 100513, 2024, doi: 10.1016/j.hazadv.2024.100513.
- [9] X. Li, H. Wei, T. Song, H. Lu, and X. Wang, “A review of the photocatalytic degradation of organic pollutants in water by modified TiO₂,” *Water Sci. Technol.*, vol. 88, no. 6, pp. 1495–1507, 2023, doi: 10.2166/wst.2023.288.
- [10] J. Li, Y. Wang, and X. Yu, “Magnetic molecularly imprinted polymers: synthesis and applications in the selective extraction of antibiotics,” *Front. Chem.*, vol. 9, pp. 1–17, 2021, doi: 10.3389/fchem.2021.706311.

- [11] J. Yi *et al.*, “Targeted degradation of refractory organic pollutants in wastewater based on molecularly imprinted catalytic materials: Adsorption process and degradation mechanism,” *Sep. Purif. Technol.*, vol. 311, no. December 2022, p. 123244, 2023, doi: 10.1016/j.seppur.2023.123244.
- [12] N. Hlongwa, K. M. Gani, S. Kumari, K. Pillay, and F. Bux, “Exploring chlorination as a removal process for antiretroviral drugs (Nevirapine and Efavirenz) from water: Effect of operational parameters, kinetics, and trihalomethane formation,” *J. Water Process Eng.*, vol. 57, no. September 2023, p. 104604, 2024, doi: 10.1016/j.jwpe.2023.104604.
- [13] K. Poonia *et al.*, “Magnetic molecularly imprinted polymer photocatalysts: synthesis, applications and future perspective,” *J. Ind. Eng. Chem.*, vol. 113, pp. 1–14, 2022, doi: 10.1016/j.jiec.2022.05.029.
- [14] D. T. Ruziwa *et al.*, “Pharmaceuticals in wastewater and their photocatalytic degradation using nano-enabled photocatalysts,” *J. Water Process Eng.*, vol. 54, no. March, p. 103880, 2023, doi: 10.1016/j.jwpe.2023.103880.
- [15] X. Li, B. Yang, K. Xiao, H. Duan, J. Wan, and H. Zhao, “Targeted degradation of refractory organic compounds in wastewaters based on molecular imprinting catalysts,” *Water Res.*, vol. 203, no. July, p. 117541, 2021, doi: 10.1016/j.watres.2021.117541.
- [16] T. Xolo and P. Mahlambi, “Molecularly imprinted polymers as solid-phase and dispersive solid-phase extraction sorbents in the extraction of antiretroviral drugs in water: adsorption, selectivity and reusability studies,” *J. Anal. Sci. Technol.*, vol. 15, no. 1, Dec. 2024, doi: 10.1186/s40543-024-00418-4.
- [17] O. A. Abafe *et al.*, “LC-MS/MS determination of antiretroviral drugs in influents and effluents from wastewater treatment plants in KwaZulu-Natal, South Africa,” *Chemosphere*, vol. 200, pp. 660–670, 2018, doi: 10.1016/j.chemosphere.2018.02.105.

- [18] S. P. Mtolo, P. N. Mahlambi, and L. M. Madikizela, "Synthesis and application of a molecularly imprinted polymer in selective solid-phase extraction of efavirenz from water," *Water Sci. Technol.*, vol. 79, pp. 356–365, 2019, doi: 10.2166/wst.2019.054.
- [19] A. Sibali *et al.*, "Removal of efavirenz in wastewater effluents using a magnetic molecularly imprinted polymer: Synthesis, multivariate optimization and application," *J. Water Process Eng.*, vol. 74, no. December 2024, 2025, doi: 10.1016/j.jwpe.2025.107786.
- [20] R. Netshithothole, M. Managa, T. L. Botha, and L. M. Madikizela, "Occurrence of selected pharmaceuticals in wastewater and sludge samples from wastewater treatment plants in Eastern Cape province of South Africa," pp. 7–14, 2024.
- [21] C. Schoeman, M. Mashiane, M. Dlamini, and O. Okonkwo, "Quantification of selected antiretroviral drugs in a wastewater treatment works in South Africa using GC-TOFMS," *J. Chromatogr. Sep. Tech.*, vol. 06, no. 04, pp. 1–8, 2015, doi: 10.4172/2157-7064.1000272.
- [22] H. Shi, Y. Wang, C. Tang, W. Wang, M. Liu, and G. Zhao, "Mechanism investigation on the enhanced and selective photoelectrochemical oxidation of atrazine on molecular imprinted mesoporous TiO₂," *Appl. Catal. B Environ.*, vol. 246, no. January, pp. 50–60, 2019, doi: 10.1016/j.apcatb.2019.01.018.
- [23] R. Liu, X. Han, R. Liu, Z. Qi, B. Ren, and Y. Sun, "Molecularly imprinted Fe₃O₄/g-C₃N₄/TiO₂ catalyst for selective photodegradation of chlorotetracycline," *Colloids Surfaces A Physicochem. Eng. Asp.*, vol. 680, no. October 2023, p. 132691, 2024, doi: 10.1016/j.colsurfa.2023.132691.
- [24] L. C. Motue Waffo *et al.*, "Electrochemical production of sulfate radicals for degradation of Tenofovir in aqueous solution," *Case Stud. Chem. Environ. Eng.*, vol. 6,

- no. July, p. 100235, 2022, doi: 10.1016/j.cscee.2022.100235.
- [25] Y. A. Bhembe *et al.*, “Photocatalytic degradation of nevirapine with a heterostructure of few-layer black phosphorus coupled with niobium (V) oxide nanoflowers (FL-BP@Nb₂O₅),” *Chemosphere*, vol. 261, p. 128159, 2020, doi: 10.1016/j.chemosphere.2020.128159.
- [26] D. Li, R. Yuan, B. Zhou, and H. Chen, “Selective photocatalytic removal of sulfonamide antibiotics: The performance differences in molecularly imprinted TiO₂ synthesized using four template molecules,” *J. Clean. Prod.*, vol. 383, no. December 2022, p. 135470, 2023, doi: 10.1016/j.jclepro.2022.135470.
- [27] S. Mokhtari, H. Faghihian, and M. Mirmohammadi, “A core/shell TiO₂ magnetized molecularly imprinted photocatalyst (MMIP@TiO₂): synthesis and its photodegradation activity towards sulfasalazine,” *Environ. Sci. Pollut. Res.*, vol. 30, no. 5, pp. 13624–13638, 2023, doi: 10.1007/s11356-022-22792-5.
- [28] L. Bi *et al.*, “Selective adsorption and enhanced photodegradation of diclofenac in water by molecularly imprinted TiO₂,” *J. Hazard. Mater.*, vol. 407, no. September 2020, p. 124759, 2021, doi: 10.1016/j.jhazmat.2020.124759.
- [29] J. Y. Zhang *et al.*, “Selective removal of sulfamethoxazole by a novel double Z-scheme photocatalyst: Preferential recognition and degradation mechanism,” *Environ. Sci. Ecotechnology*, vol. 17, p. 100308, 2024, doi: 10.1016/j.es.2023.100308.
- [30] Q. Li *et al.*, “Hollow C, N-TiO₂@C surface molecularly imprinted microspheres with visible light photocatalytic regeneration availability for targeted degradation of sulfadiazine,” *Sep. Purif. Technol.*, vol. 299, no. June, p. 121814, 2022, doi: 10.1016/j.seppur.2022.121814.

- [31] L. Tabana, D. R. Booyens, and S. Tichapondwa, "Photocatalytic degradation of efavirenz and nevirapine using visible light-activated Ag-AgBr-LDH nanocomposite catalyst," *J. Photochem. Photobiol. A Chem.*, vol. 444, no. June, p. 114997, 2023, doi: 10.1016/j.jphotochem.2023.114997.
- [32] P. Ncube, C. Zvinowanda, M. Belaid, and F. Ntuli, "Heterogeneous photocatalytic degradation of nevirapine in wastewater using the UV/TiO₂/H₂O₂ process," *Environ. Process.*, vol. 10, no. 1, pp. 1–24, 2023, doi: 10.1007/s40710-022-00615-6.
- [33] T. An, J. An, H. Yang, G. Li, H. Feng, and X. Nie, "Photocatalytic degradation kinetics and mechanism of antiviral drug-lamivudine in TiO₂ dispersion," *J. Hazard. Mater.*, vol. 197, pp. 229–236, 2011, doi: 10.1016/j.jhazmat.2011.09.077.

GENERAL CONCLUSIONS

Two hybrid polymers, MMIP and MMIP@TiO₂ were successfully synthesized via bulk polymerization. The characterization was done to determine their physiochemical properties. The TGA results showed that the two polymers maintained its weight up to 250°C and then degrade to about 350°C. For the FTIR it was observed that magnetite exhibited typical -OH and Fe-O absorption bands. After co-polymerization, these stretches were suppressed indicating that the magnetite lost the H₂O particles from its surface as it was incorporated into the MIP during co-polymerization. The adsorption kinetics were studied and indicated that pseudo second order was the best fit model with R² of 0.9833 and favoured a Langmuir model with R² of 0.9975. The multivariate optimization was performed to identify the optimum conditions for MIPs performance. The optimum conditions were pH 6, initial concentration 1 mg L⁻¹ and contact time 40min. Re-usability studies were also done and showed that the MMIP can be used up to 5 cycles. The MMIP was applied as a sorbent for removal of efavirenz from wastewater effluents and achieved 44.8% removal efficiencies. It's fit for purpose prediction was verified statistically using central composite design outputs such as coefficient plots, summary of fit and contour plots. Although the removal efficiency was relatively low, the smart sorbent was optimized using environmental wastewater effluent polluted with efavirenz. A hybrid MMIP/TiO₂ smart polymer also successfully synthesized and applied for the photodegradation of efavirenz in wastewater effluents. Incorporation of TiO₂ into the MMIP cavities it gave greater degradation efficiencies of up to 99%. This was obtained using a multivariate optimization where concentration was the only significant factor which explains that an increase in concentration decreases the degradation efficiency of efavirenz in the solution.

APPENDIX FOR PAPER 1

PUBLISHED REVIEW ARTICLE



Applications of molecularly imprinted titania-based photocatalysis for degradation of pharmaceutical pollutants in the aqueous environment

Asenathi Sibali^a, Thabang Hendrica Mokhothu^a, Samson Masulubanye Mohomane^b,
Vusumzi Emmanuel Pakade^c, Ramakwala Christinah Chokwe^c, Somandla Ncube^{a,*}

^a Department of Chemistry, Durban University of Technology, P O Box 1334, Durban 4000, South Africa

^b Department of Chemistry, KwaDlangezwa Campus, University of Zululand, Empangeni 3886, South Africa

^c Department of Chemistry, University of South Africa, Private Bag X6, Florida, 1710, South Africa

ARTICLE INFO

Keywords:

MIPs
TiO₂
Photocatalytic degradation
Pharmaceuticals
Pollution

ABSTRACT

Pharmaceutical residues and their ecotoxicological impact on aquatic organisms are well documented which has forced researchers to shift focus towards finding sustainable pollution control technologies that can effectively control their levels in the environment. Photocatalytic degradation has offered a viable alternative with the ability to eliminate pharmaceutical residues through degradation and eventual mineralization to less-toxic products. Despite its documented successes, photocatalysis still has its challenges that relate to the presence of scavengers of photogenerated radicals and decomposed matrices accumulating on the surface of the photocatalyst. This has led to the incorporation of molecularly imprinted polymers on the surface of the photocatalyst to allow only selected targets to reach the photocatalyst. This review provides a concise yet comprehensive look at the integration of photocatalysis with molecular imprinting technology focussing on titania-based photocatalysts combined with molecularly imprinted polymers for selective degradation of pharmaceutical pollutants in the aqueous environment. The principles, applications, challenges and future directions of molecularly imprinted photocatalytic degradation as a technology for the remediation of pharmaceuticals in aqueous environments are highlighted.

1. Introduction

Photocatalytic degradation represents a promising approach for mitigating environmental pollution by harnessing the power of light and semiconductor catalysts to degrade organic contaminants. As research progresses and technology matures, photocatalysis is expected to play a pivotal role in achieving sustainable development goals related to water and air quality management worldwide. However, there still exists some challenges that have hindered progress towards total acceptance of doped-TiO₂ as an ultimate remedial tool for pollutants in the aqueous environment, and this has opened some avenues for improvement including integration with molecular imprinting technology. Various photocatalysts in combination with molecularly imprinted polymers (MIPs) and their applications in eradicating organic pollutants in general have been presented in literature (Sajini et al., 2019; Ali et al., 2024; Krakowiak et al., 2021; Singh and Borthakur, 2018; Bagheri et al., 2021;

Lai et al., 2018; Chen et al., 2020; Guan et al., 2021; Zhang et al., 2023a; Wang et al., 2023; Koe et al., 2019; Li et al., 2023). Some reviews have detailed synthesis techniques for MIPs modified with TiO₂ and their application in pollution remediation (Sun et al., 2018; Luo et al., 2022). Reviews that touch on different nanostructure-based photocatalysts for degradation of pharmaceuticals (Ruziwa et al., 2023; Majumder et al., 2021), antibiotics (Yi et al., 2023; Basavarajappa et al., 2020; Chen et al., 2022), antivirals (Rana et al., 2024), antipsychotics (Mohamadpour and Mohamadpour, 2024), nonsteroidal anti-inflammatory drugs and analgesics (Vahidifar et al., 2022), and some that target specific pharmaceuticals such as sulfamethoxazole (Musial et al., 2023) have been presented in literature. A recent review also presented studies that have reported remediation of antibiotics using various hybrid MIPs (Mumtaz et al., 2024). The application of photocatalytic degradation and molecular imprinting in environmental pollution research has gained much interest and their integration towards the

Abbreviations: ARG, antibiotic resistant genes; g-C₃N₄, graphitic carbon nitride; MIPs, molecularly imprinted polymers; MOFs, Metal-Organic Frameworks; PEDOT, poly-3,4-ethylenedioxythiophene; POPD, poly-o-phenylenediamine.

* Corresponding author.

E-mail address: SomandlaN@dut.ac.za (S. Ncube).

<https://doi.org/10.1016/j.hazadv.2024.100513>

Received 29 August 2024; Received in revised form 20 October 2024; Accepted 24 October 2024

Available online 28 October 2024

2772-4166/© 2024 The Author(s). Published by Elsevier B.V. This is an open access article under the CC BY-NC license (<http://creativecommons.org/licenses/by-nc/4.0/>).

production of hybrid schemes targeting pharmaceutical pollution is an area that deserves a focussed review. The current review seeks to provide a concise yet comprehensive look at the principles, applications, challenges, and future directions of molecularly imprinted TiO_2 -based photocatalytic degradation of pharmaceutical residues in the environment. It differs from all other reviews in that it is a focussed review that details the integration of titania-based photocatalysts with molecular imprinting technology for the purposes of pharmaceutical remediation in aqueous environments. Other molecularly imprinted photocatalysts are also discussed to better understand the potential value that molecular imprinting might bring to pharmaceutical pollution control based on semiconductor photocatalysts. Interest in the applications of molecularly imprinted TiO_2 as a technology for the remediation of pharmaceuticals in aqueous environments is a recent niche area with 83 % of the referenced studies done in the last 5 years (2019–2024). Only three studies were done more than 10 years ago. The three papers were all published in 2012 for the degradation of oxytetracycline (Huo et al., 2012a), ciprofloxacin (Huo et al., 2012b) and tetracycline (Wang et al., 2012).

2. Overview of pharmaceutical pollution in the aqueous environment

Pharmaceuticals are critical components of modern healthcare systems, contributing significantly to public health improvements and quality of life. Their production is regulated by health authorities in each country to ensure they meet stringent standards for safety, quality, and efficacy. However, their fate after performing their therapeutic effect in the body has not been prioritized with most of the residues making their way into the aqueous environment, thus creating a challenge to environmental sustainability and water quality. Various scholars have observed that developing countries are the most affected because they still use conventional wastewater treatment processes with limited abilities to remove pharmaceutical residues from effluents (Madikizela et al., 2020; Fekadu et al., 2019). The situation is made worse because of the lack of disposal directives to guide monitoring programs resulting in an uncontrolled release of improperly treated wastewater with no repercussions or reparations for those responsible.

The presence of pharmaceutical residues in the aqueous environment poses a significant concern due to their potential ecotoxicological and health impacts on the organisms that depend on water if the water gets polluted. Pharmaceutical residues originate from the excretion of pharmaceuticals by humans and animals, as well as improper disposal of unused medications either by consumers or pharmaceutical manufacturing companies. A plethora of studies have attributed the presence of pharmaceutical residues in the aqueous environments to high pharmaceutical consumption trends, the inability of conventional wastewater treatment processes to fully degrade the pharmaceuticals, and the lack of pollution directives in some countries (Madikizela et al., 2020; Fekadu et al., 2019). Most pharmaceuticals enter aqueous environments primarily through wastewater effluents from hospitals, households, and pharmaceutical industries while relatively low amounts enter via improper disposal of unused or expired pharmaceuticals (Bavumiragira et al., 2022).

A wide range of pharmaceuticals exist but the most common ones can be classified under antibiotics, painkillers, anti-inflammatory drugs, antivirals, antiretrovirals, hormones, and antidepressants. Antibiotics and antiretrovirals are probably the worst pharmaceuticals to enter the aquatic environment. Chronic exposure to low concentrations of antibiotics can contribute to antibiotic resistance in bacteria (Theuretzbacher, 2013; Larsson and Flach, 2022; Skandalis et al., 2021) while antiretrovirals have the potential to promote drug resistance in the human body if not taken according to prescription (Ncube et al., 2018). The other classes also have endocrine-disrupting effects with the potential to cause behavioural changes in aquatic organisms. Detection and monitoring of these residues have been crucial in pollution

management. The provision of monitoring data has led to a better understanding of the potential risks of pharmaceuticals to ecosystems and human health and the drafting of policies that address pharmaceutical residues in water bodies. Efforts typically focus on monitoring of pharmaceuticals in aqueous environments, health risk assessment, and setting limits for permissible concentrations in effluents. However, it is important to note that regulatory frameworks vary globally and most developing countries have not yet defined frameworks for pharmaceuticals in wastewater effluents. Another challenge is that the availability of pharmaceutical pollution directives does not guarantee compliance with those directives due to a lack of stringent measures against those that defy or ignore the guideline limits in effluents. With data showing evidence of the presence of elevated levels of pharmaceutical residues in the aqueous environment, researchers have since diverted to remediation. This is because pharmaceutical consumption continues to rise globally with new medicines being introduced regularly. In addition, attempts at keeping effluents within guideline limits have failed due to a lack of measures that enforce compliance. Remedial action that eliminates pharmaceuticals by mineralization has provided hope for pollution management. Photocatalytic degradation using radicals generated through the illumination of semiconductor materials has gained traction in pollution remediation. Its intergradation with molecular imprinting technology has offered a viable direction towards more effective management of pharmaceutical contaminants in the environment.

3. Principles of photocatalytic degradation

Photocatalytic degradation is an advanced oxidation process that utilizes light and a semiconductor catalyst to degrade organic pollutants into harmless by-products. It differs from photolysis in that UV photolysis of H_2O molecules is a result of light at 309nm with energy of about 4eV resulting in dissociation of H_2O molecules into $\bullet\text{OH}$ species and H_2O_2 . On the other hand, photocatalysis is a process that harnesses the power of light to accelerate chemical reactions on the surface of semiconductor materials used as catalysts (Chen et al., 2020; Koe et al., 2019). When a semiconductor absorbs light, electrons are excited from the valence band to the conduction band leaving behind positively charged holes in the valence band (Basavarajappa et al., 2020). These electron-hole pairs can initiate oxidation or reduction reactions with surrounding molecules. Electrons in the conduction band are free to move within the semiconductor material and can participate in reduction reactions by donating their energy to react with molecules on the surface or dissolved in the surrounding solution. The holes in the valence band are positively charged and decompose pollutants through oxidation. In the presence of water and O_2 , the electrons in the conduction band reduce O_2 into superoxide radicals ($\bullet\text{O}_2^-$), while the holes can attract electrons from water molecules and hydroxyl ions (OH^-) forming hydroxyl radicals ($\bullet\text{OH}$) with strong oxidant properties (Basavarajappa et al., 2020). The $\bullet\text{OH}$ and $\bullet\text{O}_2^-$ radicals are highly reactive and initiate the decomposition of organic molecules in solution breaking down complex molecules into simpler, less-toxic substances. The $\bullet\text{OH}$ radical achieves this by either removing an electron or H atom, or by adding itself to unsaturated bonds. The process is depicted in Fig. 1.

The most common semiconductor photocatalyst that has been utilized extensively in pollution control is TiO_2 . Its preference as a photocatalyst stems from the fact that it is low-cost, readily available and it is more stable in an aqueous solution (Teixeira et al., 2016). Furthermore, TiO_2 is non-corrosive, highly stable and the degradation products are largely non-toxic compared to other semiconductors with better photocatalytic activity such as ZnO (Li et al., 2021). Other important photodegraders include graphitic carbon nitride ($\text{g-C}_3\text{N}_4$), Metal-Organic Frameworks (MOFs) as well as some organic semiconductors such as poly-o-phenylenediamine (POPD). These photocatalytic semiconductors have been applied in the photodegradation of pharmaceuticals in aqueous environments and some reviews on them are available in the literature (Singh and Borthakur, 2018, Xia et al., 2021). However, the

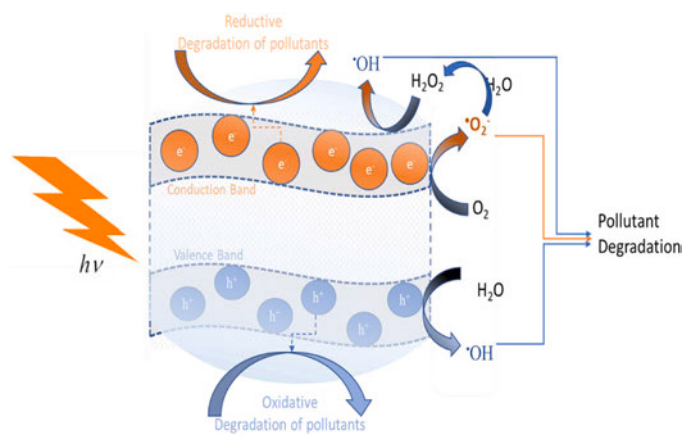


Fig. 1. Photocatalytic degradation schematic diagram.

focus of the current review is TiO_2 and its modification with MIPs for application in the remediation of pharmaceutical residues in aqueous environments.

4. Integration of molecularly imprinted polymers with TiO_2 photodegradation catalysts

4.1. Principle of titania photodegradation

The wavelength range in which TiO_2 shows light response has been reported between 200 to 400 nm due to electron transition from the valence band (O_{2p}) to the conduction band (Ti_{3d}). The valence band position for TiO_2 is at 2.77 eV while the conduction band is at -0.33 eV giving a band gap of 3.1 eV (Liu et al., 2024). Electron transitions therefore only occurs when TiO_2 is illuminated with photons having $h\nu > 3.1$ eV. The band gap of the different types of TiO_2 is larger than 3 eV (~3.0 eV for rutile to ~3.2 eV for anatase), thus making pure TiO_2 primarily active for UV light. Anatase TiO_2 with 3.2 eV, corresponds to the absorption of light at 387 nm and below which falls at the lowest end of visible light (Krakowiak et al., 2021). The mechanism of photodegradation by TiO_2 doped with either metals or non-metals has been detailed in different review articles (Chen et al., 2020; Koe et al., 2019; Basavarajappa et al., 2020). The reviews emphasized that dopants act by minimizing the bandgap of TiO_2 allowing it to use higher wavelengths in the visible light region to transfer its photoelectrons to the conduction band. The doped- TiO_2 therefore becomes active in the visible light region.

4.2. Applications of titania-based photocatalyst in degradation of pharmaceutical residues

Applications of TiO_2 as a single isolated photocatalyst in the degradation of pharmaceutical residues have been less represented in literature with relatively lower degradation efficiencies compared to advanced or doped TiO_2 photocatalysts. For example, Shaykhi and Zinatizadeh (2014) reported a photocatalytic-perozonation ($\text{O}_3/\text{H}_2\text{O}_2/\text{UV}/\text{TiO}_2$) reactor for degradation of amoxicillin in a simulated wastewater treatment plant achieving 58 % removal efficiencies in 250 min. The degradation of carbamazepine has been reported to attain complete mineralization after 6 h of irradiation (Haroune et al., 2014). It is however, important to mention that most of the reported efficiencies are comparable with advanced degradation schemes. A study reported TiO_2 irradiated with UV rays at 365 nm resulting in 90 % removal of amoxicillin and 98 % for metformin over 150 min in a laboratory-scale synthetic hospital wastewater (Chinnaiyan et al., 2019). Recently, some researchers arguably reported commercial Degussa P25 TiO_2 with the ability to remove three pharmaceuticals (propranolol-99.3 %,

mebeverine-98.5 %, and carbamazepine-83.2 %) after irradiation with light of 253 nm for 30 min (Navidpour et al., 2024). A large portion of TiO_2 -based photocatalysis has been reported for the remediation of antiviral drugs. For example, a $\text{TiO}_2/\text{H}_2\text{O}_2$ system irradiated at 300 nm yielded 89.23 % degradation rates of nevirapine in wastewater within 60 min (Ncube et al., 2023) while 87.1 % was reported for lamivudine (An et al., 2011).

Doped TiO_2 has been explored successfully as a replacement for plain TiO_2 and its application in the removal of pharmaceuticals has been a success story with various studies reporting better catalytic performance and degradation efficiency under visible light. The purpose of doping is to narrow the band gap or provide acceptors of the photoelectrons from the conduction band. Decreasing the band gap results in more electrons being excited to the conduction band. The end result is an improved photocatalytic activity. When doped, a hybridized valence band occupying a higher energy level is formed which results in the reduction of the band gap. For example, for a graphene/ TiO_2 , a new hybridized valence band consisting of C_{2p} (from graphene) and O_{2p} (from TiO_2) is formed (Li et al., 2013). The resultant graphene/ TiO_2 can be attributed to graphene's enhanced quantum efficiency due to the plasmon resonance effect on its surface which relates to its strong light absorbing ability. Another example is that of a TiO_2/Ge photocatalyst with a band gap of 2.83 eV compared to 3.21 eV for TiO_2 (Chun et al., 2015). TiO_2 doped with other semiconductors has been explored successfully in pharmaceutical pollution remediation and a plethora of studies are presented in literature reporting impressive photocatalytic activity towards target pharmaceuticals (Basavarajappa et al., 2020; Varma et al., 2020; Ahmadvipour et al., 2024).

4.3. Challenges of photocatalytic degradation of pharmaceuticals in aqueous environments

Despite advancements in photocatalytic degradation approaches as shown by the applications of doped semiconductors for removal of pharmaceutical residues in aqueous environments, total pharmaceutical elimination still presents several challenges. Notably is the issue of matrix effects. Water samples contain numerous organic and inorganic compounds (Zhu et al., 2023; Chianese et al., 2020), which can limit the ability of a photodegrader to effectively perform its photocatalytic activity on the intended pharmaceutical residue (Liu et al., 2024; Bi et al., 2021; Peng et al., 2024). Another important challenge that complicates the task of comprehensive remediation of pharmaceuticals is their existence in aqueous environments at extremely low concentrations compared to matrices. Furthermore, aqueous surface sources contain multiple pollutants that require remediation simultaneously (Du et al., 2020). Most photodegraders are non-specific and their photogenerated radicals will react with anything organic that exist on their surfaces. In this regard, it is observed that researchers have recently introduced MIPs with the aim of selectively bringing the target pollutants to the surface of the photodegrader (Sajini et al., 2019; Guan et al., 2021). MIPs are valued for their tailor-made selectivity, which can be advantageous in applications requiring precise recognition and manipulation of specific molecules (Belbruno, 2019; Martín-Esteban, 2013; Kaya et al., 2023). The interrelationship between the MIP and the nanoparticle is synergistic. The MIP offers specific binding sites that bring the target pollutant to the surface of the photodegrader nanoparticle, while embedding the MIP on the nanoparticle itself enhances its binding capability by offering a high surface area with more binding sites per unit area.

4.4. Principle of molecular imprinting technology

A MIP is created by polymerization of functional monomers with peripheral vinyl groups in the presence of a template molecule. In most cases, the template molecule is the target compound for which the MIP is intended to absorb from the aqueous solution. The functional monomer and the template molecule must have complementary functional groups

that interact through weak non-covalent intermolecular forces such as Van der Waals forces and H-bonding. Once the functional monomers have occupied strategic positions around the monomer, a cross linker with terminal vinyl groups is added to the reaction mixture. Polymerization is then initiated using a radical initiator such as azobisisobutyronitrile. The crosslinker helps create a link between the functional monomers allowing them to maintain their positions around the template molecules as the polymerization process progresses. Ethylene glycol dimethacrylate is commonly used as the crosslinker (Madikizela et al., 2018). The final product is a covalent solid structure with the template molecules still trapped within its matrix. Since the interaction between the monomer functional groups and those of the template are non-covalent, the trapped template molecules can be washed out using an appropriate organic solvent leaving behind cavities or imprints that are complementary in shape, size and functionality to the template molecule (Gkika et al., 2024; Vasapolo et al., 2011). These cavities have the ability to selectively isolate the target molecule or molecules with similar structures and functional groups from aqueous solution in the presence of potential interferents. These features have since permitted intergradation of molecular imprinting technology with photocatalysis as remediation tools for pharmaceuticals in the environment. Notably, the imprinted layer does not take part in photocatalysis but merely provides recognition sites that help bring the targeted pollutant to the photocatalyst. In this regard, the presence of the MIP on the surface of the photocatalyst is not expected to affect the degradation pathways but offers channels that allow specific targets to reach the photocatalyst. Various studies have reported applications of MIPs for isolation of pharmaceuticals from aqueous samples and some review articles are present in literature (Villarreal-Lucio et al., 2022; Speltini et al., 2017; Huang et al., 2015a). The current review assesses the integration of MIPs with photocatalysts including TiO_2 for remediation of pharmaceutical residues in the aqueous environment.

4.5. Applications of molecularly imprinted TiO_2 photodegradation catalysts

While the purpose of doping TiO_2 is to reduce the band gap, in MIP- TiO_2 systems the target is to create specific binding sites to bring specific targets closer to TiO_2 . The concept of molecularly imprinted photocatalytic degradation has been clearly illustrated in a graphical abstract by Feng et al. (Fig. 2) that represented a MIP- TiO_2 for degradation of norfloxacin (Fang et al., 2023). The schematic diagram shows TiO_2 nanoparticles embedded within a MIP particle with holes/cavities that channel towards the nanoparticles. The advantage is that the MIP isolates the target pollutant from a complex aqueous system. The isolated pollutant is brought closer to the TiO_2 and this minimizes potential interference from matrices in solution. With the process of photocatalysis dependent on the photogenerated radicals, molecular imprinting on the surface of photocatalysts has also been shown to greatly reduce the impact of radical scavengers on the photocatalytic activity by keeping them away from the surface of the photocatalyst (Yuan et al., 2020). While photocatalysis offers a green alternative to chemical oxidation methods, the environmental impact of photocatalytic nanoparticles that can potentially leach into the environment is another drawback for using metal oxides as photocatalysts (Zhang et al., 2022a; Renzi and Blašković, 2019; Nguyen et al., 2020a). However, copolymerization during synthesis of the MIP ensures that these nanoparticles remain trapped within the polymer reducing their potential to leach into the environment. Recent studies have further incorporated magnetite nanoparticles for the purpose of trapping the MIP- TiO_2 nano-scheme and keeping it stationary and also remove it from aqueous solution using an external magnetic field (Poonia et al., 2022; Huang et al., 2018; Cui et al., 2022). This helps prevent the entire polymer from washing away with the water in cases where they need to be deployed in the environment. The concept of application of a magnetic MIP- TiO_2 scheme for degradation of pharmaceuticals in aqueous environment is summarized in Fig. 3. This simplified version represents a pharmaceutical compound being selectively trapped within the MIP- TiO_2 scheme

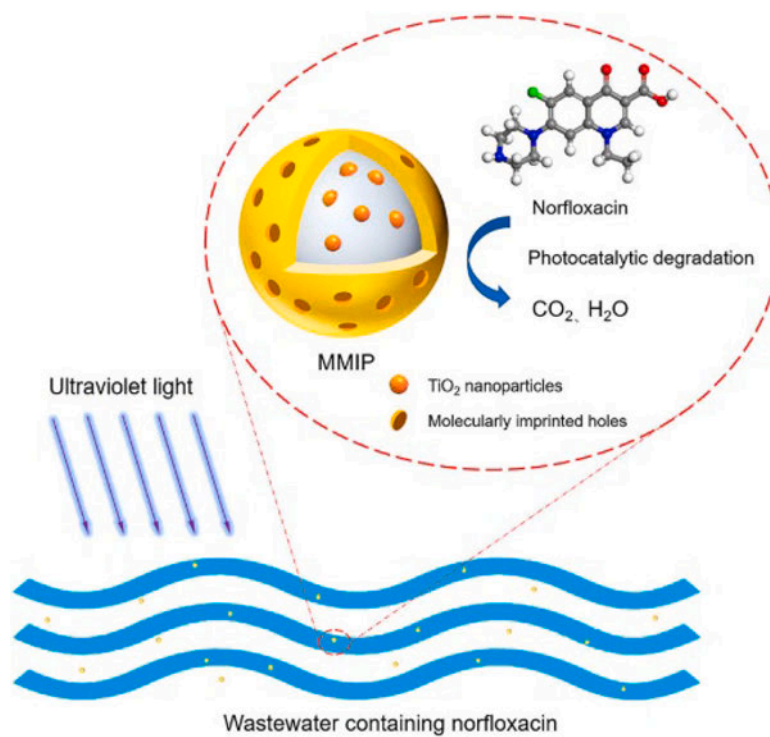


Fig. 2. Graphical representation of magnetic molecularly imprinted photocatalytic degradation of norfloxacin. Adapted with permission from Taylor & Francis (Fang et al., 2023).

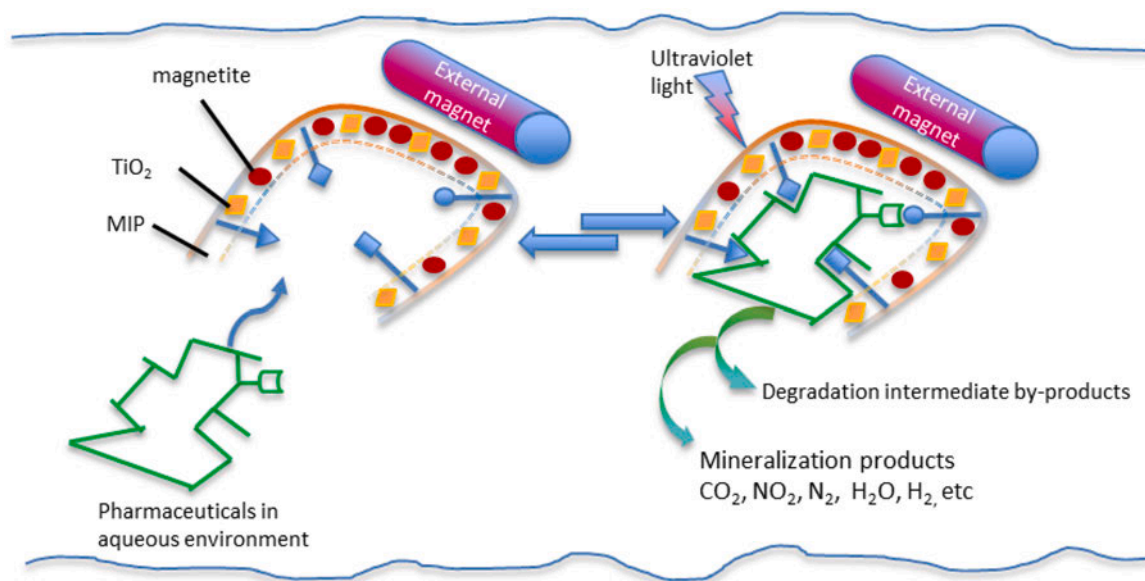


Fig. 3. Degradation schematic diagram for pharmaceutical pollutants based on a magnetized molecularly imprinted polymer embedded with titania.

and eventually getting mineralized to less toxic products.

TiO₂ embedded on MIP cavities for photocatalytic degradation of pharmaceutical residues in the environment has been reported in literature as shown in Table 1. Diclofenac is well studied with the first application of MIP-TiO₂ yielding just over 48 % degradation efficiencies in 2018 (de Escobar et al., 2018). However, the preceding studies have observed better efficiencies such as 91.4 % efficiency in 10 min (Bi et al., 2021). Diclofenac has also been included in multiresidue remediation using MIP-TiO₂ as the photocatalyst with fairly high degradation rates observed (Table 1). For example, a study that reported degradation rates for seven pharmaceuticals, the rates for diclofenac ranked second with about 42 % (de Escobar et al., 2016). Diclofenac is one of the most

commonly used over-the-counter anti-inflammatory medication for mild to moderate pain and is frequently detected in the aqueous environment (Sathishkumar et al., 2020).

Double heterojunction schemes have also been investigated in the photodegradation of pharmaceuticals using molecularly imprinted TiO₂-based photocatalysts. Examples include a novel molecularly imprinted TiO₂ doped with Fe₂O₃ and g-C₃N₄ (Zhang et al., 2024). The two doping materials were reported to reduce the rate of recombination of e⁻/h⁺ pairs. Fe₂O₃ provided a Z-heterojunction with TiO₂ while g-C₃N₄ provided a second charge transfer mechanism. Due to the MIP in the scheme, their double Z-scheme was able to selectively isolate sulfamethoxazole from synthetic wastewater in the presence of

Table 1
Molecularly imprinted-TiO₂ photocatalysts applied in pharmaceutical degradation.

Target(s)	Photocatalyst	Template	Time (min)	Efficiency (%)	Reference
Chlortetracycline	Fe ₃ O ₄ /g-C ₃ N ₄ /TiO ₂ /MIP	Chlortetracycline	120	91.87	(Liu et al., 2024)
Ciprofloxacin	MIP/C/TiO ₂	Ciprofloxacin	90	87	(Li et al., 2020)
	MIP/POPD/TiO ₂ /fly-ash	Ciprofloxacin	60	70	(Huo et al., 2012)
Diclofenac	MIP/TiO ₂	Diclofenac	120	48.72	(de Escobar et al., 2018)
	MIP/TiO ₂	Diclofenac	10	91.4	(Bi et al., 2021)
Enrofloxacin	TiO ₂ @SiO ₂ @Fe ₃ O ₄ /MIP	Enrofloxacin	90	-	(Lu et al., 2014)
Norfloxacin	CoFe ₂ O ₄ @TiO ₂ @MMIP	Norfloxacin	150	84.2	(Fang et al., 2023)
Oxytetracycline	MIP/POPD/TiO ₂ /fly-ash	Oxytetracycline	60	76	(Huo et al., 2012)
Sulfadiazine	N-TiO ₂ /C/MIP	Sulfadiazine	140	99.25	(Li et al., 2022)
Sulfamethoxazole	MIP-TiO ₂ @Fe ₂ O ₃ @g-C ₃ N ₄	Sulfamethoxazole		96.8	(Zhang et al., 2024)
Sulfasalazine	MMIP@TiO ₂	Sulfasalazine	10	92	(Mokhtari et al., 2023)
Tetracycline	MIP/TiO ₂	Tetracycline	180	-	(Wang et al., 2012)
Sulfadiazine	MIP/TiO ₂	Aniline (dummy)	80	99.9	(Li et al., 2023)
Sulfamethoxazole			15	99.9	
Diclofenac	MIP/TiO ₂	Diclofenac	60	86.6	(Eslami et al., 2023)
Ibuprofen		Ibuprofen		75	
Norfloxacin	CoFe ₂ O ₄ @TiO ₂ @MMIP	Norfloxacin		99.4	(Fang et al., 2021)
Ciprofloxacin				85.9	
Tetracycline	TiO ₂ @MIP	Tetracycline	50	95	(Sheng et al., 2022)
Norfloxacin				80	
Sulfamethoxazole				59	
Thiamphenicol				45	
Chloramphenicol				39	
Diclofenac Valsartan	MIP/TiO ₂	Diclofenac	60	42	(de Escobar et al., 2016)
Tioconazole				46	
Ketoconazole				25	
Ibuprofen Atorvastatin Gentamicine				24	
				19	
				19	
				11	

sulfadiazine, ibuprofen and bisphenol A as potential interferents. Sulfamethoxazole degradation efficiency was found to be 96.8 % which was more than double the efficiency observed for the potential interferents.

Most of the degradation studies using molecularly imprinted TiO₂ photocatalysts have validated the need for molecular imprinting by comparing the photocatalytic activity of the target with that of potential competing pharmaceuticals. For example, to prove selectivity, Fang and colleagues investigated the degradation performance of norfloxacin-imprinted CoFe₂O₄@TiO₂_MMIP towards norfloxacin, ciprofloxacin, ibuprofen, carbamazepine and phenol then observed its specificity towards fluoroquinolones (norfloxacin-91.1 % and ciprofloxacin-85.9 %) compared to other classes of pharmaceuticals with degradation of ibuprofen at 34 %, carbamazepine at 3.4 % and phenol at only 2.9 % (Fang et al., 2021). This was attributed to the imprinted cavities on the surface of TiO₂ which preferentially brought the fluoroquinolones closer to the surface of the TiO₂ while the other compounds remained in solution. Another study imprinted TiO₂ with tetracycline and tested it against five antibiotics; sulfamethoxazole, thiamphenicol, chloramphenicol, norfloxacin and tetracycline. The tetracycline-imprinted TiO₂ achieved 95 % degradation for tetracycline, 80 % for norfloxacin while sulfamethoxazole, thiamphenicol and chloramphenicol had 59, 45 and 39 % degradation, respectively (Sheng et al., 2022). The preference towards tetracycline was attributed to the shape and size of imprinted cavities.

5. Photodegradation activities of other molecularly imprinted photocatalysts

5.1. Molecularly imprinted metal oxides

Some metal oxide nanoparticles with semiconductor properties have been utilized in combination with molecular imprinting for photocatalytic degradation of pharmaceuticals. ZnO is considered to have better semiconductor properties than TiO₂ and its molecularly imprinted version has been utilized in pharmaceutical pollution management. Cantarella et al. (2018) has reported molecularly imprinted ZnO nanonuts with the ability to selectively degrade all the paracetamol within 3 h in the presence of four other water pollutants. Similarly, Du et al. (2020) reported a molecularly imprinted ZnO composite doped with NH₂-UiO-66 MOF that removed 61.9 % in 30 min. Wang et al. (2023) reported a Fe₃O₄/ZnO@MIP composite that achieved 90.72 % degradation of amoxicillin over 140 min. Interaction between ZnO with the dopants had synergistic effects which limited the e⁻/h⁺ recombination. Other molecularly imprinted metal oxides have also been investigated. A NiO-CuS/MIP nanocomposite for removal of letrozole in wastewater was found to exhibit over 90 % degradation rates (Rabizadeh et al., 2020). A MIP-CuFeO₂@MnO₂ nanocomposite was group-imprinted using aniline and pyrrole copolymers and acrylamide as a dummy template for targeting tetracycline (Peng et al., 2024). The nanocomposite selectively degraded tetracycline achieving 92 % efficiency. A surface BiOCl/Bi₃NbO₇ photocatalyst imprinted with ceftriaxone has also been reported with a 92 % degradation of ceftriaxone after 100 min (Zhang et al., 2023).

5.2. Molecularly imprinted graphene-based semiconductors

Molecularly imprinted graphene-based photocatalytic degradation has been utilized in pharmaceutical pollution control in the environment. The application of graphene-based nanomaterials in photocatalysis is due to the plasmonic resonance effect possessed by carbon nanoparticles. This integrated approach utilizes the advantages that both molecular imprinting and plasmon resonance can bring in photocatalytic degradation. A magnetic molecularly imprinted bismuth phosphate/graphene oxide (BiPO₄@GO-MMIP) was developed for selective degradation of ciprofloxacin (Kumar et al., 2020). Its photocatalytic activity was attributed to Bi(PO₄) and GO with the authors

noting that Bi(PO₄) has more energy gap than GO resulting in the transfer of photoelectrons from LUMO of GO to HOMO of Bi(PO₄) via π to π^* transitions. About 75 % of ciprofloxacin was degraded over 80 min. Li et al. (2022) have developed a molecularly imprinted C-doped TiO₂ nanomaterial for sulfadiazine and recorded a 99.25 % degradation efficiency in 140 min. This was an indication that the selectivity of the molecularly imprinted surface coupled with the surface plasmon effect brought by the thin sheets of graphene greatly improved the photocatalytic activity of TiO₂. An Fe₃O₄/g-C₃N₄/TiO₂ heteroscheme imprinted with diclofenac achieved 68.34, 84.76 and 86.27 % degradation rates towards diclofenac in wastewater, river water, and tap water (Liu et al., 2024). It was obvious that the complexity of the sample affects the performance of the photocatalyst with its performance in wastewater lower compared to river and tap water.

5.3. Molecularly imprinted organic semiconductors

The potential of organic semiconductors as replacements for TiO₂ and other metal oxide semiconductors has been investigated for pharmaceutical remediation with a list of studies reported in literature where MIPs were combined with organic material as the photocatalysts or as dopants for photocatalysts. The main advantage of organic semiconductors is that their energy level positions can be adjusted. In their study, Huang et al. (2021) synthesized a magnetic molecularly imprinted photocatalyst based on poly-o-phenylenediamine doped with silver (Ag-POPD) as an organic semiconductor for selective degradation of ciprofloxacin achieving a 70.85 % degradation rate in 90 min. Similarly, an imprinted Ag-POPD was used elsewhere for the same pharmaceutical with similar degradation rates (73.25 %) in 90 min (Liu et al., 2022). Huo et al. (2012) has modified molecularly imprinted TiO₂/fly ash cenospheres with POPD for degradation of ciprofloxacin in wastewater yielding 70 % efficiency in 60 min. The same authors presented a similar approach but this time imprinting their cenospheres with oxytetracycline and La³⁺ for degradation of oxytetracycline yielding 76 % in 60 min (Huo et al., 2012). However, La³⁺ did not impact the catalytic activity of the cenospheres but merely enhanced the imprinting of oxytetracycline by acting as a bridge between the O atoms of oxytetracycline and the N atoms of the acrylamide monomers. A novel Cu²⁺-imprinted POPD-CoFe₂O₄ heterojunction mesoporous photocatalyst has been reported with the ability to reduce Cu²⁺ and simultaneously degrade tetracycline (He et al., 2019). CoFe₂O₄ acted as an acceptor of photo-induced holes from POPD. The CoFe₂O₄ holes were responsible for degradation of tetracycline while Cu²⁺ was reduced by photoelectrons from the conduction band of POPD.

Other semiconducting polymers have been reported in molecularly imprinted photocatalytic degradation of pharmaceuticals. For example, polyaniline integrated with a WS₂ semiconducting material where it acted by transferring charge carriers has been investigated in the photocatalytic degradation of nitrofurantoin with an efficiency of 92 % in 75 min (Fatima et al., 2024). Polyaniline is an organic conducting polymer which tends to keep the e⁻/h⁺ pairs separated by transferring charge carriers from WS₂. Lu et al. (2020) developed a magnetic imprinted nanoreactor based on poly-3,4-ethylenedioxythiophene (PEDOT) and CdS with double photocatalytic activity towards danofloxacin. CdS acted as the photocatalyst, magnetite enhanced transfer of conduction band photoelectrons while PEDOT extracted the photoinduced holes. Molecular imprinting enhanced selectivity towards the danofloxacin with photocatalyst achieving 84.8 % degradation of danofloxacin. Its photocatalytic activity towards three other pharmaceuticals (gatifloxacin, ciprofloxacin and tetracycline) ranged between 37 and 50 %.

5.4. Molecularly imprinted metal organic frameworks

MIPs imbedded on MOFs is another area that has been explored in the degradation of pharmaceutical pollutants in the environment. Yi et al. (2023) recently reported a MIL100@MIP for sulfamethoxazole

with the study observing a 63.6 % increase in the degradation performance compared to non-imprinted scheme. Magnetic MIPs grafted on a MIL-100 MOF have been reported for elimination of ciprofloxacin from wastewater effluents (Li et al., 2022), sulfamethoxazole in wastewater (Xie et al., 2022) and tetracycline in lake water (Fu et al., 2024). The reported $\text{Fe}_3\text{O}_4@\text{MIL-100}(\text{Fe})@\text{MIP}$ nanocomposites were imprinted with ciprofloxacin, sulfamethoxazole and tetracycline, respectively. The imprinted frameworks displayed a strong preference towards the target pharmaceuticals in the presence of other pharmaceutical residues as potential competitors. In both cases, the presence of $\text{Fe}_3\text{O}_4@\text{MIP}$ on the surface of MOF allowed specific targets only to channel into the MOF. The photocatalytic activity was further enhanced by addition of H_2O_2 which helped to capture the photogenerated electrons to form more $\bullet\text{OH}$ radicals. For MOF-based schemes, photodegradation occurs by photo-Fenton processes. Liu et al. (2021) has also reported a molecularly imprinted MOF anchored on porous carbon forms that selectively removed norfloxacin, ibuprofen, naproxen, sulfadimethoxine and caffeine. Another study created molecularly imprinted MOF channels utilizing the 3D structural configuration of β -cyclodextrin for selective degradation of sulfamethoxazole (Tang et al., 2022). Over 91 % degradation rates in complex matrices including polluted river water were achieved in 60 min.

5.5. Molecularly imprinted schemes based on novel semiconductors

Other hybrid schemes in which molecularly imprinted polymers were embedded on novel semiconductor materials have been reported in photocatalytic degradation of pharmaceutical pollutants. These include a $\text{ZnGa}_2\text{O}_4/\text{Cr}^{3+}$ heterojunction photocatalyst for degradation of tetracycline (Zhang et al., 2022). This heterojunction scheme had afterglow photocatalysis abilities in which tetracycline could be degraded day-and-night. A molecularly imprinted magnetic $\gamma\text{-Fe}_2\text{O}_3/\text{H}_2\text{O}_2/\text{chitosan}$ composite has been reported for the removal of norfloxacin in pharmaceutical wastewater through Fenton-like oxidative degradation (Huang et al., 2015; Wu et al., 2016). Yan et al. (2022) has reported an imprinted P25@IL nanoreactor in which a MIP was synthesized using an imidazole ionic liquid as a monomer and levofloxacin as the template. This novel MIP was embedded on the surface of a TiO_2 photocatalyst for the degradation of levofloxacin and tetracycline in aqueous media. The imprinted nanoreactor had a strong preference for levofloxacin compared to the non-imprinted nanoreactor with degradation rates of 50.69 and 25.58 %, respectively. The authors attributed this to the specificity of the levofloxacin-imprinted reactor towards levofloxacin.

6. Challenges and considerations

Despite its promise, photocatalytic degradation still faces several challenges as a potential remedial tool for pharmaceutical pollution control. TiO_2 may be readily available as a commercial photocatalyst but it still needs to be modified or doped appropriately for it to effectively degrade the target pollutant. Commercial TiO_2 is marketed as P25, a combination of about 80 % anatase and 20 % rutile (Krakowiak et al., 2021). Modification of TiO_2 with selective imprinted polymer cavities may help bring the target closer to the photocatalyst's surface however, embedding a solid matrix on the surface may create challenges related to incident light accessibility. Effective photocatalytic degradation solely depends on light striking the semiconductor (Lu et al., 2014). In this regard, one of the major questions focuses on whether light can fully transmit through the imprinting layer. Currently, there are limited studies that have reported on the light permeability of imprinted polymers and the potential impact it can have if the imprinted TiO_2 was to be upscaled. The most appropriate position of the TiO_2 nanoparticles within the MIP matrix that could result in better accessibility of the incident light has not yet been reported. More research is required in this regard to assess the potential of upscaling molecularly imprinted photocatalysts for application in the environment.

Another notable observation in the applications of molecularly imprinted TiO_2 -based photocatalysts and any other imprinted photocatalyst is the lack of pilot-scale studies and industrial applications to demonstrate their feasibility and economic viability in large-scale environmental remediation projects. MIPs are tailored for single specific targets and currently, most studies have reported molecularly imprinted photodegraders that target a single pharmaceutical (Table 1). This approach is not environmentally plausible because pharmaceuticals exist in the environment as mixtures, all of which are of ecotoxicological concern, indicating a need for multiresidue remedial tools. It should be noted that some studies have already initiated this approach (de Escobar et al., 2016; Sheng et al., 2022). However, the results are not yet convincing with efficiencies ranging between 11 and 46 % for 7 pharmaceuticals (de Escobar et al., 2016), and 39–95 % for 5 pharmaceuticals (Sheng et al., 2022). Importantly, a single pharmaceutical was used as the imprinting template which might explain the low degradation efficiencies towards the targeted compounds (Table 1). Multitemplate imprinting might be a solution to this problem.

The type of matrix is also a contributing factor that has proven to limit the potential upscaling and commercialization of photocatalysts. Liu et al. (2024) recently observed that their molecularly imprinted $\text{Fe}_3\text{O}_4/\text{g-C}_3\text{N}_4/\text{TiO}_2$ heteroscheme attained different degradation rates towards diclofenac in tap water (86.27 %), polluted river water (84.76 %), pulping wastewater (65.69 %), and pharmaceutical wastewater (68.34 %), despite the scheme being imprinted with diclofenac. Tang et al. (2022) also observed a reduction in the degradation abilities of a MIP/ ZnO/MOF towards sulfamethoxazole in polluted river water (91 %) compared to tap water (97 %). It is obvious that degradation is lower for samples with more complex matrices and there is a need for proper optimization strategies in consideration of matrices. Related to matrices is the issue of interferents, which reduce the photocatalytic activity by adsorbing on the photocatalyst surface and blocking the active sites, scavenging $\bullet\text{OH}$ and $\bullet\text{O}_2$ radicals, and competition for incident light. For example, Liu et al. (2024) observed that photodegradation of chlorotetracycline using $\text{Fe}_3\text{O}_4/\text{g-C}_3\text{N}_4/\text{TiO}_2/\text{MIP}$ decreased significantly from 91.87 % to 61.29 % in the presence of humic acids. They mentioned that humic acid adsorbed on the surface and scavenged for photogenerated O_2 radicals. It also decomposed under continuous illumination and further accumulated on the surface of the photocatalyst. This observation creates a challenge because humic substances including fulvic acids and humic acids are always a part of wastewater treatment (Zhu et al., 2023; Chianese et al., 2020). They possess other advantages such as the removal of toxic trace metals and other lipophilic constituents from wastewater. Various other important scavengers that inhibit the degradation activities of molecularly imprinted photocatalysts have been mentioned in the literature. One study observed that the degradation rates for diclofenac decreased from 91.4 % to 84.8, 61.7, and 29.5 % in the presence of butanol, EDTA-2Na and p-benzoquinone, respectively (Bi et al., 2021). Another study reported that isopropanol, triethanolamine, and p-benzoquinone led to a reduction in tetracycline rates from 92 % to 62.5, 54.38 and 78.9 %, respectively (Peng et al., 2024). Alcohols such as isopropanol are scavengers of $\bullet\text{OH}$ radicals, p-benzoquinone targets $\bullet\text{O}_2$ radicals while triethanolamine scavenges the holes. Save for humic acids, the levels of these radical scavengers in municipal wastewater are not well defined. In this regard, the focus should shift towards those potential scavengers that are known to exist in relevant concentrations in the aqueous environment.

Other inhibitors to commercialization have been raised when discussing the potential of molecularly imprinted photocatalysts. The production of commercial MIPs has always been a challenge for researchers because they need to be synthesized for a specific target (Lowdon et al., 2020). This has failed because priority pollutants cannot be the same for potential customers from different areas. Another challenge is that regeneration studies which focus on the stability of molecularly imprinted photocatalysts if deployed in the environment have not yet been fully explored. Impressive regeneration results have

been presented for most of the molecularly imprinted TiO₂ photocatalysts in which the photocatalyst is reused based on lab-scale stagnant water, usually between 5 and 10 cycles. However, the challenge is that if the photocatalyst was to be applied in the environment it would have to be deployed and be continuously in contact with flowing water. Reusability studies should therefore consider photocatalyst deployment times.

There is also a challenge of the parent pharmaceutical achieving 100 % degradation without being completely mineralized. An example was presented by (Li et al., 2015) in which amoxicillin, methyl orange and 3-chlorophenol all achieved 100 % degradation but their mineralization was 78.1, 47.9 and 35.7 %, respectively. Another study observed that while diclofenac achieved 89 % degradation after 10 min, its mineralization was only 17 % (Bi et al., 2021). These observations raise the issue of the toxicity of intermediate degradation products that do not achieve complete mineralization. It is however important to point out that molecularly imprinted photocatalysts give less products since the intermediates can remain in the cavities to permit mineralization (Tang et al., 2022), but the toxicity of the unmineralized products remains a concern. Different studies have observed different ecotoxicities of the intermediates depending on the target pharmaceutical. For example, Peng et al. (2024) observed that the intermediate products of tetracycline were less toxic towards aquatic organisms compared to tetracycline. However, An et al. (2015) noted that acyclovir's inhibition towards bacteria, algae, and daphnia ranged between 4.8 and 35.1 %, but the ecotoxicities increased to 14.3–79.0 % when the same organisms were exposed to the treated solution of acyclovir indicating the cumulative ecotoxicity due to intermediates. Even after complete degradation of acyclovir, the bio-toxicities remained between 7.2 and 14.4 %. The implication was that the unmineralized intermediates were toxic towards bacteria, algae, and daphnia. These conflicting observations are an indication of the challenge of intermediates and the need for further studies that can provide more informed ecotoxicity data.

7. Perspectives

Research continues to seek methodologies that can either substitute or enhance the applicability of photocatalysts for the remediation of pollutants in the environment. The potential of co-doping is one area that could potentially elevate the applicability of molecularly imprinted TiO₂ photocatalysts for the remediation of pharmaceuticals (Basavarajappa et al., 2020). For example, a typical single Z-scheme has the disadvantage that migration of charge carriers to higher valence bands and lower conduction bands is coupled with a loss of catalytic redox potential. Utilizing multiple heterojunction schemes where TiO₂ is coupled with other semiconductors is one approach that could help increase the catalytic conduction band potential and improve the photocatalytic activity. A recent study has investigated a novel molecularly imprinted TiO₂@Fe₂O₃@g-C₃N₄ in which Fe₂O₃ and g-C₃N₄ were used as co-dopants on the surface of the MIP-TiO₂ (Zhang et al., 2024). The inclusion of g-C₃N₄ provided a second charge transfer mechanism in addition to the Fe₂O₃ Z-heterojunction thus reducing the rate of recombination of e⁻/h⁺ pairs. Another study observed that TiO₂@Zn-Fe₂O₄/Pd gave better catalytic performance than TiO₂@ZnFe₂O₄ (Ahmadpour et al., 2020), while co-doping TiO₂ with carbon and nitrogen gave better photocatalytic performances (Li et al., 2022; Nguyen et al., 2020). These are indications of the potential of co-doping in enhancing the photocatalytic abilities of TiO₂.

Having mentioned the potential ecotoxicity effects due to the leaching of nanoparticles into the environment, some researchers have substituted inorganic nanoparticles including metal oxides and graphene with organic semiconductors (Huang et al., 2021). These include POPD, PEDOT, and some MOFs as discussed in Sections 5.3–5.5. More of these materials need to be identified and their potential as substitutes for TiO₂ should be investigated. Furthermore, the use of organic solvents in synthesizing MIPs requires careful assessment and regulation. With

green chemistry procedures advocating for the use of environmentally friendly solvents, deep eutectic solvents and ionic liquids have been mentioned in the synthesis of MIPs (Madikizela et al., 2022). This approach could be adopted in the synthesis of MIP-based photocatalysts.

With most studies still focussing on remediation of single pharmaceuticals, a shift towards multiresidue degradation can be an important approach that could result in upscaling molecularly imprinted photocatalysts. Nearly 10 years ago, de Escobar et al. (2016) attempted a MIP/TiO₂ imprinted with cavities for seven pharmaceuticals belonging to different classes (atorvastatin, diclofenac, ibuprofen, tioconazole, valsartan, ketoconazole, and gentamicine). They observed that degradation rates for the multitemplate imprinted TiO₂ photocatalyst were enhanced by over 400 %. Multiple pharmaceutical degradation is an area that needs serious attention because pollutants do not exist in isolation in the environment and photocatalysts with multiresidue degradation capabilities are required. Multiple imprinted photocatalysts with two or more heterojunctions can be further explored to enhance the degradation abilities of imprinted photocatalysts to remediate multifarious pharmaceuticals from the environment. Furthermore, some studies have observed that using dummy templates results in better degradation activities than when target pharmaceuticals are used as the templates. For example, Li et al. (2023) synthesized a MIP/TiO₂ with sulphonamide and sulfamethoxazole as templates. They compared their activities with a MIP/TiO₂ prepared using aniline as a dummy template and observed that it performed better than target-imprinted MIP/TiO₂, with the additional advantage of producing fewer intermediates and by-products.

Various other novel methods that could be further explored have been mentioned in the literature. Zhang et al. (2022) have initiated the concept of afterglow photocatalysis with the ability to degrade pollutants day and night. Another area that might excite researchers in the near future has been recently mentioned in literature where a MIP-based photocatalyst was utilized for the mitigation of antibiotic resistant genes (ARGs) in aqueous environment (Yuan et al., 2020). In their study, the researchers synthesized guanine-imprinted g-C₃N₄ nanosheets and used them to degrade plasmid-encoded (bla_{NDM-1}) multi-drug ARG in wastewater effluents. Imprinting g-C₃N₄ with guanine enhanced the adsorption of the ARG on its surface resulting in photodegradation efficiencies that were 37-fold faster than bare g-C₃N₄. ARGs are of global concern because of their persistence in the environment and photocatalytic degradation might provide a potentially effective way of removing them in the environment. Photodegradation helps fragment and mineralize the DNA of the ARG thus preventing it from repair.

Common MIP/doped-TiO₂ photocatalysts still underperform when compared to MIP/TiO₂ schemes with dopants that possess plasmonic resonance properties. The future of molecularly imprinted photocatalysts might fall on utilizing the advantages of molecularly imprinting and dopants with plasmonic resonance properties. Studies that integrated molecular imprinting with graphene-doped photocatalysts have observed better performances compared to individual techniques combined with TiO₂. For example, a molecularly imprinted C-doped TiO₂ nanomaterial for sulfadiazine recorded a 99.25 % degradation efficiency in 140 min (Li et al., 2022). A tetracycline imprinted Ag/Ag₃VO₄/g-C₃N₄ photocatalyst that utilized Ag⁰ for its surface plasmon resonance resulted in a 90 % degradation efficiency of tetracycline over 120 min (Sun et al., 2019). These observations are an indication that combined utilization of molecular imprinting and plasmon resonance could shape the future of photocatalytic degradation of organic pollutants, necessitating further studies in this area.

8. Conclusions

Photocatalytic degradation represents a promising approach to controlling environmental pollution. Its integration with molecular imprinting technology is expected to play a pivotal role in achieving sustainable goals related to pharmaceutical control in the environment.

Currently, the approach has several drawbacks that need to be addressed before it can be considered as a plausible alternative in pharmaceutical pollution control. One notable drawback is the lack of pilot-scale studies and industrial applications to demonstrate their feasibility and economic viability in large-scale environmental remediation projects. Continued research is therefore essential to further explore innovative solutions around molecularly imprinted photocatalysts for sustainable pharmaceutical residue management including substituting metal oxide nanoparticles with organic semiconductors and exploring multiresidue photodegradation. The review identifies that the integration of molecularly imprinted polymers with semiconductor materials for photodegradation of pollutants is a relatively new niche area with 83 % of the studies so far done within the last 5 years (2019–2024) and more studies are expected in the few coming years.

CRediT authorship contribution statement

Asenathi Sibali: Writing – original draft, Conceptualization. **Thabang Hendrica Mokhothu:** Writing – review & editing, Supervision, Conceptualization. **Samson Masulubanye Mohomane:** Writing – review & editing, Conceptualization. **Vusumzi Emmanuel Pakade:** Writing – review & editing, Conceptualization. **Ramakwala Christinah Chokwe:** Writing – review & editing, Conceptualization. **Somandla Ncube:** Writing – original draft, Supervision, Conceptualization.

Declaration of competing interest

The authors declare that they have no known competing financial interests or personal relationships that could have appeared to influence the work reported in this paper.

Funding

This research did not receive any specific grant from funding agencies in the public, commercial, or not-for-profit sectors.

Data availability

Data will be made available on request.

References

- Ahmadpour, N., Nowrouzi, M., Madadi Avargani, V., Sayadi, M.H., Zendejboudi, S., 2024. Design and optimization of TiO₂-based photocatalysts for efficient removal of pharmaceutical pollutants in water: recent developments and challenges. *J. Water Process Eng.* 57, 104597. <https://doi.org/10.1016/j.jwpe.2023.104597>.
- Ahmadpour, N., Sayadi, M.H., Sobhani, S., Hajiani, M., 2020. Photocatalytic degradation of model pharmaceutical pollutant by novel magnetic TiO₂/ZnFe₂O₄/Pd nanocomposite with enhanced photocatalytic activity and stability under solar light irradiation. *J. Environ. Manage.* 271, 110964. <https://doi.org/10.1016/j.jenvman.2020.110964>.
- Ali, Y., Hadj, E., Azzouz, A., Ahrouch, M., Lamaoui, A., Raza, N., Ait, A., 2024. Molecular imprinting technology for next-generation water treatment via photocatalysis and selective pollutant adsorption. *J. Environ. Chem. Eng.* 12, 112768. <https://doi.org/10.1016/j.jece.2024.112768>.
- An, T., An, J., Gao, Y., Li, G., Fang, H., Song, W., 2015. Photocatalytic degradation and mineralization mechanism and toxicity assessment of antiviral drug acyclovir: experimental and theoretical studies. *Appl. Catal. B Environ.* 164, 279–287. <https://doi.org/10.1016/j.apcatb.2014.09.009>.
- An, T., An, J., Yang, H., Li, G., Feng, H., Nie, X., 2011. Photocatalytic degradation kinetics and mechanism of antiviral drug-lamivudine in TiO₂ dispersion. *J. Hazard. Mater.* 197, 229–236. <https://doi.org/10.1016/j.jhazmat.2011.09.077>.
- Bagheri, A., Aramesh, N., Arif, A., Gul, I., Ghotekar, S., Bilal, M., 2021. Molecularly imprinted polymers-based adsorption and photocatalytic approaches for mitigation of environmentally-hazardous pollutants – A review. *J. Environ. Chem. Eng.* 9, 104879. <https://doi.org/10.1016/j.jece.2020.104879>.
- Basavarajappa, P.S., Patil, S.B., Ganganagappa, N., Reddy, K.R., Raghu, A.V., Reddy, C. V., 2020. Recent progress in metal-doped TiO₂, non-metal doped/codoped TiO₂ and TiO₂ nanostructured hybrids for enhanced photocatalysis. *Int. J. Hydrogen Energy* 45, 7764–7778. <https://doi.org/10.1016/j.ijhydene.2019.07.241>.
- Bavumiragira, J.P., Ge, J., Yin, H., 2022. Fate and transport of pharmaceuticals in water systems: a processes review. *Sci. Total Environ.* 823, 153635. <https://doi.org/10.1016/j.scitotenv.2022.153635>.

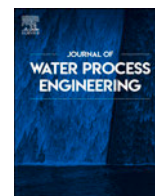
- Belbruno, J.J., 2019. Molecularly imprinted polymers. *Chem. Rev.* 119, 94–119. <https://doi.org/10.1021/acs.chemrev.8b00171>.
- Bi, L., Chen, Z., Li, L., Kang, J., Zhao, S., Wang, B., Yan, P., Li, Y., Zhang, X., Shen, J., 2021. Selective adsorption and enhanced photodegradation of diclofenac in water by molecularly imprinted TiO₂. *J. Hazard. Mater.* 407, 124759. <https://doi.org/10.1016/j.jhazmat.2020.124759>.
- Cantarella, M., Di Mauro, A., Gulino, A., Spitaleri, L., Nicotra, G., Privitera, V., Impellizzeri, G., 2018. Selective photodegradation of paracetamol by molecularly imprinted ZnO nanonuts. *Appl. Catal. B Environ.* 238, 509–517. <https://doi.org/10.1016/j.apcatb.2018.07.055>.
- Chen, D., Cheng, Y., Zhou, N., Chen, P., Wang, Y., Li, K., Huo, S., Cheng, P., Peng, P., Zhang, R., Wang, L., Liu, H., Liu, Y., Ruan, R., 2020. Photocatalytic degradation of organic pollutants using TiO₂-based photocatalysts: a review. *J. Clean. Prod.* 268. <https://doi.org/10.1016/j.jclepro.2020.121725>.
- Chen, Y., Yang, J., Zeng, L., Zhu, M., 2022. Recent progress on the removal of antibiotic pollutants using photocatalytic oxidation process. *Crit. Rev. Environ. Sci. Technol.* 52, 1401–1448. <https://doi.org/10.1080/10643389.2020.1859289>.
- Chianese, S., Fenti, A., Iovino, P., Musmarra, D., Salvestrini, S., 2020. Sorption of organic pollutants by Humic acids: a review. *Molecules* 25, 1–17. <https://doi.org/10.3390/molecules25040918>.
- Chinnaiyan, P., Thampi, S.G., Kumar, M., Balachandran, M., 2019. Photocatalytic degradation of metformin and amoxicillin in synthetic hospital wastewater: effect of classical parameters. *Int. J. Environ. Sci. Technol.* 16, 5463–5474. <https://doi.org/10.1007/s13762-018-1935-0>.
- Chun, S.Y., Chung, W.J., Kim, S.S., Kim, J.T., Chang, S.W., 2015. Optimization of the TiO₂/Ge composition by the response surface method of photocatalytic degradation under ultraviolet-a irradiation and the toxicity reduction of amoxicillin. *J. Ind. Eng. Chem.* 27, 291–296. <https://doi.org/10.1016/j.jiec.2015.01.003>.
- Cui, Y., Ding, L., Ding, J., 2022. Recent advances of magnetic molecularly imprinted materials: from materials design to complex sample pretreatment. *TrAC - Trends Anal. Chem.* 147, 116514. <https://doi.org/10.1016/j.trac.2021.116514>.
- de Escobar, C.C., Lansarin, M.A., Zimnoch dos Santos, J.H., 2016. Synthesis of molecularly imprinted photocatalysts containing low TiO₂ loading: evaluation for the degradation of pharmaceuticals. *J. Hazard. Mater.* 306, 359–366. <https://doi.org/10.1016/j.jhazmat.2015.11.035>.
- de Escobar, C.C., Moreno Ruiz, Y.P., dos Santos, J.H.Z., Ye, L., 2018. Molecularly imprinted TiO₂ photocatalysts for degradation of diclofenac in water. *Coll. Surf. A Physicochem. Eng. Asp.* 538, 729–738. <https://doi.org/10.1016/j.colsurfa.2017.11.044>.
- Du, Q., Wu, P., Sun, Y., Zhang, J., He, H., 2020. Selective photodegradation of tetracycline by molecularly imprinted ZnO @ NH₂-UiO-66 composites. *Chem. Eng. J.* 390, 1–11. <https://doi.org/10.1016/j.cej.2020.124614>.
- Eslami, A., Rafiee, M., Sedghi, R., Aliyari, A., Heidari, B., 2023. Simultaneous and selective removal of diclofenac and ibuprofen from aqueous matrices by a hybrid TiO₂-dual-template molecularly imprinted polymer. *Int. J. Environ. Anal. Chem.* 00, 1–23. <https://doi.org/10.1080/03067319.2023.2178917>.
- Fang, L., Miao, Y., Wei, D., Zhang, Y., Zhou, Y., 2021. Efficient removal of norfloxacin in water using magnetic molecularly imprinted polymer. *Chemosphere* 262. <https://doi.org/10.1016/j.chemosphere.2020.128032>.
- Fang, L., Tang, K., Wei, D., Zhang, Y., Zhou, Y., 2023. Photocatalytic degradation of norfloxacin by magnetic molecularly imprinted polymers: influencing factors and mechanisms. *Environ. Technol. (United Kingdom)* 44, 1438–1449. <https://doi.org/10.1080/09593330.2021.2003442>.
- Fatima, T., Husain, S., Khanuja, M., 2024. Optimization of WS2 modified polyaniline for superior photocatalytic degradation and electrochemical detection of pharmaceutical drug. *FlatChem* 44, 100624. <https://doi.org/10.1016/j.flatc.2024.100624>.
- Fekadu, S., Alemayehu, E., Dewil, R., Van der Bruggen, B., 2019. Pharmaceuticals in freshwater aquatic environments: a comparison of the African and European challenge. *Sci. Total Environ.* 654, 324–337. <https://doi.org/10.1016/j.scitotenv.2018.11.072>.
- Fu, J.X., Li, S.Y., Li, Q.Y., Bell, E., Yang, D.D., Li, T., Li, Y.J., He, J.Y., Di Zhou, L., Zhang, Q.H., Yuan, C.S., 2024. Preparation of surface molecular-imprinted MOFs for selective degradation of tetracycline antibiotics in wastewater. *Coll. Surf. A Physicochem. Eng. Asp.* 687, 133575. <https://doi.org/10.1016/j.colsurfa.2024.133575>.
- Gkika, D.A., Tolkou, A.K., Lambropoulou, D.A., Bikiaris, D.N., Kokkinos, P., Kalavrouziotis, I.K., Kyzas, G.Z., 2024. Application of molecularly imprinted polymers (MIPs) as environmental separation tools. *RSC Appl. Polym.* 2, 127–148. <https://doi.org/10.1039/d3lp00203a>.
- Guan, G., Pan, J.H., Li, Z., 2021. Innovative utilization of molecular imprinting technology for selective adsorption and (photo)catalytic eradication of organic pollutants. *Chemosphere* 265, 129077. <https://doi.org/10.1016/j.chemosphere.2020.129077>.
- Haroune, L., Salaun, M., Ménard, A., Legault, C.Y., Bellenger, J.P., 2014. Photocatalytic degradation of carbamazepine and three derivatives using TiO₂ and ZnO: effect of pH, ionic strength, and natural organic matter. *Sci. Total Environ.* 475, 16–22. <https://doi.org/10.1016/j.scitotenv.2013.12.104>.
- He, F., Lu, Z., Song, M., Liu, X., Tang, H., Huo, P., Fan, W., Dong, H., Wu, X., Han, S., 2019. Selective reduction of Cu²⁺ with simultaneous degradation of tetracycline by the dual channels ion imprinted POPD-CoFe₂O₄ heterojunction photocatalyst. *Chem. Eng. J.* 360, 750–761. <https://doi.org/10.1016/j.cej.2018.12.034>.
- D. Huang, R. Wang, Y. Liu, Application of molecularly imprinted polymers in wastewater treatment: a review, (2015a) 963–977. doi:10.1007/s11356-014-3599-8.

- Huang, M., Zhou, T., Wu, X., Mao, J., 2015b. Adsorption and degradation of norfloxacin by a novel molecular imprinting magnetic Fenton-like catalyst. *Chin. J. Chem. Eng.* 23, 1698–1704. <https://doi.org/10.1016/j.cjche.2015.08.030>.
- S. Huang, J. Xu, J. Zheng, F. Zhu, L. Xie, G. Ouyang, Synthesis and application of magnetic molecularly imprinted polymers in sample preparation, (2018) 3991–4014.
- Huang, Y., Wang, P., Chen, F., Zhou, G., Song, M., Liu, X., Ma, C., Han, S., Yan, Y., Lu, Z., 2021. Enhanced controllable degradation ability of magnetic imprinted photocatalyst via photoinduced surface imprinted technique for ciprofloxacin selectively degradation. *J. Photochem. Photobiol. A Chem.* 410, 113159. <https://doi.org/10.1016/j.jphotochem.2021.113159>.
- Huo, P., Lu, Z., Liu, X., Liu, X., Gao, X., Pan, J., Wu, D., Ying, J., Li, H., Yan, Y., 2012a. Preparation molecular/ions imprinted photocatalysts of La³⁺@POPD/TiO₂/fly-ash cenospheres: preferential photodegradation of TCs antibiotics. *Chem. Eng. J.* 198–199, 73–80. <https://doi.org/10.1016/j.cej.2012.05.089>.
- Huo, P., Lu, Z., Liu, X., Wu, D., Liu, X., Pan, J., Gao, X., Guo, W., Li, H., Yan, Y., 2012b. Preparation photocatalyst of selected photodegradation antibiotics by molecular imprinting technology onto TiO₂/fly-ash cenospheres. *Chem. Eng. J.* 189–190, 75–83. <https://doi.org/10.1016/j.cej.2012.02.030>.
- Kaya, S.I., Cetinkaya, A., Ozkan, S.A., 2023. Molecularly imprinted polymers as highly selective sorbents in sample preparation techniques and their applications in environmental water analysis. *Trends Environ. Anal. Chem.* 37, e00193. <https://doi.org/10.1016/j.teac.2022.e00193>.
- Koe, W.S., Lee, J.W., Chong, W.C., 2019. An overview of photocatalytic degradation: photocatalysts, mechanisms, and development of photocatalytic membrane. *Environ. Sci. Pollut. Res.* 27, 1–44. <https://doi.org/10.1007/s11356-019-07193-5>.
- Krakowiak, R., Musiał, J., Bakun, P., Spychała, M., Czarzynska-Goslinska, B., Mlynarczyk, D.T., Koczarowski, T., Sobotta, L., Stanisł, B., Goslinski, T., 2021. Titanium dioxide-based photocatalysts for degradation of emerging contaminants including pharmaceutical pollutants. *Appl. Sci.* 11. <https://doi.org/10.3390/app11188674>.
- Kumar, S., Karfa, P., Majhi, K.C., Madhuri, R., 2020. Photocatalytic, fluorescent BiPO₄@ Graphene oxide based magnetic molecularly imprinted polymer for detection, removal and degradation of ciprofloxacin. *Mater. Sci. Eng. C* 111. <https://doi.org/10.1016/j.msec.2020.110777>.
- Lai, C., Zhou, X., Huang, D., Zeng, G., Cheng, M., 2018. A review of titanium dioxide and its highlighted application in molecular imprinting technology in environment. *J. Taiwan Inst. Chem. Eng.* 91, 517–531. <https://doi.org/10.1016/j.jtice.2018.05.035>.
- Larsson, D.G.J., Flach, C.F., 2022. Antibiotic resistance in the environment. *Nat. Rev. Microbiol.* 20, 257–269. <https://doi.org/10.1038/s41579-021-00649-x>.
- Li, D., Yuan, R., Zhou, B., Chen, H., 2023b. Selective photocatalytic removal of sulfonamide antibiotics: the performance differences in molecularly imprinted TiO₂ synthesized using four template molecules. *J. Clean. Prod.* 383, 135470. <https://doi.org/10.1016/j.jclepro.2022.135470>.
- Li, D., Zhu, Q., Han, C., Yang, Y., Jiang, W., Zhang, Z., 2015. Photocatalytic degradation of recalcitrant organic pollutants in water using a novel cylindrical multi-column photoreactor packed with TiO₂-coated silica gel beads. *J. Hazard. Mater.* 285, 398–408. <https://doi.org/10.1016/j.jhazmat.2014.12.024>.
- Li, K., Xiong, J., Chen, T., Yan, L., Dai, Y., Song, D., Lv, Y., Zeng, Z., 2013. Preparation of graphene/TiO₂ composites by anionic surfactant strategy and their simulated sunlight and visible light photocatalytic activity towards representative aqueous POPs degradation. *J. Hazard. Mater.* 250–251, 19–28. <https://doi.org/10.1016/j.jhazmat.2013.01.069>.
- Li, L., Zheng, X., Chi, Y., Wang, Y., Sun, X., Yue, Q., Gao, B., Xu, S., 2020. Molecularly imprinted carbon nanosheets supported TiO₂: strong selectivity and synergic adsorption-photocatalysis for antibiotics removal. *J. Hazard. Mater.* 383, 121211. <https://doi.org/10.1016/j.jhazmat.2019.121211>.
- Li, Q., Huang, Y., Pan, Z., Ni, J., Yang, W., Chen, J., Zhang, Y., Li, J., 2022a. Hollow C, N-TiO₂@C surface molecularly imprinted microspheres with visible light photocatalytic regeneration availability for targeted degradation of sulfadiazine. *Sep. Purif. Technol.* 299, 121814. <https://doi.org/10.1016/j.seppur.2022.121814>.
- Li, X., Chen, X., Lv, Z., Wang, B., 2022b. Ultrahigh ciprofloxacin accumulation and visible-light photocatalytic degradation: contribution of metal organic frameworks carrier in magnetic surface molecularly imprinted polymers. *J. Coll. Interface Sci.* 616, 872–885. <https://doi.org/10.1016/j.jcis.2022.02.130>.
- Li, X., Wei, H., Song, T., Lu, H., Wang, X., 2023a. A review of the photocatalytic degradation of organic pollutants in water by modified TiO₂. *Water Sci. Technol.* 88, 1495–1507. <https://doi.org/10.2166/wst.2023.288>.
- Li, X., Yang, B., Xiao, K., Duan, H., Wan, J., Zhao, H., 2021. Targeted degradation of refractory organic compounds in wastewaters based on molecular imprinting catalysts. *Water Res.* 203, 117541. <https://doi.org/10.1016/j.watres.2021.117541>.
- Liu, R., Han, X., Liu, R., Qi, Z., Ren, B., Sun, Y., 2024. Molecularly imprinted Fe₃O₄/g-C₃N₄/TiO₂ catalyst for selective photodegradation of chlorotetracycline. *Coll. Surf. A Physicochem. Eng. Asp.* 680, 132691. <https://doi.org/10.1016/j.colsurfa.2023.132691>.
- Liu, X., Tang, L., Xu, L., Zhou, G., Liu, Q., Song, M., Ma, C., Lu, Z., Yan, Y., 2022. A temperature-sensitive modified imprinted Ag-Poly (o-phenylenediamine) photocatalyst synthesized by microwave method for efficient degradation of ciprofloxacin. *React. Kinet. Mech. Catal.* 135, 2137–2151. <https://doi.org/10.1007/s11444-022-02208-8>.
- Liu, Z., Chen, G., Lu, X., 2021. In-situ growth of molecularly imprinted metal-organic frameworks on 3D carbon foam as an efficient adsorbent for selective removal of antibiotics. *J. Mol. Liq.* 340, 117232. <https://doi.org/10.1016/j.molliq.2021.117232>.
- Lowdon, J.W., Diliën, H., Singla, P., Peeters, M., Cleij, T.J., van Grinsven, B., Eersels, K., 2020. MIPs for commercial application in low-cost sensors and assays – an overview of the current status quo. *Sens. Actuat. B Chem.* 325. <https://doi.org/10.1016/j.snb.2020.128973>.
- Lu, Z., Chen, F., He, M., Song, M., Ma, Z., Shi, W., Yan, Y., Lan, J., Li, F., Xiao, P., 2014. Microwave synthesis of a novel magnetic imprinted TiO₂ photocatalyst with excellent transparency for selective photodegradation of enrofloxacin hydrochloride residues solution. *Chem. Eng. J.* 249, 15–26. <https://doi.org/10.1016/j.cej.2014.03.077>.
- Lu, Z., Zhou, G., Song, M., Liu, X., Tang, H., Dong, H., Huo, P., Yan, F., Du, P., Xing, G., 2020. Development of magnetic imprinted PEDOT/CdS heterojunction photocatalytic nano-reactors: 3-Dimensional specific recognition for selectively photocatalyzing danofloxacin mesylate. *Appl. Catal. B Environ.* 268, 118433. <https://doi.org/10.1016/j.apcatb.2019.118433>.
- Luo, Y., Feng, X., Chen, Z., Shen, X., 2022. Molecularly imprinted photocatalysts: fabrication, application and challenges. *Mater. Adv.* 3, 8830–8847. <https://doi.org/10.1039/d2ma00848c>.
- Madikizela, L.M., Ncube, S., Chimuka, L., 2020. Analysis, occurrence and removal of pharmaceuticals in African water resources: a current status. *J. Environ. Manage.* 253, 109741. <https://doi.org/10.1016/j.jenvman.2019.109741>.
- Madikizela, L.M., Ncube, S., Nomngongo, P.N., Pakade, V.E., 2022. Molecular imprinting with deep eutectic solvents: synthesis, applications, their significance, and benefits. *J. Mol. Liq.* 362, 119696. <https://doi.org/10.1016/j.molliq.2022.119696>.
- Madikizela, L.M., Tavengwa, N.T., Chimuka, L., 2018. Applications of molecularly imprinted polymers for solid-phase extraction of non-steroidal anti-inflammatory drugs and analgesics from environmental waters and biological samples. *J. Pharm. Biomed. Anal.* 147, 624–633. <https://doi.org/10.1016/j.jpba.2017.04.010>.
- Majumder, A., Saidulu, D., Gupta, A.K., Ghosal, P.S., 2021. Predicting the trend and utility of different photocatalysts for degradation of pharmaceutically active compounds: a special emphasis on photocatalytic materials, modifications, and performance comparison. *J. Environ. Manage.* 293, 112858. <https://doi.org/10.1016/j.jenvman.2021.112858>.
- Martín-Esteban, A., 2013. Molecularly-imprinted polymers as a versatile, highly selective tool in sample preparation. *TrAC - Trends Anal. Chem.* 45, 169–181. <https://doi.org/10.1016/j.trac.2012.09.023>.
- Mohamadpour, F., Mohamadpour, F., 2024. Photodegradation of six selected antipsychiatric drugs; carbamazepine, sertraline, amisulpride, amitriptyline, diazepam, and alprazolam in environment: efficiency, pathway, and mechanism—a review. *Sustain. Environ. Res.* 34, 1–26. <https://doi.org/10.1186/s42834-024-00214-0>.
- Mokhtari, S., Faghian, H., Mirmohammadi, M., 2023. A core/shell TiO₂ magnetized molecularly imprinted photocatalyst (MMIP@TiO₂): synthesis and its photodegradation activity towards sulfasalazine. *Environ. Sci. Pollut. Res.* 30, 13624–13638. <https://doi.org/10.1007/s11356-022-22792-5>.
- Mumtaz, F., Atif, M., Naz, F., Li, B., Wang, K., Alshehri, M.R., 2024. Advanced hybrid molecular imprinted polymers for antibiotics remediation from wastewater. *ChemBioEng Rev.* 11, 495–512. <https://doi.org/10.1002/cben.202300057>.
- Musiał, J., Mlynarczyk, D.T., Stanisł, B.J., 2023. Photocatalytic degradation of sulfamethoxazole using TiO₂-based materials – Perspectives for the development of a sustainable water treatment technology. *Sci. Total Environ.* 856, 159122. <https://doi.org/10.1016/j.scitotenv.2022.159122>.
- Navidpour, A.H., Ahmed, M.B., Zhou, J.L., 2024. Photocatalytic degradation of pharmaceutical residues from water and sewage effluent using different TiO₂ nanomaterials. *Nanomaterials* 14. <https://doi.org/10.3390/nano14020135>.
- Ncube, P., Zvinowanda, C., Belaid, M., Ntuli, F., 2023. Heterogeneous photocatalytic degradation of nevirapine in wastewater using the UV/TiO₂/H₂O₂ process. *Environ. Process.* 10, 1–24. <https://doi.org/10.1007/s40710-022-00615-6>.
- Ncube, S., Madikizela, L.M., Chimuka, L., Nindi, M.M., 2018. Environmental fate and ecotoxicological effects of antiretrovirals: a current global status and future perspectives. *Water Res.* 145, 231–247. <https://doi.org/10.1016/j.watres.2018.08.017>.
- Nguyen, L.T., Nguyen, H.T., Pham, T.D., Tran, T.D., Chu, H.T., Dang, H.T., Nguyen, V.H., Nguyen, K.M., Pham, T.T., Van der Bruggen, B., 2020b. UV-Visible light driven photocatalytic degradation of ciprofloxacin by N,S Co-doped TiO₂: the effect of operational parameters. *Top. Catal.* 63, 985–995. <https://doi.org/10.1007/s11244-020-01319-7>.
- Nguyen, M.K., Moon, J.Y., Lee, Y.C., 2020a. Microalgal ecotoxicity of nanoparticles: an updated review. *Ecotoxicol. Environ. Saf.* 201. <https://doi.org/10.1016/j.ecoenv.2020.110781>.
- Peng, J., Deng, F., Shi, H., Wang, Z., Li, X., Zou, J., Luo, X., 2024. Target recognition and preferential degradation of toxic chemical groups by innovative group-imprinted photocatalyst with footprint cavity. *Appl. Catal. B Environ.* 340, 123179. <https://doi.org/10.1016/j.apcatb.2023.123179>.
- Poonia, K., Raizada, P., Singh, A., Verma, N., Ahamad, T., Alshehri, S.M., Khan, A.A.P., Singh, P., Hussain, C.M., 2022. Magnetic molecularly imprinted polymer photocatalysts: synthesis, applications and future perspective. *J. Ind. Eng. Chem.* 113, 1–14. <https://doi.org/10.1016/j.jiec.2022.05.029>.
- Rabizadeh, H., Feizbakhsh, A., Panahi, H.A., Konoz, E., 2020. A convenient synthesis of NiO-CuS/molecularly imprinted polymer nanocomposites with highly enhanced adsorption activity and selectivity for removal of Letrozole. *Polym. Technol. Mater.* 59, 619–629. <https://doi.org/10.1080/25740881.2019.1669658>.
- Rana, G., Dhiman, P., Kumar, A., Chauhan, A., Sharma, G., 2024. Recent advances in photocatalytic removal of antiviral drugs by Z-scheme and S-scheme heterojunction. *Environ. Sci. Pollut. Res.* 31, 40851–40872. <https://doi.org/10.1007/s11356-024-33876-9>.

- Renzi, M., Blašković, A., 2019. Ecotoxicity of nano-metal oxides: a case study on daphnia magna. *Ecotoxicology* 28, 878–889. <https://doi.org/10.1007/s10646-019-02085-3>.
- Ruziwa, D.T., Oluwalana, A.E., Mupa, M., Meili, L., Selvasembian, R., Nindi, M.M., Sillanpaa, M., Gwenzi, W., Chaukura, N., 2023. Pharmaceuticals in wastewater and their photocatalytic degradation using nano-enabled photocatalysts. *J. Water Process Eng.* 54, 103880. <https://doi.org/10.1016/j.jwpe.2023.103880>.
- Sajini, T., Gigimol, M.G., Mathew, B., 2019. A brief overview of molecularly imprinted polymers supported on titanium dioxide matrices. *Mater. Today Chem.* 11, 283–295. <https://doi.org/10.1016/j.mtchem.2018.11.010>.
- Sathishkumar, P., Meena, R.A.A., Palanisami, T., Ashokkumar, V., Palvannan, T., Gu, F. L., 2020. Occurrence, interactive effects and ecological risk of diclofenac in environmental compartments and biota - a review. *Sci. Total Environ.* 698, 134057. <https://doi.org/10.1016/j.scitotenv.2019.134057>.
- Shaykhi, Z.M., Zinatizadeh, A.A.L., 2014. Statistical modeling of photocatalytic degradation of synthetic amoxicillin wastewater (SAW) in an immobilized TiO₂ photocatalytic reactor using response surface methodology (RSM). *J. Taiwan Inst. Chem. Eng.* 45, 1717–1726. <https://doi.org/10.1016/j.jtice.2013.12.024>.
- Sheng, S., Zhang, Z., Wang, M., He, X., Jiang, C., Wang, Y., 2022. Synthesis of MIL-125 (Ti) derived TiO₂ for selective photoelectrochemical sensing and photocatalytic degradation of tetracycline. *Electrochim. Acta* 420, 140441. <https://doi.org/10.1016/j.electacta.2022.140441>.
- Singh, P., Borthakur, A., 2018. A review on biodegradation and photocatalytic degradation of organic pollutants: A bibliometric and comparative analysis. *J. Clean. Prod.* 196, 1669–1680. <https://doi.org/10.1016/j.jclepro.2018.05.289>.
- Skandalis, N., Maelisli, M., Papafotis, D., Miller, S., Lee, B., Theologidis, I., Luna, B., 2021. Environmental spread of antibiotic resistance. *Antibiotics* 10, 1–14. <https://doi.org/10.3390/antibiotics10060640>.
- Speltini, A., Scalabrini, A., Maraschi, F., Sturini, M., Profumo, A., 2017. Newest applications of molecularly imprinted polymers for extraction of contaminants from environmental and food matrices: a review. *Anal. Chim. Acta* 974, 1–26. <https://doi.org/10.1016/j.aca.2017.04.042>.
- Sun, L., Guan, J., Xu, Q., Yang, X., Wang, J., Hu, X., 2018. Synthesis and applications of molecularly imprinted polymers modified TiO₂ nanoparticles: a review. *Polymers (Basel)* 10, 1–26. <https://doi.org/10.3390/polym10111248>.
- Sun, L., Li, J., Li, X., Liu, C., Wang, H., Huo, P., Sheng Yan, Y., 2019. Molecularly imprinted Ag/Ag₃VO₄/g-C₃N₄ Z-scheme photocatalysts for enhanced preferential removal of tetracycline. *J. Coll. Interface Sci.* 552, 271–286. <https://doi.org/10.1016/j.jcis.2019.05.060>.
- Tang, M., Wan, J., Wang, Y., Yan, Z., Ma, Y., Sun, J., Ding, S., 2022. Developing a molecularly imprinted channels catalyst based on template effect for targeted removal of organic micropollutants from wastewaters. *Chem. Eng. J.* 445, 136755. <https://doi.org/10.1016/j.cej.2022.136755>.
- Teixeira, S., Gurke, R., Eckert, H., Ku, K., Fauler, J., Cuniberti, G., 2016. Photocatalytic degradation of pharmaceuticals present in conventional treated wastewater by nanoparticle suspensions. *J. Environ. Chem. Eng.* 4, 287–292. <https://doi.org/10.1016/j.jece.2015.10.045>.
- Theuretzbacher, U., 2013. Global antibacterial resistance: the never-ending story. *J. Glob. Antimicrob. Resist.* 1, 63–69. <https://doi.org/10.1016/j.jgar.2013.03.010>.
- Vahidifar, M., Es'haghi, Z., Oghaz, N.M., Mohammadi, A.A., Kazemi, M.S., 2022. Multi-template molecularly imprinted polymer hybrid nanoparticles for selective analysis of nonsteroidal anti-inflammatory drugs and analgesics in biological and pharmaceutical samples. *Environ. Sci. Pollut. Res.* 29, 47416–47435. <https://doi.org/10.1007/s11356-021-18308-2>.
- Varma, K.S., Tayade, R.J., Shah, K.J., Joshi, P.A., Shukla, A.D., Gandhi, V.G., 2020. Photocatalytic degradation of pharmaceutical and pesticide compounds (PPCs) using doped TiO₂ nanomaterials: a review. *Water-Energy Nexus* 3, 46–61. <https://doi.org/10.1016/j.wen.2020.03.008>.
- Vasapollo, G., Del Sole, R., Mergola, L., Lazzoi, M.R., Scardino, A., Scorrano, S., Mele, G., 2011. Molecularly imprinted polymers: present and future prospective. *Int. J. Mol. Sci.* 12, 5908–5945. <https://doi.org/10.3390/ijms12095908>.
- Villarreal-Lucio, D.S., Vargas-Berrones, K.X., Díaz de León-Martínez, L., Flores-Ramírez, R., 2022. Molecularly imprinted polymers for environmental adsorption applications. *Environ. Sci. Pollut. Res.* 29, 89923–89942. <https://doi.org/10.1007/s11356-022-24025-1>.
- Wang, H.T., Wu, X., Zhao, H.M., Quan, X., 2012. Enhanced photocatalytic degradation of tetracycline hydrochloride by molecularly imprinted film modified TiO₂ nanotubes. *Chin. Sci. Bull.* 57, 601–605. <https://doi.org/10.1007/s11434-011-4897-x>.
- Wang, J., Feng, J., Wei, C., 2023b. Molecularly imprinted polyaniline immobilized on Fe₃O₄/ZnO composite for selective degradation of amoxicillin under visible light irradiation. *Appl. Surf. Sci.* 609, 155324. <https://doi.org/10.1016/j.apsusc.2022.155324>.
- Wang, L., Yu, J., Wang, X., Li, J., Chen, L., 2023a. Molecular imprinting-based nanocomposite adsorbents for typical pollutants removal. *J. Hazard. Mater. Lett.* 4, 100073. <https://doi.org/10.1016/j.hazl.2022.100073>.
- Wu, X., Huang, M., Zhou, T., Mao, J., 2016. Recognizing removal of norfloxacin by novel magnetic molecularly imprinted chitosan/γ-Fe₂O₃ composites: selective adsorption mechanisms, practical application and regeneration. *Sep. Purif. Technol.* 165, 92–100. <https://doi.org/10.1016/j.seppur.2016.03.041>.
- Xia, T., Lin, Y., Li, W., Ju, M., 2021. Photocatalytic degradation of organic pollutants by MOFs based materials: a review. *Chin. Chem. Lett.* 32, 2975–2984. <https://doi.org/10.1016/j.ccllet.2021.02.058>.
- Xie, Y., Wan, J., Yan, Z., Wang, Y., Xiao, T., Hou, J., Chen, H., 2022. Targeted degradation of sulfamethoxazole in wastewater by molecularly imprinted MOFs in advanced oxidation processes: degradation pathways and mechanism. *Chem. Eng. J.* 429, 132237. <https://doi.org/10.1016/j.cej.2021.132237>.
- Yan, H., Ren, Y., Zhou, G., Wang, P., Xu, Y., Song, M., Liu, X., Ma, C., Han, S., Lu, Z., 2022. Aqueous-phase synthesis of heterojunction molecularly imprinted photocatalytic nanoreactor via stable interaction forces for improved selectivity and photocatalytic property. *Appl. Surf. Sci.* 579, 152174. <https://doi.org/10.1016/j.apsusc.2021.152174>.
- Yi, J., Wan, J., Ye, G., Wang, Y., Ma, Y., Yan, Z., Zeng, C., 2023. Targeted degradation of refractory organic pollutants in wastewater based on molecularly imprinted catalytic materials: adsorption process and degradation mechanism. *Sep. Purif. Technol.* 311, 123244. <https://doi.org/10.1016/j.seppur.2023.123244>.
- Yuan, Q., Zhang, D., Yu, P., Sun, R., Javed, H., Wu, G., Alvarez, P.J.J., 2020. Selective adsorption and photocatalytic degradation of extracellular antibiotic resistance genes by molecularly-imprinted graphitic carbon nitride. *Environ. Sci. Technol.* 54, 4621–4630. <https://doi.org/10.1021/acs.est.9b06926>.
- Zhang, F., Wang, Z., Peijnenburg, W.J.G.M., Vijver, M.G., 2022a. Review and prospects on the ecotoxicity of mixtures of nanoparticles and hybrid nanomaterials. *Environ. Sci. Technol.* 56, 15238–15250. <https://doi.org/10.1021/acs.est.2c03333>.
- Zhang, H., Xiao, Y., Peng, Y., Tian, L., Wang, Y., Tang, Y., Cao, Y., Wei, Z., Wu, Z., Zhu, Y., Guo, Q., 2023b. Selective degradation of ceftriaxone sodium by surface molecularly imprinted BiOCl/Bi₃NbO₇ heterojunction photocatalyst. *Sep. Purif. Technol.* 315, 123716. <https://doi.org/10.1016/j.seppur.2023.123716>.
- Zhang, J.Y., Ding, J., Liu, L.M., Wu, R., Ding, L., Jiang, J.Q., Pang, J.W., Li, Y., Ren, N.Q., Yang, S.S., 2024. Selective removal of sulfamethoxazole by a novel double Z-scheme photocatalyst: preferential recognition and degradation mechanism. *Environ. Sci. Technol.* 17, 100308. <https://doi.org/10.1016/j.jese.2023.100308>.
- Zhang, Y., Wang, Z.W., Yang, X.T., Zhu, Y.Z., Wang, H.F., 2022b. Afterglow-catalysis and molecular imprinting: a promising union for elevating selectivity in degradation of antibiotics. *Appl. Catal. B Environ.* 305, 121025. <https://doi.org/10.1016/j.apcatb.2021.121025>.
- Zhang, Y., Zhang, X., Wang, S., 2023a. Recent advances in the removal of emerging contaminants from water by novel molecularly imprinted materials in advanced oxidation processes - a review. *Sci. Total Environ.* 883, 163702. <https://doi.org/10.1016/j.scitotenv.2023.163702>.
- Zhu, X., Liu, J., Li, L., Zhen, G., Lu, X., Zhang, J., Liu, H., Zhou, Z., Wu, Z., Zhang, X., 2023. Prospects for humic acids treatment and recovery in wastewater: a review. *Chemosphere* 312, 137193. <https://doi.org/10.1016/j.chemosphere.2022.137193>.

APPENDIX FOR PAPER 2

PUBLISHED ARTICLE



Removal of efavirenz in wastewater effluents using a magnetic molecularly imprinted polymer: Synthesis, multivariate optimization and application

Asenathi Sibali^a, Devrani Naicker^a, Nompumelelo Pretty Cele^a, Vusumzi Emmanuel Pakade^b, Ramakwala Christinah Chokwe^b, Thabang Mokhothu^a, Somandla Ncube^{a,*}

^a Department of Chemistry, Durban University of Technology, P O Box 1334, Durban 4000, South Africa

^b Department of Chemistry, University of South Africa, Private Bag X6, Florida 1710, South Africa

ARTICLE INFO

Editor: Tzyy Haur Chong

Keywords:

Central composite design
Efavirenz
Molecularly imprinted polymer
Pollution
Wastewater

ABSTRACT

Efavirenz is the most detected antiretroviral drug in the aqueous environment and its levels are way higher compared to other antiretroviral drugs. This is a cause for concern and requires a shift towards finding remedial ways to minimize its potential impact to aquatic organisms. In the current study, a magnetic molecularly imprinted polymer was synthesized, optimized via central composite design and finally applied to remove of efavirenz from wastewater effluents. The magnetic smart polymer was synthesized via a bulk polymerization technique owing to its simplicity, low cost yet it yields a polymer of high purity. Efavirenz was used as the template and p-vinyl benzoic acid as the functional monomer. Based on coefficient plots, summary of fit and contour plots, the removal of efavirenz was directly affected by contact time, initial concentration of efavirenz and the mass of the magnetic polymer used under neutral conditions. The optimal binding capacity achieved after 40 min of contact time and neutral conditions was $44.9 \mu\text{g g}^{-1}$. The polymeric sorbent could achieve 44.8 % removal efficiencies from real wastewater effluents polluted with 3.99 ng mL^{-1} of efavirenz. Reusability studies showed <4 % average loss in the binding capacity with every reuse cycle, while there was no loss in binding capabilities when the polymer was utilized at about half its binding capacity.

1. Introduction

The release of pharmaceuticals into the aqueous environment has negative effects on humans and other aquatic species. Antiretroviral drugs (ARVDs) are among a group of pharmaceuticals with potentially serious ecotoxicological effects when they make their way into the environment. Exposure to them via contaminated water may be consequential especially for those already taking ARVDs and for new infections because ARVDs work against a virus that easily mutates if the drugs are not taken according to prescription. The analysis of ARVDs in the aqueous environment in South Africa started about 10 years ago and the first paper was published in 2015 [1]. Since then, there has been a plethora of other studies that have detected ARVDs in wastewater, rivers and dams in South Africa and the African continent at large [2,3]. Major sources of the ARVDs in the environment are mainly through effluents from wastewater treatment plants (WWTPs) as well as illicit or indiscriminate disposal of expired drugs [2,3]. Poor sanitation in most African regions, unavailability of modern ablution facilities that can be

flushed with water to direct the human waste into WWTPs and improper disposal of expired or unused medications have contributed to the direct contamination of surface water with pharmaceuticals.

A further challenge for Africa is that the infection rates continue to surge resulting in more ARVDs released into the environment as part of excreta [4,5]. South Africa in particular has been identified as a hotspot regarding ARVD contamination due to the relatively high therapeutic application and lack of wastewater treatment processes that can effectively minimize their release via effluents. In this regard, the presence of ARVDs in various aqueous systems such as wastewater effluents, surface water, ground water, and even drinking water has been reported extensively in South Africa [1,6,7]. Efavirenz is the most detected ARVD in surface environments and some scholars now consider it as a priority pollutant in African water bodies [4,8]. The performance of conventional wastewater treatment processes in South Africa has recently been observed to be less effective in the removal of efavirenz [9]. For example, four WWTPs in the Gauteng Province could only remove between 21 and 27 % of efavirenz [10]. In the Eastern Cape Province,

* Corresponding author.

E-mail address: SomandlaN@dut.ac.za (S. Ncube).

<https://doi.org/10.1016/j.jwpe.2025.107786>

Received 8 December 2024; Received in revised form 16 April 2025; Accepted 20 April 2025

Available online 23 April 2025

2214-7144/© 2025 The Authors. Published by Elsevier Ltd. This is an open access article under the CC BY-NC license (<http://creativecommons.org/licenses/by-nc/4.0/>).

WWTPs were reported to achieve between 2 and 12 % removal efficiencies [11], while in the KwaZulu Natal Province, removal efficiencies for four of the five WWTPs ranged between 19 and 38 % [12]. In view of these observations, it is crucial that alternative removal strategies are explored to minimize entry of efavirenz into the environment through WWTP effluents.

In the current study, we have investigated a magnetic molecularly imprinted polymer (MMIP) as a potential remedial tool for efavirenz in WWTP effluents. MIPs are the synthetic materials with structural cavities designed to selectively isolate a specific target from complex matrices. The MIPs have been utilized in separation science to selectively isolate target analytes from complicated samples [13]. Despite the documented advantages that include low-cost production and stability, classic MIPs still have the challenge of isolating them from the sample matrix once they have adsorbed the target molecule. In this regard, recent studies have emphasized the need for incorporating magnetic materials to allow for their removal using an external magnetic field [14–17]. In our study, the MMIP was synthesized, characterized and its performance was optimized before its application as a sorbent to remove efavirenz from real effluent samples from a WWTP in Durban, South Africa. With the view that the smart polymer needs to be deployed in wastewater effluents, it was magnetized with magnetite (iron oxide) to offer the advantage of trapping it at the deployment site using an external magnetic force [18,19]. The MMIP could be recovered from wastewater effluents, cleaned, and re-deployed to continue adsorbing efavirenz from the effluents. Previously, MIPs for ARVDs have been utilized as sorbents for solid phase extraction (SPE) for the purposes of quantifying ARVDs in various aqueous samples, including efavirenz [12,20–22]. Nevirapine was included in the study as a competitor of efavirenz for the active binding sites on the magnetic polymer cavities.

2. Methods and materials

2.1. Chemicals and reagents

Analytical grade efavirenz and nevirapine as well as all organic solvents of HPLC grade (acetonitrile, methanol, ethyl acetate, dimethylformamide and toluene) were purchased from Merck (Pty) Ltd., Johannesburg, South Africa. Chemicals for synthesis of the MIP including ethylene glycol dimethacrylate (EGDMA) (the cross-linker), p-vinyl benzoic acid (the monomer) and 1,1'-azobis(isobutyronitrile) (AIBN) as the initiator were also purchased from Merck (Pty) Ltd., Johannesburg, South Africa.

2.2. Gas chromatography mass spectrometry

Chromatographic quantitation was carried out on a gas chromatograph coupled with triple quadrupole mass spectrometry (GC-TQMS) by Scion instruments, Goes, Netherlands. A 100-ng mL⁻¹ standard was first run in full scan mode to determine a suitable temperature program and the retention times of the efavirenz and nevirapine. A temperature program from 170 to 280 °C gave retention times of 4.15 and 5.12 min, respectively. The transfer line temperature and source temperature were set at 290 °C and 250 °C, respectively. The spectra of the two ARVDs were searched in the NIST library and positively identified with 87 and 92 % matches for efavirenz and nevirapine, respectively. A single ion monitoring (SIM) method was then created by setting the 4.15 and 5.12 min as retention times while the *m/z* values were set at 316 and 266 for efavirenz and nevirapine, respectively. The mass error was set at ±5 ppm. The GC-TQMS was then calibrated using 10 calibration standards of efavirenz in the concentration range of 10–100 ng mL⁻¹. The limit of detection (LOD) and limit of quantitation (LOQ) were computed using the linear regression method based on the Linest function in Excel. These were further used to determine the method detection limit (MDL) and method quantitation limit (MQL) based on the amount of MMIP used and the volume of the effluents.

2.3. Synthesis of a magnetic smart sorbent

2.3.1. Synthesis of magnetite

For synthesis of magnetite, 3 g of FeCl₃·6H₂O and 1.5 g of FeSO₄·7H₂O were dissolved in 100 mL of deionized water in a round bottom flask. The solution was heated to 50 °C and then 12 mL of concentrated ammonia solution was added and the mixture stirred vigorously for 30 min. The temperature was then increased and maintained at 90 °C for 30 min. Magnetic nanoparticles were magnetically retained at the bottom of the flask, washed with water and ethanol and dried in an oven overnight at 60 °C.

2.3.2. Synthesis of a magnetic molecularly imprinted polymer

The synthesis of MMIP was done by transferring 0.0736 mmol of efavirenz as a template into a 50 mL round bottom flask containing 3 mL dimethylformamide as a porogen. The resulting homogeneous solution was stirred at 200 rpm and 40 °C for 5 min to completely dissolve the monomer templates in dimethylformamide. Then 41 mg of p-vinyl benzoic acid as a functional monomer was added and the mixture stirred for a further 5 min. A 0.2 g mass of magnetite from Section 2.3.1 was added to the solution followed by mild ultrasonic treatment for 15 min. Then 208 µL of EGDMA was added as a crosslinker followed by 100 mg of the AIBN initiator. The mixture was allowed to pre-polymerize in an inert atmosphere (nitrogen) for 10 min and the temperature of the mixture was then increased to 70 °C and maintained for 30 min. The temperature was finally increased to 90 °C until a polymer was formed. The polymer was formed within 2 h but it was allowed to remain in the silicon bath at 90 °C for a further 2 h to stabilize. The product was dried in an oven overnight at 70 °C. The dried MMIP was then crushed into a fine powder and washed with methanol/acetic acid (9:1 v/v) to remove the ARVD template molecules creating cavities within each grain of the polymer powder. The magnetic polymer was then characterized using Fourier transform infrared spectroscopy (FTIR) and thermogravimetric analysis (TGA). The MIP was synthesized using the same procedure as MMIP in the absence of the magnetite.

2.4. Optimization experiments using central composite design

The interactive effects of four factors that could affect the adsorption of efavirenz from aqueous solution were optimized simultaneously using central composite design (CCD) created on MODDE Pro statistical software by Sartorius, Göttingen, Germany. These were sample pH (4–9), mass of MMIP (5–15 mg), initial concentration of efavirenz (0.1–1 ng mL⁻¹) and contact time (10–120 min). The design output based on a quadratic model with star points placed on the faces of the sides composed of 27 experiments of which three of the experiments were randomly set for repeated design runs. The CCD output was then experimented and the peak area was chosen as a response factor. All the 27 design runs were done in triplicate and the average peak area was used for data analysis.

2.5. Investigating the mechanism and kinetics of adsorption

To investigate the extent of adsorption of efavirenz, 50 mg of the MMIP was dispersed into 5 mL spiked solutions over a concentration range of 10–300 ng mL⁻¹. The extraction process was allowed to take place under ambient conditions for 10 min. The results were then used to plot two important isotherm models; the Langmuir and Freundlich adsorption isotherms. The Langmuir adsorption isotherm predicts linear adsorption and a maximum surface coverage [23]. The model explains that all binding sites are homogeneous with uniform adsorption energy and that each site can accommodate only one molecule, thus only a single layer of adsorption (a monolayer) occurs [24]. The mathematical representation of the linearized form of the Langmuir model is summarized using Eq. 1. On the other hand, the Freundlich adsorption isotherm model predicts a heterogeneous binding site distribution,

meaning binding sites with different adsorption energies [23]. The linearized mathematical representation of the Freundlich model is summarized using Eq. 2. These linearized equations are used to plot linear graphs based on the $y = mx + c$ form. The model whose linear plot gives a higher coefficient of determination (R^2) is accepted as the model that explains the extent of adsorption.

$$1/q_e = \left(1/K_L Q_{max}\right) \left(\frac{1}{C_e}\right) + 1/Q_{max} \quad (1)$$

where q_e is the adsorption capacity of the ARVDs at equilibrium (ng g^{-1}), Q_{max} is the monolayer maximum adsorption capacity of the sorbent (ng g^{-1}) and K_L is the Langmuir equilibrium constant (L g^{-1}) and C_e is the concentration of ARVDs (ng g^{-1}).

$$\log q_e = \log K_F + \frac{1}{n} \log C_i \quad (2)$$

where K_F is the Freundlich constant (L g^{-1}) and n is the heterogeneity factor.

The pseudo-first-order (PFO) and pseudo-second-order (PSO) adsorption kinetic models are the most commonly used in understanding adsorption kinetics. To investigate the kinetics, a 50 mg mass of the MMIP was added in centrifuge tubes containing 5 mL of water spiked at 200 ng mL^{-1} of efavirenz. Three tubes were randomly collected for analysis at specific time intervals over a period of 10 to 120 min. The analysis data was then used to plot the linear forms of the PFO and PSO models based on Eq. 3 and 4, respectively. The model with a better R^2 value was accepted as the one that explained the mechanism of adsorption of efavirenz onto the MMIP cavities. PFO predicts that adsorption occurs by physisorption while PSO predicts chemisorption.

$$\ln(q_e - q_t) = \ln q_e - k_1 t \quad (3)$$

$$t/q_e = 1/k_2 q_e^2 + t/q_e \quad (4)$$

where k_1 and k_2 are the rate constants for the pseudo first- and second-order models (min^{-1}), respectively.

2.6. Reusability studies

To investigate the possibility of reusing the polymer to extract efavirenz from effluent samples, the MMIP was used and regenerated repeatedly under its maximum binding capacity and at half its binding capacity. This was done by placing 10 mg of the MMIP in 5 mL of water spiked at 50 and 100 $\mu\text{g mL}^{-1}$ of efavirenz then allowing adsorption to occur at 25 °C for 40 min. This was followed by trapping the MMIP using an external magnet and the spiked sample decanted. Thereafter, the MMIP was washed with 5 mL methanol to determine the amount of efavirenz extracted. The same MIP was used repeatedly for five consecutive cycles of adsorption/desorption.

2.7. Application of the MMIP in wastewater effluent samples

2.7.1. Wastewater effluent collection and analysis

Samples were collected from a WWTP in Durban, South Africa that treats both domestic and industrial wastewater using conventional treatment methods with chlorination as the final step. After chlorination, the effluents are discharged into a nearby river. Wastewater was collected at the exit point where the treated wastewater discharges into a river after chlorination. All samples were collected into 2.5 L brown glass bottles and transported to the laboratory in cooler boxes. In the laboratory, the samples were sonicated and immediately filtered through 0.45 μm filter paper. The filtered samples were then extracted using solid phase extraction (SPE) with Hydrophilic-Lipophilic-Balance (HLB) (6 cc Vac, 200 mg) cartridges by Waters Corporation, Milford, USA as sorbents followed by analysis using a gas chromatography coupled with triple quadrupole mass spectrometry (GC-TQMS). For SPE,

50 mL of wastewater effluent samples was diluted with 50 mL deionized water. The HLB cartridges were first conditioned with 5 mL of methanol followed by equilibrating with 3 mL of deionized water. The diluted wastewater effluent samples (100 mL) were then loaded at about 1 mL min^{-1} . The pumping process was continued for a further 5 min to dry the cartridges. About 1 mL of 2 % methanol in water was then used to wash the cartridges. Finally, 5 mL of methanol was used to elute the analytes from the cartridges followed by immediate analysis using GC-TQ/MS. This process was repeated three times.

2.7.2. Removal of efavirenz using the magnetic polymer

Once the amount of efavirenz had been determined in effluents using SPE-GC-TQMS, the MMIP was then applied to the effluent samples to remove the ARVDs. A volume of 100 mL of undiluted wastewater effluent sample was poured into a 250 mL beaker. Then 20 mg of the MMIP was added and the mixture allowed to settle. After 30 min, a magnet was used to trap the MMIP at the bottom of the beaker and the effluent was decanted. The MMIP was then washed with 5 mL of methanol to determine the amount of efavirenz trapped by the polymer. The amount trapped was then compared with the amount found in the effluents using SPE. This was used to determine the efficiency of the MMIP in removing the ARVDs from wastewater effluents using Eq. 5.

$$\text{Removal efficiency} = n_{MMIP}/n_E \times 100\% \quad (5)$$

where n_{MMIP} is the amount removed by the MMIP, n_E is the amount of efavirenz in effluents.

3. Results and discussion

3.1. Characterization results

All the significant peaks observed for the MIP in Fig. 1A agreed with the information acquired from previous studies in which p-vinyl benzoic acid and EDGMA were used during polymer formation [25]. The FTIR of the synthesized magnetite exhibited typical -OH and Fe—O absorption bands as evidence of the purity of the synthesized magnetite nanoparticles [26]. The broad signal band at around 3400 cm^{-1} represented -OH stretching while the two bands at around 1650 and 1480 cm^{-1} were due to -OH and O—H vibrational modes of water particles on the surface of the nanoparticle. The Fe—O stretching was observed at around 580 cm^{-1} . The presence of -OH and Fe—O bands was an indication that the synthesized magnetite nanoparticles were of high purity. After co-polymerization, the -OH stretch initially observed for magnetite was suppressed both at 3400, 650 and 1480 cm^{-1} which was an indication that the magnetite lost the H_2O particles from its surface as it was incorporated into the MIP during co-polymerization.

The TGA results in Fig. 1B show that the MMIP polymer maintains its weight up to 250 °C and only degrades to about 80 % at 350 °C. The incorporation of the magnetite nanoparticles tends to destabilize the polymer because the MIP maintained almost 100 % stability up to 350 °C. Results of similar nature where MIPs maintain >80 % of their weight at temperatures above 300 °C have been reported in literature [27–29]. These observations are an indication that the polymer can be used under extreme environmental conditions without degradation.

3.2. Optimization results

3.2.1. Method validity and interactive effects

The performance of the design model and its fit-for-purpose summary is presented visually in Fig. 2. The coefficient plots in Fig. 2A show that initial concentration of the ARVD in solution, the mass of the MMIP used as the sorbent and the time it remains in contact with efavirenz had a positive significant effect on the adsorption kinetics. However, a change in pH of the solution seemed to have a minimal effect which is similar to other studies from the literature [4]. The coefficient plots

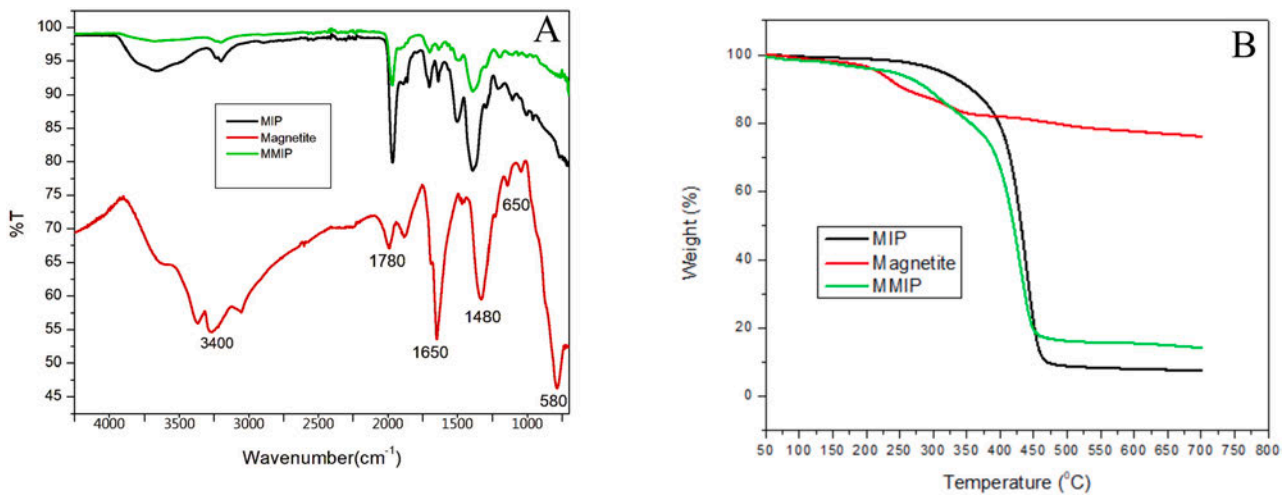


Fig. 1. FTIR spectrum (A) and TGA thermogram (B) of the sorbents.

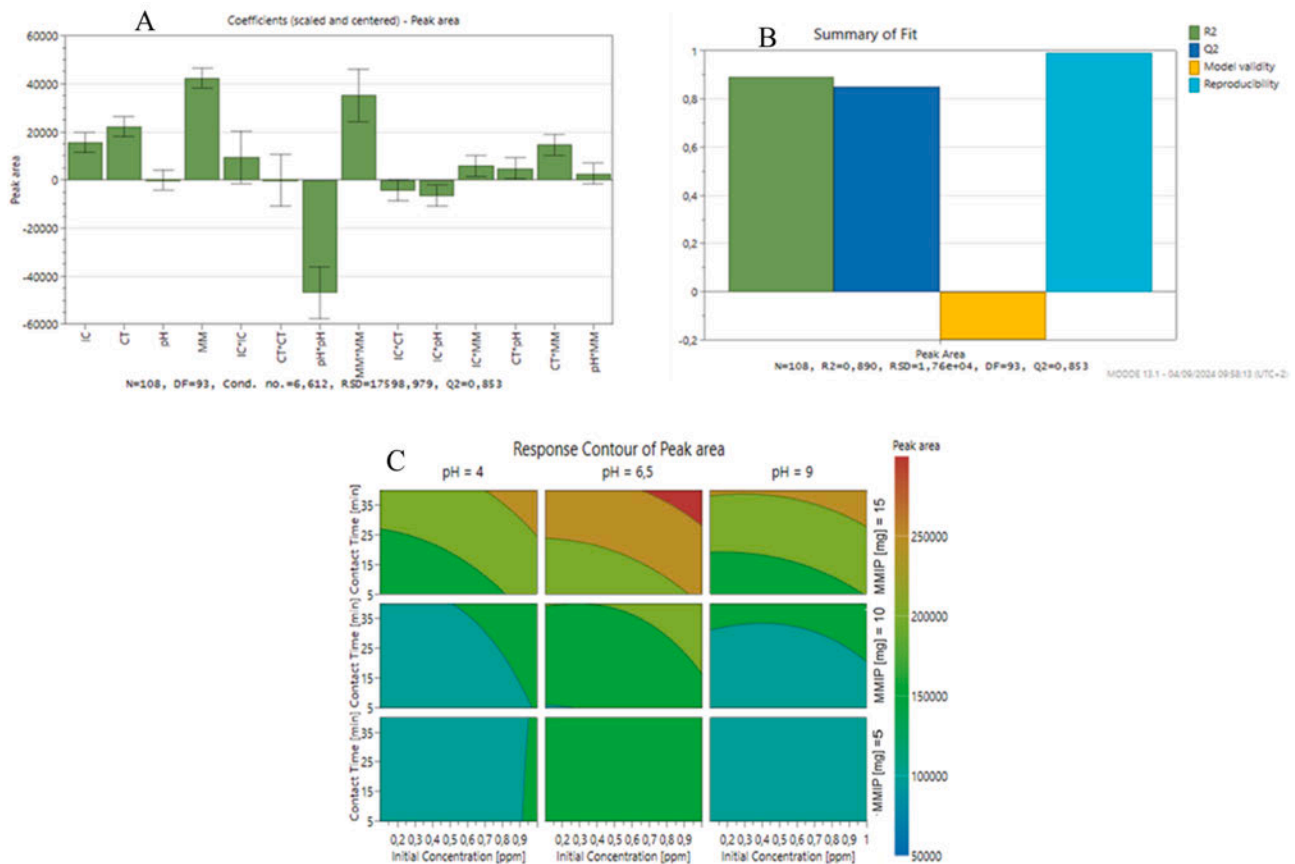


Fig. 2. Coefficient plots (A), summary of fit (B) and contour plots (C) of the optimized factors. IC – initial concentration; CT – contact time; MM – mass of the magnetic molecularly imprinted polymer.

further show that most factors had minimal dependence on interactive effects except for the pH*pH dual interaction which led to a significant negative effect on the MMIP's performance, while the MMIP*MMIP interaction had a significantly positive effect. The reliability of these observations is presented as a summary of fit plots (Fig. 2B). Acceptable values for coefficient of determination (R^2), predictive relevance (Q^2), and reproducibility were observed for the model with $R^2 = 0.890$, $Q^2 = 0.833$ and reproducibility of 0.99 indicating minimal error in the response output. The negative value of the model validity in Fig. 2B does

not necessarily imply an incorrect model form but rather represents an artificial lack of fit since acceptable values are observed for R^2 , Q^2 and reproducibility. This implies that the model error is still in the same range as the pure error, therefore it can be utilized as a valid model.

Surface response outputs obtained through simultaneous investigation of effects of initial concentration, contact time, sample pH and mass of MMIP were visualized in form of contour plots as shown in Fig. 2C. From the plots, it was observed that initial concentration, mass of the MMIP and contact time had a direct effect on the amount of efavirenz

extracted from solution which corroborated with the results of coefficient plots in Fig. 2A. As for pH, efavirenz was adsorbed better under neutral conditions with both basic and acidic conditions resulting in less adsorption.

3.2.2. Adsorption kinetics and mechanism

The adsorption of efavirenz followed pseudo second order kinetics (Table 1) suggesting that the interaction between the MMIP and the efavirenz was through chemisorption attaining a maximum adsorption of $44.9 \mu\text{g g}^{-1}$ within 40 min (Fig. 3). Similar adsorption kinetics has been observed where a MMIP was used for extraction of other pharmaceuticals including 17β -estradiol [30]. Other studies on MMIP for pharmaceuticals have obtained faster kinetics including Dai and colleagues who investigated adsorption kinetics of carbamazepine and clofibric acid and achieved equilibrium after 15 min [31]. When the MMIP was used to bind nevirapine as an interferent, it was observed that its maximum binding capacity towards nevirapine was just $11.5 \mu\text{g g}^{-1}$.

For the adsorption modelling results, it was observed that the Langmuir model was favoured with a higher R^2 value of 0.9975 compared to 0.991 for the Freundlich model (Table 1). The Freundlich model value is still relatively high but Fig. 4B shows that it fails to explain the adsorption mechanism at low concentrations of efavirenz. The Langmuir isotherm model was therefore accepted as the model that explains the extent of adsorption of the efavirenz onto the MMIP cavities. In addition, the R_L value was in the favourable range of $0 < R_L < 1$, while the predicted maximum adsorption capacity of $48.9 \mu\text{g g}^{-1}$ (Table 1) is comparable with the experimental maximum value of $53.6 \mu\text{g g}^{-1}$ (Fig. 3). The Langmuir isotherm model assumes that all binding sites are homogeneous with uniform adsorption energy and the adsorption process gives a monolayer coverage. This was an indication that once a MIP cavity is occupied, no further adsorption occurs on that cavity. This agrees with the adsorption kinetic results in which interaction between efavirenz and the MIP cavity functional groups was predicted to occur through chemisorption [12,20,22].

3.3. Reusability studies

MMIP regeneration studies in Fig. 5A show a slight gradual decrease in the adsorption capacity if the MMIP is used close to its maximum capacity, however losing only 19 % after five consecutive cycles. The reusability of the synthesized MIP corresponds to the behaviour reported in literature for the extraction of abacavir [28]. Minimal loss is observed if the MMIP is used repeatedly at half its binding capacity maintaining an almost 100 % reusability (Fig. 5B) which is advantageous considering the concentrations of efavirenz that have been reported in the environment [6,12,22].

3.4. Application in wastewater samples

3.4.1. Method validation and levels of efavirenz in wastewater effluents

Validation parameters for analysis of efavirenz using GC-TQMS are presented in Table 2. Good sensitivity of the SPE-GC-TQMS was observed with the MDL and MQL for efavirenz at 0.0265 and $0.0804 \text{ ng mL}^{-1}$, respectively. All relative standard deviation values based on triplicate analysis were $<14\%$. Most studies have reported LODs such as $0.41 \mu\text{g L}^{-1}$ [12], and 0.16 ng mL^{-1} , [32]. Studies that report MDLs for

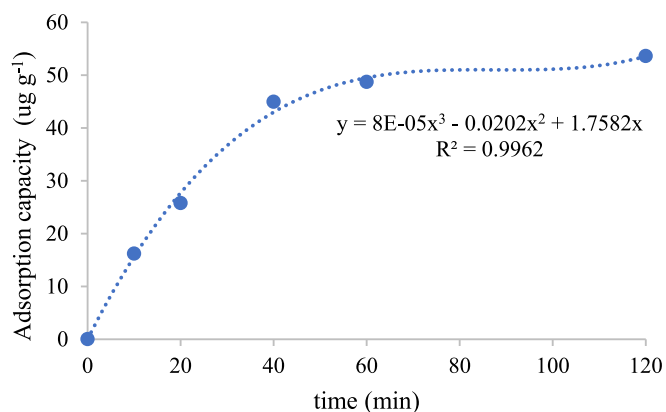


Fig. 3. Effects of contact time on the adsorption capacity. Experimental conditions: initial concentration of efavirenz – 200 ng mL^{-1} , sample pH – 6, adsorbent mass – 50 mg and sample volume – 5 mL .

efavirenz remain limited in literature [33]. For example, the MDL values were 0.12 and 0.84 ng L^{-1} in river and estuary samples, respectively [11], while 0.70 up to 9 ng L^{-1} have been reported in WWTP effluents using LC-MS [6,10,33].

The amount of efavirenz detected in the effluent using SPE-GC-TQMS was found to be 3.99 ng mL^{-1} (Table 2). The results are comparable with those reported in WWTP effluents across South Africa. In the KwaZulu Natal Province where the current study was conducted, researchers have reported varying concentrations of efavirenz mostly between 0.028 and 34 ng mL^{-1} [6,12,22] while higher concentrations of 46 – 96.11 ng mL^{-1} have also been recently reported [34]. In other provinces within South Africa, levels of efavirenz in wastewater effluents range between 0.021 and 7.6 ng mL^{-1} [10,35–38]. Nevirapine was not detected in the current study which corroborates with other studies where it was either not detected or just reported in very low levels $<1.92 \text{ ng mL}^{-1}$ [6,10,22,35,36,38,39]. Extreme concentrations of up to 92.11 ng mL^{-1} have also been reported [34].

3.4.2. Removal of efavirenz from wastewater effluents

The application of the MMIP as a sorbent that removes efavirenz from undiluted raw wastewater effluents gave an average of 44.8% (Table 2). This performance was considered relatively effective since the effluents were undiluted and unspiked which represented true wastewater effluent with its matrices. These performances are comparable with other advanced treatment processes that have been applied on wastewater effluents for the purposes of removing ARVDs from the effluents. For example, photolysis based on $\text{UV}/\text{H}_2\text{O}_2$ has been reported to remove between 20 and 50% of nevirapine from effluents [40]. However, other processes that perform better than the current method have been reported in the literature. Adeola and colleagues used graphene wool and reported 80% removal efficiency for efavirenz [4]. An exfoliated graphene sorbent for removal of ARVDs including efavirenz achieved up to 81% efficiency for ARVDs [34]. The same research group further reported up to 86% removal efficiency using activated macadamia nutshells [41]. While the reported sorbents from the literature performed better, the MMIP sorbent used in the current study boasts the magnetic advantage that allows it to be held static and can be removed

Table 1
Modelling results.

Pseudo-1st order	Pseudo-2nd order		Freundlich model	Langmuir model			
R^2	R^2	$K_2 (\text{g } \mu\text{g}^{-1} \text{ min}^{-1})$	R^2	R^2	$K_L (\mu\text{L g}^{-1})$	R_L	$Q_{\text{max}} (\mu\text{g g}^{-1})$
0.9752	0.9833	1.51	0.9910	0.9975	0.1199	0.199	48.9

R^2 - coefficient of determination; K_2 pseudo-second order constant; q_e - equilibrium adsorption capacity; K_L - the Langmuir equilibrium adsorption constant (L g^{-1}); R_L - the separation factor; Q_{max} - maximum adsorption capacity.

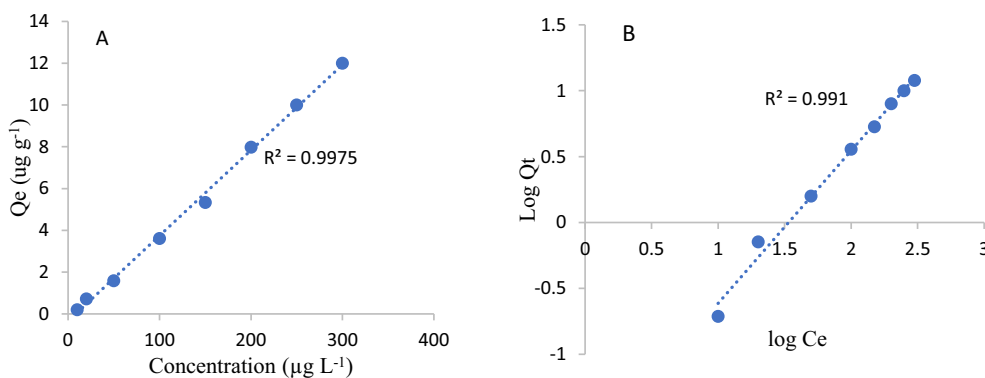


Fig. 4. Effects of initial concentration on the adsorption capacity. A - Langmuir model; B - Freundlich model.

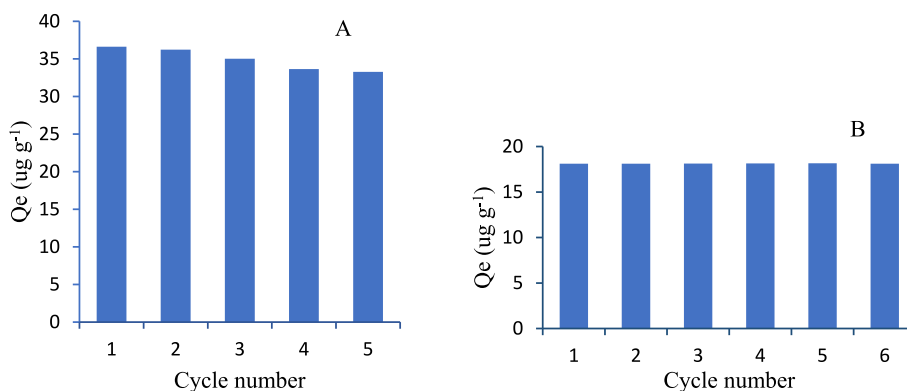


Fig. 5. Reusability of efavirenz in five consecutive cycles at the MMIP maximum binding capacity (A) and at half its capacity (B).

Table 2

Method validation, concentration of ARVDs in effluents and removal efficiencies.

Analyte	SIM ion (<i>m/z</i>)	R^2	Calibration accuracy (%)	MDL (ng mL ⁻¹)	MQL (ng mL ⁻¹)	Concentration in effluent (ng mL ⁻¹)	Removal efficiency (% ± RSD %)
Efavirenz	315	0.9908	92.2–104.7	0.0265	0.0804	3.99	44.8 ± 11
Nevirapine	266	0.9981	92.3–104	0.0331	0.100	n.d	–

n.d - not detected.

from the real effluents in the environment using an external magnetic field. It is noteworthy mentioning that most studies that have mentioned recoveries of ARVDs from effluents are almost always done for the purposes of quantitation while studies that report removal efficiencies as a remedial tool remain limited. In this regard, the magnetic sorbent presented in the current study might be a viable remedial approach with potential applicability in the environment.

4. Conclusions

A magnetic smart polymer has been successfully synthesized and applied as a sorbent for efavirenz from wastewater effluents achieving 44.8 % removal efficiencies. Its fit for purpose prediction was verified statistically using central composite design outputs such as coefficient plots, summary of fit and contour plots. Although the removal efficiency is still relatively low, the smart sorbent was optimized using environmental wastewater effluent polluted with efavirenz. The sorbent has a further advantage of being magnetized which could permit for its deployment in the environment and its eventual recovery for reuse using an external magnetic field. The magnetic sorbent has shown great potential and could be a viable alternative to remediation of efavirenz and other ARVDs from surface water sources.

CRediT authorship contribution statement

Asenathi Sibali: Writing – original draft, Methodology, Investigation, Formal analysis, Conceptualization. **Devrani Naicker:** Writing – review & editing, Validation, Formal analysis, Conceptualization. **Nompumelelo Pretty Cele:** Writing – review & editing, Validation, Formal analysis, Conceptualization. **Vusumzi Emmanuel Pakade:** Writing – review & editing, Validation, Supervision, Conceptualization. **Ramakwala Christinah Chokwe:** Writing – review & editing, Validation, Conceptualization. **Thabang Mokhothu:** Writing – review & editing, Validation, Supervision, Conceptualization. **Somanda Ncube:** Writing – review & editing, Validation, Supervision, Resources, Conceptualization.

Funding

This research did not receive any specific grant from funding agencies in the public, commercial, or not-for-profit sectors.

Declaration of competing interest

The authors declare that they have no known competing financial interests or personal relationships that could have appeared to influence

the work reported in this paper.

Acknowledgment

In loving memory of Nompumelelo Pretty Cele.

Data availability

Data will be made available on request.

References

- T.P. Wood, C.S.J. Duvenage, E. Rohwer, The occurrence of anti-retroviral compounds used for HIV treatment in South African surface water, *Environ. Pollut.* 199 (2015) 235–243. Available at: <https://doi.org/10.1016/j.envpol.2015.01.030>.
- W. Gwenzi, N. Chaukura, Organic contaminants in African aquatic systems: current knowledge, health risks and future research directions, *Sci. Total Environ.* 619–620 (2018) 1493–1514. Available at: <https://doi.org/10.1016/j.scitotenv.2017.11.121>.
- L.M. Madikizela, S. Ncube, L. Chimuka, Analysis, occurrence and removal of pharmaceuticals in African water resources: a current status, *J. Environ. Manage.* 253 (August 2019) (2020) 109741. Available at: <https://doi.org/10.1016/j.jenvman.2019.109741>.
- A.O. Adeola, J. de Lange, P.B.C. Forbes, Adsorption of antiretroviral drugs, efavirenz and nevirapine from aqueous solution by graphene wool: kinetic, equilibrium, thermodynamic and computational studies, *Applied Surface Science, Advances* 6 (2021) 100157. Available at: <https://doi.org/10.1016/j.apsadv.2021.100157>.
- S. Ncube, et al., Environmental fate and ecotoxicological effects of antiretrovirals: a current global status and future perspectives, *Water Res.* 145 (2018) 231–247. Available at: <https://doi.org/10.1016/j.watres.2018.08.017>.
- O.A. Abafe, et al., LC-MS/MS determination of antiretroviral drugs in influents and effluents from wastewater treatment plants in KwaZulu-Natal, South Africa, *Chemosphere* 200 (2018) 660–670. Available at: <https://doi.org/10.1016/j.chemosphere.2018.02.105>.
- B. Moslah, et al., Pharmaceuticals and illicit drugs in wastewater samples in north-eastern Tunisia, *Environ. Sci. Pollut. Res.* 25 (2018) 18226–18241. Available at: <https://doi.org/10.1007/s11356-017-8902-z>.
- C. Nannou, et al., Analytical strategies for the determination of antiviral drugs in the aquatic environment, *Trends in Environmental, Anal. Chem.* 24 (2019) e00071. Available at: <https://doi.org/10.1016/j.teac.2019.e00071>.
- R. Wang, et al., Antiviral drugs in wastewater are on the rise as emerging contaminants: a comprehensive review of spatiotemporal characteristics, removal technologies and environmental risks, *J. Hazard. Mater.* 457 (May) (2023) 131694. Available at: <https://doi.org/10.1016/j.jhazmat.2023.131694>.
- C. Schoeman, M. Dlamini, O.J. Okonkwo, The impact of a wastewater treatment works in southern Gauteng, South Africa on efavirenz and nevirapine discharges into the aquatic environment, *Emerging Contaminants* 3 (2) (2017) 95–106. Available at: <https://doi.org/10.1016/j.emcon.2017.09.001>.
- R. Netshithothole, L.M. Madikizela, Occurrence of selected pharmaceuticals in the East London coastline encompassing major rivers, estuaries, and seawater in the Eastern Cape Province of South Africa, *ACS Measurement Science* 4 (3) (2024) 283–293. Available at: <https://doi.org/10.1021/acsmesurescia.4c00004>.
- S.P. Mtolo, P.N. Mahlambi, L.M. Madikizela, Synthesis and application of a molecularly imprinted polymer in selective solid-phase extraction of efavirenz from water, *Water Science & Technology* 79 (2019) 356–365. Available at: <https://doi.org/10.2166/wst.2019.054>.
- J.J. Belbruno, Molecularly imprinted polymers, *Chem. Rev.* 119 (1) (2019) 94–119. Available at: <https://doi.org/10.1021/acs.chemrev.8b00171>.
- C. Dong, et al., Molecularly imprinted polymers by the surface imprinting technique, *Eur. Polym. J.* 145 (December 2020) (2021) 110231. Available at: <https://doi.org/10.1016/j.eurpolymj.2020.110231>.
- M.S. Eissa, et al., Magnetic molecularly imprinted polymers and carbon dots molecularly imprinted polymers for green micro-extraction and analysis of pharmaceuticals in a variety of matrices, *Microchem. J.* 205 (April) (2024) 111235. Available at: <https://doi.org/10.1016/j.microc.2024.111235>.
- Y. Liu, et al., Rigorous recognition mode analysis of molecularly imprinted polymers—rational design, challenges, and opportunities, *Progr. Polym. Sci.* 150 (2024), <https://doi.org/10.1016/j.procpolymsci.2024.101790> (Available at).
- M. Sobiech, et al., Impact of structure and magnetic parameters of nanocrystalline cores on surface properties of molecularly imprinted nanoconjugates for analysis of biomolecules – a case of tyramine, *Microchem. J.* 179 (February) (2022), <https://doi.org/10.1016/j.microc.2022.107571> (Available at).
- S.I. Kaya, A. Cetinkaya, S.A. Ozkan, Molecularly imprinted polymers as highly selective sorbents in sample preparation techniques and their applications in environmental water analysis, *Trends in Environmental, Anal. Chem.* 37 (September 2022) (2023) e00193. Available at: <https://doi.org/10.1016/j.teac.2022.e00193>.
- R. Nisticò, Magnetic materials and water treatments for a sustainable future, *Res. Chem. Intermed.* 43 (12) (2017) 6911–6949. Available at: <https://doi.org/10.1007/s11164-017-3029-x>.
- S. Khulu, et al., Multivariate optimization of a two-way technique for extraction of pharmaceuticals in surface water using a combination of membrane assisted solvent extraction and a molecularly imprinted polymer, *Chemosphere* 286 (2022) 131973. Available at: <https://doi.org/10.1016/j.chemosphere.2021.131973>.
- S. Sigonya, et al., Synthesis of a multi-template molecular imprinted bulk polymer for the adsorption of non-steroidal inflammatory and antiretroviral drugs, *Appl. Sci.* 14 (8) (2024), <https://doi.org/10.3390/app14083320> (Available at).
- T. Xolo, P. Mahlambi, Molecularly imprinted polymers as solid-phase and dispersive solid-phase extraction sorbents in the extraction of antiretroviral drugs in water: adsorption, selectivity and reusability studies, *J. Anal. Sci. Technol.* 15 (1) (2024), <https://doi.org/10.1186/s40543-024-00418-4> (Available at).
- M.A. Al-ghouti, D.A. Da, Guidelines for the use and interpretation of adsorption isotherm models: a review, *J. Hazard. Mater.* 393 (January) (2020) 122383. Available at: <https://doi.org/10.1016/j.jhazmat.2020.122383>.
- M. Patel, et al., Pharmaceuticals of emerging concern in aquatic systems: chemistry, occurrence, effects, and removal methods, *Chem. Rev.* 119 (6) (2019) 3510–3673. Available at: <https://doi.org/10.1021/acs.chemrev.8b00299>.
- S. Bakhtiar, S.A. Bhawani, S.R. Shafiqat, Synthesis and characterization of molecular imprinting polymer for the removal of 2-phenylphenol from spiked blood serum and river water, *Chem. Biol. Technol. Agric.* 6 (1) (2019) 1–10. Available at: <https://doi.org/10.1186/s40538-019-0152-5>.
- M. Veneranda, et al., FTIR spectroscopic semi-quantification of iron phases: a new method to evaluate the protection ability index (PAI) of archaeological artefacts corrosion systems, *Corros. Sci.* 133 (2018) 68–77. Available at: <https://doi.org/10.1016/j.corsci.2018.01.016>.
- S. Khulu, S. Ncube, T. Kgame, Synthesis, characterization and application of a molecularly imprinted polymer as an adsorbent for solid-phase extraction of selected pharmaceuticals from water samples, *Polym. Bull.* 79 (2) (2022) 1287–1307. Available at: <https://doi.org/10.1007/s00289-021-03553-9>.
- S.N. Qwane, P.S. Mdluli, L.M. Madikizela, Synthesis, characterization and application of a molecularly imprinted polymer in selective adsorption of abacavir from polluted water, *South African, J. Chem.* 73 (2020) 84–91. Available at: [10.17159/0379-4350/2020/V73A13](https://doi.org/10.17159/0379-4350/2020/V73A13).
- S.S. Zungu, et al., Synthesis and application of a molecularly imprinted polymer in the solid-phase extraction of ketoprofen from wastewater, *C. R. Chim.* 20 (5) (2017) 585–591. Available at: <https://doi.org/10.1016/j.crci.2016.09.006>.
- L. Bi, et al., Preparation and adsorption properties of magnetic molecularly imprinted polymers for selective recognition of 17 β -estradiol, *Separations* 9 (381) (2022) 1–15.
- C. Dai, J. Zhang, Y. Zhang, Removal of carbamazepine and clofibrac acid from water using double templates – molecularly imprinted polymers, 2013, pp. 5492–5501 (Available at), <https://doi.org/10.1007/s11356-013-1565-5>.
- H. Mokgope, et al., Quantification of some ARVs' removal efficiency from wastewater using a moving bed biofilm reactor, *Water Sci. Technol.* 86 (11) (2022) 2928–2942. Available at: <https://doi.org/10.2166/wst.2022.353>.
- L. Yao, et al., Development and validation of sensitive methods for simultaneous determination of 9 antiviral drugs in different various environmental matrices by UPLC-MS/MS, *Chemosphere* 282 (May) (2021) 131047. Available at: <https://doi.org/10.1016/j.chemosphere.2021.131047>.
- P.N. Kunene, P.N. Mahlambi, T. Ndlovu, Adsorption of antiretroviral drugs, abacavir, nevirapine, and efavirenz from river water and wastewater using exfoliated graphite: isotherm and kinetic studies, *J. Environ. Manage.* 360 (May) (2024) 121200. Available at: <https://doi.org/10.1016/j.jenvman.2024.121200>.
- V. Mhuka, S. Dube, M.M. Nindi, Occurrence of pharmaceutical and personal care products (PPCPs) in wastewater and receiving waters in South Africa using LC-Orbitrap™ MS, *Emerging Contaminants* 6 (2020) 250–258. Available at: <https://doi.org/10.1016/j.emcon.2020.07.002>.
- T.T. Mosekiamang, M.A. Stander, A. de Villiers, Simultaneous quantification of commonly prescribed antiretroviral drugs and their selected metabolites in aqueous environmental samples by direct injection and solid phase extraction liquid chromatography - tandem mass spectrometry, *Chemosphere* 220 (2019) 983–992. Available at: <https://doi.org/10.1016/j.chemosphere.2018.12.205>.
- R. Netshithothole, et al., Occurrence of selected pharmaceuticals in wastewater and sludge samples from wastewater treatment plants in Eastern Cape province of South Africa, 2024, pp. 7–14.
- C. Schoeman, et al., Quantification of selected antiretroviral drugs in a wastewater treatment works in South Africa using GC-TOFMS, *Journal of Chromatography & Separation, Techniques* 06 (04) (2015) 1–8. Available at: <https://doi.org/10.4172/2157-7064.1000272>.
- M.N. Akawa, K.M. Dimpe, P.N. Nomngongo, Amine-functionalized magnetic activated carbon as an adsorbent for preconcentration and determination of acidic drugs in environmental water samples using HPLC-DAD, *Open Chem.* 18 (2020) 1218–1229.
- E. Ngumba, A. Gachanja, T. Tuhkanen, Removal of selected antibiotics and antiretroviral drugs during post-treatment of municipal wastewater with UV, UV/chlorine and UV/hydrogen peroxide, *Water Environ. J.* 34 (4) (2020) 692–703. Available at: <https://doi.org/10.1111/wej.12612>.
- L. Simelane, et al., Removal of antiretroviral drugs from wastewater using activated macadamia nutshells: adsorption kinetics, adsorption isotherms, and thermodynamic studies, *Water Environ. Res.* 96 (4) (2024) 1–16. Available at: <https://doi.org/10.1016/wer.11020>.

APPENDEIX FOR PAPER 3

All supplementary work in this section is for paper 2

Table S2-1: MODDE software multivariate optimization

Exp No	Exp Name	Run Order	Incl/Excl	Initial Concentration	Contact time	pH	MIP mass
1	N1	55	Incl	0.1	5	4	5
2	N2	31	Incl	1	5	4	5
3	N3	57	Incl	0.1	40	4	5
4	N4	42	Incl	1	40	4	5
5	N5	4	Incl	0.1	5	9	5
6	N6	98	Incl	1	5	9	5
7	N7	65	Incl	0.1	40	9	5
8	N8	77	Incl	1	40	9	5
9	N9	104	Incl	0.1	5	4	15
10	N10	99	Incl	1	5	4	15
11	N11	69	Incl	0.1	40	4	15
12	N12	47	Incl	1	40	4	15
13	N13	95	Incl	0.1	5	9	15
14	N14	49	Incl	1	5	9	15
15	N15	44	Incl	0.1	40	9	15
16	N16	56	Incl	1	40	9	15
17	N17	15	Incl	0.1	22.5	6.5	10

18	N18	45	Incl	1	22.5	6.5	10
19	N19	102	Incl	0.55	5	6.5	10
20	N20	73	Incl	0.55	40	6.5	10
21	N21	35	Incl	0.55	22.5	4	10
22	N22	2	Incl	0.55	22.5	9	10
23	N23	17	Incl	0.55	22.5	6.5	5
24	N24	107	Incl	0.55	22.5	6.5	15
25	N25	64	Incl	0.55	22.5	6.5	10
26	N26	12	Incl	0.55	22.5	6.5	10
27	N27	41	Incl	0.55	22.5	6.5	10
28	N28	21	Incl	0.1	5	4	5
29	N29	11	Incl	1	5	4	5
30	N30	5	Incl	0.1	40	4	5
31	N31	36	Incl	1	40	4	5
32	N32	24	Incl	0.1	5	9	5
33	N33	43	Incl	1	5	9	5
34	N8	1	Incl	0.1	40	9	5
35	N35	53	Incl	1	40	9	5
36	N36	54	Incl	0.1	5	4	15
37	N37	25	Incl	1	5	4	15
38	N38	74	Incl	0.1	40	4	15
39	N39	6	Incl	1	40	4	15

40	N40	96	Incl	0.1	5	9	15
41	N41	29	Incl	1	5	9	15
42	N42	14	Incl	0.1	40	9	15
43	N43	89	Incl	1	40	9	15
44	N44	9	Incl	0.1	22.5	6.5	10
45	N45	3	Incl	1	22.5	6.5	10
46	N46	16	Incl	0.55	5	6.5	10
47	N47	81	Incl	0.55	40	6.5	10
48	N48	46	Incl	0.55	22.5	4	10
49	N49	82	Incl	0.55	22.5	9	10
50	N50	62	Incl	0.55	22.5	6.5	5
51	N51	23	Incl	0.55	22.5	6.5	15
52	N52	20	Incl	0.55	22.5	6.5	10
53	N53	100	Incl	0.55	22.5	6.5	10
54	N54	50	Incl	0.55	22.5	6.5	10
55	N55	66	Incl	0.1	5	4	5
56	N56	32	Incl	1	5	4	5
57	N57	27	Incl	0.1	40	4	5
58	N58	103	Incl	1	40	4	5
59	N59	58	Incl	0.1	5	9	5
60	N60	71	Incl	1	5	9	5
61	N9	108	Incl	0.1	40	9	5

62	N62	52	Incl	1	40	9	5
63	N63	87	Incl	0.1	5	4	15
64	N64	76	Incl	1	5	4	15
65	N65	83	Incl	0.1	40	4	15
66	N66	40	Incl	1	40	4	15
67	N67	93	Incl	0.1	5	9	15
68	N68	7	Incl	1	5	9	15
69	N69	61	Incl	0.1	40	9	15
70	N70	19	Incl	1	40	9	15
71	N71	101	Incl	0.1	22.5	6.5	10
72	N72	91	Incl	1	22.5	6.5	10
73	N73	106	Incl	0.55	5	6.5	10
74	N74	86	Incl	0.55	40	6.5	10
75	N75	90	Incl	0.55	22.5	4	10
76	N76	84	Incl	0.55	22.5	9	10
77	N77	79	Incl	0.55	22.5	6.5	5
78	N78	48	Incl	0.55	22.5	6.5	15
79	N79	18	Incl	0.55	22.5	6.5	10
80	N80	80	Incl	0.55	22.5	6.5	10
81	N81	88	Incl	0.55	22.5	6.5	10
82	N82	51	Incl	0.1	5	4	5
83	N83	78	Incl	1	5	4	5

84	N84	8	Incl	0.1	40	4	5
85	N85	105	Incl	1	40	4	5
86	N86	28	Incl	0.1	5	9	5
87	N87	97	Incl	1	5	9	5
88	N10	85	Incl	0.1	40	9	5
89	N89	94	Incl	1	40	9	5
90	N90	75	Incl	0.1	5	4	15
91	N91	59	Incl	1	5	4	15
92	N92	63	Incl	0.1	40	4	15
93	N93	92	Incl	1	40	4	15
94	N94	67	Incl	0.1	5	9	15
95	N95	60	Incl	1	5	9	15
96	N96	10	Incl	0.1	40	9	15
97	N97	39	Incl	1	40	9	15
98	N98	26	Incl	0.1	22.5	6.5	10
99	N99	38	Incl	1	22.5	6.5	10
100	N100	68	Incl	0.55	5	6.5	10
101	N101	70	Incl	0.55	40	6.5	10
102	N102	72	Incl	0.55	22.5	4	10
103	N103	34	Incl	0.55	22.5	9	10
104	N104	13	Incl	0.55	22.5	6.5	5
105	N105	30	Incl	0.55	22.5	6.5	15

106	N106	22	Incl	0.55	22.5	6.5	10
107	N107	33	Incl	0.55	22.5	6.5	10
108	N108	37	Incl	0.55	22.5	6.5	10

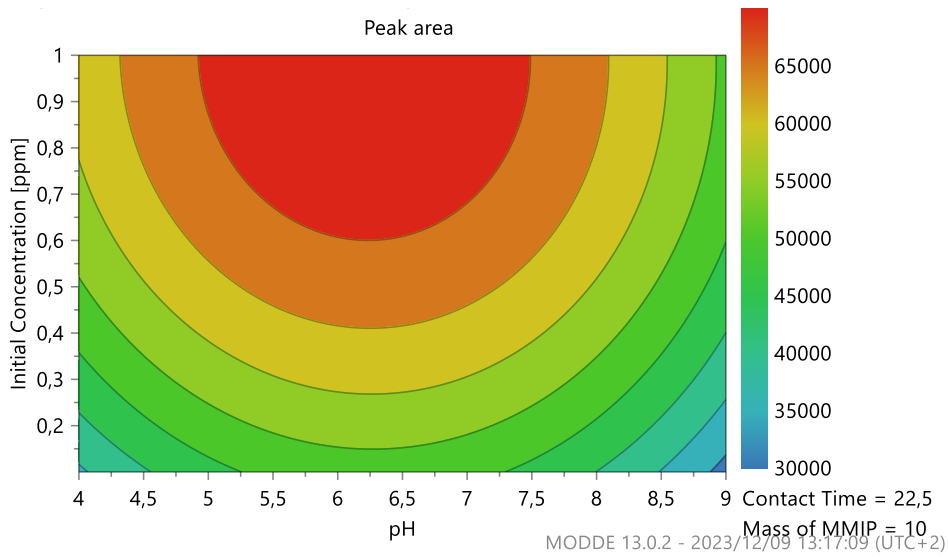


Fig S2-1: Response contour plot for initial concentration vs pH

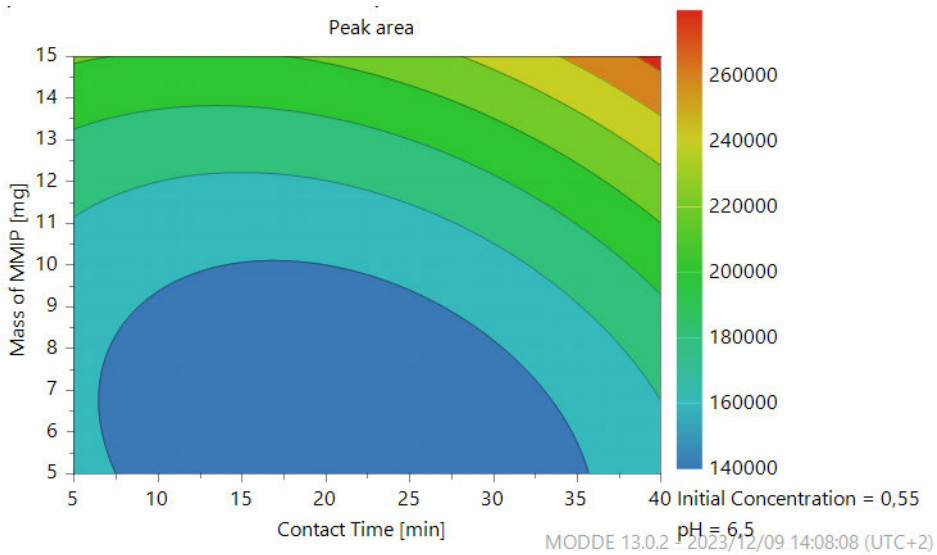


Fig S2-2: Response contour plot for mass of MMIP vs contact time

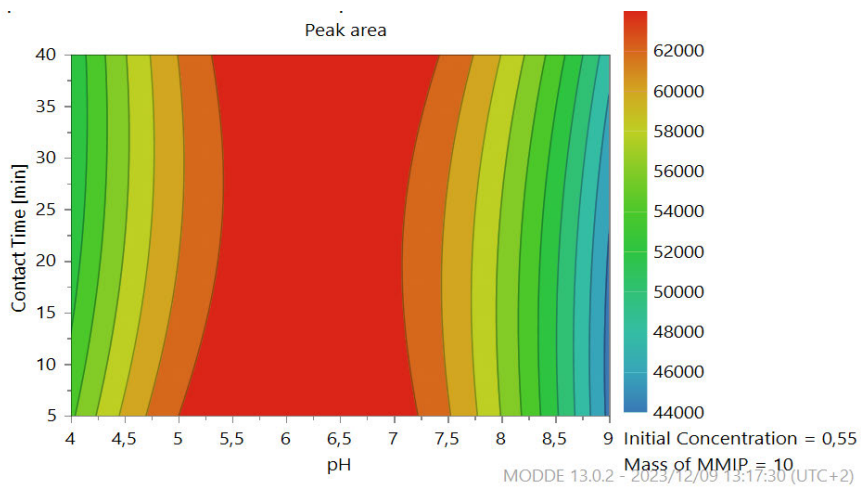


Fig S2-3: Response contour plot for contact time vs pH

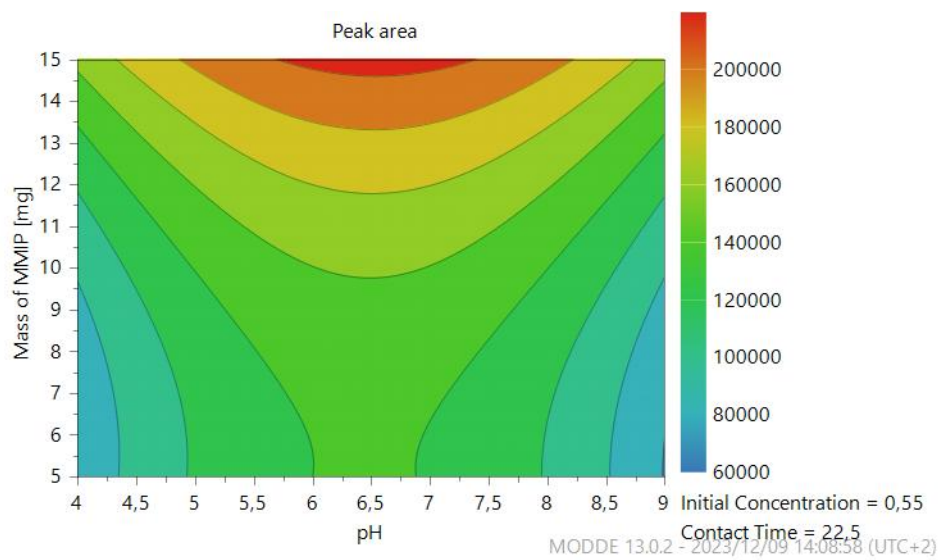


Fig S2-4: Response contour plot for mass of mass of MMIP vs pH

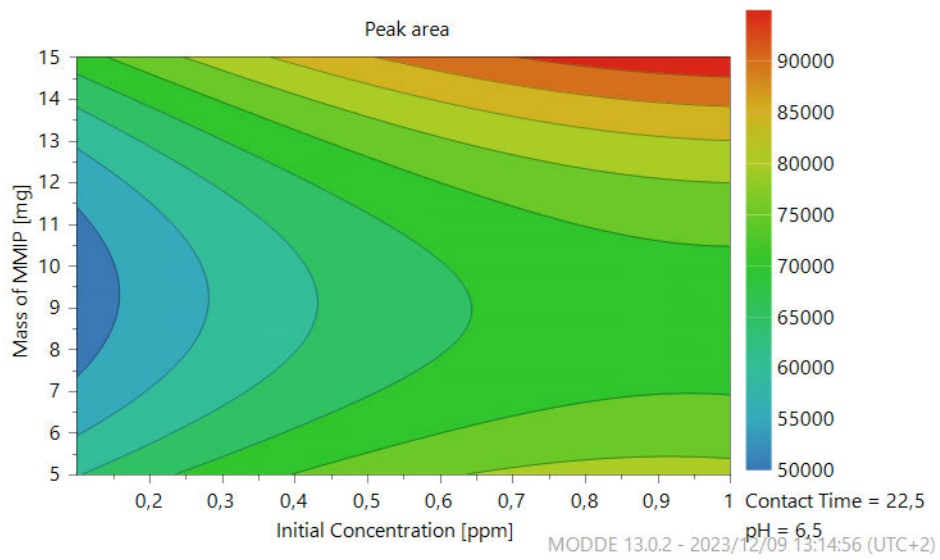


Fig S2-5: Response contour plot for initial concentration vs mass of MMIP

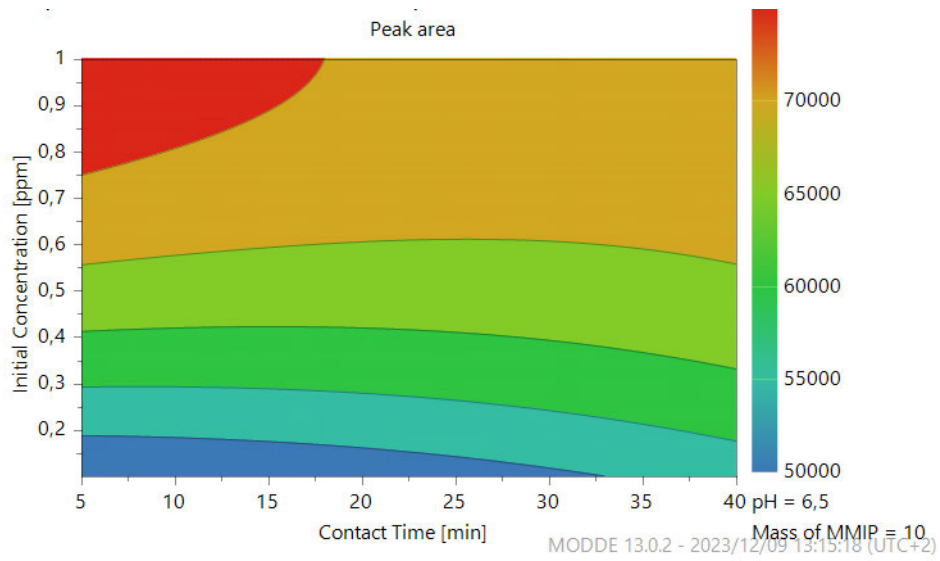


Fig S2-6: Response contour plots for initial concentration vs contact time

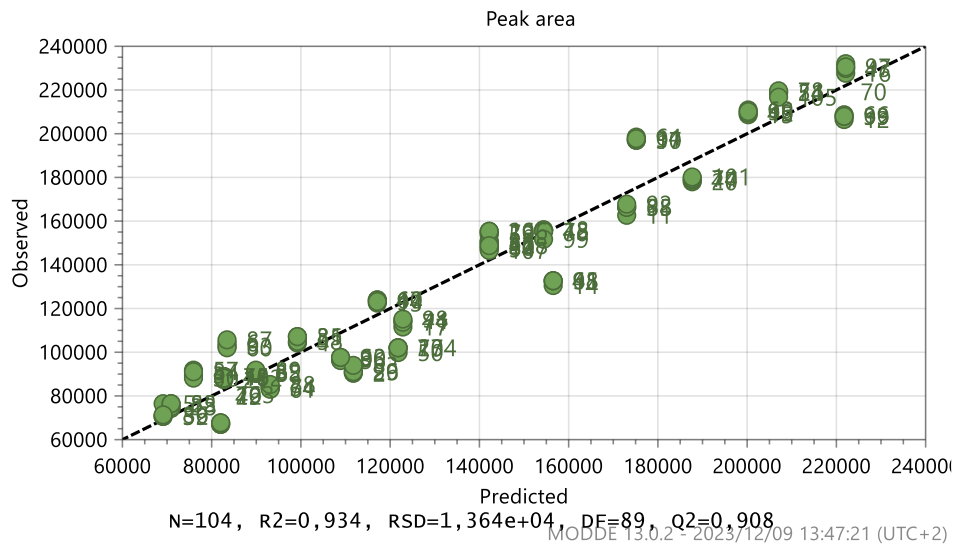


Fig S2-7: Observed vs predicted- Modde results

APPENDIX FOR PAPER 3

All supplementary work in this section is for paper 3

Initial Conc	Mass of M	Time of Irradiation	Peak area	Final Conc	Efficiency
60	15	40	100	1.5	98
40	1.591	30	88	1.3	97
40	10	30	45	0.7	98
40	10	30	112	1.7	96
60	5	20	67	1.0	98
40	10	46.8179	68	1.0	97
60	5	40	195	2.9	95
40	10	30	146	2.2	95
20	15	20	129	1.9	90
73.6359	10	30	79	1.2	98
40	10	13.1821	23	0.3	99
60	15	20	99	1.5	98
40	10	30	207	3.1	92
20	15	40	109	1.6	92
20	5	40	45	0.7	97
6.3641	10	30	192	2.9	55
20	5	20	69	1.0	95
40	18.409	30	81	1.2	97
40	10	30	131	2.0	95
40	10	30	188	2.8	93
40	10	30	188	2.8	93

Initial Conc	Mass of MM	Time of Irra	Peak area	Conc	Efficiency
60	15	40	529	7.935	87
40	1.591	30	216	3.24	92
40	10	30	332	4.98	88
40	10	30	433	6.495	84
60	5	20	263	3.945	93
40	10	46.8179	573	8.595	79
60	5	40	639	9.585	84
40	10	30	433	6.495	84
20	15	20	581	8.715	56
73.6359	10	30	244	3.66	95
40	10	13.1821	782	11.73	71
60	15	20	530	7.95	87
40	10	30	237	3.555	91
20	15	40	257	3.855	81
20	5	40	458	6.87	66
6.3641	10	30	241	3.615	43
20	5	20	353	5.295	74
40	18.409	30	338	5.07	87
40	10	30	408	6.12	85
40	10	30	421	6.315	84

APPENDIX 4– Poster Presentation

Understanding the adsorption kinetics of efavirenz using molecularly imprinted nanosorbent based on central composite design

Asenathi Sibali^a, Thabang Mokhothu^a, Dervan Naicker^a, Nompumelelo Cele^a, Samson Mohamane^b, Yusumzi Pakade^b and Somandla Ncube^a

^aDepartment of Chemistry, Durban University of Technology, P.O Box 1334, Durban, 4001, South Africa

^bDepartment of Chemistry, KwaDlangezwa Campus, University of Zululand, Empangeni 3886, South Africa

^cDepartment of Chemistry, University of South Africa, Private Bag X6, Florida, 1710, South Africa

Email: 21404005@dut4life.ac.za.

INTRODUCTION

Efavirenz is the most detected antiretroviral drug in the aqueous environment and its levels are way higher compared to other antiretroviral drugs. This is a cause for concern and requires a shift towards finding remediation ways to minimize its potential impact to aquatic organisms. In the current study we have synthesized a magnetic molecularly imprinted polymer, optimized it via central composite design and finally applied it in the removal of efavirenz in wastewater effluents.

AIM AND OBJECTIVES

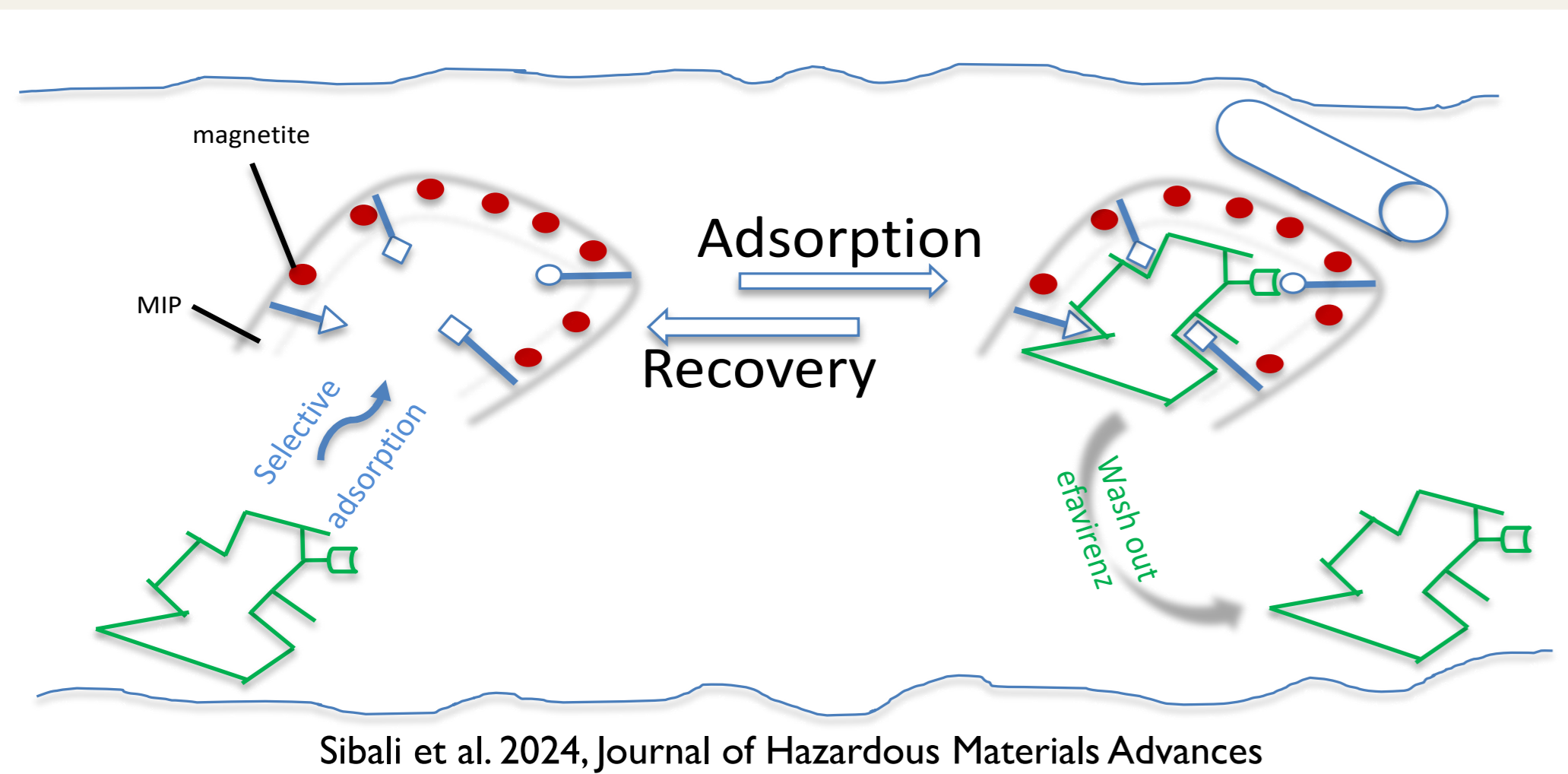
Aim

To synthesize a MMIP nanocomposite for removal of efavirenz from wastewater effluents.

Objectives

- To determine the best working conditions of efavirenz using MMIP.
- To characterize MMIP, MIP and magnetite.
- To predict the extent of adsorption of ARVDs onto the nanocomposite based on the Langmuir and Friedrich.

METHODOLOGY



Bulk polymerization in the presence of magnetite nanoparticles

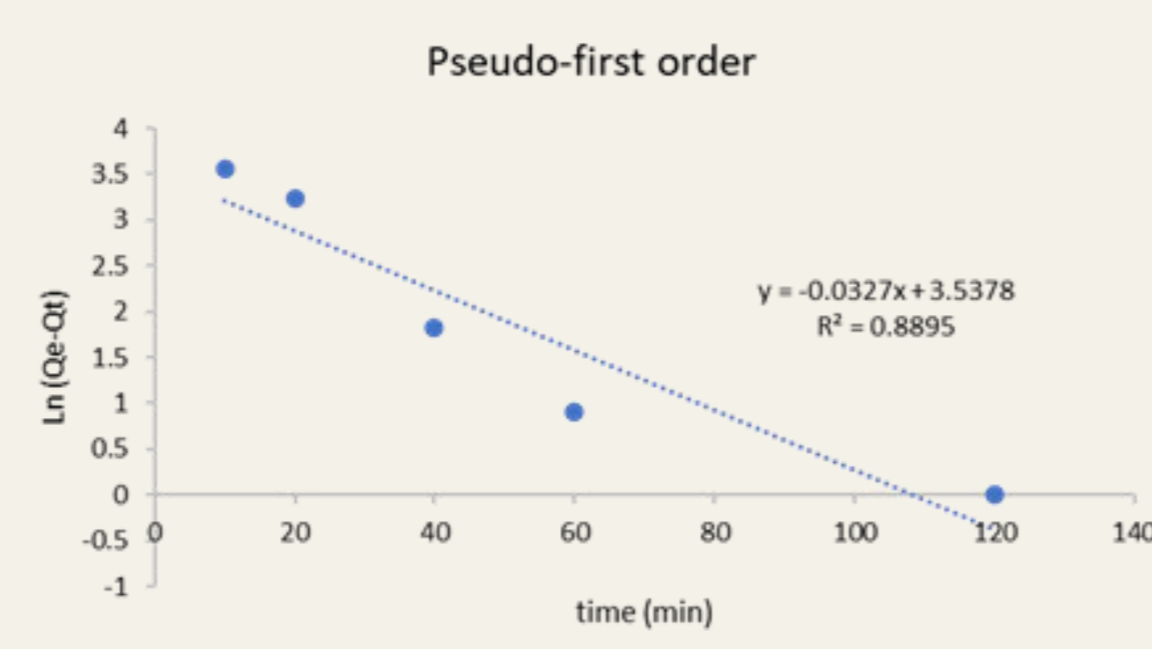
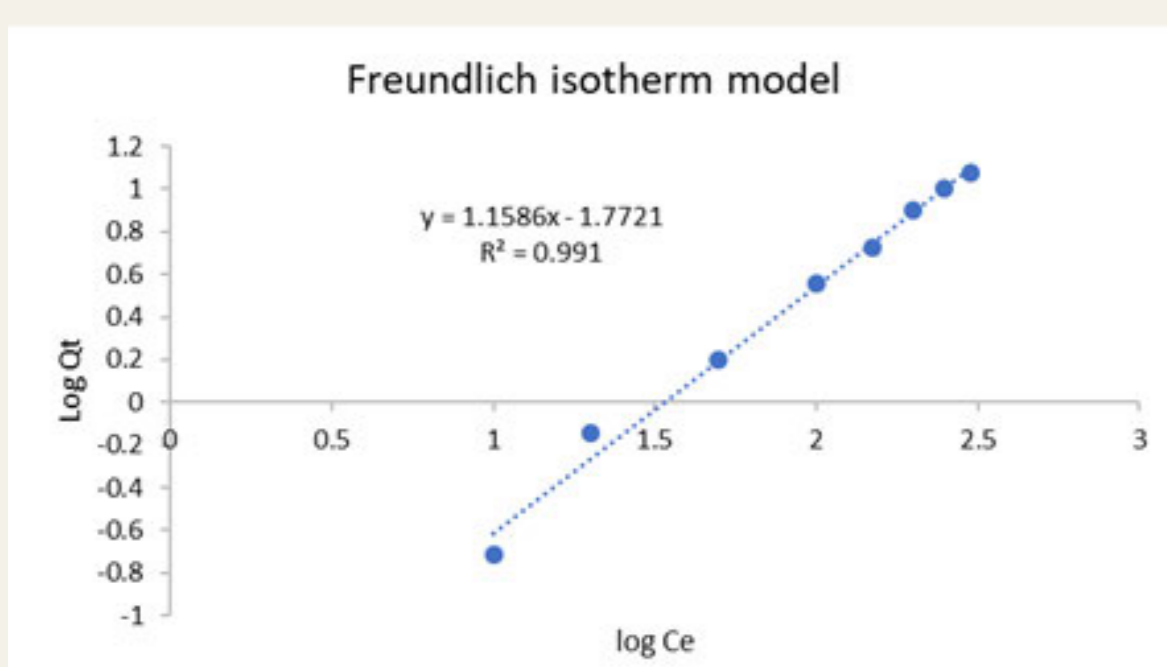
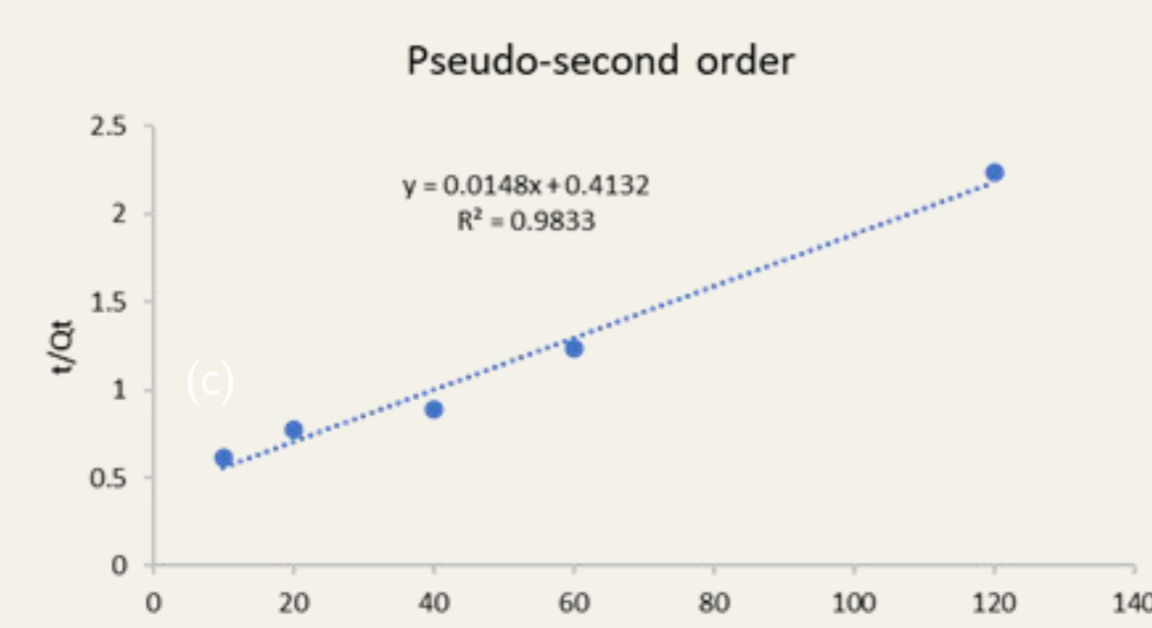
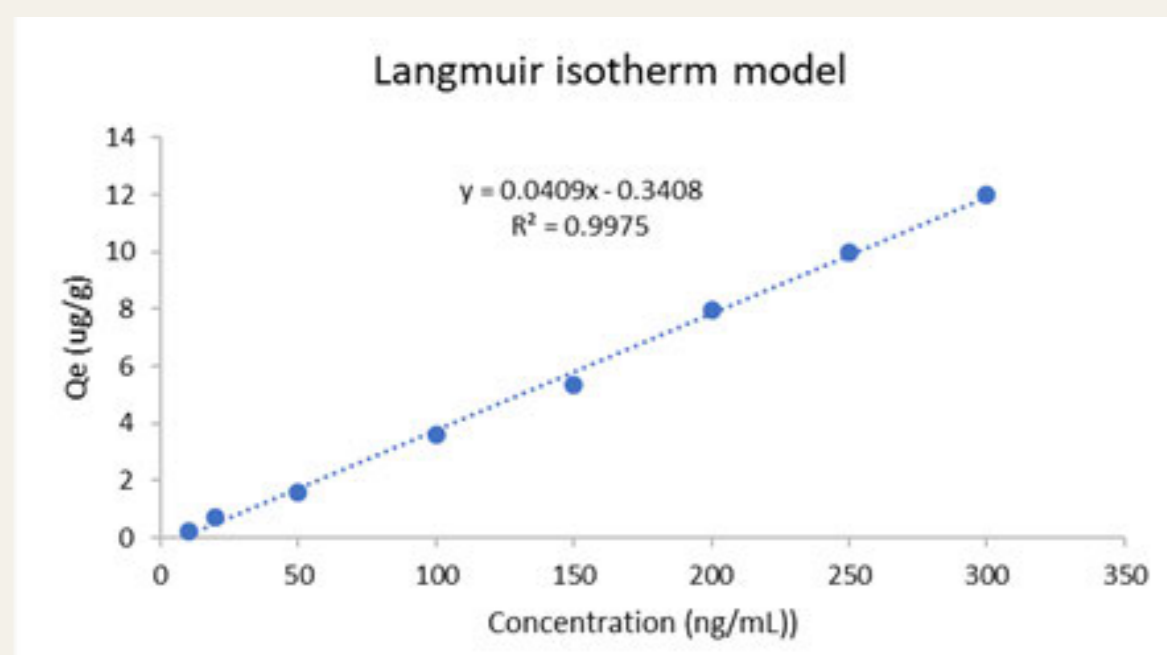
- Efavirenz as a template
- p-vinylbenzoic acid as a functional monomer
- EGDMA as a crosslinker

Optimization using Central Composite Design

Application in polluted wastewater effluents

RESULTS AND DISCUSSION

Modelling results



Adsorption of efavirenz fits the following models;

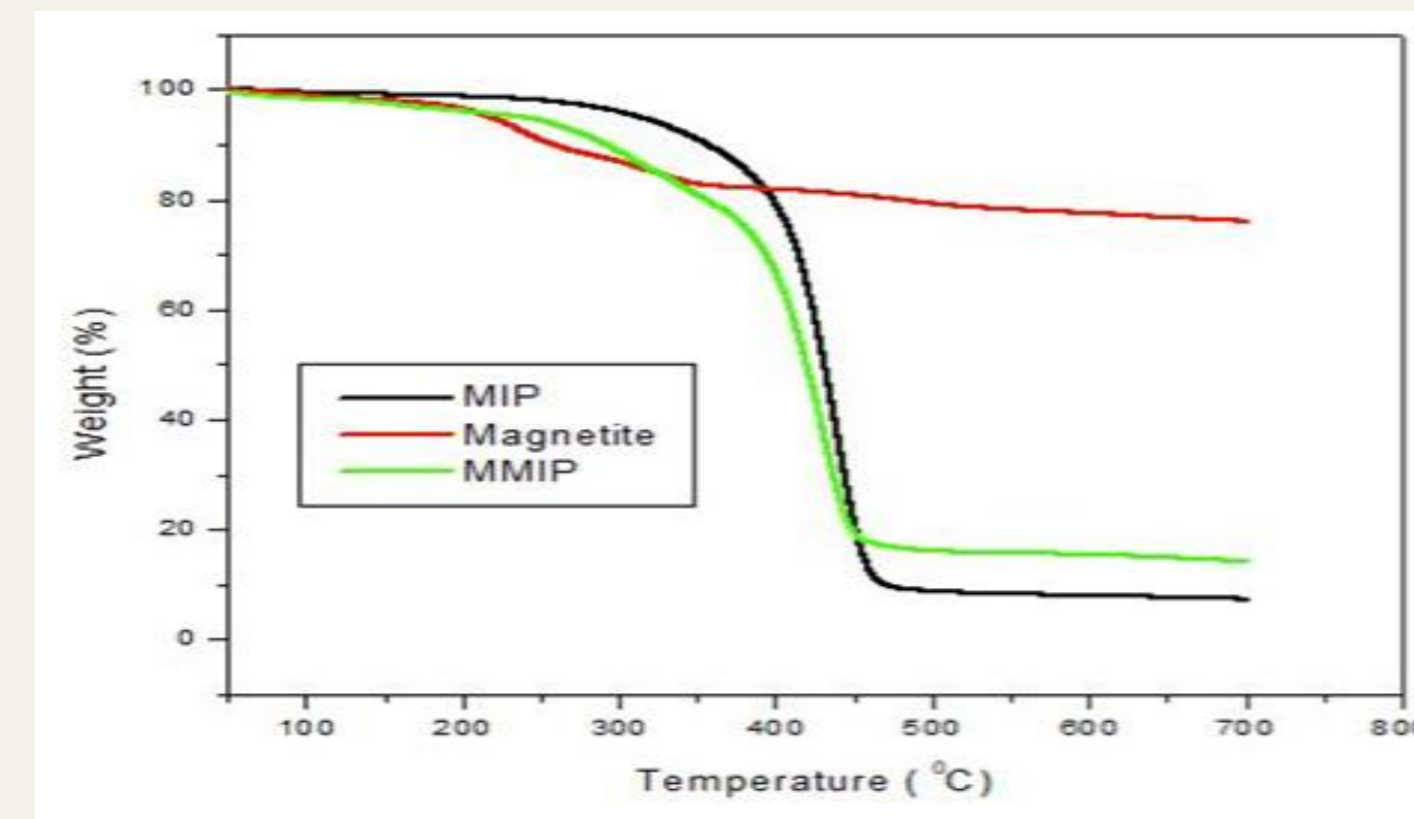
- Langmuir isotherm** - model assumes that all binding sites are homogeneous with uniform adsorption energy and the adsorption process gives a monolayer coverage.
- Pseudo 2nd order model** - the interaction between the MMIP and efavirenz is through chemisorption

ACKNOWLEDGEMENTS

DUT Internal Master's Scholarship

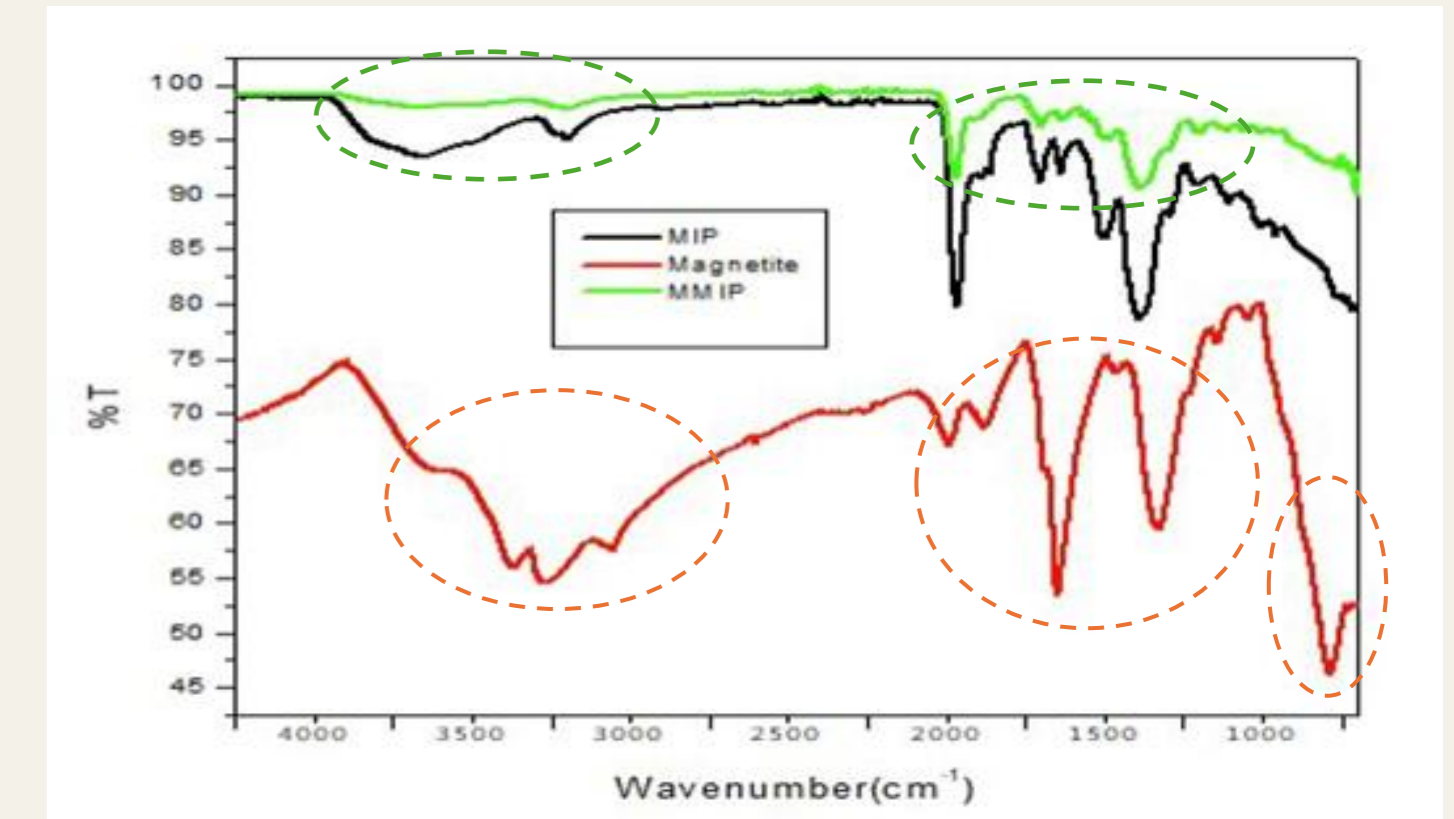
CHARACTERIZATION

Thermogravimetric analysis



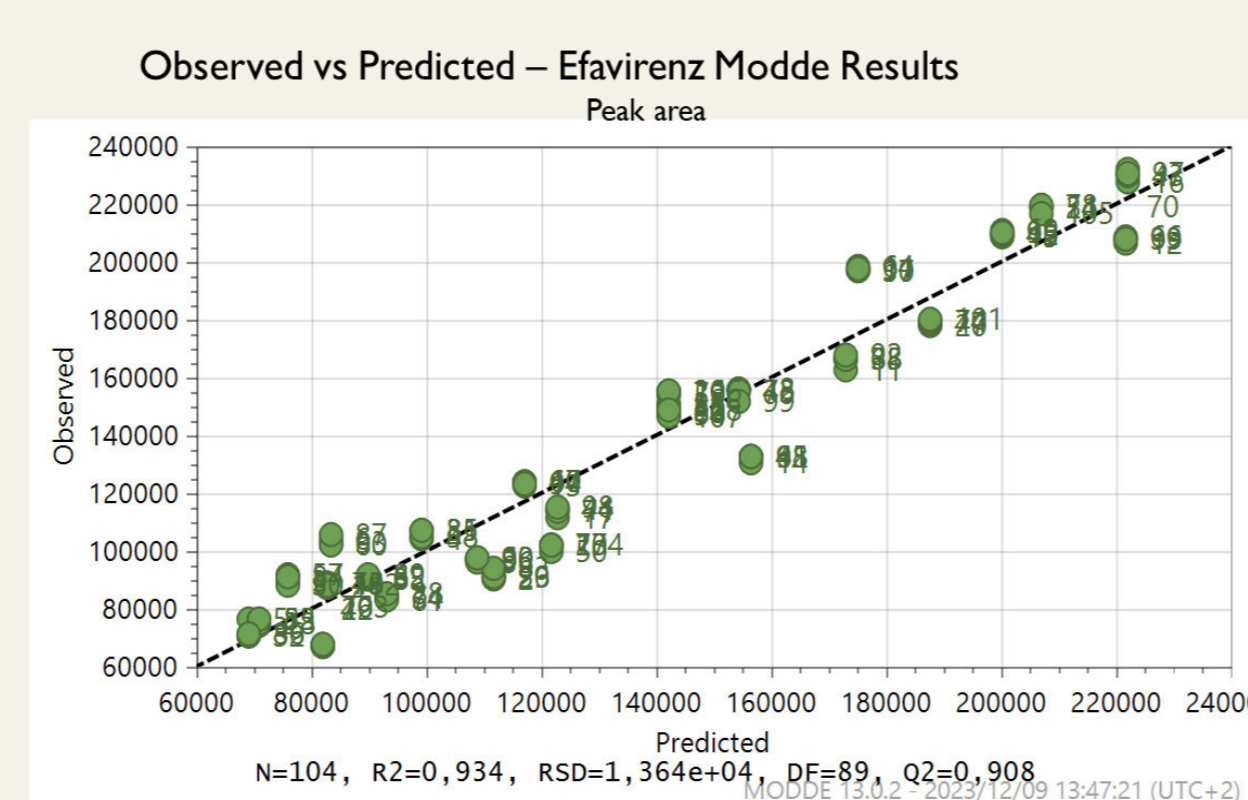
- MMIP stable up to 300 °C

Fourier transform infrared spectroscopy

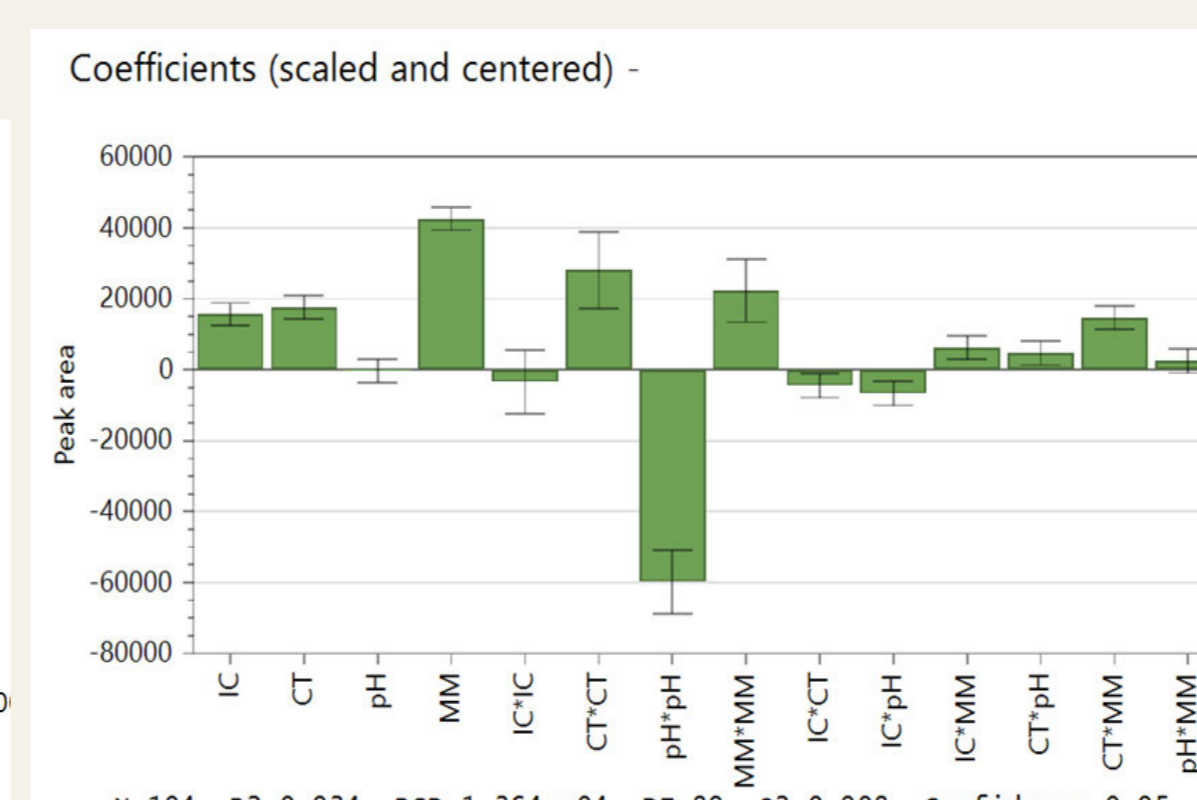


- Magnetite exhibited typical -OH and Fe-O absorption bands
- After co-polymerization, these stretches were suppressed indicating that the magnetite lost the H₂O particles from its surface as it was incorporated into the MIP during co-polymerization

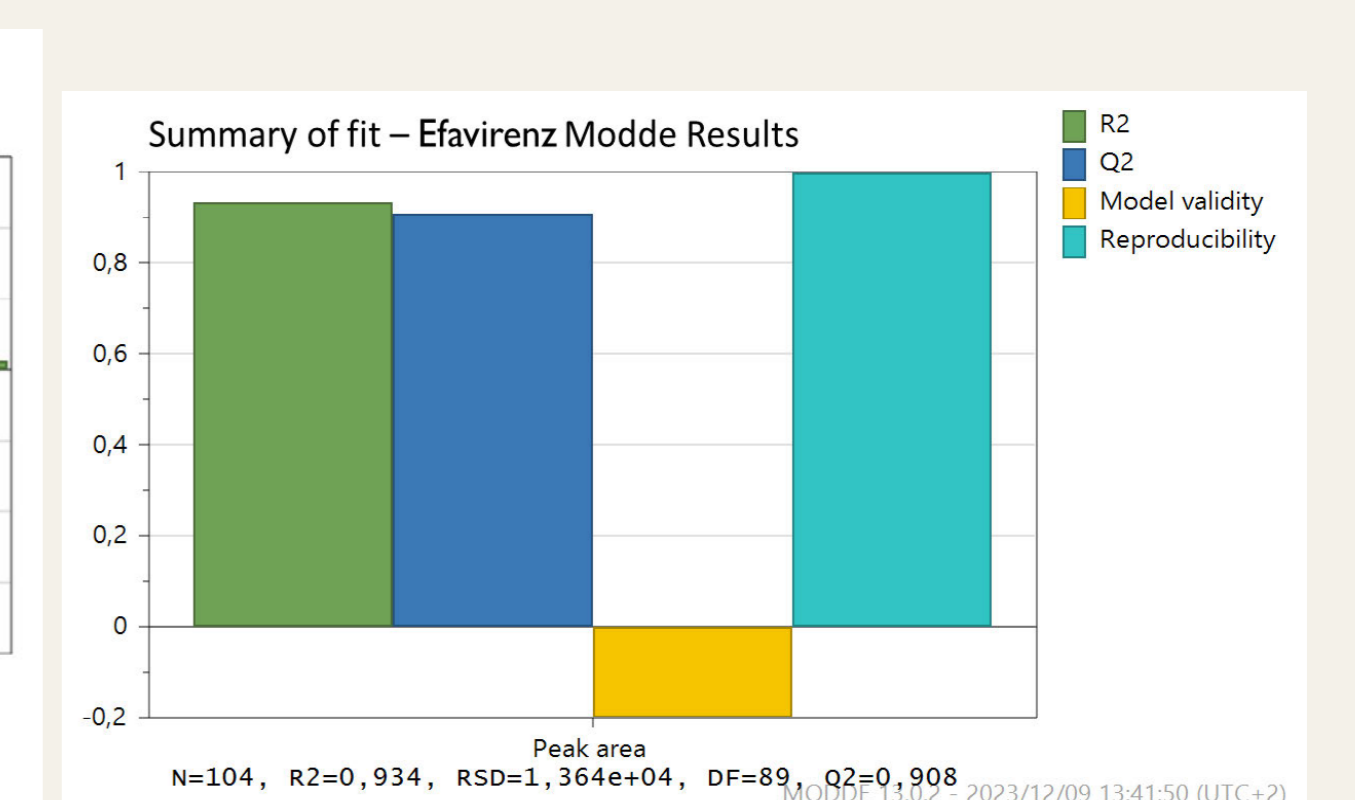
CENTRAL COMPOSITE DESIGN – Modde Statistical software



- Strong correlation between predicted and experimental values

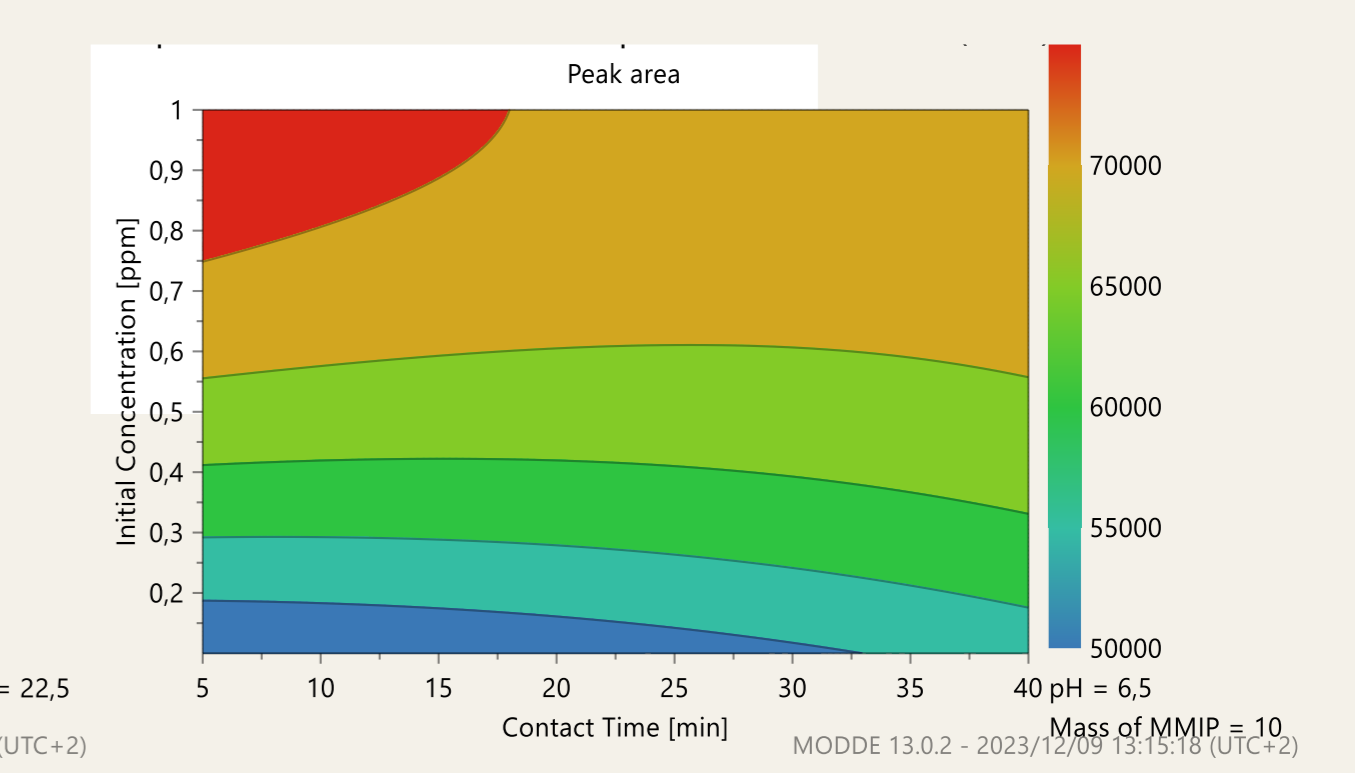
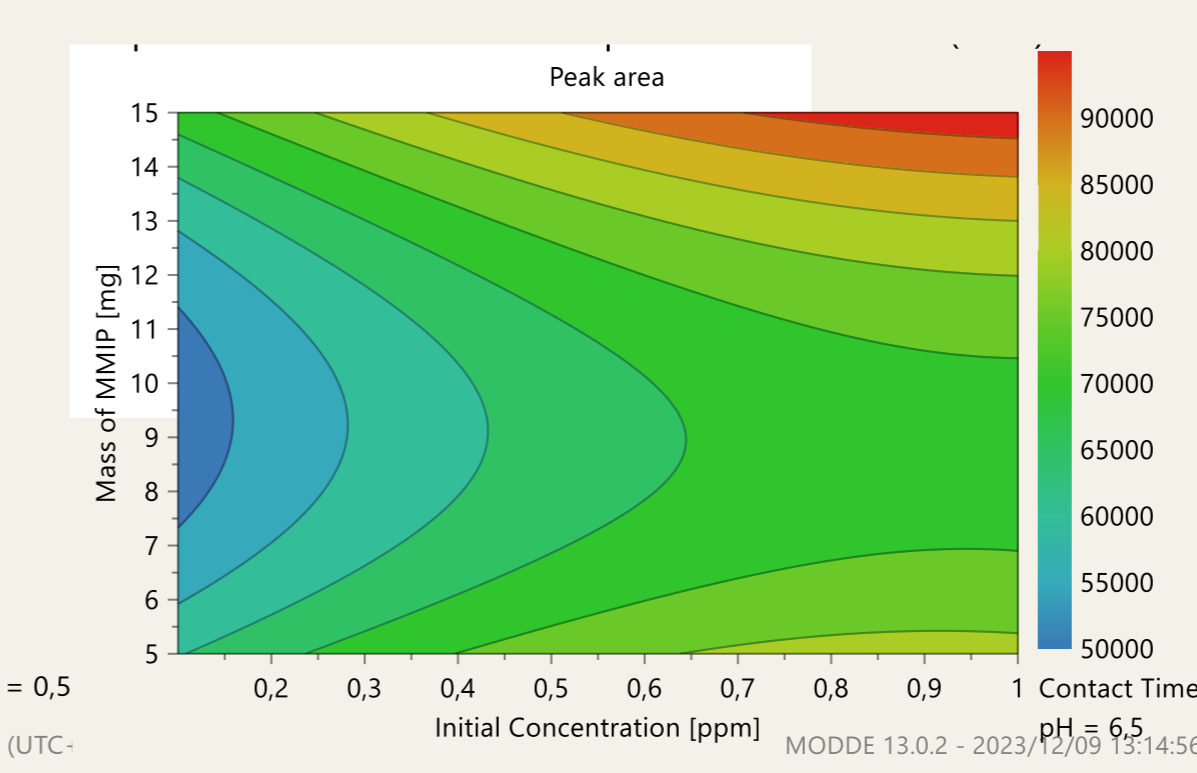
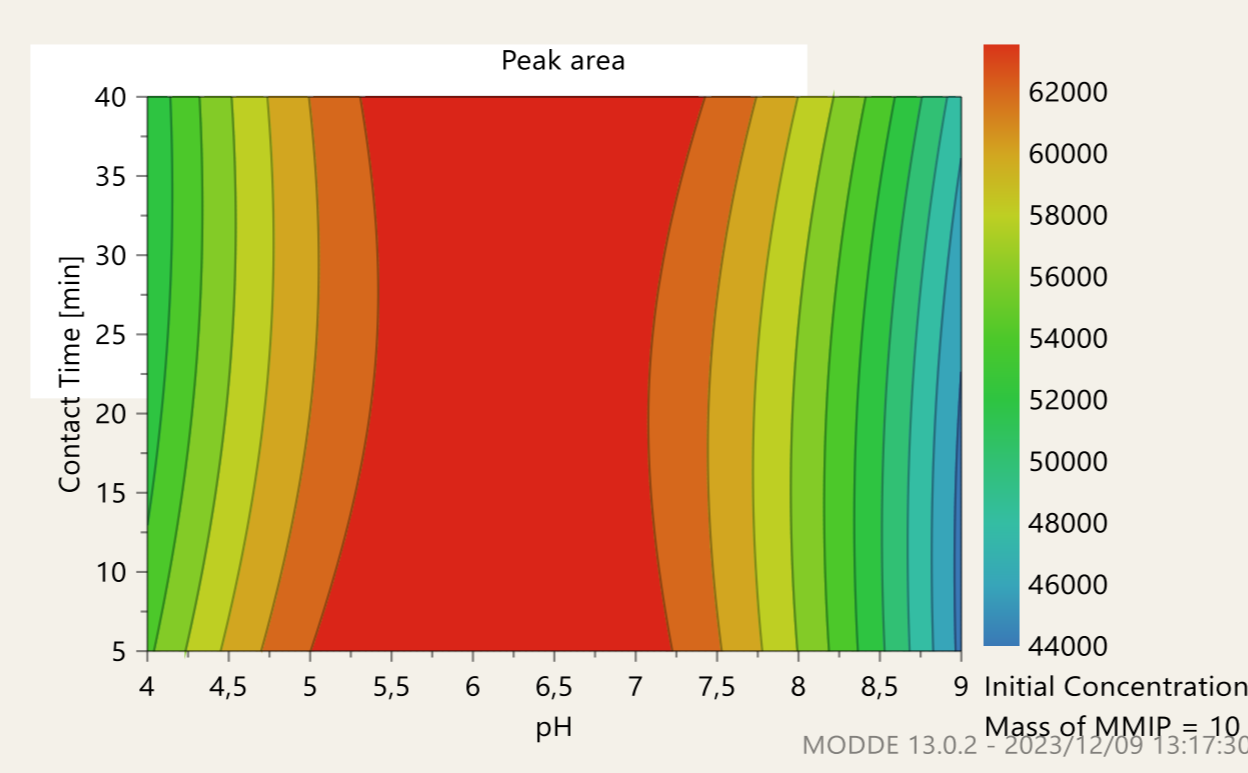
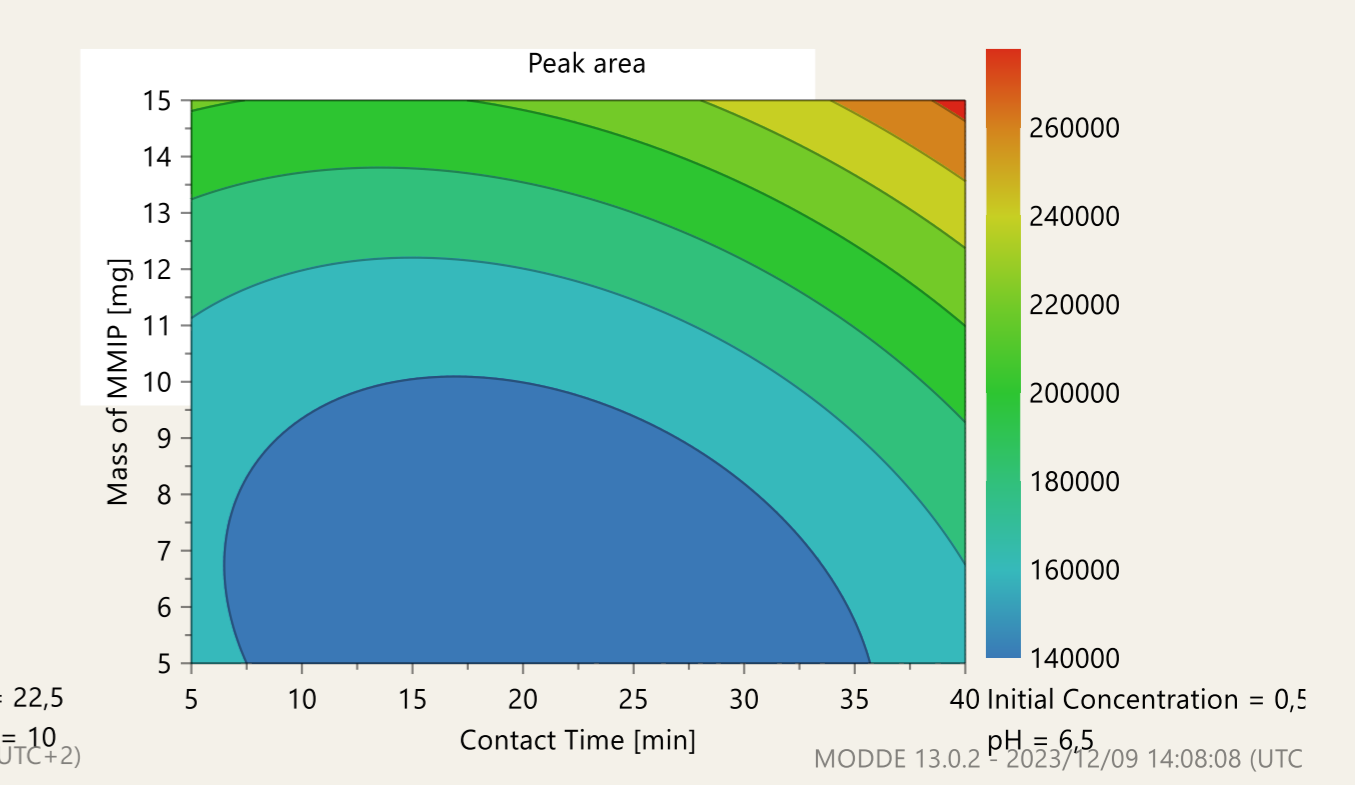
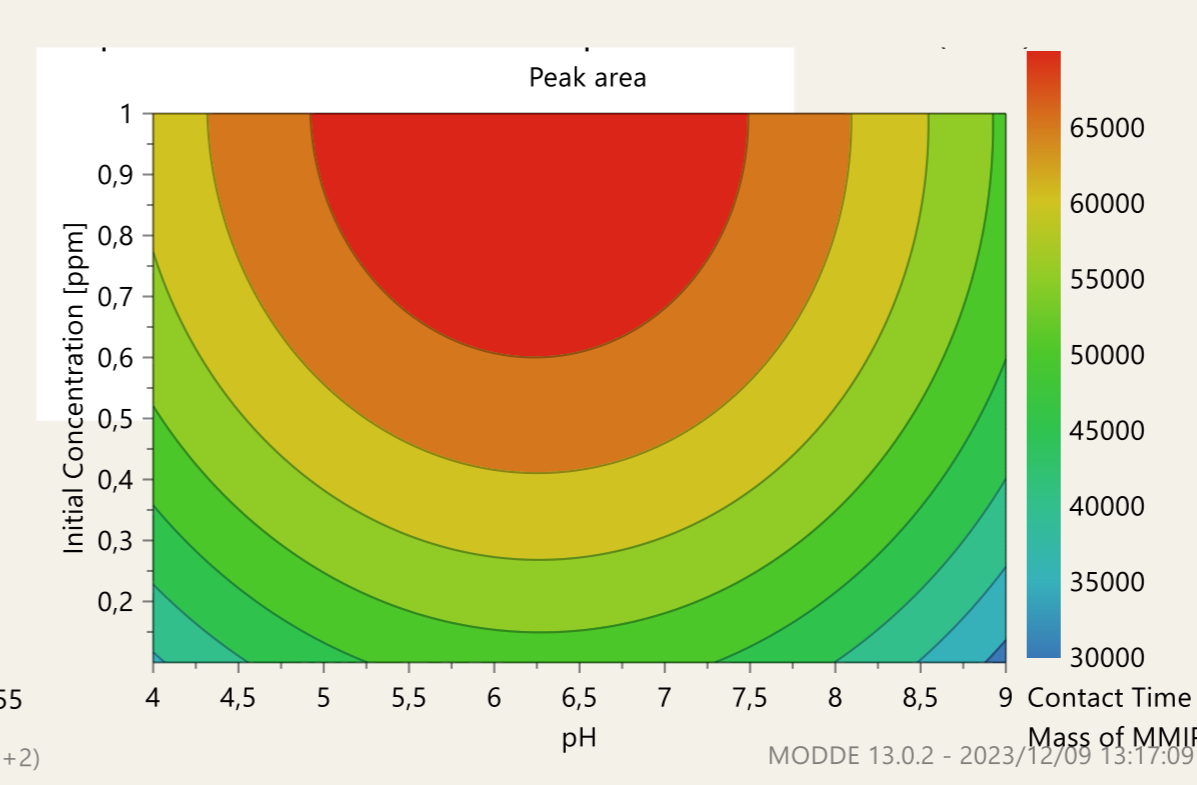
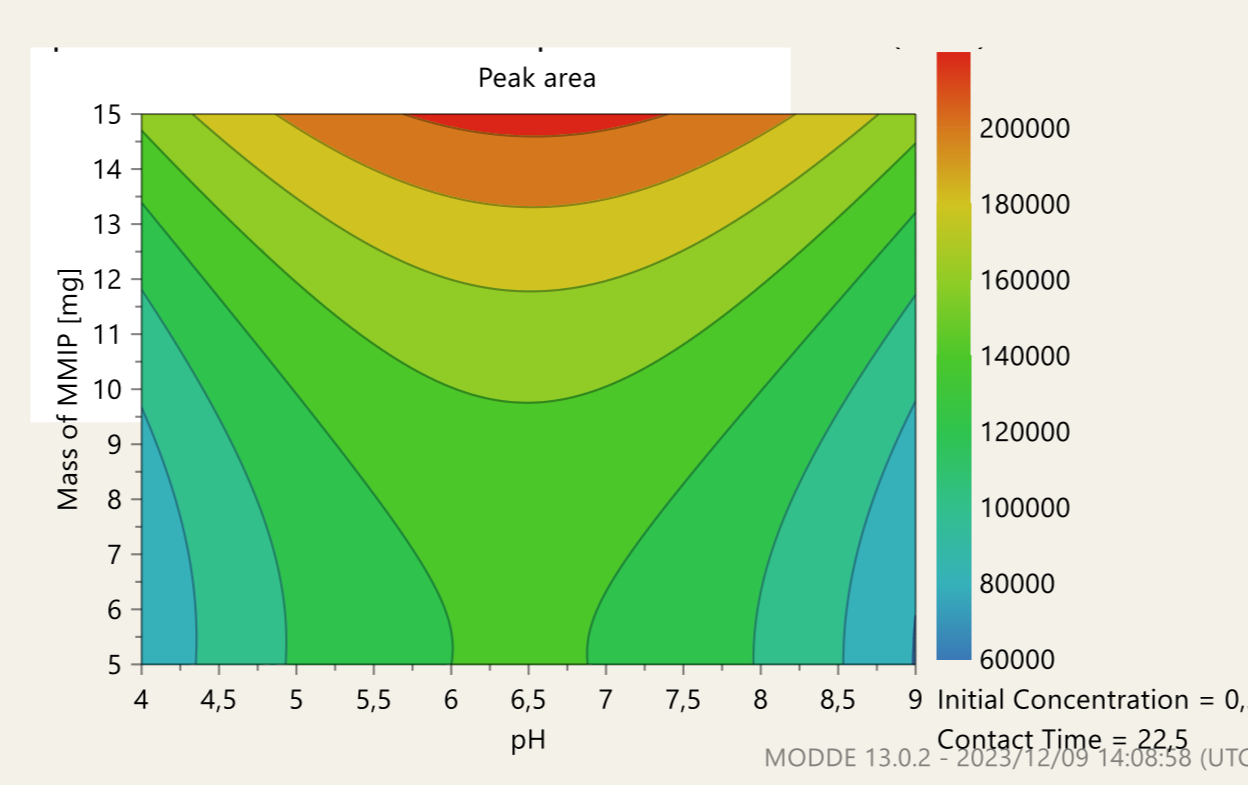


- Positive response for contact time, initial concentration, and mass of the MMIP
- Minimum effect due to pH



Good values for R², Q² and reproducibility were observed for the model with R² = 0.890, Q² = 0.833 but with a better reproducibility of 0.99 indicating minimal error in the response output

Response Contour plots



Optimum conditions:

- pH – neutral
- Initial Concentration – 1 ppm
- Contact Time – 40 min
- Mass of the MMIP – 15 mg

Method validation and application in contaminated wastewater

Analyte	SIM ion (m/z)	R ²	Calibration Accuracy (%)	MDL (ng mL ⁻¹)	MQL (ng mL ⁻¹)	*Concentration in effluent (ng mL ⁻¹)	Removal efficiency (% ± RSD%)
Efavirenz	315	0.9908	92.2 - 104.7	0.0265	0.0804	3.99	44.8 ± 11
Nevirapine	266	0.9981	92.3 - 104	0.0331	0.100	n.d.	-

n.d. - not detected;

*Done using SPE

CONCLUSION

- Based on coefficient plots, summary of fit and contour plots, the removal of efavirenz was directly affected by contact time, initial concentration of efavirenz and the mass of the magnetic polymer used under neutral conditions.
- Its optimal binding capacity achieved after 40 min contact time was 44.9 μg g⁻¹.
- The magnetic polymer could achieve 44.8% removal efficiencies from real wastewater effluents polluted with 3.99 ng mL⁻¹ of efavirenz.

REFERENCES

- Sibali et al., 2024. Journal of Hazardous Materials Advances
- Khulu et al., 2022. Chemosphere
- Mtolo, Mahlambi, Madikizela, 2019. Water Science & Technology
- Kunene, Mahlambi, Ndlovu, 2024. Journal of Environmental Management